**UNIVERSIDAD COMPLUTENSE DE MADRID**
FACULTAD DE MEDICINA


# TESIS DOCTORAL

## Influencia de las estructuras profundas sobre el EEG y su estudio invasivo y no invasivo

## Influence of deep structures on the EEG and their invasive and non-invasive assessment

MEMORIA PARA OPTAR AL GRADO DE DOCTOR

PRESENTADA POR

**David Martín López**

Directores

**Gonzalo Alarcón Palomo**
**Jorge García Seoane**
**Antonio Valentín Huete**

Madrid

UNIVERSIDAD COMPLUTENSE DE MADRID

FACULTAD DE MEDICINA

PROGRAMA DE DOCTORADO EN INVESTIGACIÓN BIOMÉDICA

DEPARTAMENTO DE FISIOLOGÍA


# INFLUENCIA DE LAS ESTRUCTURAS PROFUNDAS SOBRE EL EEG Y SU ESTUDIO INVASIVO Y NO INVASIVO

# INFLUENCE OF DEEP STRUCTURES ON THE EEG AND THEIR INVASIVE AND NON-INVASIVE ASSESSMENT

David Martín López

Madrid 2019

UNIVERSIDAD COMPLUTENSE DE MADRID

FACULTAD DE MEDICINA

PROGRAMA DE DOCTORADO EN INVESTIGACIÓN BIOMÉDICA

DEPARTAMENTO DE FISIOLOGÍA


# INFLUENCIA DE LAS ESTRUCTURAS PROFUNDAS SOBRE EL EEG Y SU ESTUDIO INVASIVO Y NO INVASIVO

# INFLUENCE OF DEEP STRUCTURES ON THE EEG AND THEIR INVASIVE AND NON-INVASIVE ASSESSMENT

David Martín López

Directores:

Prof Dr Gonzalo Alarcón Palomo

Prof Dr Jorge García Seoane

Dr Antonio Valentín Huete

Madrid 2018

UNIVERSIDAD COMPLUTENSE MADRID

# DECLARACIÓN DE AUTORÍA Y ORIGINALIDAD DE LA TESIS PRESENTADA PARA OBTENER EL TÍTULO DE DOCTOR

D./Dña. David Martín López,
estudiante en el Programa de Doctorado Investigación biomédica,
de la Facultad de Medicina de la Universidad Complutense de Madrid, como autor/a de la tesis presentada para la obtención del título de Doctor y titulada:

INFLUENCIA DE LAS ESTRUCTURAS PROFUNDAS SOBRE EL EEG Y SU ESTUDIO INVASIVO Y NO INVASIVO

y dirigida por: Jorge Juan García Seoane, Gonzalo Alarcón Palomo y Antonio Valentín Huete.

**DECLARO QUE:**

La tesis es una obra original que no infringe los derechos de propiedad intelectual ni los derechos de propiedad industrial u otros, de acuerdo con el ordenamiento jurídico vigente, en particular, la Ley de Propiedad Intelectual (R.D. legislativo 1/1996, de 12 de abril, por el que se aprueba el texto refundido de la Ley de Propiedad Intelectual, modificado por la Ley 2/2019, de 1 de marzo, regularizando, aclarando y armonizando las disposiciones legales vigentes sobre la materia), en particular, las disposiciones referidas al derecho de cita.

Del mismo modo, asumo frente a la Universidad cualquier responsabilidad que pudiera derivarse de la autoría o falta de originalidad del contenido de la tesis presentada de conformidad con el ordenamiento jurídico vigente.

En Madrid, a 13 de junio de 2019

Digitally signed by David Martin Lopez
Date: 2019.06.13 17:20:42 +01'00'

Fdo.: _____

A Laura.

*“The science of electroencephalography was at once new and old. It was old in the sense that the knowledge of the microcurrents generated by nerve cells of living beings belonged to that immense category of human knowledge whose origin was completely lost. It was knowledge that stretched back as far as the earliest remnants of human history– And yet it was new, too. The fact of the existence of microcurrents slumbered through the tens of thousands of years of Galactic Empire as one of those vivid and whimsical, but quite useless, items of human knowledge. Some had attempted to form classifications of waves into waking and sleeping, calm and excited, well and ill – but even the broadest conceptions had had their hordes of vitiating exceptions.” (…)*

*"Neural microcurrents, carry within them the spark of every varying impulse and response, conscious and unconscious. The brain-waves recorded on neatly squared paper in trembling peaks and troughs are the mirrors of the combined thought-pulses of billions of cells. Theoretically, analysis should reveal the thoughts and emotions of the subject, to the last and least. Differences should be detected that are due not only to gross physical defects, inherited or acquired, but also to shifting states of emotion, to advancing education and experience, even to something as subtle as a change in the subject's philosophy of life."*

***Isaac Asimov***

*Second Foundation - 1953*

# *Agradecimientos*

Voy a empezar la casa por el tejado y voy a agradecer en primer lugar la labor de mi tutora y mis directores de tesis a caballo entre Madrid y Londres. A María del Carmen y Jorge por su ayuda y guía desde la distancia sin la cual nada de esto sería posible. Al energético Antonio por demostrarme que muchas veces investigar es básicamente usar la imaginación, especialmente en el campo administrativo. Pero sobre todo gracias a Gonzalo por ser una constante fuente de inspiración incluso desde la distancia. Sin su capacidad de contemplar simultáneamente los aspectos clínicos, matemáticos, históricos e incluso artísticos de cualquier fenómeno, todos los sistemas implicados en este trabajo estarían fuera de control. ¿Quién iba a decir que de aquellos esbozos de idea saldría una teoría tan bien fundamentada?

A mis maestros en el campo de la neurofisiología clínica tanto en Inglaterra como en Madrid. A todos los adjuntos del Marañón, en especial a Carmen y Julio, por enseñarme el lado "duro" (en el buen sentido) y científico de la neurofisiología y a los del Gómez Ulla por enseñarme su lado amigable. A los profesores de la Universidad Autónoma de Madrid que me otorgaron la poderosa arma de la programación en MatLAB, en particular a Liset Menéndez de la Prida y su equipo del laboratorio de circuitos neuronales.

Quiero dedicar unas líneas a mi compañero de armas de programación Diego, por su entusiasmo inagotable y su capacidad compiladora. No sé qué hubiera hecho sin tus bases de datos. También recordar aquí a Narciso Serra por las nociones prácticas de teoría del caos.

No puedo dejar de expresar mi agradecimiento a todas esas otras personas que han avivado la chispa del interés científico. La ciencia no es sólo una vocación, es una forma de entender la vida, un método que nos transforma en seres diferentes. En mi caso dar las gracias a mis padres. A mi madre la estimulación temprana y responder a mis constantes dudas sin dejar de alentar más preguntas y por iniciarme en la ciencia a través del conocimiento de los animales. A mi padre por iniciarme en la informática, la química y las matemáticas y enseñarme a hacer raíces cuadradas a la antigua usanza (ganándome la enemistad de profesores de primaria amantes de la mediocridad). A Álvaro, experto autodidacta en ciencias aplicadas y electrónica por ayudarme a trastear en dicha materia. A Rubén, por su sentido del humor y por ser durante décadas el único capaz de comprender y criticar tanta jerga a la hora de la cena. Y cómo no a mi abuelo José María, quien me enseñó la belleza y crueldad de la realidad física y la naturaleza en todos los sentidos.

Por último, a Laura, "sabia" del orden y hedonista del caos por su apoyo crítico. Gracias por vivir la ciencia conmigo día a día y por el don del sueño más allá de la realidad inmediata.

A todos vosotros y al dios desconocido, gracias.

# INDEX

# STRUCTURED SUMMARY

## Title

Influence of deep structures on the EEG and their invasive and non-invasive assessment.

## Introduction

The EEG is the most valuable diagnostic test in epilepsy. In essence, it mainly consists in a graphical representation of the summated postsynaptic potentials generated in the pyramidal neurons from the cortex. The electrical fields can be generated on the scalp by two mechanisms: volume conduction from nearby regions and synaptic inter-neuronal propagation. Pyramidal cells align conforming local microcircuit configurations which activation lead to the generation of EEG rhythms. One of the main challenges of EEG is to decipher the relation between the recorded EEG activity and the activity in the neuronal networks. To find the source of EEG activity, complex non-linear and linear mechanisms as well as volume conduction effect and influence of the shape and electrical properties of the brain and skull need to be taken in consideration. In addition, brain regions are profusely interconnected and functionally connected regions often produce mutual modulation that adds additional complexity. In epilepsy it is particularly relevant to find out the initiation of the epileptiform activity and seizures as well as their propagation to connected areas. This is particularly difficult for generalised activity which involve large cortical regions bilaterally by the time it is recorded on the scalp, thus hiding any contributing deeper source. Invasive techniques are often employed to record intracranial fields and better define the

epileptogenic zone. Advances in signal analysis have contributed to improve the detection of deep sources using different mathematical methods. Our group has developed an alternative approach employing single pulse electrical stimulation to investigate both, functional connectivity and increased epileptogenicity.

The aim of this thesis is to tease out the contributions of deep and superficial structures to the EEG in several conditions.

## Objectives

1. To determine whether scalp EEG contains enough information to reliably identify focal hippocampal epileptiform discharge sources in temporal lobe epilepsy.
2. To identify the structures originating K-complexes.
3. To estimate the role of centromedian thalamic nucleus in the initiation and maintenance of seizures in humans.
4. To develop a method to characterise the morphology of responses to single pulse electrical stimulation (SPES) that could explain the oscillatory behaviour of the spontaneous EEG.
5.

## Material, Methods and Results

For objective 1, we employed simultaneous scalp and intracranial foramen ovale recordings. The aim was to develop an algorithm capable of detecting on the scalp EEG epileptiform discharges generated in the mesial temporal region but not visually detectable

in the scalp EEG. The sensitivity and specificity of scalp detections were compared with the gold standard of hippocampal EEG recorded simultaneously with foramen ovale electrodes. Our algorithm obtained a 65% accuracy based in time-frequency features.

For objective 2, we reviewed responses to SPES from patients assessed with intracranial electrodes and identified 6 patients in which SPES elicited responses similar to spontaneous K-complexes. In all patients stimulation of the cingulate gyrus elicited the response of greatest similarity to spontaneous K-complexes.

For objective 3, we studied ictal and interictal thalamic and surface recordings from 3 patients being assessed for deep brain stimulation of the centromedial nucleus of the thalamus. The first patient showed cortical seizure onset and late thalamic activation which was associated with increased rhythmicity of the ictal discharges. Patient two showed independent interictal epileptiform discharges and simultaneous scalp and thalamic seizure onset, with a thalamic leading role as demonstrated by quantitative analysis. The last patient had a frontal onset with later spreading to the thalamus.

For objective 4, we developed a model based in control systems to explain the morphology of early responses to SPES. We successfully modelled the responses employing either one or two control systems. We compared the spontaneous EEG frequency content with the frequency content predicted by the control models used. We found a great degree of similarity between spontaneous frequency content and that predicted by our models. Interestingly, activity not present in the spontaneous EEG but predicted by our model (such as alpha rhythm or epileptiform discharges) was explained by identification of such activity with eyes closed or in longer EEG periods.

## *Conclusions*

Specific conclusions obtained from the first paper:

- It is possible to detect scalp-visible and nonscalp-visible intracranial IED signatures on the scalp EEG employing a mathematical algorithm.

- The probabilistic classifier provided successful detections with a low number of false positives both, when trained with within-subject data and when trained on a pool of patients with epilepsy.

Specific conclusions obtained from the second paper:

- Electrical stimulation of the anterior cingulate gyrus initiates widespread synchronous activity that resembles K-complexes.

- Cingulate stimulation can induce responses similar to K-complexes during wakefulness.

Specific conclusions obtained from the third paper:

- Generalised seizures may show complex patterns of initiation, with various relative cortical and thalamic involvements.

- In the generalised seizures recorded in our patients, the thalamus may become involved early or late in the seizure but, once it becomes involved, it leads the cortex.

- In frontal seizures the thalamus gets involved late in the seizure and, once it becomes involved, it lags behind the cortex.

- The thalamus is capable of generating focal unilateral epileptiform discharges restricted to thalamic structures

Specific conclusions obtained from the fourth paper

- It is possible to describe the oscillatory behaviour of the EEG to SPES in terms of control theory employing one or two control systems.

- The described method can estimate the oscillatory coupling between connected cortical regions and may have the potential to identify frequencies at which cortical regions are able to oscillate.

General conclusions:

It is well known that scalp EEG activity emerges from the interaction of superficial and deep cortical and subcortical structures within a conductive medium. In the present work we show that It is possible to detect epileptiform activities generated in deep areas of the mesial temporal lobe at the scalp level. This was achieved employing time-frequency algorithms to examine low amplitude information in the scalp EEG arising from deep sources (the intracranial signatures).

Electrical stimulation of the cingulate gyrus is able to produce EEG responses resembling K-complexes. Therefore, we have assessed with SPES the ability to produce cortically-generated phasic events similar to those physiologically generated by the cortex.

Assessing the role of deep mesial structures in generalised seizures with thalamic centromedian electrodes we have observed that seizure onset in generalised seizures can be complex but once the thalamus is involved, it becomes the leading structure over the cortex acting as a pacemaker.

Responses to SPES can be characterised by a set of control systems. The properties of the summated systems can predict intrinsic properties of the cortex such as background rhythms, and capability to generate epileptiform activity and possibly seizures.

This work shows how quantitative methods can help to improve our understanding of the relative contribution of deep structures to the EEG and the interplay between different areas leading to physiological and pathological scenarios.

# RESUMEN ESTRUCTURADO

## Título

Influencia de las estructuras profundas sobre el EEG y su estudio invasivo y no invasivo

## Introducción

El EEG es la prueba diagnóstica de mayor utilidad en el diagnóstico de la epilepsia. Consiste esencialmente en la representación gráfica de los potenciales postsinápticos generados en las neuronas piramidales de la corteza. Los campos eléctricos registrados en la superficie tienen principalmente dos mecanismos de origen: conducción de volumen desde regiones adyacentes y propagación interneuronal sináptica. Las neuronal piramidales se agrupan formando microcircuitos locales siendo estos circuitos los responsables de la generación de los ritmos registrados en el EEG. Uno de los principales retos de la electroencefalografía consiste en descifrar la relación entre la actividad registrada y la actividad subyacente en las redes neuronales. Para encontrar la fuente de dichas actividades, es necesario tener en cuenta complejos mecanismos tanto no lineales como lineales, así como el efecto de la conducción de volumen y la influencia de la morfología y las propiedades eléctricas del cerebro y el cráneo. Además, las regiones cerebrales se encuentran profusamente interconectadas a menudo produciendo una modulación recíproca que añade un mayor grado complejidad. En epilepsia es particularmente importante averiguar dónde se inician las actividades epilépticas y cómo se propagan a áreas conectadas. Esto es particularmente difícil en el caso de actividad generalizada en la que en el momento en que la actividad

epileptiforme es registrada en el EEG grandes áreas corticales se encuentran activadas de forma simultánea, ocultando de este modo la contribución de cualquier fuente profunda. Hoy en día es muy común la utilización de técnicas invasivas para registrar la actividad intracraneal y definir la zona epiléptica. Los avances en análisis de señal, han contribuido a mejorar la detección de actividad epileptiforme generada en fuentes profundas utilizando diferentes métodos matemáticos. Nuestro grupo ha desarrollado un enfoque alternativo que emplea la estimulación eléctrica de pulso único (SPES) para investigar tanto la conectividad funcional como el aumento de la epileptogenicidad.

El objetivo de esta tesis es analizar la contribución de las estructuras profundas y superficiales al EEG en varias situaciones.

## *Objetivos*

- Determinar si el EEG de superficie contiene información suficiente para identificar de forma consistente las fuentes profundas de las descargas epileptiformes hipocampales en epilepsia del lóbulo temporal.
- Identificar las estructuras responsables de la generación de complejos K.
- Estudiar el papel del núcleo talámico centromediano en el inicio y mantenimiento de las crisis en humanos.
- Desarrollar un método que caracterice la morfología de las respuestas a la estimulación eléctrica de pulso único (SPES) que pueda explicar el comportamiento del EEG espontáneo.

## *Material, Métodos y Resultados*

Para el objetivo 1, empleamos registros simultáneos de EEG de superficie e intracraneales de foramen oval. El objetivo era desarrollar un algoritmo capaz de detectar en el EEG de superficie las descargas epilépticas generadas en la región mesial temporal no detectables visualmente en el EEG de superficie. Comparamos la sensibilidad y especificidad del algoritmo comparando las detecciones basadas únicamente en el EEG de superficie con los registros hipocampales adquiridos simultáneamente con los electrodos de foramen oval. Nuestro algoritmo se basó características tiempo-frecuencia de la señal y obtuvo una precisión del 65%.

Para el objetivo 2, revisamos las respuestas a SPES de pacientes evaluados con electrodos intracraneales e identificamos 6 pacientes en los que la estimulación SPES obtuvo respuestas similares a complejos K espontáneos. En todos los pacientes, la estimulación del giro cingulado produjo las respuestas de mayor similitud con los complejos K espontáneos.

Para el objetivo 3, estudiamos registros ictales e interictales talámicos y de superficie de 3 pacientes que fueron evaluados para estimulación del núcleo centromediano del tálamo. En el primer paciente la crisis tuvo un inicio cortical y una posterior activación talámica que se asoció a un aumento de ritmicidad de las descargas ictales. En el segundo paciente se observaron descargas epileptiformes interictales independientes en tálamo y las crisis tuvieron un inicio simultáneo en superficie y tálamo, liderando este último de acuerdo con el análisis cuantitativo. En el último paciente las crisis tuvieron un inicio frontal con posterior diseminación al tálamo.

Para el objetivo 4, desarrollamos un modelo basado en sistemas de control para explicar la morfología de las respuestas tempranas a SPES. Modelamos con éxito las respuestas empleando uno o dos sistemas de control combinados. Comparamos el contenido en frecuencia del EEG espontáneo con el contenido en frecuencia estimado de acuerdo con los modelos de sistemas de control empleados para cada canal. Encontramos un gran grado de similitud entre el contenido espontáneo en frecuencia y el predicho por nuestro modelo. Cabe resaltar que algunas actividades en determinadas frecuencias que no estaba presentes en el EEG espontáneo seleccionado (tales como el ritmo alfa y las actividades epileptiformes), pero que aparecían en las curvas de estimación predichas con nuestro modelo pudieron ser explicadas en todos los casos como actividades con ojos abiertos o actividades infrecuentes que solo podían observarse en periodos EEG más largos.

## *Conclusiones*

Conclusiones específicas deducidas de la primera publicación:

- Es posible detectar las firmas intracraneales de las descargas intercríticas tanto visibles como invisible en superficie mediante el uso de algoritmos matemáticos.

- El clasificador probabilístico detecta satisfactoriamente las descargas intercríticas con un número bajo de falsos positivos tanto cuando se entrena con datos del mismo sujeto como cuando se entrena con datos de un grupo de pacientes epilépticos.

Conclusiones específicas deducidas de la segunda publicación:

- La estimulación electrica del giro cingulado anterior es capaz de iniciar una actividad sincrónica difusa similar a los complejos K.

- La estimulación del giro cingulado durante vigilia puede producir respuestas similares a complejos K.

Conclusiones específicas deducidas de la tercera publicación:

- Las crisis generalizadas pueden mostrar patrones de inicio complejos con diferentes grados de implicación de la corteza y el tálamo.

- En las crisis generalizadas registradas en nuestros pacientes, el tálamo puede activarse antes o después en el curso de la crisis, pero una vez implicado ejerce un papel de liderazgo sobre el cortex.

- En las crisis frontales el tálamo se implica tardíamente en el curso de la crisis y, una vez implicado, su actividad queda rezagada respecto al cortex.

- El tálamo es capaz de generar descargas epileptiformes unilateral restringidas a las estructuras talámicas.

Conclusiones específicas deducidas de la cuarta publicación:

- Es posible describe el comportamiento oscilatorio del EEG en respuesta al SPES en términos de teoría de control utilizando uno o dos sistemas de control.

- El método matemático descrito puede explicar el comportamiento oscilatorio entre regiones corticales interconectadas e identificar las frecuencias a las que las regiones corticales estudiadas son capaces de oscilar.

Conclusiones generales:

Es bien sabido que la actividad del EEG de superficie es el resultado de la interacción de estructuras corticales y subcorticales superficiales y profundas dentro de un medio conductor. En este trabajo mostramos que es posible detectar a nivel de superficie actividades epilépticas generadas en áreas profundas del lóbulo temporal mesial gracias al uso de algoritmos basados en características tiempo-frecuencia para examinar la información de baja amplitud en el EEG de superficie que se origina en fuentes profundas (las “firmas intracraneales”).

La estimulación eléctrica del giro cingulado es capaz de producir respuestas EEG que se asemejan a complejos K. Por lo tanto, se ha comprobado mediante SPES la capacidad de producir eventos fásicos similares a los generados fisiológicamente por la corteza.

Mediante el análisis del papel de las estructuras mesiales profundas en las crisis epilépticas generalizadas mediante electrodos talámicos centromedianos hemos comprobado que el inicio de crisis generalizadas puede ser complejo, pero una vez que el tálamo está implicado, se convierte en la estructura principal liderando sobre la corteza, actuando como marcapasos.

Las respuestas a SPES pueden caracterizarse por un conjunto de sistemas de control. Las propiedades de los sistemas sumados pueden predecir las propiedades intrínsecas de la corteza, como los ritmos de fondo, y la capacidad de generar actividad epiléptica y posiblemente crisis.

Este trabajo muestra cómo los métodos cuantitativos pueden ayudarnos a mejorar nuestra comprensión de la contribución relativa de las estructuras profundas al EEG y la interacción entre áreas cerebrales dando lugar a diferentes escenarios fisiológicos y patológicos.

# 1. INTRODUCTION

## • Epilepsy

The International League Against Epilepsy (ILAE) defines epilepsy as "*a disorder of the brain characterised by and enduring predisposition to generate epileptic seizures and by the neurobiological, cognitive, psychological, and social consequences of this condition*". For diagnosis the occurrence of at least one epileptic seizure is required(1).

According with the ILAE, an epileptic seizure is "*a transient occurrence of signs and/or symptoms due to abnormal excessive or synchronous neuronal activity in the brain*"(1).

Due to the fact that suffering a single seizure without epilepsy is common in the general population, translating these definitions into clinical practice has been a matter of some controversy which has led the ILAE to set out a practical definition of epilepsy as "*a disease of the brain defined by any of the following conditions: 1. At least two unprovoked (or reflex) seizures occurring >24 h apart. 2. One unprovoked (or reflex) seizure and a probability of further seizures similar to the general recurrence risk (at least 60%) after two unprovoked seizures, occurring over the next 10 years. 3. Diagnosis of an epilepsy syndrome*". In addition, individuals are no longer considered epileptics if they have a diagnosis of an age-dependent epilepsy syndrome but are older than the applicable age or if they have remained seizure-free for the last 10 years without antiepileptic treatment for the last 5 years(2).

The overall incidence of epilepsy in the world is 61.44 cases per 100.000 habitants and its prevalence 6.38 per 1000 habitants. Incidence is higher in paediatric and elderly population and higher in males than females (3). Prevalence reaches its highest level during

adolescence and early adulthood and decreases after 30, only to increase again in old age mainly due to stroke. Geographically, the incidence of epilepsy is higher in low and middle-income countries but there is no difference in prevalence, possibly due to associated mortality in lower-income countries.

- ***The role of EEG in epilepsy***

According with the second item in the practical definition of the ILAE, patients can have the diagnosis of epilepsy even if they have presented with a single epileptic seizure if they are considered to be at a high risk of recurrence. Here is where the electroencephalography (EEG) plays its major role in predicting the risk of new seizures. Although a single seizure plus epileptiform EEG spikes does not automatically satisfy criteria for this operational definition of recurrence risk of epilepsy(2), multicentre studies demonstrate a high risk of recurrence if the EEG is abnormal after a first seizure(4-7).

In addition, the diagnosis of epilepsy in the case of unwitnessed seizures and/or in the absence of a concomitant video-EEG study can be extremely difficult as there are many conditions that can mimic epilepsy including syncope, sleep disorders, migraines, movement disorders and non-epileptic seizures among others (8, 9). Excluding these conditions is fundamental and justifies the use of EEG in many cases were the diagnosis is unclear.

The sensitivity of a routine standard EEG for the detection of epileptiform abnormalities is between 32-59%(10, 11) with a higher yield if performed within 24-48 h within first seizure (12, 13) or after sleep deprivation(13).

Nowadays, despite of the massive advances in neuroimaging, the EEG still is the most helpful diagnostic tests in epilepsy with an excellent cost-effectivity relation when directed based in clinical information(11). As a diagnostic tool, it helps in the differential diagnosis of paroxysmal neurological events, often distinguishes between focal and generalised disorders and also provides evidence of photosensitivity(14). Neurologist often use it as a management tool assessing risk of recurrence after a first seizure, in the assessment of withdrawal of antiepileptic medication after long seizure-free periods or for monitoring and detection of non-convulsive status(14).

- ***Historical background***

The dawn of our journey through the neurophysiological analysis of the brain started back in 1875 with the first recordings of varying electric currents between pairs of scalp and brain located electrodes in rabbit and monkey by Richard Caton(15). It took another four decades for the first electroencephalographic recordings to be applied in humans by Berger(16). However, it wasn't until the mid-thirties when the technique gained some acceptance after demonstrating that the oscillations observed in the electroencephalographic traces, in particular the posterior alpha rhythms, were truly originated in cerebral structures and were not artefactual(17). Less than a century later, our knowledge about the processes transforming the single unit activity from large populations of neurons into the now familiar EEG traces has improved significantly but we are far from the complete understanding of brain currents.

- ***Origins of EEG activity***

First, we need to consider that the EEG consist in a graphical representation of the summation of extracellular potentials. EEG rhythms arise basically from the synchronous firing of postsynaptic potentials of thousands to millions of geometrically aligned pyramidal neurons contained within a circuit. To a minor degree, other cells including glial cells and other subtypes of neurons(18, 19) either excitatory or inhibitory contribute to the extracellular potentials.

The negative and positive electrical charges of the ions moving within, across and outside the nerve cells generate electrical fields that can be described by measuring the difference in the electric potential between two points. According with Coulomb's law a particle with electric charge $q_1$ at position $x_1$ exerts a force (F) on a particle with charge $q_0$ at position $x_0$ (Eq. 1)

$$F = \frac{1}{4\pi\varepsilon_0}\frac{q_1 q_0}{(x_1 - x_0)^2}\hat{r}_{1,0} \qquad (1)$$

Where $\hat{r}_{1,0}$ is the unit vector in the direction from point $x_1$ to point $x_0$ and $\varepsilon_0$ is the electric constant in $C^2\ m^{-2}\ N^{-1}$. The charge $q_1$ produces an electric field electric (E) at point $x_0$ (Eq. 2).

$$E(x_0) = \frac{F}{q_0} = \frac{1}{4\pi\varepsilon_0}\frac{q_1}{(x_1 - x_0)^2}\hat{r}_{1,0} \qquad (2)$$

The formula defines a vector field equal to the F per unit that a charge would experience at the position $x_0$. An electric field due to a point charge is directed away from the charge if it is

positive, and toward the charge if it is negative, and its magnitude decreases with the inverse square of the distance from the charge(20).

In essence, all electric processes produced within a volume superimpose and produce a potential at an extracellular point with respect to a reference potential. The features of the recorded potentials will depend on the contributing sources and their position. For instance, the amplitude of the recorded signal attenuates with the distance between the source and the recording electrode following an inverse law. But not everything follows that simplistic relation as the geometrical position, density and firing synchronicity of the sources leads to a spatial averaging of the signals (18) and while electrical fields due to a single charge decrease with the square of distance as it can be deducted from equation 1, electrical fields due to dipoles decrease with the cube of the distance(20).

In a broader sense, not all the recorded potentials recorded from the brain are EEG. Depending on the location of the recording electrodes we strictly speak about EEG when referring to differences in electrical potentials at the scalp level. Intracranial recordings by contrast are grouped in a few modalities; electrocorticography (ECoG) when recorded at the cortical surface mainly by grid or strip electrodes; depth electrodes, consisting in flexible bundles of contacts (macroelectrodes) able to record from grey and white matter; and local field potentials (LFP) when recorded by small-size depth electrodes in the brain(18).

But to really find what are the cellular substrates of these activities we need to look into the cerebral cortex. The human brain cortex contains approximately $86.1 \pm 8.1 \times 10^9$ neurons. About 19% of them are located in the cerebral cortex(21) profusely interconnected by approximately $1.5 \times 10^{14}$ cortical synapses(22). Cortical neurons receive two types of synaptic inputs; excitatory postsynaptic potentials (EPSPs) and inhibitory postsynaptic

potentials (IPSPs), each type respectively facilitating or inhibiting the production of an action potential(19). EPSPs and IPSPs contribute to the generation of dipoles where an area of positive charge (source) is separated from other with negative charge (sink). Postsynaptic potentials in pyramidal neurons are then the major contributors to the extracellular electrical fields but any excitable membrane and other non-synaptic events have the potential to contribute to them(18). Pyramidal cells have a relatively larger contribution to the EEG than other cells because of their number, morphology, geometrical location and cortical location. In contrast with spherical neurons, with dendrites emanating in all directions producing a close field effect when activated(23), pyramidal neurons present as strong dipoles along the somato-dendritic axis due to the apical distribution of their dendrites (with considerable spatial separation of the source from the return currents) generating open fields (18). In addition, their apical dendrites run parallel with apical dendrites from other pyramidal cells and also receive perpendicular inputs from other neurons. Thanks to this distribution, neurons placed in the same column or its vicinity are activated synchronously and their dipoles overimpose generating larger detectable fields(24, 25).

Pyramidal cells are mainly grouped in columns perpendicularly oriented to the cortical surface in layers II/III, V and VI of the neocortex following the shape of the circumvolution(26, 27) facilitating an easy detection of their potentials on the scalp. The folded nature of the cortex also affects the magnitude of the extracellular current flow as dendrites in gyri sides are closer, producing a higher current density on the brain surface and scalp than neurons located in sulci(28). The hippocampus also shares this convolute dipolar layer structure but the surface current dipole moment density is considerably larger

than that of the cortex explaining its contribution to the scalp potential, larger than expected for its deep location (27).

Cortical EPSPs and IPSPs are in summary the major contributors to the scalp EEG but a marginal contribution has been attributed to secondary mechanisms. Among these secondary contributors, a relevant role has been attributed to long lasting $Ca^{2+}$ mediated spikes which have the ability to propagate within the neuronal body, then modifying the extracellular fields within the cortex(18, 29). $Na^{+}$ action potentials can also generate spikes, but its duration is short and their contribution to the extracellular fields in the generation of activities with frequencies <100 Hz is not substantial(30) only contributing to the high frequency components(18). Currents flowing through hyperpolarization de-inactivated cyclic nucleotide-gated channels and low-threshold transient $Ca^{2+}$ currents are intrinsic voltage-dependent membrane responses that have been proposed as the basis of the intrinsic resonance and oscillatory properties observed in the membrane potential(31). This is an interesting property as several neurons have the ability to produce self-sustained oscillating responses following depolarisation mediated by inputs of a particularly frequency range and voltage (32, 33). Nevertheless, these responses have great variability depending on the input and the synchronicity between neighbouring neurons, being their influence in the extracellular field very variable and reduced(18). Intracellular ionic changes induce inwards flow of other ions through ligand-gated channels contributing to the extracellular field that can often have a long-lasting effect(34). To a minor extent, direct communication between neurons through gap junctions(35) and ephaptic transmission(36, 37) can participate to the extracellular field indirectly by affecting neuronal excitability. In last place, glial cells

potentials also add to the extracellular potentials producing slow variations in field patterns below 0.1 Hz (38, 39).

The electrical fields predominantly generated in these large columns of neurons can be propagated to other areas. These potentials can travel through a conductive medium, for instance brain tissue, by a linear phenomenon known as volume conduction. The nature of the transmission depends on the relations between the current dipole and the characteristic of the conductive medium(18, 24). In addition to volume conduction, electrical activities (as epileptiform activities) can follow neural propagation to synaptically connected regions(40). Moreover, electrical fields attenuate very fast with distance, being inversely proportional to the square of the distance.

- ***Circuits and oscillations***

We know how the cellular-level neuronal currents generate but the conceptual jump between the generation of this electrical activities and the content of the EEG signal is far from being fully understood(41). EEG is the result of large-scale synchronous events produced by geometrically aligned pyramidal neurons(28) but different microcircuit configurations can converge in similar EEG elements(42). Local circuit configurations are shaped during the formation of functional networks in order to perform specific tasks. The activation of these networks will lead to the generation of EEG rhythms(43).

We can be tempted to think that the variety of activity patterns that a great group of neurons is able to produce is virtually infinite. Strikingly, it has being observed that the firing patterns produced by cortical circuits are in fact limited(42) and tend to group in defined

sequences of spikes (spatio-temporal firing patterns) lasting up to 450ms(44). These patterns are linked to consistent chains of neurons that constitute the simplest levels of feed-forward network (the theoretical “synfire chains”(45, 46)). A given neuron can be part of different chains of neurons. If many neurons have the ability to participate in several links among the same chain they can produce a reverberant activation of the stereotypic sequence. Different stimulus and spontaneous activities produce similar patterns of expression at the population level. In fact, variations in the spiking timing of individual neurons do not significantly affect final output. This means that the order of firing of the group of neurons is highly stereotyped even considering some variations in the sequence(42, 44). This might seem to be redundant but it might in fact constitute an error-proof mechanism to avoid pattern errors and allow an accurate information output. Once produced, these stimulus have the ability to propagate through the layers of pyramidal cells(47).

The summated activity of neurons at either intracranial or scalp levels mainly adopts a sinusoidal morphology. These regular oscillations have classically been classified into frequency bands: delta (1–4 Hz), theta (4–8 Hz), alpha (8– 12 Hz), beta (15–30 Hz), gamma (30–90 Hz), and high gamma (>50 Hz)(24). It has been proposed that oscillations play an active role in neural communication and different frequencies interact with one another in phase and amplitude to code information in what has been called cross-frequency coupling(48). For instance, it has been proposed that the phase of slower frequencies modulates the power of faster frequencies in a process known as phase–amplitude coupling(49). These activities can easily be analysed employing a crucial method in signal analysis, the Fourier transform (24), which basically decomposes the EEG signal into the sine

waves that form it. Then, a representation of the relative dominance of the frequencies can be constructed: the power spectrum, where the power of a signal is the square of the Fourier amplitude. The Fourier method therefore transforms a signal defined in the time domain, into another defined in the frequency domain. This serves to quantify the distribution of power across frequencies.

- ***Finding the source: the inverse problem***

With today's processing power acquisition systems, we are able to achieve high sampling frequencies providing excellent temporal resolution with EEG, ECoG or LFP recordings. However, spatial resolution is still the main problem of such techniques(24).

"The inverse problem" consists in calculating the neural field generator's position and features based on the activity detected by the recording electrodes(24). The root of the problem relays on revealing the relation between the activity generated at the neuronal networks and the electrical signals detected at the recording electrodes. Brain activity is considered to be a consequence of various coupled non-linear mechanisms originated at cellular and network levels(50) but also influenced by other linear interferences such as volume conduction(51).

The problem is even more complicated when considering that the electrical detected at the scalp level are also determined by the electrical properties of the head. To understand the impact of these "inert" structures, simplistic models describe the head as a three or four spherical compartment volume: scalp, skull, cerebrospinal fluid and brain. Inside each compartment, electrical conductivity is in general assumed to be linear, isotropic and

homogeneous(52). However, it is not that simple to locate sources of activity as the head is not spherical, the skull is pierced by several holes and its tissues are far from being homogeneous or isotropic. Assuming a spherical shape and ignoring the presence of holes can led to errors of location up to 30 mm(53, 54). While the effect of volumes filled with cerebrospinal fluid can be ignored for small fissures, it can lead to localisation errors up to 7.5 mm in large fissures(55). Also, conductivities in white matter are anisotropic. There is 10 times lower conductivity in directions perpendicular to the cell membranes and myelin layers compared with conductivity parallel to the fibres(56). The skull is likewise an anisotropic media where the outer layers are solid bone and the middle layer consists on spongy bone filled with blood with ten times higher conductivity in a tangential direction(52). If this was already complicated, often epileptic patients have intracranial lesions of different densities and electrical properties. Depending on their nature, these lesions can have higher conductivity, like in cerebrospinal fluid cysts or haemorrhages with up to five times the brain conductivity(57); or lower, like in calcified lesions showing a "bone-like" conductivity 1/80 of that of the brain(58). Potentials generated nearby high conductivity lesions increased when oriented radial to the lesion while an opposite effect is observed when dipoles are oriented tangentially(52). Similarly, the ventricles (containing highly conductive CSF) can increase the potential when sources are located within a few centimetres with a larger effect observed when the ventricle is located between the source and the surface(52). More complex is the influence of holes in the skull as also depends on dipole orientation and location. Radially oriented dipoles are better detected from the outside, particularly if located in the proximity of the hole. Although the effect is noticeable over a large area of the scalp, the measured potential is stronger in the vicinity of the hole

but attenuates rapidly with the distance (52, 59, 60). Altogether, these factors can lead to localisation errors of several centimetres, particularly when sources are more deeply located.

As we have seen, when looking at the raw EEG signal, we need to consider that signals obtained from each pair of recording electrodes are not merely the brain activity recorded from neighbouring sources, but a superposition of multiple brain sources, filtered by different layers and influenced by volume conduction effects from several sources (51). The later may lead to spurious detection of functional/effective couplings not caused by brain interactions but from volume conduction artefacts. Some techniques have been developed in order to get rid of the undesirable influence of linear volume conduction artefacts at the same time. Among others the imaginary part of coherency(61), the phase lag index(62), weighted phase lag index(63) and sensitivity index(51) produce a good estimate of functional connectivity minimising volume conduction effects.

When considering the distribution of dipoles inside the brain, classical mathematical models have contemplated two different approaches depending on the scale. Distributed models consider the overall behaviour of uniformly distributed dipoles. These methods provide a general estimation of widely distributed cortical sources and are therefore capable of modelling the behaviour of relatively wide areas of the cortex(64-68). Point dipole models just consider one or few dipoles are more practical to understand how focal epileptiform activities are generated in a smaller scale (50). Some more physiological models intend to mimic the cellular or network structure of the brain by modelling small individual elements and then interconnect a great amount of them(69, 70) to describe the overall behaviour, while others model the overall properties of large populations as a group(71-74).

- ***Effective connectivity***

Most studies related to the dynamics of EEG activity and connectivity concentrate on the analysis of phase and amplitude measures of spontaneous EEG activity. Latency analysis has been employed to describe conduction times and connectivity to study patterns of propagation (40, 75, 76). The phase spectrum of Fourier analysis has also been used to identify leading regions and propagation patterns. However, Fourier analysis suffers from relatively poor time resolution. Moreover, since Fourier analysis can only be defined for oscillatory (periodic) activity, when phase differences are recorded between two sites, it may be difficult or arbitrary to define the leading site.

As cerebral regions are profusely interconnected in a reciprocal way (77), it is difficult to find out the influence of a particular cortical region over other and how this external input affects the spectrum of the activity recorded at the contacted area. Each region responds, modifies and feeds back activity from other connected regions. Functionally, connected regions can better be viewed as coupled, i.e. each region engaging in receiving and feeding back activity from other regions, a process modulated by on-going processed in many other regions. In this process of mutual and multiple modulation of oscillatory activity by many regions, it is difficult to isolate the amount of coupling between any two.

- ***Scratching the surface***

In clinical settings, EEGs are routinely interpreted by visual analysis and the electroencephalographic elements “translated” into clinically relevant information such as

seizure onset, spreading, duration and morphological features of the abnormalities usually linked to particular manifestations or syndromes.

But surface abnormalities can be misleading due to volume or distance from the scalp recording electrode(78, 79). What we see at the surface is most of the times just the tip of the iceberg. Early studies already suggested that cortical activities need to have certain temporo-spatial characteristics to produce an EEG element able to be detected at a scalp level due to its amplitude against the background voltage(80). A famous in vitro study(81) performed employing a piece of skull and an artificial dura determined that a source of at least 6cm$^2$ was required for being able to detect the electrical signals from outside the scalp. The experiment had its limitations as no background activities were considered and the cortex is not a perfectly flat lamina as the one modelled, but a complexly folded structure. A recent model taking in account the convoluted anatomy of the cortex, the anatomical location of neuronal sources and their coupled behaviour estimated a minimum cortical surface of 3 cm$^2$ to produce a spike with 1.5 higher amplitude than the background activity but a cortical source of 24 cm$^2$ to obtain a clearly distinguishable spike (2.8 times the background amplitude)(50). In vivo simultaneous scalp and intracranial recordings have indeed suggested that synchronous cortical activation of at least 10cm$^2$ are needed for scalp recordable activities and >20cm$^2$ for prominent spikes(82-84). Interestingly it has been observed that a mean cortical surface of 19cm$^2$ is required to produce a rhythmic ictal activity at seizure onset detectable from the scalp (83). There has been observed that the sources required to produce detectable activities in the surface EEG may be different depending on the lobe studied. An area of 6– 24 cm2 is required in the lateral temporal lobe and of 6–30 cm2 in the frontal lobe(85). In contrast, intracranial EEG recordings provide a

higher signal to noise ratio being less susceptible to artefacts and showing high spatial and temporal resolution compared to scalp recordings(86).

Even when clear epileptiform discharges are obtained at the scalp, these are sometimes poorly informative as different sources can produce similar distribution of abnormalities at the surface EEG(83, 87). Simultaneous scalp and intracranial recordings have documented wrong lateralisation of scalp abnormalities in frontal, up to 8.6% of temporal, 28% of occipital and 16% of parietal seizures(88-92). Even in intracranial recordings it is not clear which interictal epileptiform patterns are a reliable biomarker to detect the cortical regions originating seizures. Some studies show that only 54% of the largest interictal epileptiform abnormalities were located at the region of focal seizure onset(40, 93). A potential explanation for the presence of such abnormalities in theoretically "healthy" areas of the cortex assumes that some types of interictal epileptiform discharges could have a protective role and its appearance can reflect high levels of inhibition. This is supported by the finding of long suppression (inhibition) periods on single cell recordings(94) during interictal spikes. If this is correct, seizures would only manifest in those areas where this protection becomes insufficient(93).

- ***Invasive techniques***

The localisation value of the scalp EEG is well recognised but invasive investigations are often required, particularly in MRI negative cases and invasive recordings are the gold standard technique to define the epileptogenic or irritative zones(95), the seizure onset patterns and its spreading.

A recent consensus paper has defined some general indications for invasive electroencephalography(96). One of the major indications is to accurately define the epileptogenic zone when non-invasive EEGs are inconclusive. This reaches its maximal relevance in epilepsy surgery. Epilepsy surgery aims for the removal of certain structures involved in the development of clinical seizures. The epileptic zone is the classical term defined by Bancaud to name the brain regions primarily involved in seizure generation(97, 98). Recent nomenclatures have also defined the seizure onset zone as the area of the cortex from which clinical seizures are generated while considering the epileptogenic zone as a "surgical term" defining it as the area of cortical resection necessary for achieve seizure freedom(95). Interestingly the original concept of epileptic zone coined by Bancaud is more in keeping with the concept of epileptogenic network as it contemplates the possibility of multiple areas interplaying in seizure generation. Another interesting concept is the irritative zone, the area where epileptiform activities (in the form of interictal spikes or high frequency oscillations(99)) are more persistently recorded. Lastly, the area where we can find a structural lesion is named lesional zone(100). Given the complexity of the physiopathology of epilepsy these areas may have variable degrees of overlapping. The main role of the neurophysiological assessment for epilepsy surgery is to discriminate between areas identifying the seizure onset, with the final aim of patient's seizure freedom but also limiting the loss of eloquent functions to the minimum(100). There is also need for invasive assessment when non-invasive data point to two or more regions involved in seizure generation(96).

There are a few types of electrodes available for invasive EEG: Subdural (strips or grids), intracerebral (depth), epidural peg, wick and foramen ovale electrodes(96). Each modality

has its strengths and limitations. Subdural arrays cover extensive surfaces but neglecting deep sources(101) while depth electrodes can provide excellent cover of selected deep structures but their strength is also their weakness, as they spatial sampling is very limited to the selected region(102). Foramen ovale recordings consist in the insertion of an electrode bundle through the foramen ovale(103). These are of particular interest in the assessment of temporal lobe epilepsy. The deepest contacts lie in close proximity to mesial temporal structures. In contrast to more invasive methods requiring removal of skull areas, foramen ovale electrodes are introduced through natural holes, allowing for simultaneous scalp-EEG without distorting the conductive properties of the different head compartments(104, 105).

- ***Depth structures***

One of the main difficulties of EEG is to detect the low contribution of deep sources to the surface-recorded activities due to their anatomical location. It has been repeatedly shown that intracranial recorded activity is often undetectable at the scalp level(40, 84, 104-107). Insular cortex, fronto-parietal opercular cortex, inferomedial temporal lobe, interhemispheric fissure, basal orbitofrontal cortex, hippocampal inferior parietal-occipital cortices and deep sulcal generators are underrepresented in the scalp EEG(40, 108). For some nucleus, this is not only related to distance to the source; tangentially oriented generators in the sulci do not generally contribute significantly to the EEG(11) and other structures, such as the basal ganglia, behave as close field sources due to their cellular

architecture producing a very limited scalp electromagnetic field (such as thalamus and striatum)(27).

Mesial temporal sources are particularly difficult to record at a scalp level due not only to the depth but also due to the infolded morphology of the curved mesial cortex and the obscuring influence of the lateral temporal neocortical activity over the mesial activities (40, 102). Classically two structures have been identified in the source of temporal lobe seizures: Mesial and lateral. Linear regression analysis has identified four epileptogenic networks over the temporal region: Medial, lateral-medial, medial-lateral and lateral(109). In medial and lateral types, the onset is restricted within each given area (either mesial or lateral) with high ictal coherence within it and only late spreading, if any, to the opposite structure (to the lateral if onset was mesial and vice versa). In the medial-lateral and lateral-medial types, the onset starts in medial or lateral regions with a fast-low amplitude discharge that spreads to the neighbouring structure (either lateral or medial) in less than 3 seconds or starts simultaneously in limbic and neocortical structures but one shows a predominant influence over the other in each subtype(110). Purely mesial sources can be weakly detected as a small negativity at the ipsilateral anterior basal temporal electrodes, while combined neocortical temporal or meso-lateral sources can also be detected at fronto-centro-parietal electrodes as a positivity(102). Studies with foramen ovale electrodes revealed that about 70% of the discharges detected in deepest contacts were not detectable at the scalp level(107).

Scalp EEG also has reduced value in frontal lobe epilepsy where 12-37% of patients can manifest without any epileptiform abnormalities at the surface level and poor localisation in the remaining cases (91, 92, 111-113). A number of factors can contribute to this, first the

depth of mesial and orbital sources second to the high degree of intra and interlobar connectivity and the consequent high degree of synchronicity(114) and finally, in the case of ictal abnormalities, to the presence of movement artefacts that typically characterise frontal seizures(115). Focal frontal spikes have been related to dorsolateral cortex but bifrontal spikes can arise from medial and orbitofrontal sources(101) sometimes even showing a false lateralisation(91, 92). For orbitofrontal structures, a variable percent of patients does not show any scalp abnormality. This varies between 12.5 and 88% depending on the series(91, 92, 101, 112, 113). Most patients present with fronto-temporal spikes and the remaining shows either frontal or temporal abnormalities. However, similar to what happens in temporal lobe epilepsy, the averaging of EEG activity triggered by subdural spikes increases the signal-to-noise ratio helping to detect low amplitude spikes. This allows to identify medial, basal and dorsolateral frontal cortical sources(101). In any case, considering the electrical properties of the head, these studies however suffer from some breach effect after craniotomy. This might enhance the amplitude of the epileptiform discharges obtained at the scalp, therefore overestimating the role of EEG in the detection of deep frontal sources.

Among deep structures, the thalamus historically has had a controversial role in the generation of a particular type of seizures: the generalised seizures. These are characterised by epileptiform activity simultaneously involving all the cortex. When considering which structure could cause such a fast and massive simultaneous spreading throughout the entire cortex, subcortical structures close to the midline with the ability to diffusely project to the whole cortex were soon suggested as the main as generators of generalised seizures(116).

Over the last decades four main theories have tried to explain the origin of generalised seizures attributing different roles to cortical and subcortical structures. The "centrencephalic" (80) and "thalamic clock" (117) theories suggest a thalamic origin while the "cortico-reticular" (118) and "cortical focus" (119, 120) models point to the cortex as the initiator. A number of intracranial EEG studies in humans with absence seizures have demonstrated the presence of thalamic rhythmic activities preceding the cortical onset(121-123). However other studies reveal simultaneous or preceding onset of the cortical discharges (124-129) and experimental studies have demonstrated that electrical stimulation of the cortex (130, 131) can induce generalised abnormalities.

Overall, it is not clear which is the exact relation between thalamus and cortex during the onset and development of generalised seizures. In this work we have employed standard visual analysis and the methodology described by Meeren et al(119), to examine simultaneous scalp and thalamic centromedian recordings in patients with generalised seizures in order to find out the relative role of each structure in the origin and maintenance of seizures(132).

- ***Automated spike detection and deep sources***

Advances in signal analysis over the last decades have being followed by development of multiple methods for automatic detection of epileptiform discharges based on methods such as template matching(133, 134), morphology classification(135-137), independent component analysis(138), signal modelling(139) and field of spike detection among others(140, 141). All these methods analyse the EEG signal searching for similarities to a defined epileptiform discharge (either real or modelled) based in some extracted

features(142). The first algorithms developed in the 70's decade employed human expert-selected evaluation criteria and methodology based in parameters such as duration, amplitude, sharpness, risetime, fall-time, after-coming slow waves or background frequency across multiple channels (143-145). These algorithms set up the standard which against future methods would be compared. The main problem of this early methods was the high number of false positives(146). Artificial neural networks were employed towards the end of XXI century training the algorithms on known epileptiform discharges so they can compute the relative weight of different parameters to differentiate events of interest(141, 147). This method has suffered from poor results when applied to a new set of data(146). Wavelet, Fourier, Hilbert or chirplet(148) transform focus in time-frequency representations(149-151) are methods that convert an EEG signal into a 2-dimensional map of time vs frequencies or wavelets (wavelets and chirplets are single waveforms with spike-like morphology that are fitted to the signal). In the last decades most efforts have been focused in parameter and algorithm improvement employing nonlinear features(152), decomposition methods(153, 154) or kernel type methods(155). However nowadays none of these methods have proved reliable enough to be employed in an unsupervised fashion with the rate of false positives remaining the most important handicap for such detection algorithms(146).

As discussed before, many interictal spikes originated from depth structures are often not visible at the scalp EEG. The reality is that their activity still contributes to the scalp potentials but is buried under the on-going background activity due to its low amplitude. These signals are still susceptible of being detected on the scalp by average analysis time locked to the timing of the spikes observed in depth electrodes(102, 107). It is absolutely impossible for the EEG expert to spot such small deflexions among the myriad of

background elements and automatic detection algorithms are usually trained with only scalp visible epileptiform discharges, therefore neglecting deep sources(156).

As one of the objectives of this work(157) we have aimed to develop an algorithm capable of detecting epileptiform discharges hidden to visual analysis of the scalp EEG. Recordings were simultaneously obtained from scalp and foramen ovale electrodes while the averaging trigger (the event used to synchronise the averaging of EEG epochs) was defined only by the intracranial signals. The algorithm employs multichannel pattern classification based in time-frequency, wavelet, chirplet and time domain features.

- ***Single pulse electrical stimulation (SPES)***

An alternative approach to the study of intracranial activities goes beyond the passive observation of physiologically generated activities and jumps to the active stimulation of the brain and the later observation of the evoked response. The first attempts to record electrical responses from the brain surface to electrical stimulation were carried out in 1936 in anesthetised animals(158). Adrian described electrically elicited waveforms recorded both at cortical surface and depth structures showing great waveform variability but constant time relations when propagated to neighbouring cortical areas. Electrical stimulation has been regularly used in humans since the time of Penfield(80), particularly for functional mapping.

SPES(159) is a modification of the technique developed by Adrian and later employed in humans by Purpura(160). The new paradigm defined by our lab consists in the application of a single monophasic bipolar electrical pulse (1-8mA amplitude, 0.3-1ms duration) between

contiguous electrodes and the simultaneous recording of intracranial EEG responses (either from surface or depth electrodes) by the remaining contacts not used for stimulation. After stimulus, cortical responses with varying distribution and latency can be recorded by the recording electrodes. Similar approaches and slight variations of this technique have been employed by other groups (161-170).

Two main types of evoked responses can be induced by SPES: Early and late responses (159, 171). Early responses are deflections immediately following the stimulus artefact and occasionally merging with it. These responses can be recorded in epileptogenic and non-epileptogenic regions and are therefore considered physiological. Early responses amplitudes tend to be higher with increasing stimulation intensities and with the proximity to the stimulus but can also be recorded in distant electrodes. Late responses by contrast are not so ubiquitous and arise after the early response, showing a morphology similar to epileptiform discharges. Their presence at a stimulation point is strongly correlated with the existence of epileptogenic tissue (159, 171-173).

SPES offers an outstanding opportunity to study cortical connectivity and has been increasingly employed in connectivity mapping (77, 161, 162, 164, 166-168, 174-176) and to evaluate cortical excitability and identify potential epileptogenic zones (159, 163, 165, 169, 171, 172, 177, 178).

Our group has already demonstrated that SPES is able to induce responses that resemble epileptiform discharges both with single cell and scalp recordings(93, 94) suggesting that both phenomena can share some similar mechanisms of generation. Stimulation of depth structures by SPES is a tool to map connectivity between depth areas and other cortical regions(176). This is relevant not only in the field of epilepsy for the identification of seizure

onset and propagation, but also to unveil the mechanisms mediating physiological phenomena such as sleep elements. For instance, while the structure generating sleep spindles has being identified (reticular nucleus of the thalamus in sleep spindles for instance)(179), the structures responsible for the generation of K-complexes are still unknown. Several studies have proposed that K-complexes arise from widespread synchronized cortical areas due to hyperpolarising currents in layer III of the cortex that propagate through the cortex(180-184). There must be a particular area that starts the hyperpolarising mechanism leading to the K-complex which remains unknown. Several studies have suggested that this area could be hidden in the depths of the cingulate gyrus(185-189). Following this hypothesis, our group has conducted a comprehensive examination of the intracranial recordings obtained during SPES over deep structures in frontal regions in order to identify points where stimulation elicited the presence of K-complex-like EEG elements(190).

- ***SPES and cortical oscillations***

Despite of the increasing number of publications, there is great void in our understanding of the physiological neural mechanism underlying responses to SPES (164, 166, 174). In addition, there is no explanation for the great variability of the evoked waveforms in terms of polarity, morphology and latency (159, 166) and evoked responses frequently fail to strictly fit into any of the currently proposed descriptions.

We have observed that the morphology of early responses frequently shows several cycles of oscillations, resembling the damped sinusoids that describe the responses of linear

control systems to step inputs(191). We have developed a theory suggesting that single pulse stimuli can be interpreted as a transient function applied to the neuronal network(192). The EEG responses would then reflect the transient steady-state response of the system (the cortex) until return to the baseline state is reached. Our hypothesis assumes a number of postulates: First, that the presence of a cortical response to stimulation indicates the presence of a functional connection between the stimulated area and the area where a response is recorded. Second, that a single electrical pulse applied to the cortex behaves as a transient input function. Third and last, that the EEG response reflects the output of the cortical network activated by the connection between stimulated and recorded areas.

We aim to show that linear control models can be used to describe the morphology of early responses to SPES and that the frequency response of the connections activated by SPES can explain some of the oscillatory behaviour of the spontaneous EEG. If our hypothesis is correct, SPES can be employed to estimate functional coupling between regions and quantify the relative contribution of the connections from the stimulated region to oscillatory mechanisms in the recorded region. Therefore, it can be used to identify cortical connections and to describe their dynamics, being able to predict at which frequency is the system more likely to oscillate. This can have important implications at the time of detecting areas with increased excitability and to detect which is the resonant frequency of the system. In addition, as the technique is performed with intracranial recordings, we could obtain valuable information about the intrinsic connectivity and cortical dynamics of deep cortical regions.

In summary the overall aim of this thesis is to tease out the contributions of deep and superficial structures to the EEG.

# 2. HYPOTHESIS AND OBJECTIVES

Our broad hypothesis is that deep structures significantly contribute to the surface EEG either directly by the generation of identifiable electrical fields or indirectly by the modulation of populations of cortical neurons. The specific hypotheses are:

1) Electrical fields from focal hippocampal epileptiform discharges are not identifiable on the scalp EEG on visual inspection but may be detectable by modern analytical tools.
2) Electrical stimulation of deep cortical structures can trigger K-complex-like responses.
3) The thalamus is involved in generalised as well as focal seizures in humans.
4) Electrical responses to single pulse electrical stimulation can be described in terms of control systems with specific frequency contents which can predict the behaviour of spontaneous EEG.

Our specific objectives are:

- To determine whether by considering the timing information of the interictal epileptiform discharges from intracranial EEG electrodes at the temporal lobe, the resulting concurrent surface EEG contains enough information for the interictal discharges to reliably distinguish activity generated at deep sources.
- To determine if electrical stimulation of the cingulum can induce physiological responses similar to the patient's K-complexes.

- To study simultaneous scalp and thalamic human EEG recordings during epileptic seizures to estimate the role of centromedian thalamic nucleus in the initiation and maintenance of seizures in humans.
- To develop a model that explains the morphology of responses to single pulse electrical stimulation that would explain the oscillatory behaviour of the spontaneous EEG.

# 3. MATERIAL, METHODS AND RESULTS

Detection of Intracranial Signatures of Interictal Epileptiform Discharges from Concurrent Scalp EEG. Spyrou L, Martin-Lopez D, Valentin A, Alarcon G, Sanei S. International journal of neural systems. 26(4):1650016. Copyright@2016 World Scientific. DOI: 10.1142/S0129065716500167

Electrical Stimulation of the Anterior Cingulate Gyrus Induces Responses Similar to K-complexes in Awake Humans. Voysey Z, Martin-Lopez D, Jimenez-Jimenez D, Selway RP, Alarcon G, Valentin A. Brain Stimul. ;8(5):881-90. Copyright@2015 Elsevier. DOI: 10.1016/j.brs.2015.05.006

The Role of Thalamus Versus Cortex in Epilepsy: Evidence from Human Ictal Centromedian Recordings in Patients Assessed for Deep Brain Stimulation. Martin-Lopez D, Jimenez-Jimenez D, Cabanes-Martinez L, Selway RP, Valentin A, Alarcon G. International journal of neural systems. 27(7):1750010. Copyright@2017 World Scientific. DOI: 10.1142/S0129065717500101

Characterizing EEG Cortical Dynamics and Connectivity with Responses to Single Pulse Electrical Stimulation (SPES). Alarcon G, Jimenez-Jimenez D, Valentin A, Martin-Lopez D. International journal of neural systems. 28(6):1750057. Copyright@2018 World Scientific. DOI: 10.1142/S0129065717500575

# Detection of Intracranial Signatures of Interictal Epileptiform Discharges from Concurrent Scalp EEG

Loukianos Spyrou
Department of Computer Science, University of Surrey, UK

David Martín-Lopez
Department of Clinical Neuroscience, King's College London, Institute of Psychiatry, Psychology and Neuroscience, UK.
Department of Clinical Neurophysiology, King's College Hospital NHS FT, London, UK.
Department of Clinical Neurophysiology, Ashford and St Peter's Hospital NHS FT, Chertsey, UK.
Departamento de Fisiología, Facultad de Medicina, Universidad Complutense, Madrid, Spain.

Antonio Valentín
Department of Clinical Neuroscience, King's College London, Institute of Psychiatry, Psychology and Neuroscience, UK.
Department of Clinical Neurophysiology, King's College Hospital NHS FT, London, UK.
Departamento de Fisiología, Facultad de Medicina, Universidad Complutense, Madrid, Spain.

Gonzalo Alarcón
Department of Clinical Neuroscience, King's College London, Institute of Psychiatry, Psychology and Neuroscience, UK.
Department of Clinical Neurophysiology, King's College Hospital NHS FT, London, UK.
Comprehensive Epilepsy Center Neuroscience Institute, Academic Health Systems, Hamad Medical Corporation, Doha, Qatar.

Saeid Sanei
Department of Computer Science, University of Surrey, UK
E-mail: s.sanei@surrey.ac.uk

Interictal epileptiform discharges (IEDs) are transient neural electrical activities that occur in the brain of patients with epilepsy. A problem with the inspection of IEDs from the scalp electroencephalogram (sEEG) is that for a subset of epileptic patients, there are no visually discernible IEDs on the scalp, rendering the above procedures ineffective, both for detection purposes and algorithm evaluation. On the other hand, intracranially placed electrodes yield a much higher incidence of visible IEDs as compared to concurrent scalp electrodes. In this work, we utilize concurrent scalp and intracranial EEG (iEEG) from a group of temporal lobe epilepsy (TLE) patients with low number of scalp-visible IEDs. The aim is to determine whether by considering the timing information of the IEDs from iEEG, the resulting concurrent sEEG contains enough information for the IEDs to be reliably distinguished from non-IED segments. We develop an automatic detection algorithm which is tested in a leave-subject-out fashion, where each test subject's detection algorithm is based on the other patients' data. The algorithm obtained a 65% accuracy in recognizing scalp IED from non-IED segments with 68% accuracy when trained and tested on the same subject. Also, it was able to identify nonscalp-visible IED events for most patients with a low number of false positive detections. Our results represent a proof of concept that IED information for TLE patients is contained in scalp EEG even if they are not visually identifiable and also that between subject differences in the IED topology and shape are small enough such that a generic algorithm can be used.
*Keywords*: Epileptic discharge detection; IED; intracranial and scalp EEG; clinical diagnosis.

## 1. Introduction

Epilepsy is characterized by a chronic tendency to suffer epileptic seizures. It is associated with abnormal cortical activation patterns that can be recorded by the electroencephalogram (EEG) during seizures (ictal) and in the periods between seizures (interictal). Since seizures are relatively infrequent and brief events, it is unlikely to record seizures in a standard EEG[1] and, consequently, finding interictal abnormalities on the scalp EEG has become the most widely used test for the diagnosis of epilepsy. The presence of epileptiform

discharges is the most reliable interictal biomarker for epilepsy. However, the EEG has a relatively high rate of false negatives. In patients known to have epilepsy, only about 55% of awake EEGs and 80% of sleep EEGs show epileptiform discharges.[2,3] This leaves a significant proportion of patients with an uncertain diagnosis and delayed treatment. A method to increase the sensitivity of the EEG for the diagnosis and classification of epilepsy would lead to earlier treatment, improving the patient's quality of life and reducing the risk of sudden unexpected death in epilepsy.

The reasons for the low sensitivity of the scalp EEG to record epileptiform discharges are unclear. Around 37% of patients assessed for surgery for the treatment of their epilepsy require recording of the EEG with intracranial electrodes.[4] Such intracranial recordings have demonstrated that only a minority of epileptiform discharges recorded by intracranial electrodes are detectable by visual inspection of the scalp EEG.[5–10] Several authors[5–8,11–16] have suggested that the epileptiform discharges generated by deep structures may not be seen on the scalp because of the relatively high attenuation of electrical fields with distance from the source.

The chronic implantation of multi-contact foramen ovale (FO) electrode bundles with the purpose of recording from mesial temporal structures[17] provide a unique opportunity to investigate the scalp fields associated with mesial temporal spikes, typical of temporal lobe epilepsy (TLE), the most common type of focal epilepsy. During this procedure, electrode bundles are introduced bilaterally through the FO under fluoroscopic guidance. The deepest electrodes within each bundle lie next to mesial temporal structures, whereas the most superficial electrodes lie at or just below the FO.[18] Since the FO electrodes are introduced via anatomical holes, they provide a unique opportunity to record simultaneously from scalp and mesial temporal structures without disrupting the conducting properties of the brain coverings by burr holes and wounds, which can otherwise make simultaneous scalp and intracranial recordings unrepresentative of the habitual EEG.[6,8,16,18–20] We have previously reported that about 70% of epileptiform discharges recorded by FO electrodes involve only the deep FO contacts and are not identifiable in the scalp EEG.[9] It would be very useful in clinical practice if evidence of interictal epileptiform discharges (IED) activity can be detected from the scalp EEG (sEEG) in the cases of little or no visible IEDs. sEEG IED events may not exhibit a visible spike-like structure but can contain evidence of IED activity only visible after averaging a number of those events or by retrospectively reviewing the resulting sEEG potentials originating from known intracranial EEG (iEEG) spikes. This can be explained by realizing that although the background EEG may temporally overlap with some parts of the transient activity, hence rendering it not scalp-visible on the single-trial level, IED signatures may still be contained in sEEG. Such signatures can be partial spikes, within-electrode temporal correlation, between-electrode spatial correlations, and more generally the likelihood of scalp IEDs. Similar conclusions were also attained in Ref. 21 where the spikes from deep sources contributed to the scalp EEG signal although no detection algorithm was developed.

Current IED detection techniques are for either scalp or intracranial data separately. An iEEG[22–24] or sEEG[25–28] recording is visually inspected and time segments containing spikes are identified and further used to estimate the performance of or design a detection algorithm on either the same or different subjects. Developing algorithms that detect IEDs from sEEG scored data are not sufficient since they are tuned to detect only the visible spikes that are used as examples in the algorithm design. Such an algorithm is biased to prefer such spikes.[22] In this work, we employ concurrent iEEG and sEEG recordings in order to develop an algorithm that primarily aims to detect nonscalp-visible sEEG IED events. The algorithm is based, trained, and tested, solely on sEEG discharges where the timing information of such discharges is obtained from the concurrent iEEG. This way provides the advantage that low-amplitude scalp events are utilized in the algorithm development, a feature which is not available for traditional algorithms that are trained on scalp-visible IEDs. The presence of deep spikes from their associated low amplitude scalp fields can then be detected and evaluated against the gold standard of deep FO recordings. Our algorithm employs multichannel pattern classification in order to develop

a classifier that distinguishes IED from non-IED events in a subject-independent fashion. In order to ensure maximal performance, we focus on minimizing the between subject differences that can decrease the performance of subject-independent algorithms in the EEG field (Sec. 2.2). For each patient we detect all IED activations based on the signatures of the other patients in a leave-subject out fashion (Secs. 2.3 and 2.4). In Sec. 2.4, we also explain the performance measures we use to estimate the algorithm's capabilities. Section 3 describes the results and in Sec. 4, we discuss the algorithm's performance and usefulness. Section 5 concludes the paper.

## 2. Materials and Methods

### 2.1. Dataset

### 2.1.1. Patients

The study included 20min recordings from 18 TLE patients (11 males, seven females, mean age 25.2 years, range 13–37) studied with scalp EEG recordings and simultaneous intracranial multicontact FO electrode bundles in the Department of Clinical Neurophysiology at the Maudsley and Kings College Hospitals. Patients suffering from seizures arising from mesial temporal structures were submitted for telemetry recording with FO when history, interictal scalp EEG, neuroimaging and neuropsychological studies were not able to confidently determine the side of seizure onset, or there were doubts about a lateral temporal or extra-temporal seizure onset. In 10 patients the seizure onset was identified within mesial temporal structures preceding in at least 2 ms the scalp changes while in eight patients it was located outside the mesial temporal region (lateral temporal). Most EEG recordings only contained wakefulness (13 patients) but some (five patients) also included slow wave sleep (stages I-II) (patients S2, S9, S10, S13, S15).

### 2.1.2. Electrode placement

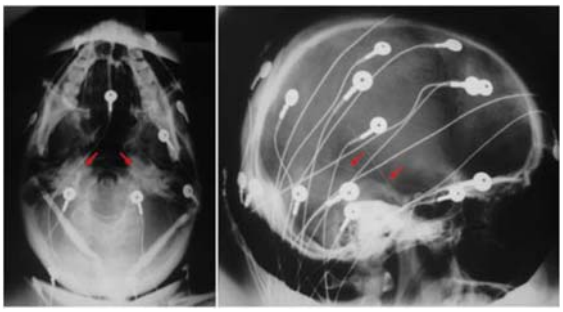

Figure 1. Basal and lateral X-rays showing scalp and intracranial FO electrodes (pointed to by red arrows)9.

For scalp EEG, 20 standard chlorided silver cup electrodes were applied according to the 'Maudsley' electrode placement system.9,16,18,29 The advantage of the Maudsley system compared to the standard 10–20 system is that it provides more extensive coverage of the lower part of the cerebral convexity and adapts itself to cranial asymmetries,30 increasing the sensitivity for recording from basal sub-temporal structures. This system is essentially similar to 10–20 system, naming of electrodes is identical, but mid-temporal, posterior-temporal and occipital electrodes in the Maudsley system are approximately 20 mm lower than in the 10–20 system.

In addition, 12 intracranial electrodes from two flexible bundles of six electrodes each, were inserted through the patients' FOs under general anaesthesia and fluoroscopic control, following the technique recommended by Ref. 17. This method has been extensively employed in several centers all around the world as a gold standard technique for the assessment of mesial TLE.5,9,16,18,30–32 Each individual electrode consisted of a 0.1 mm fully insulated stainless steel wire. The recording contacts for the three deepest electrodes were 3 mm long and those of the most superficial electrodes were 5 mm long. The distance between contiguous electrodes was 10 mm except for the two most superficial electrodes whose interelectrode distance was 15 mm. For each electrode bundle, the two deepest electrodes lay next to mesial temporal structures. The position of the FO bundles was confirmed with post-insertion radiography (Fig. 1). The labeling of the electrodes is indicated as R1 to R6 and L1 to L6 fromthe deepest to the most superficial right and left side FO,

Table 1. List of preprocessing and feature selection methods used in the algorithm.

| Preprocessing method | Parameters | Effect |
|---|---|---|
| Spectral filter | [1 70]Hz | Captures the IED frequency range |
| Detrend | Linear trend removal (per segment) | Reduces baseline drifts |
| Baseline | 162.5ms pre segment mean removal | Alleviates undesired amplitude bias |
| Channel normalization | Unit norm (per channel) | Reduces between subject temporal variability |
| Channel referencing | Common-average-reference | Reduces spatial differences between subjects |
| **Feature selection method** | **Parameters** | **Motivation** |
| Temporal ($T_m$) | Preprocessed only | — |
| Wavelet ($W_5$) | Five level coefficients | Denoises EEG data |
| Wavelet ($W_s$) | Max, min, mean, std of coefficients | Extracts primary statistical features |
| Chirplet (CL) | 3 chirplet fit | Fits more complicated waveforms |
| TF | Spectrogram (width = 40ms, overlap= 50%) | State-of-the-art in EEG classification |

respectively.

### 2.1.3. Recording system and EEG data acquisition

Cable telemetry of 32 channels (20 scalp and 12 FO) was used for data acquisition (Telefactor Beekeeper system). Data were digitized at 200 Hz and bandpass filtered (highpass cutoff frequency at 0.3 Hz and lowpass cutoff frequency at 70 Hz). The system input range was 2 mV and data were digitized using a 12 bit analog-to-digital converter (an amplitude resolution of 0.488 $\mu$V). Both scalp and FO data were recorded with respect to Pz as common reference. From each patient, a period of 20 min of simultaneous scalp and FO interictal recordings were transcribed into a digital file.

### 2.1.4. IED scoring

Scoring of the IED was performed by an expert epileptologist (DML) based on the morphology and spatial distribution of the observed waveforms. Interictal events location and morphology were evaluated in the background context. IED were evaluated in terms of morphology and distribution, following the standard definitions for epileptiform pattern, spike and sharp wave of the International Federation of Clinical Neurophysiology[33] (A glossary of terms most commonly used by clinical electroencephalographers and proposal for the report form for the EEG findings) and currently accepted EEG descriptions. Each IED was given a certainty score (1–10) and categorized to one of the following: (a) scalp-visible without considering the concurrent iEEG, (b) scalpvisible by considering the concurrent iEEG and (c) nonscalp-visible. In essence, the IEDs were scored by considering:

(1) Nonphysiological artifact: instrumental, electrode, environmental, and quantization artifacts.
(2) Physiological artifact: eye movement, electrocardiogram, muscle (lateral rectus, frontalis, temporalis, occipital), and blink artifacts.
(3) Low amplitude irregularity/physiologic “sharpened/ spiky” activities (vertex waves, K-complexes).
(4) Irregularity: IEDs barely distinguishable from the background activity and restricted to 1–2 channels.
(5) Sharp wave (restricted to at least three channels).
(6) Broad distribution sharp wave (> three channels).
(7) Spike (restricted to at least three channels).
(8) Broad distribution spike (> three channels).
(9) Spike/sharp and wave/burst.

### 2.2. Feature extraction and data slicing

Many detection algorithms for epileptic transient activity have long been proposed and applied into clinical practice, albeit with variable and dubious success. They are typically based on methods such as template matching,[25,28,34,35] classification,[36–38] through independent component analysis (ICA),[39] signal modeling[23] and many other methods[40] in common with the well-established field of spike detection. [41,42] The common characteristic of all these methods is that a description of an IED/spike signal is obtained either through modelling or through the use of real data and some similarity-based algorithm developed in order to detect those signals. This is often facilitated by obtaining useful representations of the signal that can better exploit its structure. The feature representations that are useful for IED detection has been a rather unresolved issue.[40] They can be grouped into the following categories: (a) Mimetic, where the extracted features are designed to mimic human evaluation and methodology for the presence of a spike,[43,44] (b) time-frequency (TF) representations such as Wavelet, Fourier, or Hilbert transform have been used in IED detection and with much success in EEG signal processing in general,[27,45–49] (c) nonlinear features such as Hjorth parameters, fractal dimension, mean energy[50] and through (d) decomposition methods such as ICA[51,52] and kernel type methods.[53] Apart from various feature representations, many signal conditioning and preprocessing techniques have been utilized including spectral filtering and smoothing. [54,55] The relation between the amplitude, location and propagation characteristics have been analysed extensively.[8,15,56–58] A major factor for the reduced visibility of sEEG as compared to iEEG is the reduced signal-to-noise ratio (SNR) that deteriorates the signal quality at the scalp electrodes.
In order to enable classifier training (c.f. 2.3), the raw EEG data were sliced in a $\pm$162.5ms ($\pm$32 samples) window centered at the points scored as spike from intracranial data and baselined on the preceding 162.5ms

with the resulting signal finally being linearly detrended to remove undesired drifts. Non- IED segments were also obtained from time segments where there are no scored IEDs. For each subject, the number of sliced IED and non-IED segments was chosen to be the same. The number of segments for each patient can be seen from Table 3 (column #IED: numbers in brackets). In this work, we used TF features for the detection of IEDs on scalp EEG. We also compared wavelet, chirplet, and time domain features but the highest classification performance was obtained by exploiting the TF features. Mimetic analysis methods and nonlinear operators were deemed unnecessary since iEEG timed single trial scalp IEDs do not usually contain clear spike like structures used by these methods. A fundamental assumption is that although a spike shape may not be visible or clear on the single-trial sEEG, IED information is indeed present in those cases since averaging iEEG timed sEEG IEDs provides visible spike structures.

Wavelet features were obtained by performing a discrete wavelet decomposition using the "db4" mother wavelet since it provides the highest correlation with epileptic spikes.[26,59] Similar to Ref. 26 we considered a five-level wavelet decomposition with features chosen as (a) the maximum, (b) the minimum, (c) the mean, and (d) the standard deviation of the wavelet coefficients in each of the five sub bands. Also, we considered as features the transformation to the time domain of the wavelet coefficients for the five sub-bands. For both cases, the wavelet transform was performed for each channel separately. Each IED segment consists of 20 scalp channels × $N_w$ the number of wavelet features. For the first case $N_w$ = 20 while for the second case $N_w$ = 65 which is the number of time domain samples for each segment.

Chirplet features were obtained using the matching-pursuit method with a variable number of chirplets.[60] Chirplets can accomodate signals with variable frequency over time. A chirplet is defined as:

$$ch(t) = g_{s,a}(t-u)e^{jvt} \quad (1)$$

with

$$g_{s,a}(t) = \frac{1}{\pi^{1/4}\sqrt{\sigma(s,a)}} \times \exp\left(-\left(\frac{1}{\sigma^2(s,a)} - jl(s,a)\right)\frac{t^2}{2}\right). \quad (2)$$

Each chirplet consists of four parameters controlling the scaling ($s$), chirp rate ($a$), through the functions $\sigma()$ and $l()$, the time shift ($u$) and frequency shift ($v$).[60] We fit up to 3 chirplets to the data of each channel separately obtaining four features for each case ($s, a, u, v$). Each IED segment consists of 20 scalp channels × 4 chirplet parameters ×$N$ number of chirplets.

The TF features were obtained by the spectrogram method of the preprocessed sliced data with a window length of 40ms and an overlap of 50% between the windows. The window is chosen in a way that captures the nature of IED spikes whose sub-components have a duration of less than 40ms. Each segment then consists of 1260 (20 scalp channels × 7 temporal × 9 frequency) features. The time frequency features are obtained for each IED and non-IED segment. Since the useful IED signal lies within the [1 70]Hz range,[61] the SNR was increased by bandpass filtering the raw EEG data to [1 70]Hz. A 50 Hz notch filter was also applied to eliminate the power line interference.

In order to decrease the between subject differences two extra steps were applied. Firstly, the sEEG of each subject was common-average referenced in order to reduce the spatial IED location differences between subjects, resulting in a more homogenous group. Furthermore, the scalp and intracranial segments were normalized to have unit norm per electrode channel, a step which again reduces the spike amplitude differences and has been long used in groupwise EEG signal processing.[62] These steps, reduce the individual differences between subjects enhancing the performance of the classifier since there is less between-subject variance. The shape of the responses and the correlations between and within channels is the driving factor for detecting an

IED waveform rather than its amplitude. The outliers are rejected by removing the IED and non-IED segments that are above two times the standard deviation from their respective means.

### 2.3. Classification of IED and non-IED data segments

The next step after feature extraction is to develop a method that can determine whether a specific sEEG data segment contains an IED. We include both scalp-visible and nonscalp-visible IEDs in the classifier training and when analyzing the performance of the algorithm. We employ regularized linear logistic regression[63] in order to train classifiers that can distinguish between IED and non-IED events. Logistic regression has been widely

used in EEG data obtaining state-of-the-art performance.[64] Linear classifiers work by estimating a weight vector **w** and a threshold (or bias) *b* that operate on the data **x** in the following way:

$$f(\mathrm{x}) = \sum_{j=1}^{L} \mathrm{w}(j)\mathrm{x}(j) + b,$$

(3)

where *L* is the number of features and *j* the feature index. Note that using space-TF features implies that an optimal weighting of those factors is learned from the data. For a two-class classification problem, here the two classes are the IED and non-IED segments, the sign of $f(\mathbf{x})$ denotes the prediction of class membership of data **x**. One benefit of logistic regression is that it provides a natural way to express the class membership probability from the observed data. The magnitude of $f(\mathbf{x})$ corresponds to class-membership probability ($P(\text{IED}/\,\mathbf{x})$ denoting
the probability that a segment of data **x** contains an IED) as expressed by the logistic function: $P(\text{IED}/\,\mathbf{x}) = 1/1+\exp(-f(\mathbf{x}))$, where the uncertainty of class membership is shown when $f(\mathbf{x}) = 0$, which corresponds to $P(\text{IED}/\,\mathbf{x}) = 0.5$. Also note that, $P(\text{IED}/\,\mathbf{x}) = 1 - P(\text{non-IED}/\,\mathbf{x})$.
The estimation of the weight vector **w** is performed by minimizing a quadratically regularized logistic

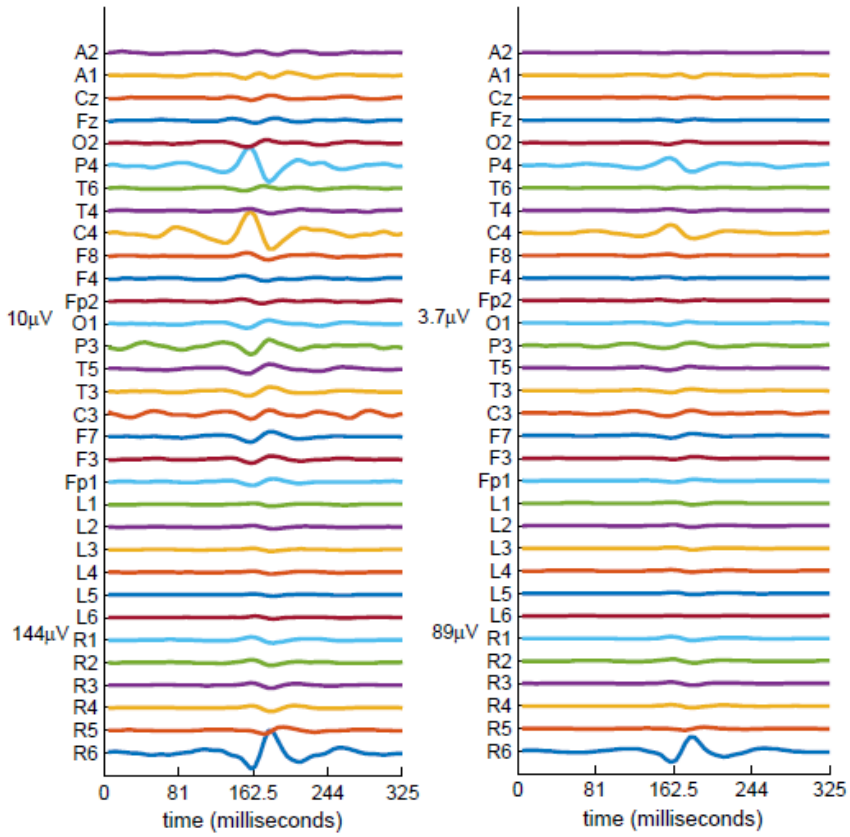


Figure 2. Average over all scalp-visible (left) and non scalp-visible (right) IEDs for Subject 1. These IEDs are obtained from the iEEG informed slicing procedure. The centre of the IED is at 162.5ms.

[a] Note that we differentiate between detection and classification performance. Detection involves identifying the time points out of a whole recording where an IED event occurs whereas the classification considers an equal number of IED and non-IED events.

regression loss function where there is a trade-off between classification accuracy and over fitting and generalization performance. The regularization parameter, which controls the trade-off, is estimated by cross-validation.[65] Cross-validation is a method for model selection that works by partitioning the training data in a number of complementary subsets (folds). In a *k*-fold cross-validation the data are split into *k* subsets. Each subset is used once to validate the model, while the rest $k - 1$ subsets are used to train the classifier. For each fold we test the following regularization parameters [125, 25, 5, 1, 0.2, 0.04, 0.008] scaled by 10% of the variance of the data and select the one that achieves the highest performance.

For IED detection we train a classifier for each subject separately. The leave-subject-out detection algorithm discards a subject's data (test subject) and combines the rest of the subjects' classifiers in a linear voting scheme where the individual classifiers are assigned equal weights. Such a weighting procedure corresponds to a naive Bayes combination of the individual classifiers.[66] The accuracy of the classifier resulting from the linear voting scheme is obtained for the sliced IED and non-IED data segments of the test subject. Individual classifiers whose

within subject or between subject classification performance was less than 55% were excluded from the ensemble. The performance of each subject's classifier is estimated through the accuracy of the best regularization parameter. Significance testing was performed through the binomial proportion confidence interval.[67]

### 2.4. IED detection

Detection[a] of IEDs is performed by sweeping through the data and applying the classifier to a $\pm$162.5ms signal window at each of the *T* samples of the scalp EEG. The scalp EEG is preprocessed the same way as in Sec. 2.2. This process generates a series of detection values $\mathbf{f}_t$ corresponding to $P(\text{IED}/\ \mathbf{x}_t)$ with $t \in \{1, \ldots, T\}$.

By choosing a target probability $p_{tgt}$ the sensitivity and specificity of the detection can be calibrated to various values and the performance of the algorithm can be evaluated for each. Sensitivity is defined as the ratio of the number of obtained IED predictions within a $\pm$40ms window of an IED as scored by the epileptology expert (true positives: TP) to the total number of true IEDs (positives: P). Specificity is calculated as the number of IED predictions that where not within the same $\pm$40ms window of a scored IED (true negatives: TN) to the total number of windows that do not contain an IED (negatives: N). A common way to depict the relation between the false and true positives is by using the receiver operating characteristics (ROC) curve.[63]

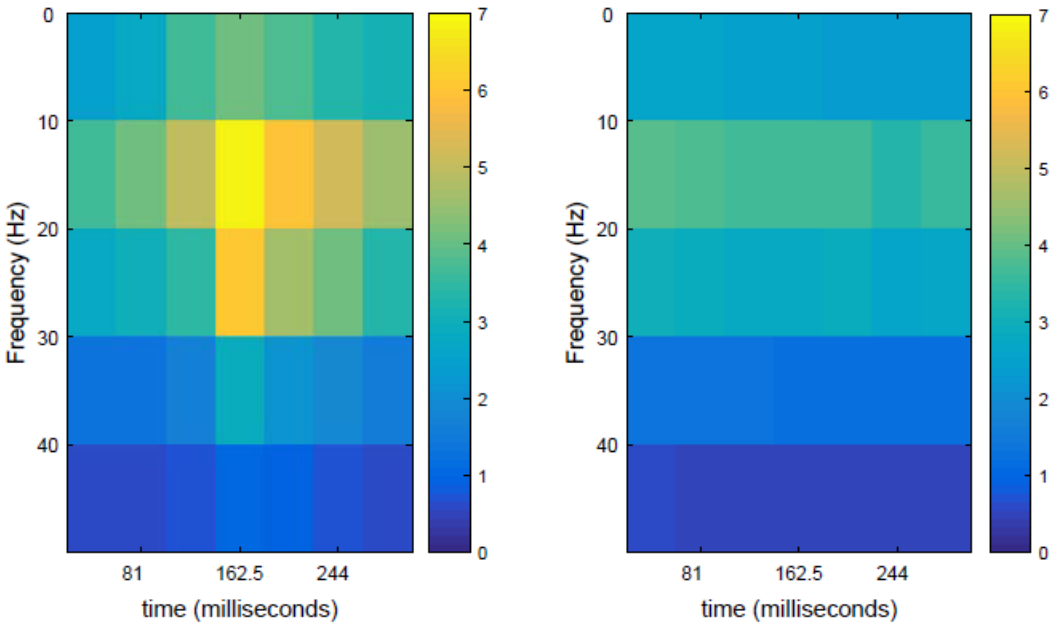


Figure 3. Example of time-frequency features used for classification. Here we show the average power spectral density for IED and non-IED segments for Subject 1 and electrode C4.

Sweeping through the data in a sample by sample basis results in consecutive data windows which are highly correlated. Hence, consecutive detections of the same event have similar probability values. *C* consecutive detections that exceed the specified threshold (i.e. $P(\text{IED}/\ \mathbf{x}_C) > p_{tgt}$ with *C* a set of consecutive predictions) are grouped into a single prediction by choosing the one with the largest probability $\max_C P(\text{IED}/\ \mathbf{x}_C)$. This results in a set of predicted IEDs that is smaller than the set of those that exceed $p_{tgt}$. This step was performed to avoid the occurence of duplicate IED detections. Then, we can calculate the false positives per minute: FP/min which is a convenient way to measure the (nonduplicate) false alarms in some specified time frame. The FP/min measure provides an estimate of the time burden of having to review false detections.
In order to estimate the statistical performance of the detection methodology we performed a classifier randomization test. 100 different random instances of the ensemble classifier were used for each subject according to a Gaussian distribution of the weights.

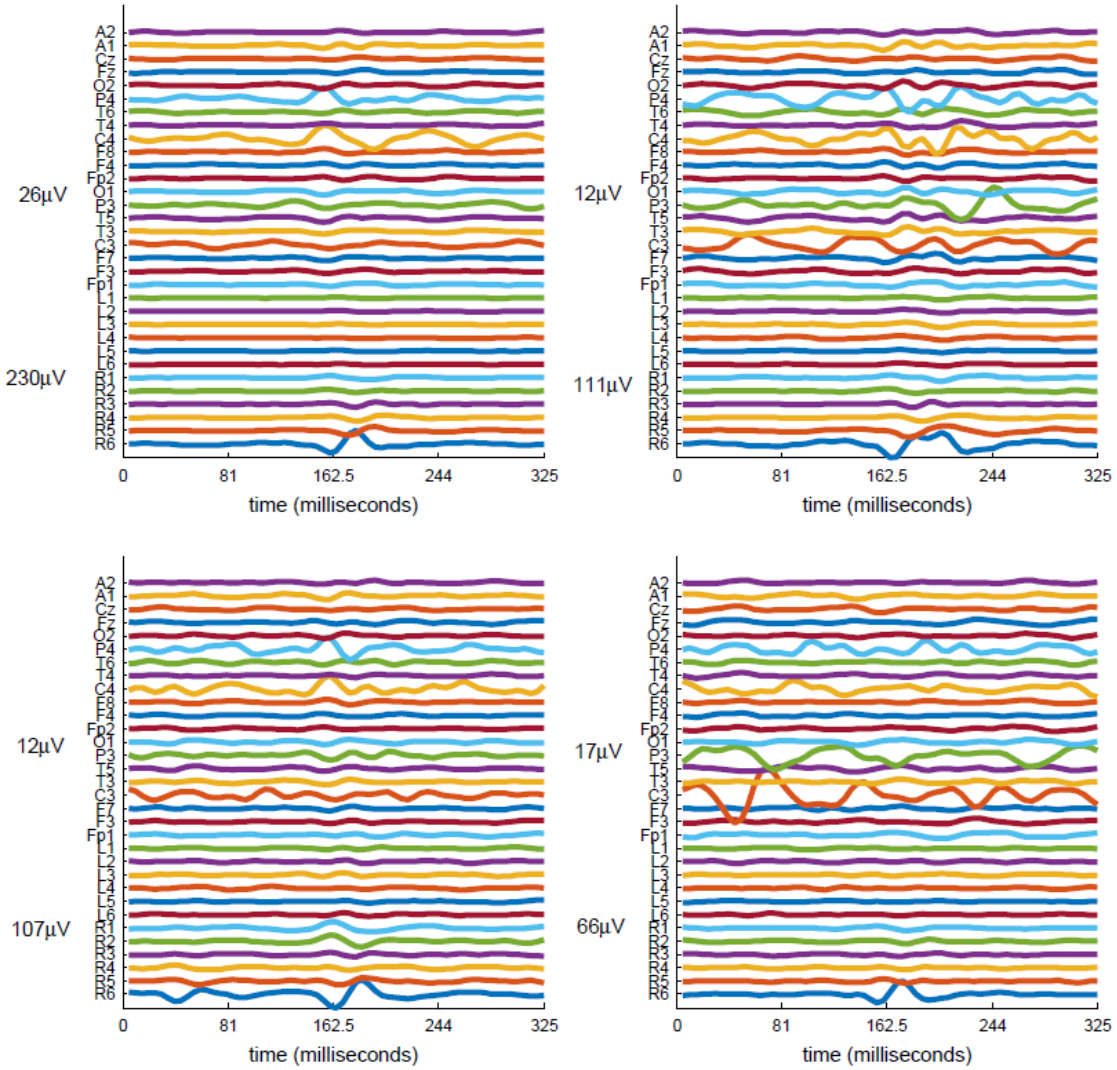


Figure 4. Examples for scalp-visible (left) and non scalp-visible (right) IEDs for Subject 1. These IEDs are obtained from the iEEG informed slicing procedure. The centre of the IED is at 162.5ms.

**3. Results**

In Fig. 2, we show an example of averages over scalp-visible and nonscalp-visible IEDs for Subject 1. This figure results from considering iEEG IEDs and performing the averaging on the concurrent sEEG segments. Examples of IEDs for different scores are shown in Fig. 4. Similarly, in Fig. 3 we show the TF average for electrode C4 for the same subject. No detection has been performed yet.

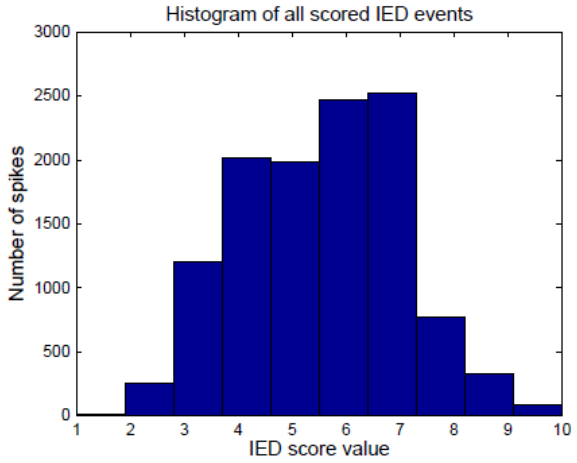


Figure 5. Epilepsy expert scored predictions histogram ove all subjects. Numbers higher than 5 denote sufficier likelihood for an epileptic spike.

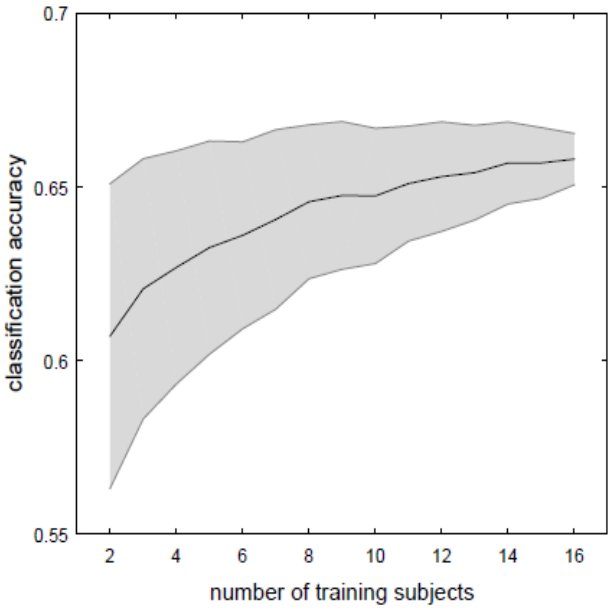


Figure 6. Classification accuracy of the ensemble classifier with regards to the number of training subjects. For each number of training subjects 100 different subsets of the full set were used in the ensemble. It can be observed that at around 10 subjects a ceiling level is reached, however the standard deviation (gray area) of the accuracy between different subsets decreases.

E ach identified IED pattern from the iEEG data was given a score by the expert epileptologist corresponding to the certainty that the pattern is an IED. The histogram of the expert's scores is shown in Fig. 5.

The baseline performance of classifying iEEG signatures on sEEG can be established by estimating the performance of the individually trained classifiers first. The different feature selection methods obtained 63%, 63%, 62%, 63%, 67% for the $T_m$, $W_5$, $W_s$, CL, and TF features, respectively, as explained in Table 1. Since the highest accuracy

Table 2. Classification accuracy of the leave-subject-out method in terms of correctly classifying the IED and non-IED segments. ACC denotes the average of the IED and non-IED classification rate. The numbers in brackets are the within-subject average of IED and non-IED classification rate.

| Subject | ACC | Non-IED | IED |
|---|---|---|---|
| S1 | 71 (78) | 79 | 63 |
| S2 | 81 (75) | 94 | 67 |
| S3 | 68 (75) | 71 | 66 |
| S4 | 58 (65) | 64 | 54 |
| S5 | 57 (57) | 61 | 53 |
| S6 | 73 (75) | 78 | 69 |
| S7 | 60 (64) | 68 | 54 |
| S8 | 58 (64) | 61 | 55 |
| S9 | 70 (72) | 75 | 65 |
| S10 | 75 (78) | 88 | 63 |
| S11 | 61 (63) | 65 | 57 |
| S12 | 67 (71) | 70 | 64 |
| S13 | 66 (72) | 70 | 62 |
| S14 | 62 (65) | 66 | 59 |
| S15 | 44 (54) | 47 | 41 |
| S16 | 61 (62) | 70 | 52 |
| S17 | 66 (74) | 71 | 60 |
| S18 | 57 (50) | 56 | 58 |
| Mean | 65 (67) | 70 | 60 |

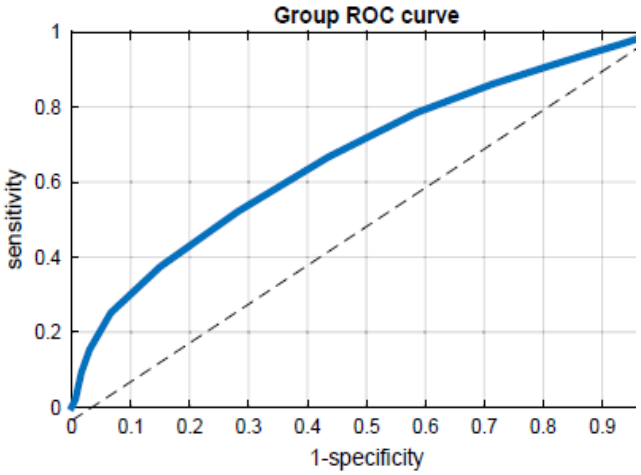


Figure 7. Group ROC curve showing the relation between the obtained sensitivity and specificity (1-FPR). By adjusting the detection threshold, a decision between the number of expected true IEDs can be tailored to user specific levels. The area under the curve (AUC) score is 0.67. The dashed line corresponds to a chance level detection algorithm.

was obtained using the TF features, subsequent analysis was performed only for TF. The individual accuracy of the individual and ensemble classifiers in recognizing IED from non-IED segments is shown in Table 2. Only S15 did not achieve the necessary significance ($p < 0.05$) level according to the binomial proportion confidence test. Also, the classifiers from subjects 15 and 18 were removed because they did not meet the criterion of >55% accuracy. The subject-independent group average accuracy was 65% with 70% and 60% accuracies on non-IED and IED segments, respectively. Furthermore, in Fig. 6 we show the classification accuracy in terms of the number of training subjects. For each number of training subjects 100 different subsets of the full dataset were used in the ensemble classifier.

The standard ROC curve of our algorithm is shown in Fig. 7. Furthermore, considering the removal of duplicate detections as described in Sec. 2.4, where consecutive detections are considered as a single event, we can estimate the proportion of detected spikes for various expert IED score values and detection thresholds in terms of FP/min (see Fig. 8). Even for low sensitivity and false positive values a high percentage of high likelihood spikes were detected by the algorithm (Fig. 8). For only nonscalp-visible IEDs the results can be seen in Fig. 9.

As seen in Fig. 8, for a low number of FPs (3.6 FP/min) the algorithm detected 26%, 21% and 12% of IEDs ranked as 10, 9 and 8, respectively, and a small number of lower ranked IEDs. For the same number of FP/min the algorithm was able to detect 20%, 17% and 7% of nonscalp-visible IEDs ranked as 10, 9 and 8, respectively. It can also be observed that the reduction of FPs is much greater than the reduction of TPs as the detection threshold is increased. For example, for IEDs ranked as 9 the FP/min was reduced by a factor of 4.58, from 16.5 to 3.6. For the TPs the reduction was from 32% to 21%, a factor of 1.5.

In Table 3, the results of an example usage of the algorithm as described in Sec. 2.4 can be seen. For each subject we show the FP/min, detected IEDs which were split into scalp-visible and nonscalpvisible. The selected decision threshold resulted in a group average of 3.6 FP/min. For 16 subjects (1, 2, 3, 4, 6, 7, 8, 9, 10, 11, 12, 13, 14, 16, 17, 18) there is improvement over only scalp-visible IED analysis since it detects nonscalp-visible IEDs as well. 10

of these subjects (3, 6, 7, 8, 9, 11, 14, 16, 17, 18) did not have any or very few scalp-visible detections but the algorithm was able to detect nonscalp-visible ones. For five subjects (1, 2, 4, 12, 13) the nonscalpvisible IEDs complemented the scalp-visible ones. Out of 18, two subjects (5, 15) had practically no IED detections and for seven subjects (3, 4, 8, 10, 16, 17, 18) there were less than 10 IED detections. It can be summarized that for

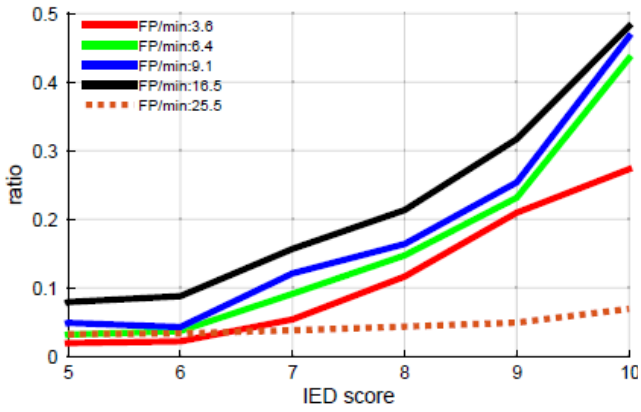


Figure 8. The ratio of detected IEDs to the total number of IEDs that were identified by the expert epileptologist per each score value (see Figure 5) for high (red) to low (black) detection thresholds. The higher the detection threshold the smaller the number of detections that are considered IEDs reducing both the true and false positives. For example 21% of IEDs with an IED score of 9 were detected by the algorithm for a detection threshold

that produced 3.6 FP=min. Increasing the detection

threshold decreases the number of detected IEDs. The dashed line indicates the average performance of the classifier randomisation test (see Section 2.4).

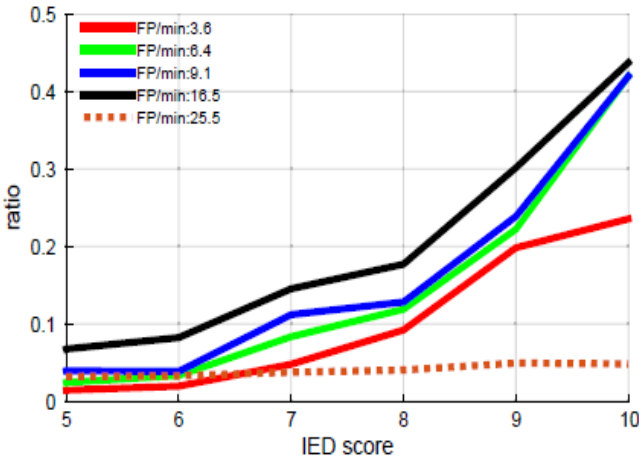


Fig. 9. The ratio of detected nonscalp-visible IEDs to the total number of nonscalp-visible IEDs per each score value (see Fig. 5) for high (red) to low (black) detection thresholds. The higher the detection threshold the smaller the number of detections that are considered IEDs reducing both the true and false positives. For example, 20% of the nonscalp-visible IEDs with an IED score of 9 were detected by the algorithm for a detection threshold that produced 3.6 FP/min. Increasing the detection threshold decreases the number of detected IEDs. The dashed line indicates the average performance of the classifier randomization test (see Sec. 2.4).

Table 3. Implementation example of the detection algorithm for a very high detection threshold that results in a group average 3.6 FP/min. We show the FP/min, the total number of detected IEDs which are subsequently split into nonscalp-visible and scalp-visible. The scalp-visible IEDs are split into IEDs that were visible with and without the need to consider the concurrent iEEG. The numbers in brackets are the total number of IEDs of each category.

| Subject | FP/min | #IED | Non-visible | Visible-without | Visible-with |
|---|---|---|---|---|---|
| S1 | 3.9 | 33(342) | 22(302) | 5(11) | 6(29) |
| S2 | 2.6 | 10(50) | 6(45) | 2(4) | 0(1) |
| S3 | 3.6 | 7(73) | 7(73) | 0(0) | 0(0) |
| S4 | 3.3 | 8(155) | 3(151) | 4(9) | 0(5) |
| S5 | 4.7 | 1(158) | 1(158) | 0(0) | 0(0) |
| S6 | 2.5 | 41(472) | 39(469) | 0(1) | 2(2) |
| S7 | 3.0 | 15(199) | 13(197) | 1(1) | 1(1) |
| S8 | 4.3 | 6(317) | 6(314) | 0(1) | 0(2) |
| S9 | 2.3 | 43(341) | 41(338) | 0(0) | 2(3) |
| S10 | 5.2 | 5(224) | 3(158) | 2(40) | 0(26) |
| S11 | 2.8 | 14(848) | 14(848) | 0(0) | 0(0) |
| S12 | 2.5 | 39(952) | 8(681) | 28(271) | 3(38) |
| S13 | 3.1 | 28(827) | 19(732) | 18(71) | 0(25) |
| S14 | 4.3 | 12(549) | 12(549) | 0(0) | (0) |
| S15 | 3.9 | 0(260) | 0(256) | 0(4) | 0(0) |
| S16 | 6.0 | 6(607) | 6(591) | 0(14) | 0(1) |
| S17 | 2.8 | 6(114) | 5(105) | 0(1) | 1(4) |
| S18 | 4.8 | 6(118) | 6(118) | 0(0) | 0(0) |

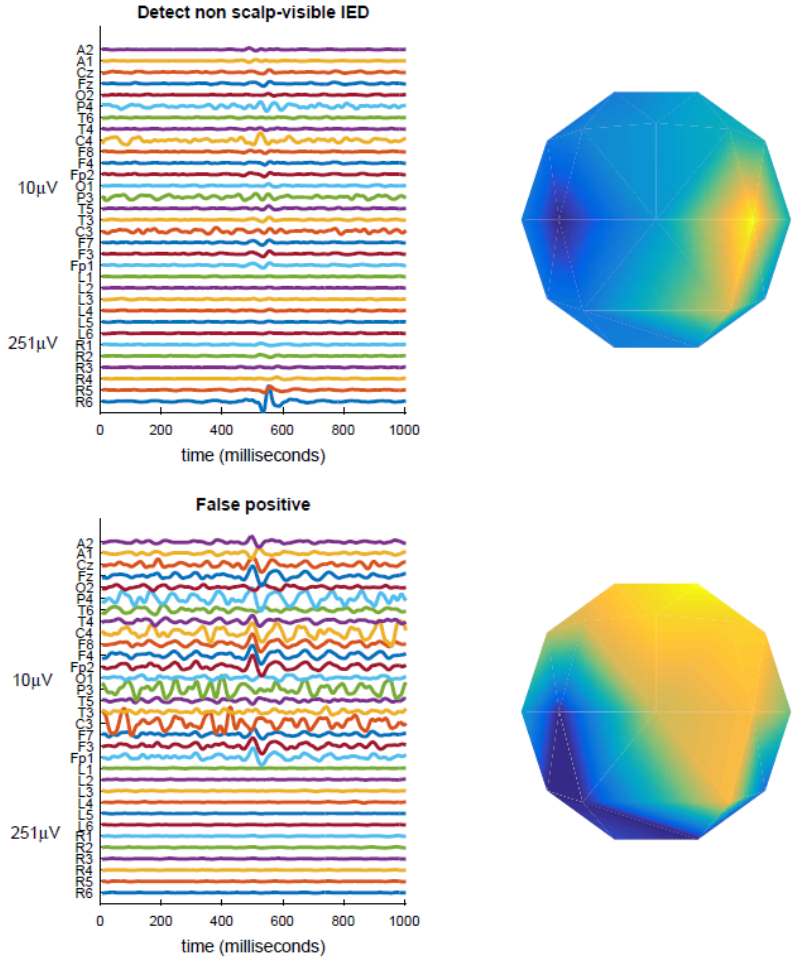


Fig. 10. Examples of detected true and false positives for Subject 1. The distinction between true (top) and false (bottom) positives can be made on the basis of the activity being focal.

nine out of 18 subjects the algorithm performed well for a 20min recording while for the other nine a longer recording would be needed.
Figures 10–12 show some representative examples of true and false positives, temporal, and spatial topographies.

**4. Discussion**

The expected discriminability of scalp IEDs against non-IED segments was initially established. It provided an indication of how well the detection algorithm can perform. Since algorithms trained and tested on the same subject data give superior performance to more generic or subject-independent algorithms, optimal classification rate can be established at the level of within subject classification rate. This was achieved at a group average of 67% indicating that there is enough discriminative information in the scalp EEG to be classified above the chance level (only S15 did not achieve a significant classification accuracy). The classification performance of unseen data performed was similar with a group average of 65% accuracy. Such performance suggests that the algorithm was able to generalize well and between subject differences did not deteriorate the performance. The performance is seemingly not very good but this is explained by the fact that we use low amplitude IEDs. Although in some studies they obtain higher performance but only consider scalp-visible IED segments (see e.g. Refs. 27, 26 and 68). Also, note that in our study we only use 20 scalp electrodes which is less than in Refs. 25–27 and by increasing the number of electrodes higher performance is expected. Increasing the number of electrodes from 19 to 256 doubled the visual detection rate in Ref. 69.
When applying the algorithm in a detection fashion, that is sweeping across the data in a sample-by sample basis, it was able to detect correctly a good number of IEDs while keeping the FP/min to an acceptable level.

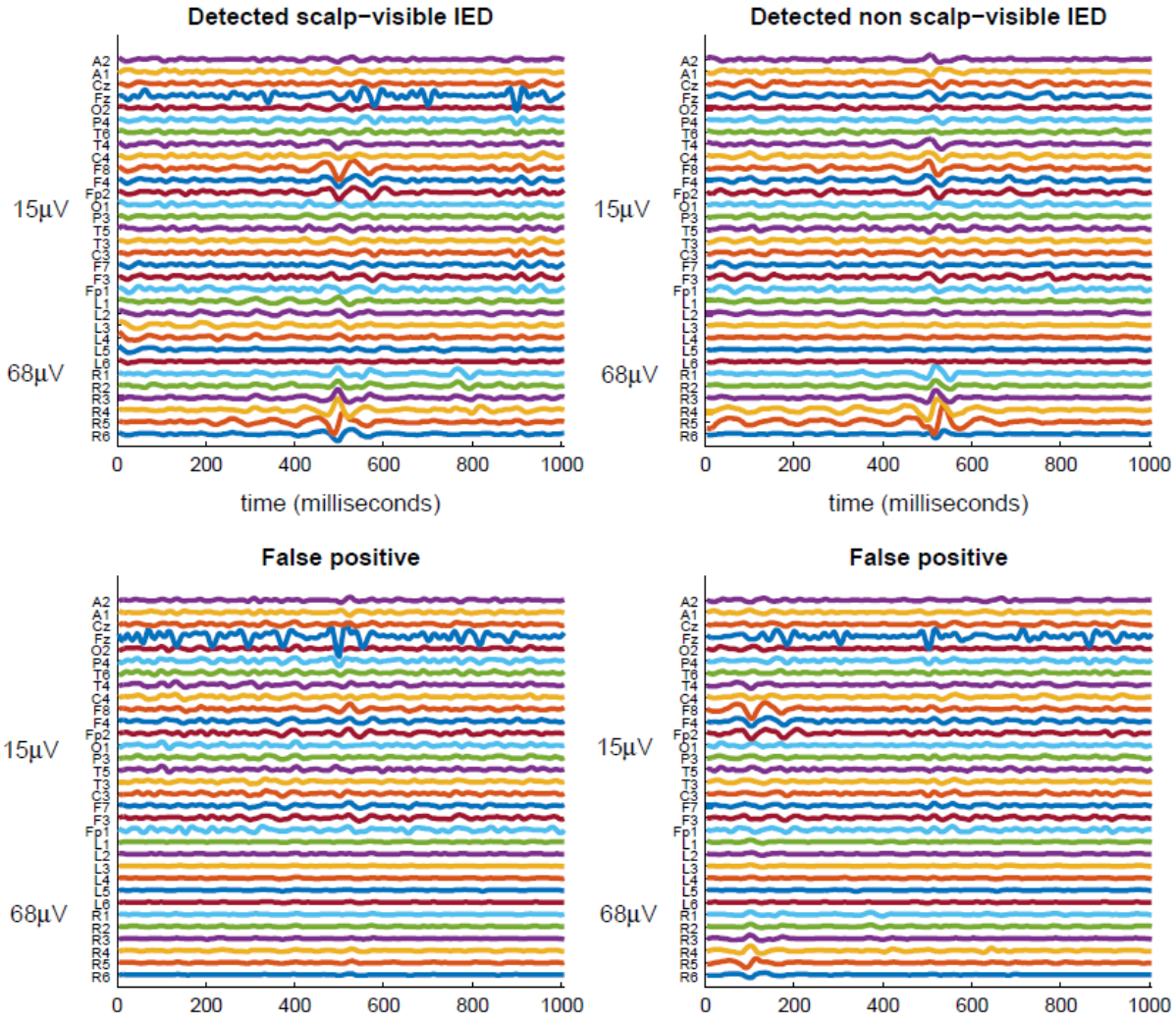


Fig. 11. Examples of scalp-visible, nonscalp-visible and two false positive detections for Subject 12. The center of the IED is at 500ms.

An acceptable maximum of FP/min can be established at 6 FP/min since that would result in maximum of 1 FPs per 10 s of data, the traditional time window size suitable to inspection of the EEG data. Detecting both nonscalp-visible and scalp-visible IEDs suggests a potential improvement on the diagnostic ability of sEEG[70] as compared to algorithms considering only scalp-visible segments. A limitation however is that the obtained results were not compared with a detection algorithm based only on scalp-visible IEDs due to their low number. Furthermore, the proposed algorithm can be effective in EEG-fMRI studies where the BOLD response needs to be estimated but there are very few scalp-visible IEDs.[28] In contrast to the study in Ref. 28 which uses only the spatial topography of the IED, our method IED signatures. Other applications can be devised, such as source localization of nonscalp-visible IEDs or the improvement of analysis methodologies for brain stimulation.[71] The methodology has the potential to be also applied to other epileptic datasets.

The presence of FPs can be problematic for the utility of the algorithm. Any algorithm that attempts to detect IEDs from EEG suffers from the inherent drawback of high class imbalance resulting in producing many more FPs. For a 20min sEEG recording our patient group had from 50 to 1000 IEDs. This corresponds to an IED duration of 1.25% to 25% within a 20min recording[b]. Also, since the IED waves exhibit similar wave shapes to other EEG sources further information has to be used to improve the detection performance. Ultimately, the decision of whether a set of candidate IED detections correspond to epileptic activity lies on the clinician performing the evaluation.

The evaluation procedure is performed in a stepwise fashion where the clinician progressively increases the number of candidate IEDs to evaluate. The candidate IEDs are selected according to their probability. Through

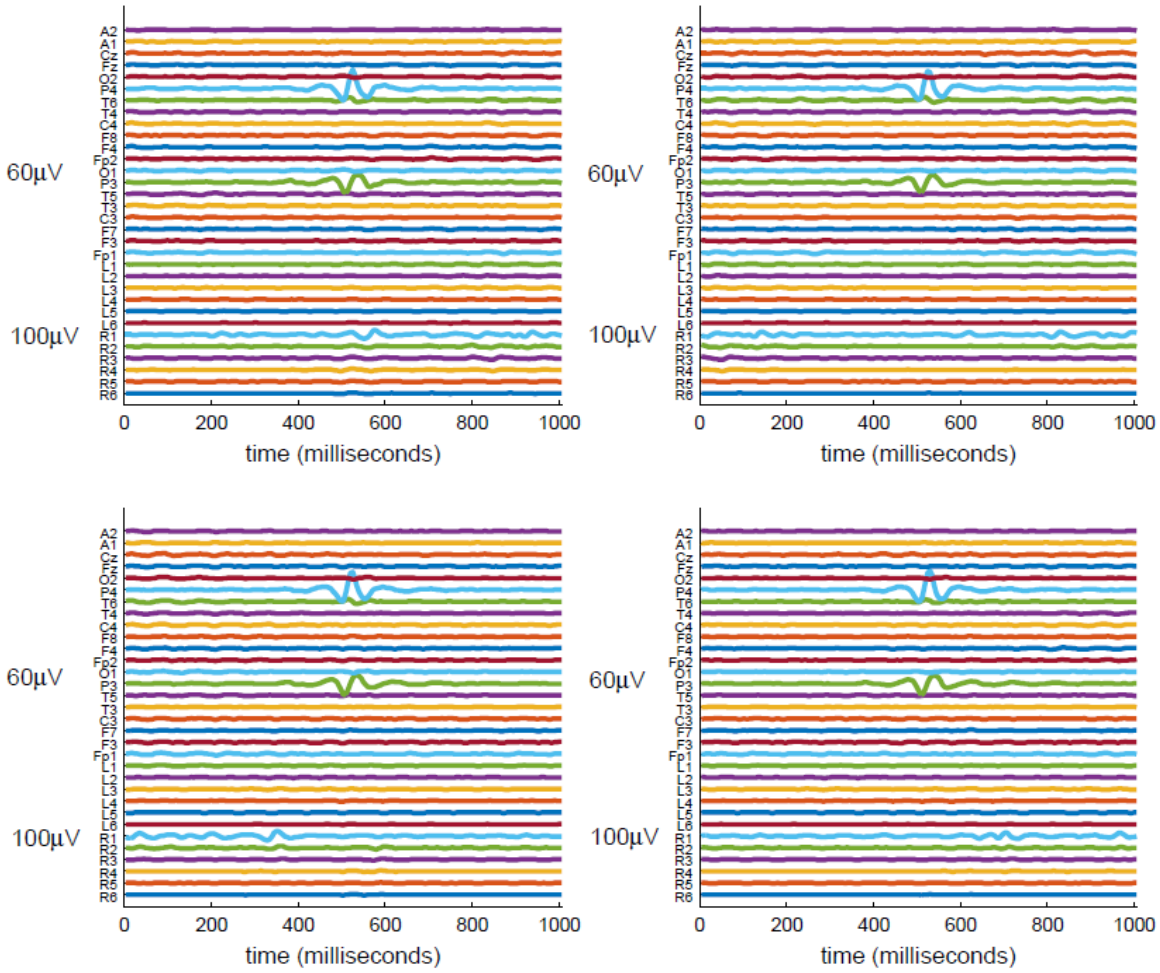


Fig. 12. Examples of four false positives for Subject 5. The center of the IED is at 500ms.

[b] We assume in this calculation that an IED lasts for 300ms.

the temporal and spatial topographies of the obtained detections the clinician can decide whether the candidate IEDs correspond to true epileptic activity.
As seen in Table 3, an example of using a high detection threshold that results in an average of 3.5 FP/min of the algorithm is able to improve upon traditional sEEG analysis since it detects IEDs that would otherwise not be detectable from the sEEG. Increasing the duration of the recording, increases the occurrence of IEDs and subsequently the number of detected IEDs and the number of patients for which such a method is useful.
The visual inspection of the candidate IEDs can provide useful information regarding the presence of epilepsy. As shown in Fig. 10, a representative case of a true positive corresponds to a focal IED source whereas the false positive is not focal. In terms of the difference between visible and nonvisible IEDs it can be seen in Fig. 11 that they show similar activity with the nonscalp-visible segment having low amplitude. The activities of the false positives are not consistent. For subjects with many false positives such as Subject 5 (Fig. 12), the false positives exhibited activities that were focal but with very little concurrent activity on other electrodes.

**5. Conclusions**

In this paper, an algorithm has been developed that is able to detect intracranial IED signatures on the scalp EEG. Both scalp-visible and nonscalp-visible IEDs were detected with a low number of FPs. We used a probabilistic classifier which provides a natural way of describing the data in terms of class membership probabilities of the obtained data of decreasing probability.[25] The IED detection methodology was successful in both cases when the algorithm was trained with within-subject data and when the classifier was trained on a pool of patients with epilepsy. Since we are aiming for generalization performance on unseen data, the algorithm was tested in a leavesubject-out fashion such that a realistic usage would be emulated. A good performance was achieved and the algorithm was able to provide a new utility of EEG[70] for TLE. Even in cases where the expert epileptologist did not mark any scalp-visible IEDs, the algorithm succeeded in detecting nonscalp-visible ones. segments. Hence, for a sEEG recording, the IED predictions can be presented and selected in order
It has to be noted that the seemingly low performance of the method is due to the scalp IEDs being segmented according to intracranial timing information. This is the first study that attempts such a procedure in contrast to defining IED segments based on only scalp-visible discharges. Detecting even a small number of IEDs is important in clinical practice since it can aid the diagnosis of epilepsy and increase the performance in related fields such as interictal fMRI bold detection[28] and electrical stimulation of the brain.[72] Since EEG only complements the diagnosis of epilepsy, the clinical efficacy and diagnostic ability of the proposed method will be further evaluated in a future study which will include longer recordings from both epileptic and healthy subjects.

**Acknowledgment**

This work has been supported by the EPSRC, UK, Grant No. EP/K005510/1.

**References**

1. S. Sanei, *Adaptive Processing of Brain Signals* (Wiley, 2013).
2. C. Marsan and L. Zivin, Factors related to the occurrence of typical paroxysmal abnormalities in the EEG records of epileptic patients, *Epilepsia* **11**(4) (1970) 361–381.
3. C. Binnie, Electroencephalography, in *A Textbook of Epilepsy*, eds. J. Laidlaw, A. Chadwick and D. Richens (Churchill Livingstone, Edinbrugh, 1992).
4. R. Kumar, Diagnostic imaging of intracranial neoplasms: How frequent are indicative findings in CT and MRI? *Int. J. Curr. Res. Rev.* **22**(5) (2013) 64–73.
5. G. Alarcon, C. N. Guy, C. D. Binnie, S. R. Walker, R. D. Elwes and C. E. Polkey, Intracerebral propagation of interictal activity in partial epilepsy: Implications for source localisation, *J. Neurol. Neurosurg. Psychiatry* **57** (1994) 435–449.
6. G. Alarcon, C. D. Binnie, J. J. Garcia Seoane, M. C. Martin Miguel, J. L. Fernandez Torre, C. E. Polkey and C. N. Guy, Mechanisms involved in the propagation of interictal epileptiform discharges in partial epilepsy, *Electroencephalogr. Clin. Neurophysiol.* **50** (1999) 259–278.
7. H. Wieser, Stereoelectroencephalography and foramen ovale electrode recording, in (eds.) E.M. Niedermeyer and Lopes da Silva, *Electroencephalography*, *Basic Principles, Clinical Applications and Related Fields* (Williams and Wilkings, London, 1999).

8. J. L. Fernandez Torre, G. Alarcon, C. D. Binnie, J. J. Seoane, J. Juler, C. N. Guy and C. E. Polkey, Generation of scalp discharges in temporal lobe epilepsy as suggested by intraoperative electrocorticographic recordings, *J. Neurol. Neurosurg. Psychiatry* **67** (1999) 51–58.
9. D. Nayak, A. Valentin, G. Alarcon, J. J. Garcia Seoane, F. Brunnhuber, J. Juler, C. E. Polkey and C. D. Binnie, Characteristics of scalp electrical fields associated with deep medial temporal epileptiform discharges, *Clin. Neurophysiol.* **115** (2004) 1423–1435.
10. J. Tao, A. Ray, S. Hawes-Ebersole and J. Ebersole, Intracranial EEG substrates of scalp EEG interictal spikes, *Epilepsia* **46** (2005) 669–676.
11. R. Cooper, A. L. Winter, H. J. Crow and W. G. Walter, Comparison of subocortical, cortical and scalp activity using chronically indwelling electrodes in man, *Electroencephalogr. Clin. Neurophysiol.* **18** (1965) 217–228.
12. G. Pfurtscheller and R. Cooper, Frequency dependence of the transmission of the EEG from cortex to scalp, *Electroencephalogr. Clin. Neurophysiol.* **38** (1975) 93–96.
13. O. Devinsky, S. Sato, C. V. Kufta, B. Ito, D. F. Rose, W. H. Theodore and R. J. Porter, Electroencephalographic studies of simple partial seizures with subdural electrode recordings, *Neurology* **39** (1989) 527–533.
14. S. Arroyo, Subdural and epidural grids and strips, *Surgical Treatment of the Epilepsies*, ed. J. Engel (Raven Press, New York, 1993).
15. G. Alarcon, J. J. Garcia Seoane, C. D. Binnie, M. C. Martin Miguel, J. Juler, C. E. Polkey, R. D. Elwes and J. M. Ortiz Blasco, Origin and propagation of interictal discharges in the acute electrocorticogram. Implications for pathophysiology and surgical treatment of temporal lobe epilepsy, *Brain* **120** (**Pt 1**) (1997) 2259–2282.
16. N. Kissani, G. Alarcon, M. Dad, C. Binnie and C. Polkey, Sensitivity of recordings at sphenoidal electrode site for detecting seizure onset: Evidence from scalp, superficial and deep foramen ovale recordings, *Clin. Neurophysiol.* **112** (2001) 232–240.
17. S. Stodieck, H. G. Wieser and C. E. Elger, The foramen ovale electrode: A new recording method for the preoperative evaluation of patients suffering from mesio-basal temporal lobe epilepsy, *Electroencephalogr. Clin. Neurophysiol.* **61** (1985) 314–322.
18. J. Fernandez Torre, G. Alarcon, C. Binnie and C. Polkey, Comparison of sphenoidal, foramen ovale and anterior temporal placements for detecting interictal epileptiform discharges in presurgical assessment for temporal lobe epilepsy, *Clin. Neurophysiol.* **110** (1999) 895–904.
19. B. C. Heasman, A. Valentin, G. Alarcon, J. J. Garcia Seoane, C. D. Binnie and C. N. Guy, A hole in the skull distorts substantially the distribution of extracranial electrical fields in an *in vitro* model, *Clin. Neurophysiol.* **19** (2002) 163–171.
20. M. Sparkes, A. Valentin and G. Alarcon, Mechanisms involved in the conduction of anterior temporal epileptiform discharges to the scalp, *Clin. Neurophysiol.* **120** (2009) 2063–2070.
21. L. Koessler, T. Cecchin, S. Colnat-Coulbois, J.-P. Vignal, J. Vespignani, G. Ramantani and L. Maillard, Catching the invisible: Mesial temporal source contribution to simultaneous EEG and SEEG recordings, *Brain Topogr.* **28** (2015) 5–20.
22. N. Gaspard, R. Alkawadri, P. Farooque, I. I. Goncharova and H. P. Zaveri, Automatic detection of prominent interictal spikes in intracranial EEG: Validation of an algorithm and relationsip to the seizure onset zone, *Clin. Neurophysiol.* **125** (2014) 1095–1103.
23. R. Janca, P. Jezdik, R. Cmejla, M. Tomasek, G. A. Worrell, M. Stead, J. Wagenaar, J. G. R. Jefferys, P. Krsek, V. Komarek, P. Jiruska and P. Marusic, Detection of interictal epileptiform discharges using signal envelope distribution modelling: Application to epileptic and non-epileptic intracranial recordings, *Brain Topogr.* **28** (2014) 172–183.
24. M. Dumpelman and C. Elger, Visual and automatic investigation of epileptiform spikes in intracranial EEG recordings, *Epilepsia* **42** (1999) 275–285.
25. S. S. Lodder and M. J. A. M. van Putten, A self-adapting system for the automated detection of inter-ictal epileptiform discharges, *PLoS ONE* **9** (2014) e85180.
26. J. J. Halford, R. J. Schalkoff, J. Zhou, S. R. Benbadis, W. O. Tatum, R. P.Turner, S. R. Sinha,N. B. Fountain, A. Arain, P. B. Pritchard, E. Kutluay, G. Martz, J. C. Edwards, C. Waters and B. C. Dean, Standardized database development for EEG epileptiform transient detection: EEGnet scoring system and machine learning analysis, *J. Neurosci. Methods* **212** (2013) 308–316.
27. F. Argoud, F. M. De Azevedo, J. Neto and E. Grillo, SADE3: An effective system for automated detection of epileptiform events in long-term EEG based on context information, *Med. Biol. Eng. Comput.* **44** (2006) 459–470.
28. F. Grouiller, R. Thornton, K. Groening, L. Spinelli, J. Duncan, K. Schaller, M. Siniatchkin, L. Lemieux, M. Seeck, C. Michel and S. Vulliemoz, With or without spikes: Localization of focal epileptic activity by simultaneous electroencephalography and functional magnetic resonance imaging, *Brain* **134** (2011) 2867–2886.
29. J. Margerison, C. Binnie and I. McCaul, Electroencephalographic signs employed in the location of ruptured intracranial arterial aneurysms, *Electroencephalogr. Clin. Neurophysiol.* **28** (1970) 296–306.
30. C. Binnie, E. Dekker, A. Smit and G. Van der Linden, Practical considerations in the positioning of EEG electrodes, *Electroencephalogr. Clin. Neurophysiol.* **53** (1982) 453–458.
31. T. Velasco, A. C. Sakamoto, J. V. Alexandre, R. Walz, C. L. Dalmagro and M. M. Bianchin, Foramen ovale electrodes can identify a focal seizure onset when surface EEG fails in mesial temporal lobe epilepsy, *Epilepsia* **47** (2006) 1300–1307.
32. H. Wieser and A. Siegel, Analysis of foramen ovale electrode-recorded seizures and correlation with outcome following amygdalohippocampectomy, *Epilepsia* **32** (1991) 838–850.

33. S. Noachtar, C. Binnie, J. Ebersole, F. Mauguiere, A. Sakamoto and B. Westmoreland, A glossary of terms most commonly used by clinical electroencephalographers and proposal for the report form for the EEG findings. The International Federation of Clinical Neurophysiology, *Electroencephalogr. Clin. Neurophysiol. Suppl.* **52** (1999) 21–41.
34. J. Zhanfeng, T. Sugi, S. Goto, X.Wang andM. Nakamura, Multichannel template extraction for automatic EEG spike detection, Proceedings of the 2011 IEEE/ICME International Conference on Complex Medical Engineering, 22–25 May (2011, Harbin, China), pp. 179–184.
35. K. Vijayalakshmi and A. M. Abhishek, Spike detection in epileptic patients EEG data using template matching technique, *Int. J. Comput. Appl.* **2** (2010) 5–8.
36. J. Zhou, R. J. Schalkoff, B. C. Dean and J. J. Halford, Morphology-based wavelet features and multiple mother wavelet strategy for spike classification in EEG signals, *Annual Int. Conf. IEEE Engineering in Medicine and Biology Society*, Vol. 2012 (2012) 3959–3962.
37. Y. C. Liu, C. C. K. Lin, J. J. Tsai and Y. N. Sun, Model-based spike detection of epileptic EEG data, *Sensors* **13** (2013) 12536–12547.
38. S. Ghosh-Dastidar, H. Adeli and N. Dadmehr, Mixed-band wavelet-chaos-neural network methodology for epilepsy and epileptic seizure detection, *IEEE Trans. Biomed. Eng.* **54**(9) (2007) 1545–1551.
39. M. De Lucia, J. Fritschy, P. Dayan and D. S. Holder, A novel method for automated classification of epileptiform activity in the human electroencephalogram-based on independent component analysis, *Med. Biol. Eng. Comput.* **46** (2008) 263–272.
40. A. T. Tzallas, M. G. Tsipouras, D. G. Tsalikakis, E. C. Karvounis, L. Astrakas, S. Konitsiotis and M. Tzaphlidou, Automated epileptic seizure detection methods: A review study, in *Epilepsy —Histological, Electroencephalographic and Psychological Aspects*, ed. D. Stevanovic (2009).
41. S. B. Wilson, C. A. Turner, R. G. Emerson and M. L. Scheuer, Spike detection II: Automatic, perceptionbased detection and clustering, *Clin. Neurophysiol* **110** (1999) 404–411.
42. S. B. Wilson and R. Emerson, Spike detection: A review and comparison of algorithms, *Clin. Neurophysiol.* **113** (2002) 1873–1881.
43. A. Gotman and P. Gloor, Automatic recognition and quantification of interictal epileptic activity in the human scalp EEG, *Electroencephalogr. Clin. Neurophysiol* **41**(5)(1976) 513–529.
44. N. Acir, I. Oztura, M. Kuntalp, B. Baklan and C. G¨uzeli, s, Automatic detection of epileptiform events in EEG by a three-stage procedure based on artificial neural networks, *IEEE Trans. Biomed. Eng.* **52** (2005) 30–40.
45. H. Adeli, Z. Zhou and N. Dadmehr, Analysis of EEG records in an epileptic patient using wavelet transform, *J. Neurosci. Methods* **123**(1) (2003) 69–87.
46. H. Adeli, S. Ghosh-Dastidar and N. Dadmehr, A wavelet-chaos methodology for analysis of EEGs and EEG sub-bands to detect seizure and epilepsy, *IEEE Trans. Biomed. Eng.* **54**(2) (2007) 205–211.
47. Z. Vahabi, R. Amirfattah, F. Ghassmi and D. Shayegh, Online epileptic seizure prediction using wavelet-based bi-phase correlation of electrical signal tomography, *Int. J. Neural Syst.* **25**(6) (2015) 1550028.
48. U. R. Acharya, S. V. Sree, A. P. C. Alvin, R. Yanti and J. S. Suri, Application of non-linear and wavelet based features for the automated identification of epileptic EEG signals, *Int. J. Neural Syst.* **22** (2012) 1250002.
49. S. Yuan, W. Zhou, Q. Yuan, X. Zhao and J. Wang, Kernel collaborative representation-based automatic seizure detection in intracranial EEG, *Int. J. Neural Syst.* **25** (2015) 1550003.
50. F. S. Bao, J.-M. Gao, J. Hu, D. Y. C. Lie, Y. Zhang and K. J. Oommen, Automated epilepsy diagnosis using interictal scalp EEG, in *Conf. Proc. IEEE Engineering in Medicine Biology Socety* (2009), pp. 6603–6607.
51. C. Wang, J. Zou, J. Zhang, M. Wang and R. Wang, Feature extraction and recognition of epileptiform activity in EEG by combining PCA with ApEn, *Cognit. Neurodyn.* **4** (2010) 233–240.
52. R. Martis, U. Acharya, J. Yan, A. Petznick, C. Chua and E. Ng, Application of intrinsic time-scale decomposition (ITD) to EEG signals for automated seizure prediction, *Int. J. Neural Syst.* **23**(5) (2013) 1350023.
53. Q. Yuan, W. Zhou, S. Yuan, X. Li, J. Wang and G. Jia, Epileptic EEG classification based on kernel sparse representation, *Int. J. Neural Syst.* **24** (2014) 1450015.
54. C. James, M. Hagan, R. Jones, P. Bones and G. Carroll, Multireference adaptive noise canceling applied to the EEG, *IEEE Trans. Biomed. Eng.* **44** (1997) 775–779.
55. L. da Silva, Detection of nonstationarities in EEGs using the autoregressive model — An application to EEGs of epileptics, in *Computerized EEG analysis*, eds. G. Dolce and H. Kunkel (Fisher, Stuttgart, 1975).
56. N. von Ellenrieder, L. Beltrachini, P. Perucca and J. Gotman, Size of cortical generators of epileptic interictal events and visibility on scalp EEG, *NeuroImage* **94** (2014) 47–54.
57. G. Ramantani, M. D¨umpelmann, L. Koessler, A. Brandt, D. Cosandier-Rim´el´e, J. Zentner, A. Schulze-Bonhage and L. G. Maillard, Simultaneous subdural and scalp EEG correlates of frontal lobe epileptic sources, *Epilepsia* **55** (2014) 278–288.
58. D. Cosandier-Rimele, I. Merlet, M. Badier, P. Chauvel and F. Wendling, The neuronal sources of EEG: Modeling of simultaneous scalp and intracerebral recordings in epilepsy, *Neuroimage* **42** (2008) 135–146.
59. K. P. Indiradevi, E. Elias, P. S. Sathidevi, S. Dinesh Nayak and K. Radhakrishnan, A multi-level wavelet approach for automatic detection of epileptic spikes in the electroencephalogram, *Comput. Biol. Med.* **38** (2008) 805–816.
60. A. Bultan, A four-parameter atomic decomposition of chirplets, *IEEE Trans. Signal Process.* **47** (1999) 731–745.
61. H. Zaveri, W. Williams, L. Iasemidis and J. Sackellares, Time-frequency representation of electrocorticograms in temporal lobe epilepsy, *IEEE Trans. Biomed. Eng.* **39** (1992) 502–509.

62. B. Reudering, J. Farquhar,M. Poel and A. Nijholt, A subject-independent brain-computer interface based on smoothed, second-order baselining, *33rd Annual Int. Conf. IEEE EMBS* (2011), pp. 46000–46004.
63. T. Hastie, R. Tibshirani and J. Friedman, *The Elements of Statistical Learning* (Springer, 2009).
64. J. Farquhar and J. Hill, Interactions between preprocessing and classification methods for event-related-potential classification: Best-practice guidelines for brain-computer interfacing, *Neuroinformatics* **11** (2013) 175–192.
65. C. Schaffer, Selecting a classification method by cross-validation, *Mach. Learn.* **13**(1) (1993) 135–143.
66. Y. Blokland, L. Spyrou, D. Thijssen, T. Eijsvogels, W. Colier, M. Floor-Westerdijk, R. Vlek, J. Bruhn and J. Farquhar, Combined EEG-fNIRS decoding of motor attempt and imagery for brain switch control: An offline study in patients with tetraplegia, *IEEE Trans. Neural Syst. Rehabil. Eng.* **22**(2) (2014) 1–8.
67. A. Agresti and B. A. Coull, Approximate is better than "exact" for interval estimation of binomial proportions, *Am. Stat.* **52**(2) (1998) 119–126.
68. F. Moraes and D. Callegari, Automated detection of interictal spikes in EEG: A literature review, UCRS Tecnical Report TR081 (2014).
69. M. Yamazaki, D. Tucker, A. Fujimoto, T. Yamazoe, T. Okanishi, T. Yokotaa, H. Enoki and T. Yamamoto, Comparison of dense array EEG with simultaneous intracranial EEG for interictal spike detection and localization, *Epilepsy Res.* **98** (2012) 166–173.
70. H. Adeli and S. Ghosh-Dastidar, *Automated EEGBased Diagnosis of Neurological Disorders — Inventing the Future of Neurology* (CRC Press, Taylor and Francis, Florida, 2007).
71. D. Kugiumtzis and K. Kimiskidis, Direct causal networks for the study of transcranial magnetic stimulation effects on focal epileptiform discharges, *Int. J.Neural Syst.* **25**(5) (2015) 1550006.
72. E. Bellistri, V. Gnatkovsky and M. de Curtis, Fast activity evoked by intracranial 50Hz stimulation as a marker of epileptogenic zone, *Int. J. Neural Syst.* **25** (2015) 1250022.

# Electrical Simulation of the Anterior Cingulate Gyrus Induces Responses Similar to K-complexes in Awake Humans

Zanna Voysey, BMBCh MA[a,*], David Martín-López, MBBS MSc CCST[a,b,c,*], Diego Jiménez-Jiménez, MBBS MSc[a,b,d], Richard P. Selway, MBBS CCST[e], Gonzalo Alarcón, MD PhD[a,b,f,#], Antonio Valentín, MD PhD[a,b,f,#]

[a] Department of Basic and Clinical Neuroscience, King's College London, Institute of Psychiatry, Psychology and Neuroscience, UK.

[b] Department of Clinical Neurophysiology, King's College Hospital NHS Trust, London, UK.

[c] Department of Clinical Neurophysiology, St Peter's Hospital, Chertsey, UK.

[d] Universidad San Francisco de Quito, School of Medicine, Quito, Ecuador.

[e] Department of Neurosurgery, King's College Hospital NHS Trust London, UK.

[f] Departamento de Fisiología, Facultad de Medicina, Universidad Complutense, Madrid, Spain.

*Drs Z. Voysey and D. Martín-López are joint first authors.

[#] Drs G. Alarcón and A. Valentín are joint senior authors.

This project did not have external funding.

No author has a conflict of interest.

Corresponding author:

Dr Antonio Valentin, MD PhD
Department of Clinical Neuroscience
Institute of Psychiatry, Psychology and Neuroscience
PO 43,De Crespigny Park, London SE5 8AF, United Kingdom

Tel: +44 20 7848 5161 / 5436
Fax: +44 20 73463725

**ABSTRACT**

*Background:* The brain region responsible for the initiation of K-complexes has not been identified to date.

*Objective:* To determine the brain region responsible for originating K-complexes.

*Methods:* We reviewed all 269 patients assessed for epilepsy surgery with intracranial electrodes and single pulse electrical stimulation (SPES) at King's College Hospital between 1999 and 2013. Intracranial EEG responses to electrical stimulation at orbitofrontal, frontal, cingulate, temporal and parietal loci were compared visually with each patient's K-complexes and the degree of resemblance was quantified.

*Results:* Among the 269 patients, K-complex-like responses were exclusively observed in all 6 patients who had depth electrodes in the cingulate cortex. In each patient, the stimulation site eliciting the response of greatest similarity to the patient's K-complex was located within the dorso-caudal anterior cingulate. The K-complex like responses were evoked when the patients were awake.

*Conclusion:* Our findings provide the first causal evidence that the cingulate gyrus initiates the widespread synchronous activity that constitutes the K-complex. The induction of K-complex-like responses during wakefulness suggests that the mechanisms required for the initiation of K-complexes are separate from those involved in sleep.

**Keywords:** K-complex, single pulse electrical stimulation, sleep phenomena, cingulate gyrus.

**Abbreviations**

EEG: Electroencephalography

SPES: Single Pulse Electrical Stimulation

r: Correlation Coefficient

SI: Similarity index

## 1. INTRODUCTION

K-complexes are electroencephalographic (EEG) phenomena occurring during sleep, arising either spontaneously or in response to sensory stimulation. They are identified as a large biphasic negative-positive wave lasting for longer than 0.5 seconds, often preceded or followed by a sleep spindle[1].

Since K-complexes were first described in 1938 by Loomis et al.[2], they have become a marker of stage II sleep. Their physiological mechanisms are largely unknown, with evidence supporting both a sleep-protective role [3], and conversely, one of arousal[4]. Likewise the axiom that they can arise spontaneously is under question, with some evidence to suggest that seemingly-spontaneous K-complexes may in fact be a response to unrecognised internal stimuli, such as borborygmi[5,6].

Above all, however, it is their generation that remains controversial. Studies combining multisite cellular, local field and scalp EEG recordings[7–12] suggest that K-complexes arise from synchronised activity across widespread cortical areas mediated by hyperpolarising currents in layer III of the cortex, such that they form a transient version of the on-going slow wave activity that predominates in stage III-IV sleep[13]. This activity then propagates via cortico-cortical connections[7] in a predominantly anterior-posterior direction[14,15]. It follows, however, that there must be a region that orchestrates and synchronises the initial hyperpolarising input to widespread cortical regions, the location of which remains unknown.

The areas originating K-complexes are much debated. As long ago as the 1950s, the cingulate gyrus was proposed as the area originating K-complexes[16,17]. Initially this was based on source-localisation from scalp EEG recordings, but such conclusions were limited by poor spatial coverage and the tendency for traditional simple dipole models to attribute diffuse bilateral cortical activity to a deep midline source. More sophisticated contemporary source localisation techniques employing high definition EEG and distributed source modelling could not provide convincing evidence for the involvement of the cingulate gyrus in the generation of K-complexes[17]. EEG-fMRI studies [20,21] have implicated deep midline structures including the cingulate gyrus in some aspects of K-complex physiology, but the area responsible for initiating K-complexes was not identified. Intracranial EEG has provided more direct insight into this question. Early studies in cats[22] and monkeys[23] highlighted a cingulate generator for the K-complex, but the transferability of such findings to humans is questionable. In contrast, intracranial EEG recordings in humans have suggested that the cingulate cortex and functionally related mesial frontal structures appear uninvolved in generating the visible human K complex waveform [24], although the site of initiation of the K-complex could not be resolved at the level of EEG macroelectrodes.

At our centre, we have developed a novel approach to investigate the generators of K-complexes. Patients studied with intracranial EEG recordings routinely undergo assessment with single pulse electrical stimulation (SPES) to aid identification of epileptogenic cortex[25–29]. Essentially, a single small electrical pulse (3-5mA amplitude, 1ms duration) is applied between contiguous electrodes, and EEG responses are recorded by remaining electrodes. In the course of our practice, we observed that stimulation of some regions induced

responses of marked similarity to the patient's K complexes. In the present work, we report these areas, and quantify the resemblance between SPES responses and K-complexes. To our knowledge, we provide the first causal evidence that K-complexes are initiated by the cingulate cortex.

## 2. METHODS

### Subjects

Records from all 269 patients assessed for epilepsy surgery with intracranial electrodes and SPES at King's College Hospital (London) between January 1999 and December 2013 were reviewed. The study included all patients who had:

1. Bihemispheric intracerebral (depth) electrodes.
2. Frontal lobe intracerebral electrodes.
3. Intracranial sleep stage II recordings.

Patients with the following criteria were excluded:

1. Previous resective neurosurgery.
2. Continuous abnormalities in the background EEG precluding identification of K-complexes and/or SPES responses.

The development of SPES was approved by the ethical committee of King's College Hospital (99-017). SPES is now part of the clinical protocol for presurgical assessment of patients with epilepsy with intracranial recordings.

### Electrodes

In all patients, bilateral multicontact flexible bundles of depth (intracerebral) electrodes (AdTech Medical Instruments Corp., WI, USA) were implanted stereotactically under MRI guidance at sites which included frontal, parietal and temporal locations. Each electrode bundle contained 6–10 cylindrical 2.3 mm platinum electrodes, with adjacent electrode centres separated by 5 mm. The location of depth electrodes was verified by postimplantation skull X-ray, brain CT or MRI. The type, number and location of the electrodes were determined by the suspected location of the ictal onset region, according to non-invasive evaluation: clinical history, scalp EEG recordings obtained with the Maudsley system[30,31], neuropsychology[32] and neuroimaging. The selection criteria and implantation procedure have been described elsewhere[25].

### Recording protocol

Recording of intracranial EEG started when the patient had recovered from electrode implantation, usually 24-48 hours after surgery. Cable telemetry with up to 64 recording channels was used for data acquisition with simultaneous video monitoring. In two patients, a Telefactor Beehive-Beekeeper system (Astro-Med, RI, USA)

was used. Data were digitized at 200 Hz and band pass filtered (high pass cut-off frequency at 0.3 Hz and low pass cut-off frequency at 70 Hz). The system input range was 2 mV and data were digitized with a 12 bit analog-to-digital converter (amplitude resolution of 0.976 μV). In four patients, a Medelec-Profile system was used (Medelec, Oxford Instruments, United Kingdom). Data were digitized at 256 Hz (two patients) or 1024 Hz (two patients) and band pass filtered (0.05-70 Hz). The input range was 10 mV and data were digitized with a 22 bit analog-to-digital converter (an amplitude resolution of 0.153 μV). Interictal awake and sleep recordings in addition to ictal recordings were permanently stored in hard drives. Data were recorded as common reference to Cz-Pz or to an intracranial electrode, and displayed in a variety of montages, including common average reference.

**SPES protocol**

SPES was applied sequentially between pairs of adjacent electrodes with a constant current neurostimulator (Medelec ST10 Sensor, Oxford Instruments or Leadpoint, Medtronic) using monophasic single pulses (0.1-0.2Hz, 1ms, 3-5mA). At least 20 stimuli were delivered at for each stimulated site. Either all electrodes (patients 1, 3, 5 and 6) or only the electrodes located in grey matter (patients 2 and 4) were used to stimulate. EEG responses to each pulse were recorded through the non-stimulating electrodes. A more detailed description of the experimental protocol for SPES is described elsewhere[26–29]. SPES protocol was always started with the patient awake. SPES responses resembling K-complexes will be called “K-complex like” responses to emphasise that, despite their resemblance to K-complexes, SPES responses did not fulfil the standard definition of K-complexes (occurrence during sleep either spontaneously or in response to sensory stimulation).

**Identification of K-complexes**

In contrast to scalp recordings, where K complexes are usually bilaterally symmetrical and largest at the midline, there are not established criteria to identify K-complexes in intracranial recordings. We have followed some of the standard scalp criteria in addition to those described by Wennberg[24] with simultaneous intracranial and scalp recordings. In essence, we identified K-complexes in our intracranial records as high amplitude (>50μV) bilateral frontal biphasic waveforms lasting longer than 0.5 sec, often preceded or followed by a sleep spindle. The presence of bilateral intracranial frontal electrodes was required in our patient population because our cohort included patients with focal frontal epilepsy, who may show unilateral sleep-activated focal discharges that could be wrongly identified as K complexes.

**Comparison of recordings**

Intracranial EEG was analysed using ASA4.8.1$^{TM}$ in referential montage (reference to Cz or Pz). Researchers undertaking EEG analysis were blinded to electrode placement and patient details. The first 20 K-complexes occurring during sleep were identified visually, and 4 second epochs centred at the event were averaged to create a per-patient averaged K-complex. K-complex selection was reviewed independently by authors AV and GA. Interictal awake recordings were also reviewed for K-complex-like spontaneous interictal epileptiform discharges. Where present, the first 20 of such discharges were averaged using the same method. Similarly, for each pair of stimulating electrodes, 20 SPES responses were averaged in 4-second epochs and compared visually against the average of K-complexes or spontaneous interictal epileptiform discharges. For each electrode bundle, the averaged responses of greatest visual similarity to the averaged K-complex and/or epileptiform discharge were submitted for quantitative analysis as below.

*Quantitative analysis*

Computer software was implemented in Matlab (The Math Works Inc., USA) to quantify the similarity between averaged SPES responses, averaged K complexes and averaged spontaneous interictal epileptiform discharges.

For each patient, averaged K-complexes, responses to SPES and spontaneous interictal epileptiform discharges (where available) were compared to each other in one-to-one comparisons. Because there was no a priori synchronising marker for recordings to be compared, an initial synchronising time for all channels was necessary. This was achieved by calculating the compound amplitude at each latency. The compound amplitude was defined as the summation of the absolute values of the amplitudes of each recording channel at the latency in question. Further synchronisation was then implemented for each recording channel in order to quantify the similarity between waveforms. Hence, for any two recordings to be compared, synchronisation was carried out in a two stage process (figure 1):

1) The two recordings were shifted and synchronised at the time of the largest compound amplitudes ("initial synchronising time") (figure 1a). After that, SPES artifact was removed by flattening the record 150ms before and after the peak of the stimulus artifact. The averaged waveforms were smoothed with a moving average of 20ms (1/50 of the sample rate) (figure 1b).
   The initial synchronising time provides a time baseline that takes into account all channels from which the following step will start.
2) A second optimized synchronisation was calculated for each channel with the data window between 500ms before and 1500ms after the initial synchronising time (figure 1c) in order to quantify the similarity between waveforms of homonymous channels. For homonymous recording channels, the correlation coefficients and their significance values were calculated after successive one-sample time shifts of one of the two recordings to be compared. This was carried out for time shifts between 175ms before and after the initial synchronising time. For each channel, the time shift used to yield the highest correlation coefficient was the "final synchronising time". Values of the final synchronising

time between 70 ms before and 100 ms after the initial synchronising time included all values between 10$^{th}$ and 90$^{th}$ percentiles of all final synchronising times. Homonymous channels with a final synchronising time beyond these limits were considered “dissimilar” channels.

In summary, the final synchronising time is defined for each channel, and is an indication of the degree of time shifting from the overall (initial) synchronising time which is required to obtain the highest correlation for each channel.

As the correlation coefficient does not take into account signal amplitude, traces markedly different in amplitude can misleadingly yield a high correlation coefficient. To minimise this effect, once each channel was synchronised at the final synchronising time, amplitudes were adjusted to yield the least square difference between waveforms (figure 1d). Amplitude adjustments consisting of increments by a factor of 3.3 or decrements by 0.3 (i. e, more than 70% of the largest amplitude) included all values between the 10$^{th}$ and 90$^{th}$ percentiles of all least square differences. Consequently, if amplitude adjustments greater than 70% of the largest were required, channels were considered too different to resemble each other (see below) and therefore considered “dissimilar” channels. This prevented low amplitude background noise from being selected for analysis.

Homonymous channels were considered “similar” to one another where the following three criteria were met:

a) The final synchronising time occurred between 70ms before or 100ms after the initial synchronising time.
b) The difference in amplitude between both channels was less than 70% of the largest.
c) The highest correlation coefficients exceeded 0.5 with $p<0.01$.

In order to quantify the similarity between two recordings, we have defined the similarity index (SI) between two recordings as the percentage of similar homonymous channels. SPES responses were deemed similar to K-complexes (*K-complex like responses*) if the overall SI exceeded 50%., i.e. 50% or more of homonymous channels were similar.

In a final phase of analysis, stimulation sites were grouped into regions: orbitofrontal, lateral frontal, parietal, temporal, rostral anterior cingulate and dorso-caudal anterior cingulate. The proportion of similar SPES responses and K-complexes elicited by stimulation of each region was calculated. The differences between these proportions were analysed using a chi-square test.

## 3. RESULTS

### Patients

Out of the initial 269 patients, the inclusion and exclusion criteria identified 6 patients (2 men, 4 women; median age 35; range 24-49). Their characteristics are shown in table 1. Patients had between 6 and 10 electrode bundles, ranging from 45 to 68 electrodes per patient. Figure 2 shows all electrodes implanted in all 6 patients. All patients had electrodes located in medial and lateral frontal areas bilaterally. In addition, 4 patients had additional electrodes located in orbitofrontal areas, 3 had electrodes located in temporal areas and 1 in the parietal lobe. Intracranial recordings in all 6 patients were obtained with reference to a midpoint between Cz and Pz.

During sleep, all six patients showed K-complexes.

Four patients subsequently underwent frontal resections for the treatment of epilepsy. Histopathology revealed Taylor type focal cortical dysplasia (type 2) in 3 subjects and a dysembryoplastic neuroepithelial tumor in one.

### Similarity between K-complexes and SPES responses

SPES responses occurred after each stimulus at 98.5% of stimulated sites and were highly stereotyped across repeats of identical stimulation at each recording electrode. Conversely, the morphology, amplitude and distribution of SPES responses varied markedly with the stimulated region, ranging from low amplitude deflections to widespread, bilateral responses. Examples are shown in Figures 3 and 4.

Visual analysis: Stimulation at sites in the anterior cingulate frequently resembled sleep K complexes. Conversely, stimulation of lateral frontal cortex, posterior cingulate, orbitofrontal cortex, temporal lobe (including hippocampal) or parietal regions did not readily elicit responses resembling K-complexes.

Quantitative analysis: Figure 5 shows the stimulation sites that induced SPES responses with SI (similarity index, see Methods) exceeding 50% (n=14) when compared to sleep K-complexes. All responses showing SI above 50% were induced by stimulation of the frontal cortex, and most were in the anterior cingulate gyrus. By contrast, no responses induced by stimulation of the posterior cingulate, temporal or parietal regions showed responses with SI above 50%.

Among the 14 recordings with SI above 50%, the median SI was 69.49% (SD= 10.37). In some cases, similarity to K-complexes was as high as 81% of channels exhibiting correlation coefficients >0.75 (Figure 3). Moreover, for each patient, the stimulation site which elicited the highest SI between SPES responses and K-complexes was located in the anterior cingulate gyrus or in the underlying white matter (figures 5 and 6); more specifically, in or by the dorso-caudal half of the anterior cingulate gyrus (red dots Figure 5, SI: mean= 75.80%, SD= 12.22).

The median amplitude of K-complexes was 464.57 µV (range 203.56-772.41 µV) and that of the most similar SPES responses was 642.68 µV (range 192.07-793.77 µV).

All patients remained awake during stimulation of the regions inducing K-complex-like responses.

Table 2 summarises the degree of similarity between K complexes and SPES responses when stimulating at different regions. For each stimulated region, Table 2 shows the number and proportion of homonymous channels meeting the criteria for similarity (see Methods). Responses to stimulation of the dorso-caudal anterior cingulate (n=24) showed the highest proportion of similar channels (63.33%). All other regions bore less than 35% of channels exhibiting similarity. Chi-square analysis revealed the existence of differences in the proportion of similar channels among regions ($p<0.0001$; 63.33% observed vs 35.88% expected), which attributable to the increased proportion of similar channels when stimulating at the dorso-caudal anterior cingulate.

**Similarity between spontaneous interictal discharges and SPES responses**

Two patients (patients 2 and 6 in table 2) exhibited interictal epileptiform discharges during wakefulness that resembled each patient's K-complex (SI: 55.54% and 70.00% respectively). Of note, both were subsequently found to have histology-confirmed focal cortical dysplasia in the anterior cingulate gyrus, in contrast to the other four patients.

## 4. DISCUSSION

We have found that electrical stimulation of the frontal lobes while awake can induce responses similar to sleep K-complexes. The responses of greatest similarity are elicited by stimulation of the anterior cingulate gyrus or its underlying white matter (red dots in figure 5). Their similarity is apparent both visually and quantitatively. Stimulation of other regions including the posterior cingulate, orbitofrontal, medial frontal, temporal, hippocampal or parietal areas did not induce such responses. Our findings are consistent with a model in which the dorso-caudal anterior cingulate initiates, and possibly coordinates, the widespread synchronous cortical process that constitutes the K-complex. Indeed, slow waves and K-complex-like responses can also be evoked by cortical transcranial magnetic stimulation over sensorimotor areas [33]. However, previous studies with intracranial EEG recordings in humans have suggested that the cingulate cortex and functionally related mesial frontal structures appear uninvolved in generating the visible human K complex waveform [24]. This discrepancy is most likely due to differences in methodology: whereas EEG localisation identifies the generator of activity at a given time, electrical stimulation used in the present work identifies the structure involved in "initiating" the course of events that will generate the K-complex.

K-complexes are thought to be related to sleep arousals rather than sleep generation. Therefore it is perhaps not surprising that K-complex-like responses can be induced by unilateral stimulation in awake patients without inducing sleep. This suggests that cingulate stimulation activates only part of the circuits involved in sleep, probably sparing the subcortical loops. This supports that K-complex generation largely relies on cortico-cortical connections. Indeed, the slow cortical oscillations involved in the genesis of K-complexes[3] appear to be intrinsically generated in cortical neurons[10]. Moreover, there are profuse bilateral connections between medial frontal cortices[34], which may be responsible for the bilateral cortical involvement seen during both, normal sleep K-complexes and electrically induced K-complexes[7]. In the generation of normal sleep K-complexes, subcortical structures could modulate cortical excitability, allowing for neuronal synchronization similar to that induced by focal stimulation of the anterior cingulate in our awake patients.

The neurochemical and electrophysiological state of the brain is very different between sleep and awake states. The fact that we can induce "sleep" phenomena while awake suggests that some sleep mechanisms are somehow present but "latent" during wakefulness, and can be activated by stimulation of the appropriate site while awake. Moreover, it is possible that by stimulating the cingulate gyrus we are activating only a sub-branch of the "K-complex" pathway. In that case we would expect only a channel subset within the SPES response to simulate K-complexes in contrast to what we have observed.

Other relatively large-amplitude evoked slow responses arising from medial cortical structures (such as the P300) during wakefulness have been proposed as a marker of conscious perception [35,36], a proposal that has been recently challenged by evidence suggesting that these responses are absent when conscious perception is present [37,38]. Our results, showing that large slow responses can be elicited by SPES of the

frontal cortex without subjects being conscious of the stimulus, provide new insight in this debate as they may represent a more general default-mode of reactivity.

Anterior cingulate stimulation consistently induced K-complex like responses but not sleep spindles. This suggests that the physiology of K-complexes is independent from that of sleep spindles. In contrast to K-complexes, spindles are expressed in the cortex via thalamo-cortical excitatory projections[9] and K-complexes appear to trigger sleep spindles probably due to connections between cortex and the reticular nucleus of the thalamus. However, our findings suggest that during wakefulness, cingulate stimulation is unable to activate these loops in a fashion which induces sleep or spindles.

This study with intracranial electrodes was necessarily limited to patients with epilepsy. Anti-epileptic medication has been shown to reduce the abundance of K-complexes[39–41] but to date there is no evidence that their morphology or distribution is altered[24]. The question of whether epilepsy itself may have influenced our findings is more complex. In our series, seizure onset in 4 out of 6 patients did not involve medial frontal cortex, suggesting that our observations are not necessarily due to abnormalities in cingulate cortex. Responses to SPES and spontaneous epileptiform discharges show similar characteristics in terms of cellular behaviour[25], EEG morphology[42,43] and cognitive effects[44]. Both appear to share similar generic physiological mechanisms and spontaneous interictal epileptiform discharges could be considered as triggered by some form of endogenous stimulation or synchronisation. Therefore, it is possible that lesions at the region whose stimulation induces K-complexes can also originate interictal discharges similar to K-complexes, as observed in two of our patients with anterior cingulate cortical dysplasia.

The beauty of this study is that the localising power is not only provided by the EEG itself, but also by the stimulation site, i.e. the initiator of a spontaneous event is identified by the site whose stimulation induces a response similar to the spontaneous event in question, making localisation independent from the montage used.

It could be argued that our patients had a predominance of frontal electrodes compared to other lobes (figure 2). Patients with bilateral frontal electrodes were deliberately chosen because stimulating at extra-frontal structures in the total population of 269 patients did not induce responses remotely similar to K-complexes. For instance, SPES responses to hippocampal stimulation induces bilateral responses only in 5% of patients [34,45], and when they occur, they are grossly asymmetrical. Furthermore, even within the frontal lobes, the similarity between SPES responses and K-complexes is highly specific of stimulation of the dorso-caudal anterior cingulate or its underlying white matter (table 2). In any case, the cortical region within the anterior cingulate responsible for K-complex like responses appears to be rather specific. For instance, in patients 1 and 6, stimulation of the deepest contacts of the bundle located at the anterior cingulate did not induce the responses with highest similarity to K-complexes, despite being located in regions apparently similar to those of the remaining four patients (figure 6). However, in these two patients, SPES responses most similar to K-complexes were induced when stimulating the white matter underlying the anterior cingulate, which could be explained by stimulation of axons projecting to the anterior cingulate gyrus.

## 5. CONCLUSIONS

This study has implications for sleep physiology. Our findings provide the first causal evidence that the anterior cingulate gyrus initiates widespread synchronous activity that resembles K-complexes. Moreover, cingulate stimulation can induce responses similar to K-complexes during wakefulness, suggesting that subcortical structures may not be required for initiating K-complexes.

**References**


[1] Iber C, Ancoli-Israel S, Chesson AL, Quan SF. AASM - Manual for the Scoring of Sleep and Associted Events. 2007.

[2] Loomis AL, Harvey EN, Hobart, Garret A. I. Distribution of disturbance-patterns in the human electroencephalogram, with special reference to sleep. J Neurophysiol 1938;1:413–30.

[3] Amzica F, Steriade M. The functional significance of K-complexes. Sleep Med Rev 2002;6:139–49.

[4] Halász P, Pál I, Rajna P. K-complex formation of the EEG in sleep. A survey and new examinations. Acta Physiol Hung 1985;65:3–35.

[5] Johnson LG, Karpan WE. Autonomic correlates of the spontaneous K-complex 1968;4:444–53.

[6] Niiyama Y, Satoh N, Kutsuzawa O, Hishikawa Y. Electrophysiological evidence suggesting that sensory stimuli of unknown origin induce spontaneous K-complexes. Electroencephalogr Clin Neurophysiol 1996;98:394–400.

[7] Amzica F, Steriade M. Short- and long-range neuronal synchronization of the slow (< 1 Hz) cortical oscillation. J Neurophysiol 1995;73:20–38.

[8] Cash SS, Halgren E, Dehghani N, Rossetti AO, Thesen T, Wang C, et al. The human K-complex represents an isolated cortical down-state. Science 2009;324:1084–7.

[9] Contreras D, Esteriade M. Cellular Basis of EEG Slow Rhythms : Corticothalamic Relationships 1995;15.

[10] Steriade M, Nuñez A, Amzica F. A novel slow (< 1 Hz) oscillation of neocortical neurons in vivo: depolarizing and hyperpolarizing components. J Neurosci 1993;13:3252–65.

[11] Steriade M, Contreras D, Curró Dossi R, Nuñez A. The slow (< 1 Hz) oscillation in reticular thalamic and thalamocortical neurons: scenario of sleep rhythm generation in interacting thalamic and neocortical networks. J Neurosci 1993;13:3284–99.

[12] Steriade M, Nuñez A, Amzica F. Intracellular analysis of relations between the slow (< 1 Hz) neocortical oscillation and other sleep rhythms of the electroencephalogram. J Neurosci 1993;13:3266–83.

[13] Hirsch JC, Fourment A, Marc ME. Sleep-related variations of membrane potential in the lateral geniculate body relay neurons of the cat. Brain Res 1983;259:308–12.

[14] Nir Y, Staba RJ, Andrillon T, Vyazovskiy V V., Cirelli C, Fried I, et al. Regional Slow Waves and Spindles in Human Sleep. Neuron 2011;70:153–69.

[15] Massimini M, Huber R, Ferrarelli F, Hill S, Tononi G. The sleep slow oscillation as a traveling wave. J Neurosci 2004;24:6862–70.

[16] Roth M, Shaw J, Green J. The form voltage distribution and physiological significance of the K-complex. Electroencephalogr Clin Neurophysiol 1956;8:385–402.

[17] Gastaut H. Etude électrographique chez l'homme et chez l'animal des décharges épileptiques dites psychomotrices. Rev Neurol 1953;88:310–52.

[18] Wennberg R, Cheyne D. On noninvasive source imaging of the human K-complex. Clin Neurophysiol 2013;124:941–55.

[19] Murphy M, Riedner BA, Huber R, Massimini M, Ferrarelli F, Tononi G. Source modeling sleep slow waves. Proc Natl Acad Sci U S A 2009;106:1608–13.

[20] Dang-Vu TT, Desseilles M, Laureys S, Degueldre C, Perrin F, Phillips C, et al. Cerebral correlates of delta waves during non-REM sleep revisited. Neuroimage 2005;28:14–21.

[21] Czisch M, Wehrle R, Stiegler A, Peters H, Andrade K, Holsboer F, et al. Acoustic oddball during NREM sleep: A combined EEG/fMRI study. PLoS One 2009;25:e6749.

[22] Hughes JR, Mazurowski JA. Studies on the supracallosal mesial cortex of unanesthetized, conscious mammals: I. Cat. B. Electrical activity. Electroencephalogr Clin Neurophysiol 1959;11:459–69.

[23] Hughes JR, Mazurowski JA. Studies on the supracallosal mesial cortex of unanesthetized, conscious mammals: II. Monkey. D. vertex sharp waves and epileptiform activity. Electroencephalogr Clin Neurophysiol 1964;16:561–74.

[24] Wennberg R. Intracranial cortical localization of the human K-complex. Clin Neurophysiol 2010;121:1176–86.

[25] Alarcón G, Martinez J, Kerai S V, Lacruz ME, Quiroga RQ, Selway RP, et al. In vivo neuronal firing patterns during human epileptiform discharges replicated by electrical stimulation. Clin Neurophysiol 2012;123:1736–44.

[26] Flanagan D, Valentín A, García Seoane JJ, Alarcón G, Boyd SG. Single-pulse electrical stimulation helps to identify epileptogenic cortex in children. Epilepsia 2009;50:1793–803.

[27] Valentín A, Alarcón G, Honavar M, García Seoane JJ, Selway RP, Polkey CE, et al. Single pulse electrical stimulation for identification of structural abnormalities and prediction of seizure outcome after epilepsy surgery: A prospective study. Lancet Neurol 2005;4:718–26.
[28] Valentín A, Alarcón G, García-Seoane JJ, Lacruz ME, Nayak SD, Honavar M, et al. Single-pulse electrical stimulation identifies epileptogenic frontal cortex in the human brain. Neurology 2005;65:426–35.
[29] Valentín A, Anderson M, Alarcón G, Seoane JJG, Selway R, Binnie CD, et al. Responses to single pulse electrical stimulation identify epileptogenesis in the human brain in vivo. Brain 2002;125:1709–18.
[30] Kissani N, Alarcon G, Dad M, Binnie CD, Polkey CE. Sensitivity of recordings at sphenoidal electrode site for detecting seizure onset: Evidence from scalp, superficial and deep foramen ovale recordings. Clin Neurophysiol 2001;112:232–40.
[31] Fernández Torre JL, Alarcón G, Binnie CD, Seoane JJ, Juler J, Guy CN, et al. Generation of scalp discharges in temporal lobe epilepsy as suggested by intraoperative electrocorticographic recordings. J Neurol Neurosurg Psychiatry 1999;67:51–8.
[32] Akanuma N, Koutroumanidis M, Adachi N, Alarcón G, Binnie CD. Presurgical assessment of memory-related brain structures: The Wada test and functional neuroimaging. Seizure 2003;12:346–58.
[33] Massimini M, Ferrarelli F, Esser SK, Riedner B a, Huber R, Murphy M, et al. Triggering sleep slow waves by transcranial magnetic stimulation. Proc Natl Acad Sci U S A 2007;104:8496–501.
[34] Lacruz ME, García Seoane JJ, Valentin A, Selway R, Alarcón G. Frontal and temporal functional connections of the living human brain. Eur J Neurosci 2007;26:1357–70.
[35] Sergent C, Baillet S, Dehaene S. Timing of the brain events underlying access to consciousness during the attentional blink. Nat Neurosci 2005;8:1391–400.
[36] Dehaene S, Changeux JP. Experimental and Theoretical Approaches to Conscious Processing. Neuron 2011;70:200–27.
[37] Melloni L, Schwiedrzik CM, Müller N, Rodriguez E, Singer W. Expectations change the signatures and timing of electrophysiological correlates of perceptual awareness. J Neurosci 2011;31:1386–96.
[38] Pitts M a., Metzler S, Hillyard S a. Isolating neural correlates of conscious perception from neural correlates of reporting one's perception. Front Psychol 2014;5:1–16.
[39] Colrain IM. The K-complex: a 7-decade history. Sleep 2005;28:255–73.
[40] Johnson LC, Hanson K, Bickford RG. Effect of flurazepam on sleep spindles and K-complexes. Electroencephalogr Clin Neurophysiol 1976;40:67–77.
[41] Legros B, Bazil CW. Effects of antiepileptic drugs on sleep architecture: A pilot study. Sleep Med 2003;4:51–5.
[42] Nayak D, Valentín A, Selway RP, Alarcón G. Can single pulse electrical stimulation provoke responses similar to spontaneous interictal epileptiform discharges? Clin Neurophysiol 2014;125:1306–11.
[43] Valentin A, Lazaro M, Mullatti N, Cervantes S, Malik I, Selway RP, et al. Cingulate epileptogenesis in hypothalamic hamartoma. Epilepsia 2011;52:e35–9.
[44] Lacruz ME, Valentín A, Seoane JJG, Morris RG, Selway RP, Alarcón G. Single pulse electrical stimulation of the hippocampus is sufficient to impair human episodic memory. Neuroscience 2010;170:623–32.
[45] Jiménez-Jiménez D, Abete-Rivas M, Martín-López D, Lacruz ME, Selway RP, Valentín A, et al. Incidence of functional bi-temporal connections in the human brain in vivo and their relevance to epilepsy surgery. Cortex 2015;5:0–10.

**Legends**

Figure 1: Four samples of the signal processing steps. For each step, the correlation coefficient (r) and the least square difference (LS) are shown. First, for each channel, an averaged K-complex and an averaged SPES response are shifted and synchronised at initial synchronising time (a). After that, SPES artifact is removed (b). The second optimized synchronisation (final synchronising time) is calculated for each channel (c) and amplitudes are adjusted (d). Different situations are reflected in each sample. Sample 1 represents an example of high similarity between the K-complex and the SPES response. Sample 2 also shows similar waveforms after some time shifting. Sample 3 reflects different waveforms that share a restricted similarity due to a positive deflection (downwards) in a segment of the recording. Sample 4 illustrates the case of very different waveforms that even reaches the limit of time shifting (step c).

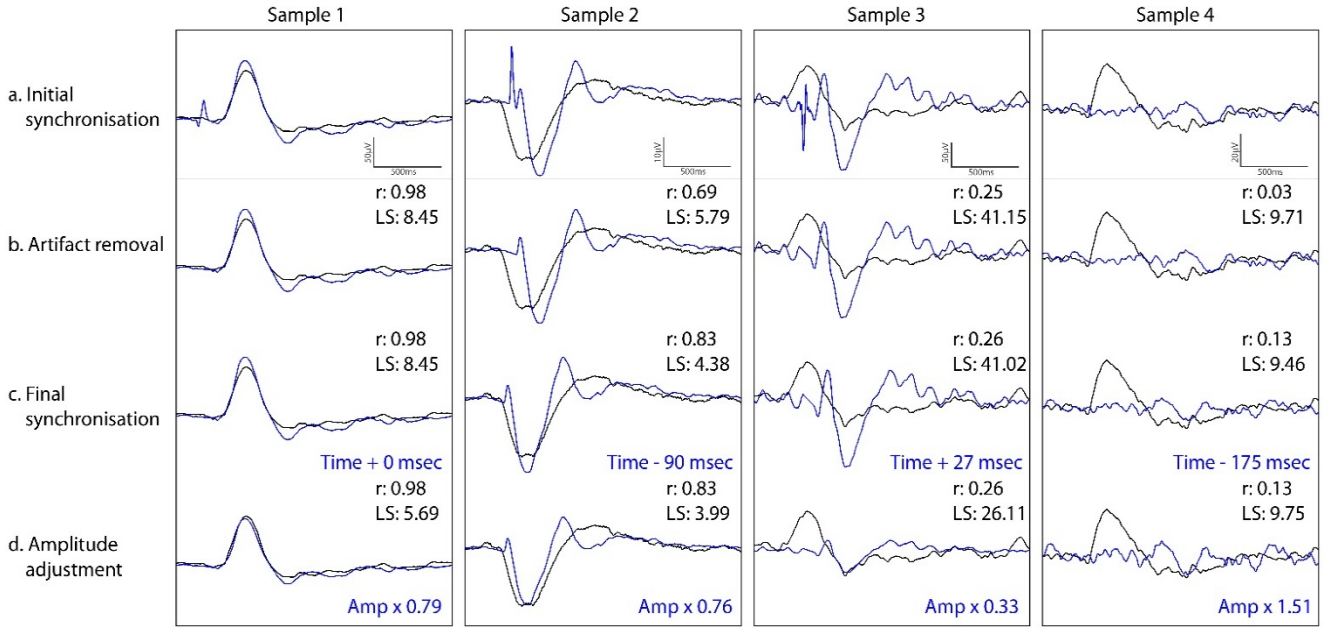

Figure 2: Spatial distribution of implanted sites (white circles) in all patients. R= Right, L=Left.

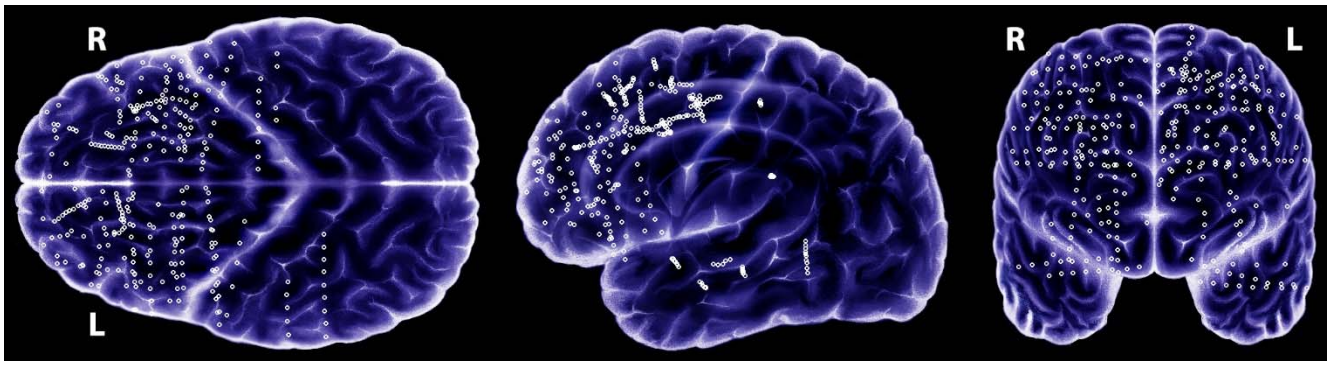

Figure 3. Example of response similar to K-complex from patient 2 after stimulation of dorso-caudal anterior cingulate. Top: Resemblance between averaged spontaneous K-complex (left) and SPES response (right). The column between the two recordings shows the correlation coefficient (r) between homonymous channels, showing values of up to 0.97. Bottom: The red dot shows the stimulation site used to induce the SPES response with the highest SI when compared to K-complexes and the yellow dots show all EEG recording sites. The pie chart shows the percentage of homonymous channels with correlation coefficients between 0-0.25 (green), 0.25-0.50 (yellow), 0.50-0.75 (orange), 0.75-1 (red). The percentage of dissimilar channels (see *Methods*) appears in blue. R= Right, L=Left, r=Correlation coefficient.

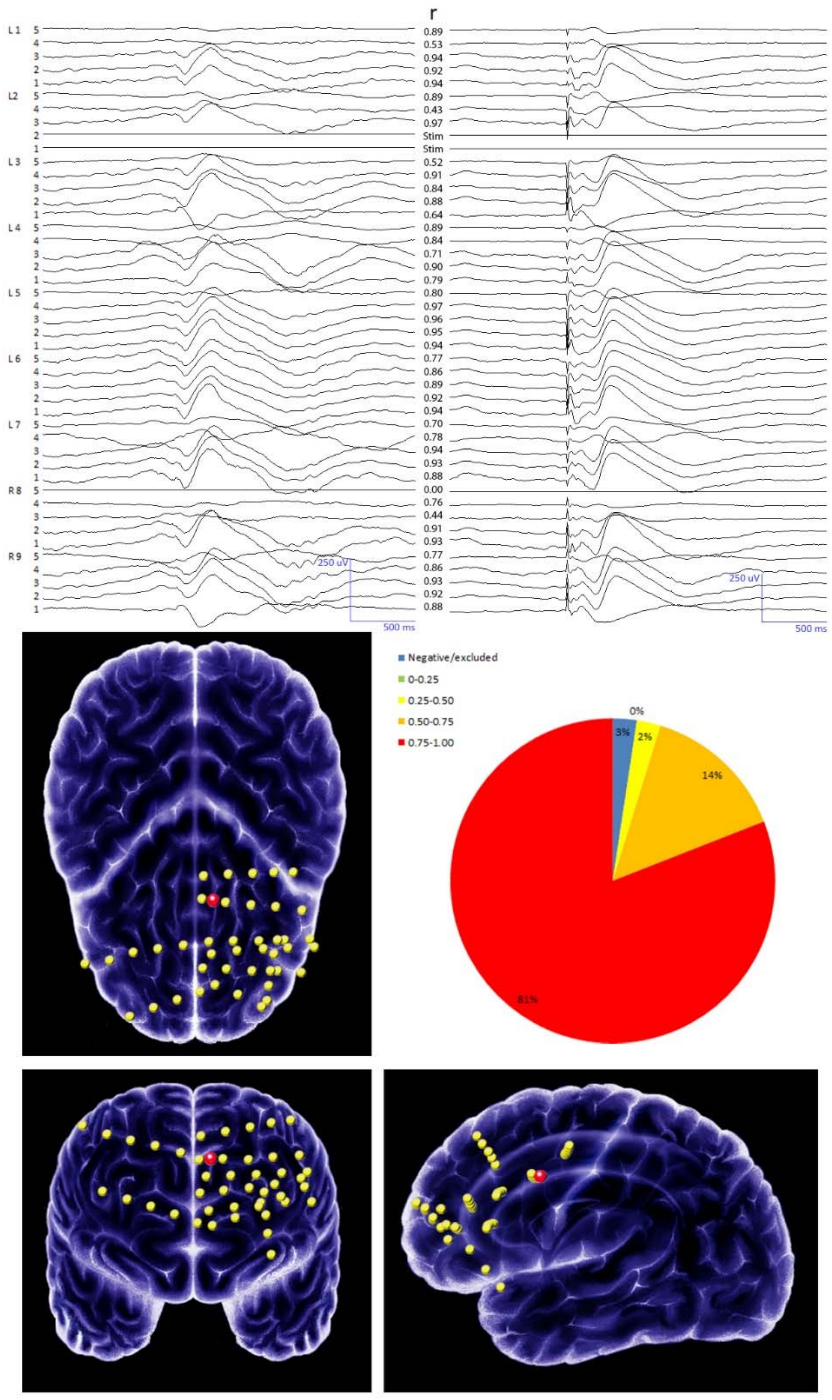

Figure 4. Example of response not similar to K-complex from patient 2 after stimulation of rostral anterior cingulate. Top: Resemblance between averaged spontaneous K-complex (left) and SPES response (right). The column between the two recordings shows the correlation coefficient (r) between homonymous channels. Bottom: The red dot shows the stimulation site used to induce the SPES response with the highest SI when compared to K-complexes and the yellow dots show all EEG recording sites. The pie chart shows the percentage of homonymous channels with correlation coefficients between 0-0.25 (green), 0.25-0.50 (yellow), 0.50-0.75 (orange), 0.75-1 (red). The percentage of dissimilar channels (see *Methods*) appears in blue. Note that most channels were considered dissimilar due to the amplitude or final synchronising time criteria detailed in methods, despite showing r values of up to 0.61. R= Right, L=Left, r=Correlation coefficient.

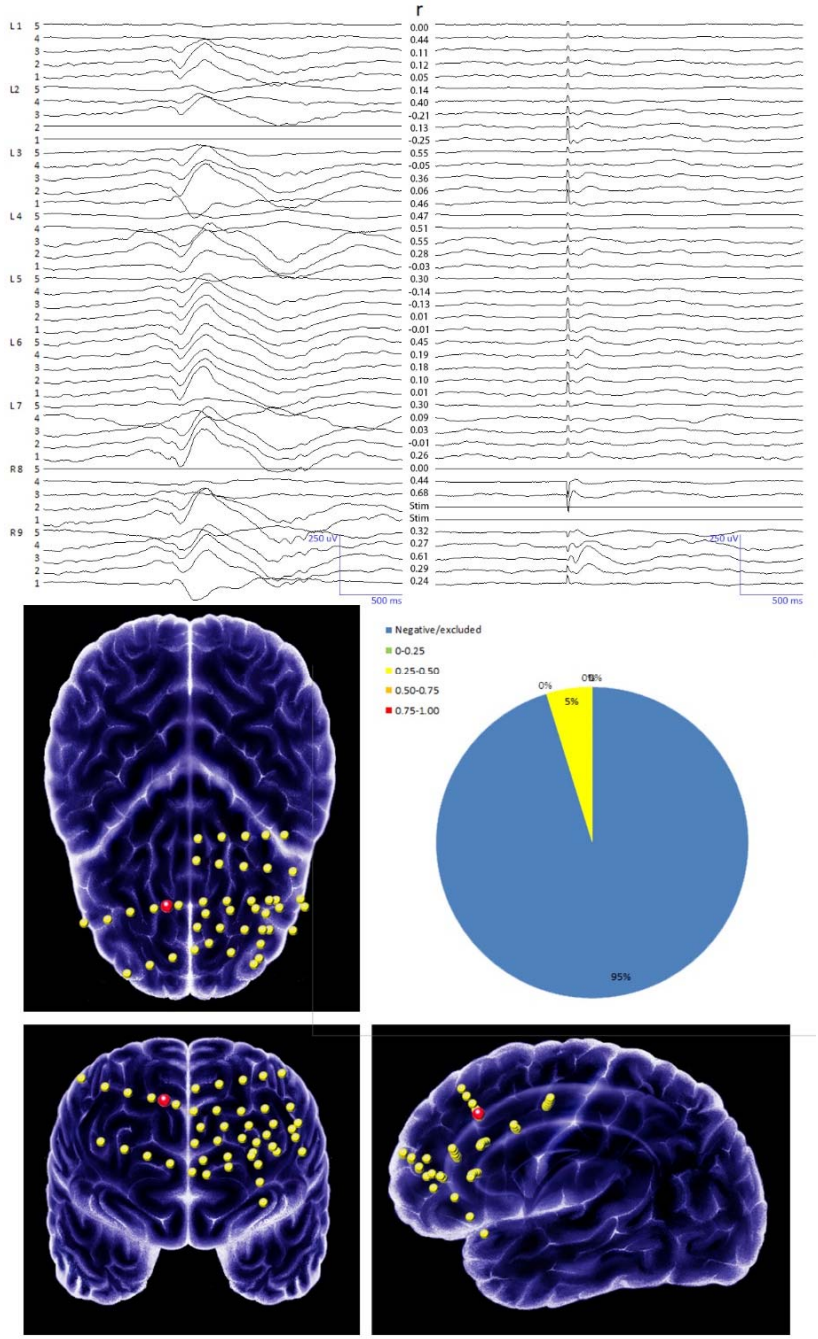

Figure 5. Sites whose stimulation induced SPES responses with SI above 50% (mean= 69.49%, SD= 10.37) when compared to averaged K-complexes in all patients. Red dots represent stimulation sites which elicit the highest SI between SPES responses and K-complexes in each patient (mean= 75.80%, SD= 12.22). R= Right, L=Left.

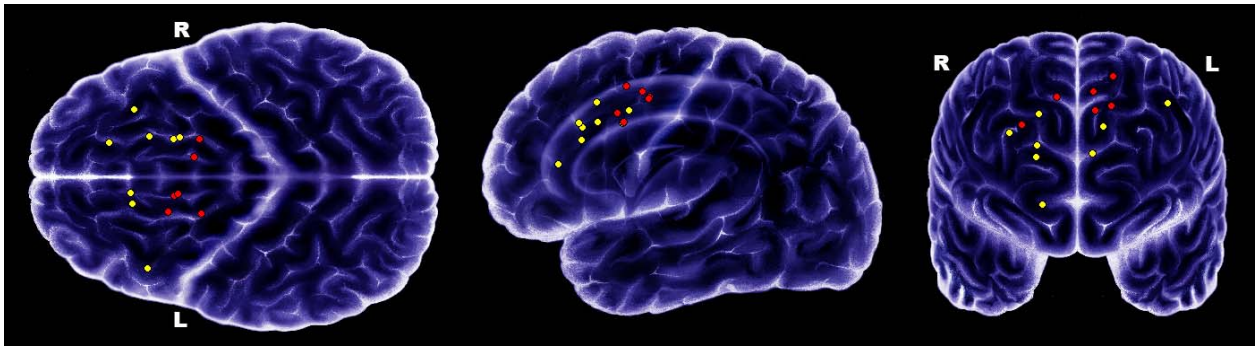

Figure 6. Averaged intracranial K-complexes from each 6 patients displayed in referential montages and topography of the electrodes used to induce the most similar K-complex-like responses. Each graph shows recordings from the electrode bundle used to stimulate the site that induced the responses resembling K-complexes the most. The electrodes used to induce such responses are shown in red. For each electrode bundle, electrode 1 is the deepest, which is located at the anterior cingulate.

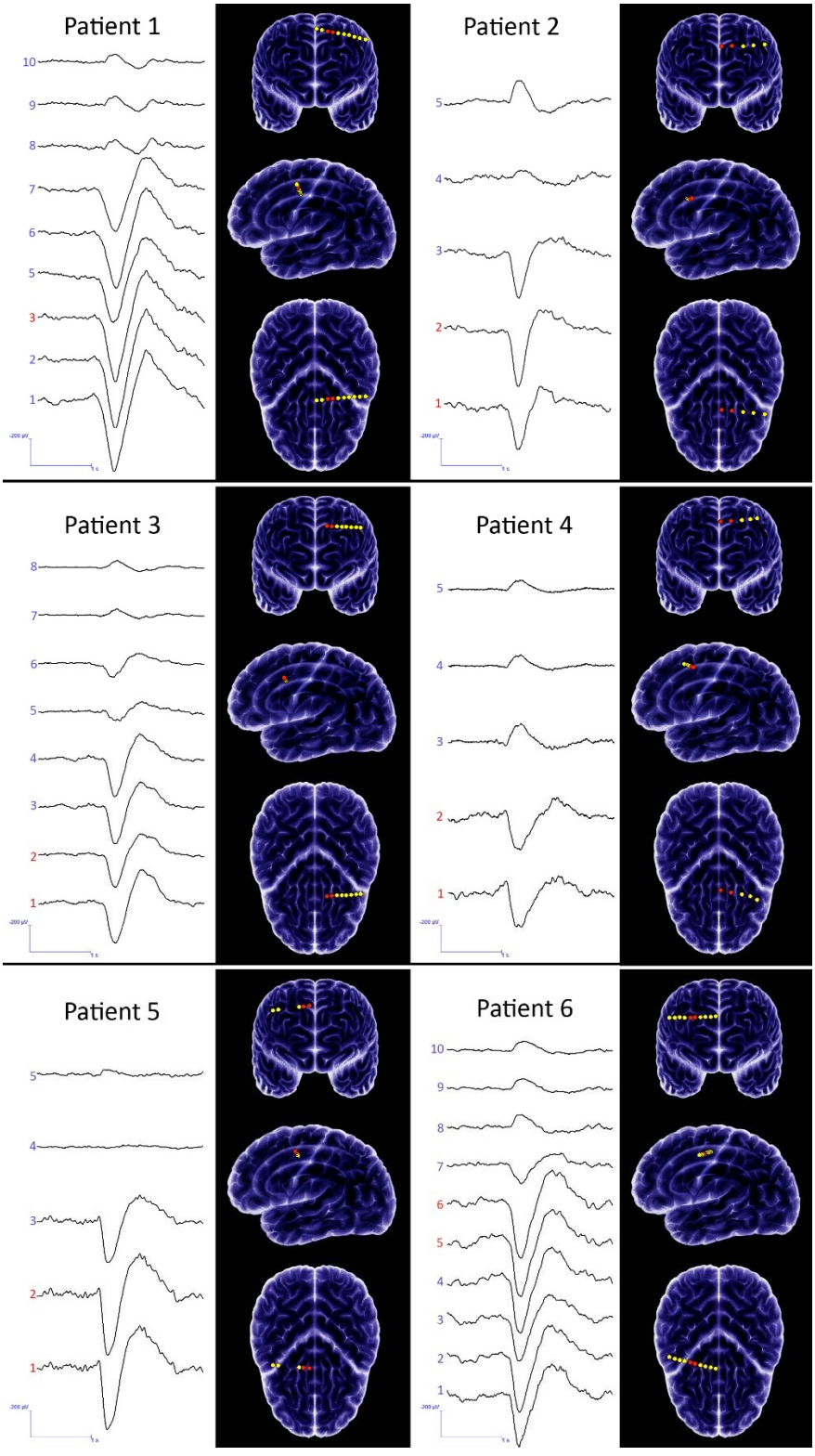

# THE ROLE OF THALAMUS VERSUS CORTEX IN EPILEPSY: EVIDENCE FROM HUMAN ICTAL CENTROMEDIAN RECORDINGS IN PATIENTS ASSESSED FOR DEEP BRAIN STIMULATION

**DAVID MARTÍN-LÓPEZ**
*Department of Clinical Neurophysiology, Kingston Hospital NHS FT, London, UK.*

*Department of Clinical Neurophysiology, St George´s University Hospitals NHS FT, London, UK.*

*Department of Clinical Neuroscience, King's College London, Institute Of Psychiatry, Psychology and Neuroscience, London, UK.*

*Departamento de Fisiología, Facultad de Medicina, Universidad Complutense, Madrid, Spain.*

*E-mail: david.martin_lopez@kcl.ac.uk*

**DIEGO JIMÉNEZ-JIMÉNEZ**
*Department of Clinical Neuroscience, King's College London, Institute Of Psychiatry, Psychology and Neuroscience, London, UK.*

*Department of Clinical Neurophysiology, King's College Hospital NHS FT, London, UK.*

*Universidad San Francisco de Quito, School of Medicine, Quito, Ecuador.*

**LIDIA CABAÑÉS-MARTÍNEZ**
*Servicio de Neurofisiología Clínica Hospital Ramón y Cajal. Madrid*

**RICHARD P. SELWAY**

*Department of Neurosurgery, King's College Hospital NHS FT, London, UK.*

**ANTONIO VALENTÍN[1]**

*Department of Clinical Neuroscience, King's College London, Institute Of Psychiatry, Psychology and Neuroscience, London, UK.*

*Department of Clinical Neurophysiology, King's College Hospital NHS FT, London, UK.*

*Departamento de Fisiología, Facultad de Medicina, Universidad Complutense, Madrid, Spain.*

**GONZALO ALARCÓN[2]**

*Comprehensive Epilepsy Center Neuroscience Institute, Academic Health Systems, Hamad Medical Corporation, Doha, Qatar*

*Department of Clinical Neuroscience, King's College London, Institute Of Psychiatry, Psychology and Neuroscience, London, UK.*

*Department of Clinical Neurophysiology, King's College Hospital NHS FT, London, UK.*

*Departamento de Fisiología, Facultad de Medicina, Universidad Complutense, Madrid, Spain.*

[1]Drs G. Alarcón and A. Valentín are joint senior authors.

Background: The onset of generalised seizures is a long debated subject in epilepsy. The relative roles of cortex and thalamus in initiating and maintaining the different seizure types are unclear. Objective: The purpose of the study is to estimate whether the cortex or the centromedian thalamic nucleus is leading in initiating and maintaining seizures in humans. Methods: We report human ictal recordings with simultaneous thalamic and cortical electrodes from three patients without anaesthesia being assessed for deep brain stimulation (DBS). Patients 1 and 2 had idiopathic generalised epilepsy whereas patient 3 had frontal lobe epilepsy. Visual inspection was combined with nonlinear correlation analysis. Results: In patient 1, seizure onset was bilateral cortical and the belated onset of leading thalamic discharges was associated with an increase in rhythmicity of discharges, both in thalamus and cortex. In patient 2, we observed bilateral independent interictal discharges restricted to the thalamus. However, ictal onset was diffuse with discharges larger in the cortex even though they were led by the thalamus. In patient 3, seizure onset was largely restricted to frontal structures, with belated lagging thalamic involvement. Conclusion: In human generalised seizures, the thalamus may become involved early or late in the seizure but, once it becomes involved, it leads the cortex. In contrast, in human frontal seizures the thalamus gets involved late in the seizure and, once it becomes involved, it lags behind the cortex. In addition, the centromedian nucleus of the thalamus is capable of autonomous epileptogenesis as suggested by the presence of independent focal unilateral epileptiform discharges restricted to thalamic structures. The thalamus may also be responsible for maintaining the rhythmicity of ictal discharges.

Keywords: Intracranial EEG, centromedian nucleus, generalised epilepsy, ictal recordings

## 1. Introduction

Since the first electroencephalographic (EEG) recordings of human absence seizures in the thirties[1], the role of the subcortical structures in human epileptogenesis has long been debated. Currently four main mechanisms have been suggested as candidates to explain the origin of generalised seizures. Each model proposes different relevance for cortical and subcortical structures. The "centrencephalic"[2] and "thalamic clock"[3] theories presume a subcortical origin whereas the "cortico-reticular"[4] and "cortical focus"[5] theories provide a model where the cortex is the leading structure. Nevertheless, the interplay between cortex and thalamus appears to be the key for maintaining typical absence seizures.

Modern advances in neuroimaging and increasing interest in deep brain stimulation (DBS) have revived the discussion. In the present article, we review the available evidence on the generation of generalised seizures and illustrate relevant issues with human ictal recordings obtained with simultaneous thalamic and scalp/subdural electrodes in three patients assessed for deep brain stimulation for the treatment of their epilepsy.

The involvement of subcortical structures such as the thalamus, in the generation of sudden bilaterally synchronous epileptiform discharges was proposed in the forties under the so called 'centrencephalic' hypothesis[2,6,7]. Jasper and Kershman suggested the existence of a deep-lying central focal pacemaker for discharges involving bilateral cortical areas, such as the 3 Hz wave and spike bifrontal synchronous discharges. Hursh observed that these rhythms remained generalised and synchronous after callosotomy suggesting a subcortical origin in the thalamus. Further supporting arguments for the pacemaker function of the thalamus on generalised seizures were suggested by the ability of the thalamic circuits to generate rhythmic patterns due to the intrinsic properties of its neurons and the profuse web of connections with the cortex[8]. Further support for a thalamic origin for generalised discharges was provided by the finding that cortical generalized discharges could be induced by thalamic stimulation in anesthetized rats[9–12].

Nevertheless, other studies fail to show a convincing primary involvement of the thalamus in the generation of spike and wave patterns. In a study with simultaneous scalp and depth electrodes in several subcortical structures[13], it was not possible to identify a thalamic origin for the generalised epileptiform activity. Simultaneous onset was reported for cortical and thalamic discharges. Frequently, 3 Hz spike and wave discharges were seen in the cortex with no changes in thalamic activity. They observed a phase reversal of this activity in or just beneath the cortex. On a few occasions, spikes were recorded independently from subcortical structures but discharges in or around the medial thalamus could not be interpreted as initiating 3 Hz spike-and-wave discharges. In a short series of 4 patients with generalised spike and wave complexes studied with scalp and deep electrodes covering the thalamic structures, no evidence for a primary thalamic focus was found[14].

A study of generalised seizures in cats triggered by metrazol found that ictal activity was always recorded first by cortical electrodes and then progressed to deep structures[15]. Another experimental study of generalised seizures in cats[16] studied with electrodes in cortex and centromedian and dorsomedial thalamic nuclei, failed to demonstrate a significant involvement of thalamic structures at the onset of generalised seizures. In contrast to previous observations in humans[7], Marcus and Watson (1966) noted a disruption in bilateral interhemispheric synchrony after callosotomy, supporting an intracortical, rather than a diencephalic or mesencephalic mechanism for the generation and propagation of generalised seizures.

Further human evidence supported the cortical origin for generalised discharges. Generalised spike-wave discharges in patients suffering petit mal seizures can be induced by injection of pentylenetetrazol and sodium amytal in the internal carotid artery, which supplies cortex, but not thalamus. Conversely, no discharges were induced after injection of the vertebral artery, which supplies thalamus but not cortex[4,17]. Furthermore, electrical stimulation of the frontal lobe in man can induce absence-like attacks[18] and generalised discharges[19].

Other studies in the feline penicillin model concluded that primary generalised epilepsies are caused by a general state of hyperexcitability of cortical neurons, originated by an enhancement of both, Glu/Asp-mediated excitation and GABA-mediated inhibition, that leads to a thalamic dysfunction via thalamo-cortical connections[20]. The thalamocortical circuits involved in the genesis of the generalised spike and wave discharges are proposed to be those sustaining physiological sleep spindles, which in a state of hyperexcitability would lead to the production of spike-wave discharges instead of spindles.

Early studies in anaesthetised humans with petit mal seizures observed the presence of epileptiform activity in the dorsomedial thalamic nucleus that was not always accompanied with cortical spike and wave activity[21]. Human intracranial recordings with electrodes in thalamus, white matter and cerebral cortex in children during petit mal attacks showed spontaneous 3Hz recruiting rhythms in the thalamus preceding cortical activity by 14 milliseconds and phase reversing within thalamic structures, supporting a thalamic origin[22]. In patients with generalised epilepsy, discharges appeared first in thalamus or simultaneously in thalamus and cortex, but never first in the cortex[23,24].

In five patients suffering generalised seizures studied with scalp and depth electrodes covering thalamic nuclei (centromedian, reticularis, reuniens and limbic nuclei of the thalamus including anterior, medial dorsal and ventral anterior nuclei) thalamic onset and simultaneous initiation in thalamic and extrathalamic structures were observed, but spike and wave discharges were commonly recorded from scalp electrodes and temporal structures preceding at least by half a second those in the thalamus[25].

The relation between thalamic and cortical epileptiform activity has been studied with simultaneous scalp and thalamic recordings (located in centromedian, parafascicularis thalami, amygdaloid and ventrolateral nucleus) in six patients with partial motor, complex partial and generalised seizures assessed for deep brain stimulation[26] . The amplitude gradients and early participation of the centromedian nucleus during the onset and maintenance of non-convulsive and tonic-clonic generalised seizures suggested a leading role of this structure in the generation and propagation of epileptiform activity leading to generalised seizures. Conversely not all epileptiform activity recorded at this nucleus developed into a cortical seizure, suggesting that, although the thalamus is able to generate epileptiform activity by itself, its isolated activation is not enough to develop generalised seizures. This would point to the existence of a nonspecific thalamo-cortical system rather than only a thalamic ascending trigger in the pathogenesis of generalised seizures. With similar methodology, Velasco also described epileptiform activity observed in the centromedian nucleus in four children with Lennox-Gastaut syndrome and different generalised seizure patterns[27]. During atypical absence seizures, epileptiform activity was simultaneously recorded from scalp and thalamic electrodes. Conversely during myoclonic seizures the spike-wave complexes recorded from centromedian nucleus preceded those recorded on the scalp, suggesting an onset for myoclonic seizures in or near this nucleus.

A multisite recording study in WAG/Rij rats[28] revealed selective activation of thalamic nuclei preceding the spike component of the spike-wave discharges, supporting that the thalamus is the leading structure in the generation of generalised epileptiform activity. Buzsaki[3] studied the rhythmical oscillations of thalamic neuronal population and its relation with cortical activities. He described the mechanisms of high-voltage spindle activity in rats (which resembled spontaneous spike-wave discharges in humans) suggesting the existence of a pacemaker in the reticular thalamic nucleus (the ‘thalamic clock’).

In addition to evidence for thalamic involvement in generalised seizures, several studies emphasise the role of cortical function. Analysis of multiunit activity at different thalamo-cortical sites in the genetic absence epilepsy rats from Strasbourg model (GAERS) observed early rhythmic burst-like activities within layers IV/V of the somatosensory cortex which preceded the diffuse cortical and thalamic spike-wave discharges[29]. Meeren et al in the light of observational and experimental findings obtained from humans and, in particular, from experiments in the WAG/Rij model, proposed the cortical focus theory[5,30]. This is a holistic model that integrates thalamic and cortical structures, under the leading influence of the later. They proposed that the perioral region of the somatosensory cortex of the rat as the triggering area for the initial spike, which would then rapidly propagate through the entire cortex via short-range intracortical fibres and long-range association fibres, some of them connecting both hemispheres across the corpus callosum. Some of the projecting axons would reach the thalamus and set a cascade of thalamo-cortical events that transform the initial spike into spike-wave activity. Once the thalamo-cortical resonant circuit has been established, thalamus and cortex drive each other and discharges are amplified and sustained. The generation of the initial spike, as well as local and distal spreading of the epileptiform activity, are possible in the context of a diffuse decrease in GABAergic activity[31], possibly more pronounced on the perioral region of the somatosensory cortex.

Modern neuroimaging has added wood to the fire. Bilateral thalamic involvement during absence seizures has also been observed with functional magnetic resonance imaging (fMRI)[32,33]. Markers of focal neuronal dysfunction had been identified with neuroimaging techniques in the thalamus of patients with typical absence epilepsy[34]. For instance, proton magnetic resonance spectroscopy revealed a decrease in N-acetylaspartate/creatine ratio at the centre of the thalamus, which has been related with neuronal and/or axonal loss. The timing of cortico-thalamic activation in patients with idiopathic generalised epilepsy revealed by EEG-fMRI suggests that the posterior intralaminar nuclei (centromedian and parafascicular part of the cortico-reticular system) are involved in the initiation and early propagation of discharges whereas the anterior nucleus is involved in their maintenance[35]. The timing and topography of the magnetic changes during generalised absence seizures studied with magnetoencephalography (MEG) suggests a source of thalamic activity 50 ms before the beginning of the seizure, immediately followed by activation of the lateral inferior frontal cortex[36]. In addition, a SPECT-EEG study in six patients with childhood absence epilepsy failed to demonstrate a focal onset during ictal or interictal discharges (Yeni et al. 2000).

Positron emission tomography (PET) studies provided further evidence supporting the role of cortical structures in the onset of absence seizures. A PET study performed with simultaneous EEG recordings[37] showed a marked increase in fluorodeoxyglucose uptake over the right frontal region in an 8 year old patient with frequent typical absence seizures. Similar studies[38–40] demonstrated marked bilateral increase in thalamic metabolism and bilateral cortical hypometabolism (mainly in frontal cortex) during absence seizures without clear thalamic activation at seizure onset providing an additional support to the corticothalamic theory.

Quantitative approaches in the study of seizure dynamics rely on identifying regions which are driving EEG activity. When activity propagates with preserved morphology, latency analysis identifying time differences between peaks can characterise propagation patterns and conduction times [41–43]. This could be useful once seizure activity becomes established and is driven by a specific region. However, at seizure onset, EEG waveforms can be different between regions due to the mutual interactions between them. When waveforms are different between recording sites, the phase spectrum of Fourier analysis, spectral coherence and cross correlation have been used to identify leading regions and propagation patterns. Such methods suffer from relatively poor time resolution, which renders them unhelpful during for the analysis of the few milliseconds when seizure onset occurs. A number of non-linear signal processing methods, have been developed over the last decades to overcome some limitations [44–47]. Therefore, for quantitative analysis we have chosen a non-linear method which runs in the time domain (analysis amount of mutual information) in order to preserve the high time resolution of the EEG during the brief period of seizure onset.

### 1.1 Objectives

Clearly, the dichotomy between cortical and thalamic driving for generalised seizures and discharges appears too simplistic, with both structures becoming involved and active during early stages, suggesting a cortico-thalamic network responsible for generalised seizures. We report here human ictal recordings with simultaneous thalamic and cortical electrodes from three patients being assessed for deep brain stimulation,

which illustrate such complexities. The objective of the study is to estimate whether the cortex or the centromedian thalamic nucleus is leading in initiating and maintaining seizures in humans.

## 2. Methods

### 2.1 Subjects

The study includes all patients (table 1) who had seizures during video telemetry with thalamic and scalp electrodes at King's College Hospital (London, United Kingdom) between January 2005 and December 2013 for the assessment of chronic DBS of the centromedian nucleus of the thalamus[48]. Three patients fulfilled these inclusion criteria.

Before implantation, patients were evaluated with clinical history, examination, neuroimaging, scalp EEG and scalp video telemetry recorded with electrodes applied according to the Maudsley System[49,50]. Essentially, the study included patients with generalised or frontal epilepsy. The specific inclusion criteria for DBS implantation have been described elsewhere[48]. Immediately following DBS implantation, patients underwent video telemetry with thalamic and scalp/subdural electrodes in order to record cortical recruiting responses and establish the best stimulation parameters for each patient. The optimal stimulation parameters were identified by the evaluation of seizure frequency and cortical responses to centromedian stimulation, including recruitment responses at 6 Hz and responses to single pulse electrical stimulation (SPES) [51–54]. After telemetry, the subdural electrodes were removed, the system was internalised (Kinetra ©Medtronic) and stimulator turned off. The study was approved by King's College Hospital Ethics Committee and the New Clinical Procedures Committee in 2005. Records from all 9 patients assessed for DBS with both, scalp and thalamic electrodes at King's College Hospital were reviewed retrospectively. The three patients showing epileptic seizures were identified and reported here. The clinical characteristics of these three patients are shown in table 1.

A four-contact electrode bundle (K-3387 or K-3389, Medtronic) was stereotactically implanted in the centromedian nucleus of each hemisphere under general anaesthesia. Within each bundle electrodes have a length of 1.5 mm and inter-electrode spacing was 1.5/0.5 mm. Target location for each electrode was determined using frame (Leksell Coordinate Frame G, Elekta, Stockholm, Sweden)-based atlas coordinates and calculated with STEALTH FRAMELINK 5 software (Medtronic, Inc., Minneapolis, MN, U.S.A.). Electrodes were implanted through bilateral frontal burr holes in a transparenchymal extraventricular trajectory under neurophysiologic monitoring. The final electrode position was decided on the basis of atlas-derived coordinates, intraoperative recordings and the thalamic location where stimulation induced the largest cortical responses. The position of implanted electrodes was checked with intraoperative X-ray or CT scan. In addition, in patient 3, one lateral frontal eight-contact subdural strip electrodes was implanted over the frontal convexity on each hemisphere. A detailed figure of electrode arrangements can be seen in figure 1 of reference[41].

Table 1. Patients' details. M: Male, F: Female. GCTS= Generalised tonic-clonic seizures.

| Patient | Sex | Age | Diagnosis | Onset age (years) | Type of seizures | MRI |
|---|---|---|---|---|---|---|
| **1** | M | 26 | Idiopathic generalised epilepsy. | 8 | Absence seizures and GTCS | Normal |
| **2** | F | 24 | Idiopathic generalised epilepsy. | 9 | Absence seizures and GTCS | Normal |
| **3** | M | 36 | Symptomatic frontal lobe epilepsy. | 9 | Blank spells, complex partial seizures and GTCS. | Mild cerebral atrophy |

**2.3 Recording protocol**

Recording of video EEG started 24-48 hours after electrode implantation after the effects of anaesthesia had ceased. Cable telemetry with up to 64 recording channels was used for data acquisition with simultaneous video monitoring. In all three patients, a Medelec-Profile system was used (Medelec, Oxford Instruments, United Kingdom). Data were digitized at 256 Hz (patients 1 and 3) or 1024 Hz (patient 2) and band pass filtered (0.05-70 Hz). The input range was 10 mV and data were digitized with a 22 bit analog-to-digital converter (an amplitude resolution of 0.153 µV). Interictal awake and sleep recordings were stored in hard drives. Data wer recorded as common reference to Cz-Pz and displayed in a variety of montages, including common averag reference and bipolar montage for the intracranial recordings. All the analysis and figures have been done i bipolar montage to avoid reference contamination. (1)

**2.4 Analysis**

An initial visual inspection was carried out by two accredited consultants in clinical neurophysiology (DML and GA). Quantitative analysis was then carried out to estimate the degree of association between any two recording channels and the corresponding time delay in order to identify the leading structures, according to the methodology described by Meeren et al.[5]. For completeness, we copy the main principles here. The nonlinear correlation coefficient $h^2$ was calculated as a function of time shift ($\tau$) between the two signals. It describes the dependency of a signal *Y* on a signal *X* in a general way. Basically, the amplitude of signal *Y* is considered as a function of the amplitude of signal *X*, the value of y given a certain value of *x* can be predicted according to a nonlinear regression curve. The variance of *Y* according to the regression curve is called the explained variance, i.e., it is explained or predicted on the basis of *X*. By subtracting the explained variance from the total variance one obtains the unexplained variance. The correlation ratio $\eta^2$ expresses the reduction of variance of *Y* that can be obtained by predicting the y values according to the regression curve as follows: $\eta^2$= (total variance - unexplained variance)/total variance. In practice, a numerical approximation of the nonlinear regression curve is obtained by describing the scatterplot of *y* versus *x* by segments of linear regression curves. The variable x is subdivided into bins; for each bin the *x* value of the midpoint ($p_i$) and the average value of *y* ($q_i$) are calculated, and the resulting points ($p_i$,$q_i$) are connected by segments of straight lines (linear regression curves). The nonlinear correlation coefficient $h^2$, can now be computed as the fraction of total variance that can be explained by the segments of linear regression lines, as follows:

$$h^2 = \frac{\sum_{i=1}^{N}(y_i - \langle y\rangle)^2 - \sum_{i=1}^{N}(y_i - f(x_i))^2}{\sum_{i=1}^{N}(y_i - \langle y\rangle)^2},$$

With *N* being the number of samples and *y* being the average of all $y_i$. The estimator $h^2$, which signifies the strength of the association between the two signals, can take values between 0 (*Y* is totally independent of *X*) and 1 (*Y* is completely determined by *X*). In the case of a linear relationship between *x* and y, the $\eta^2$ reduces to the common regression coefficient $r^2$. Similarly, as in the case of the cross-correlation, one can estimate $h^2$ as a function of time shift ($\tau$) between signal *X* and *Y* or vice versa. That shift for which the maximum value for $h^2$ is reached is used as an estimate of the time lag between the two signals.

In the present study, association strengths and their corresponding time delays were determined between all possible pairs of electrodes including scalp and intracranial cortical and thalamic electrodes.

Signals were analysed with MatLab (The Math Works Inc., USA) and subdivided into bins of the same length (100 ms). Maximum and minimum time shifts were 75 ms and 3,9ms (=one sample) for patients 1 and 3 and 75ms and 1ms (=one time sample) for patient 2. Analysis covered from 1 second before seizure onset to 4 seconds after seizure onset, by means of four consecutive time windows ($t_1$, $t_2$, $t_3$ and $t_4$) lasting for 2 seconds with 1 second overlap. For each patient, 8 seizures were selected for analysis.

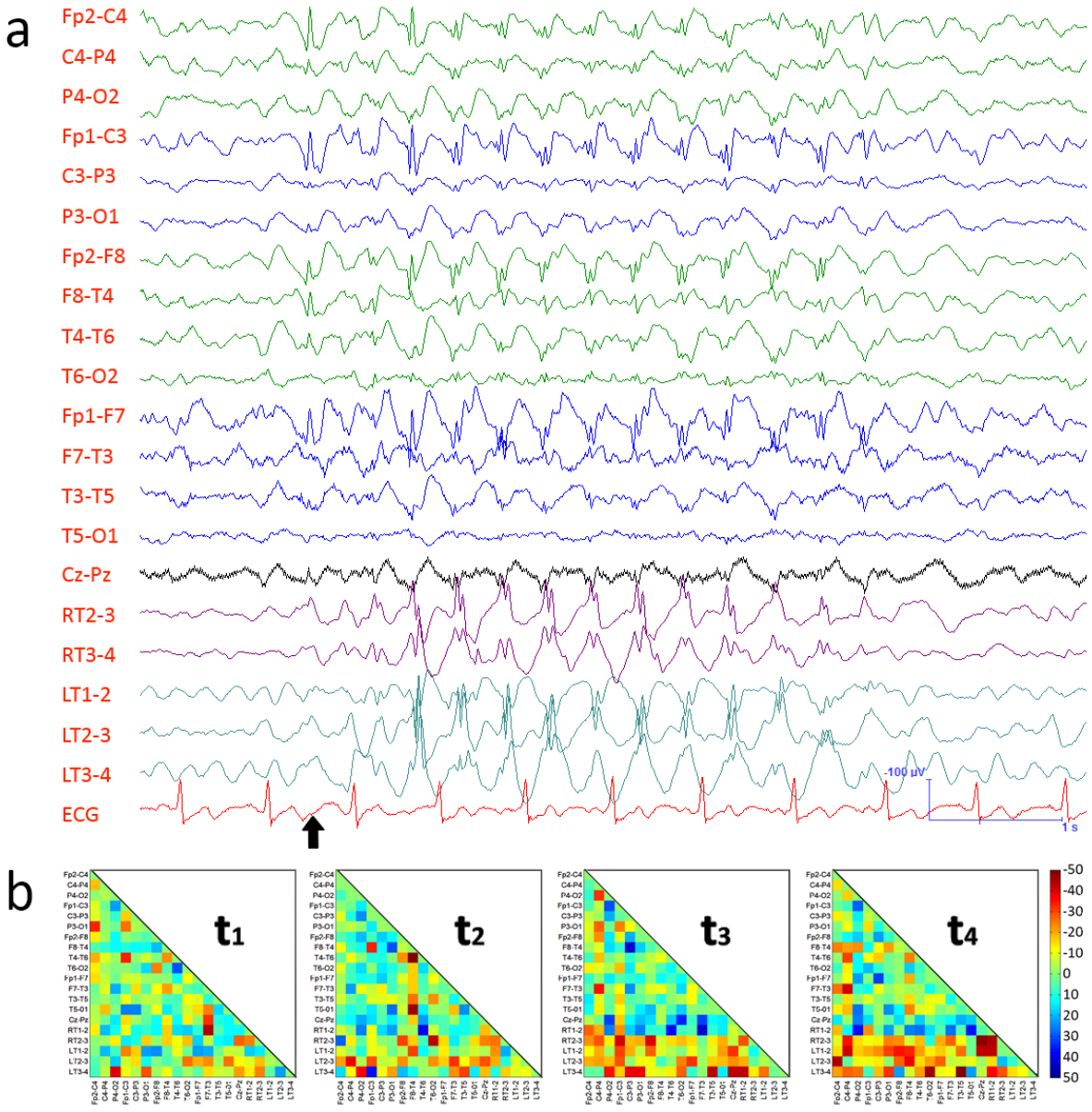


**Figure 1.** A) Scalp and thalamic EEG recordings during a typical absence seizure. Recordings are displayed in bipolar longitudinal montage. Bursts of 3 Hz generalised polyspike wave activity were initially recorded on the scalp and later recruited the centromedian nucleus. Note the rhythmicity of epileptiform activity after thalamic involvement. A black arrow marks the seizure onset identified visually. RT, right thalamic centromedian nucleus; LT, left thalamic centromedian nucleus. B) Colour matrix indicating the time differences (in milliseconds) between all possible channel pairs. Channels in the horizontal axis are compared to those in the vertical axis. Negative values (red) mean that to achieve the highest degree of association between both signals, the channel in the horizontal axis precedes (needs to be shifted to the right). Positive values (blue) indicate that to achieve the highest degree of association between both signals, the channel in the horizontal axis lags behind (needs to be shifted to the left). Note the preponderance of red-yellow squares over the four bottom rows in $t_2$ to $t_4$ (only $t_3$ and $t_4$ are statistically significant) indicating that the thalamus started to lead the cortex after seizure onset.

For each seizure, time shift values yielding the highest $h^2$ coefficient were calculated for each channel pair for every time window. For each time window, mean time delay values were obtained for each channel pair. In order to determine if time delays between cortical and thalamic electrodes significantly differ from zero, a t test was carried out for each pair of channels with 95% confidence interval.

**3. Results**

The three patients who fulfilled the inclusion criteria are described below.

**3.1 Patient 1**

Patient 1 is a 26 year old man with the diagnosis of idiopathic generalized epilepsy with absence and generalised tonic-clonic seizures. There is no history of meningitis, encephalitis, head injury or febrile convulsions. He had a normal birth and has no family history of epilepsy. He stated to suffer typical absence seizures at age 8, and had his first generalised tonic clonic seizure at 10. Typical absence seizures occurred mainly during daytime and consisted of unresponsiveness and looking blank for 2-3 seconds, associated with repetitive blinking and no recall for the episode, which was followed by immediate complete recovery. He occasionally suffered generalised tonic-clonic seizures, usually at night time, sometimes associated tongue biting and incontinence without recall for the episode. Seizure frequency was around 15 absence seizures a day and 5 convulsive seizures a month. At the time of assessment, he was taking levetiracetam, phenytoin, sodium valproate and zonisamide. MRI scan (1.5 T) failed to show any abnormality.

Scalp EEG and video-telemetry showed mild slowing of the background activity, probably due to medication. Some bursts of irregular 2-4 Hz generalised spike-wave activity were seen lasting for 5-7 seconds. Generalised bursts of polyspike-wave activity were also seen lasting for 1-2 seconds. Before thalamic implantation, he also suffered a generalised tonic-clonic seizure occurring in sleep. The onset was associated with rhythmic generalised spiking followed by a diffuse electrodecrement and then high amplitude bilateral spike and wave activity.

3.1.1 *DBS telemetry*

One thalamic electrode bundle was implanted at the centromedian nucleus on each hemisphere for DBS. Telemetry recording started 24 hours after implantation and lasted for 7 days. The ensuing video telemetry with thalamic and standard scalp electrodes showed a diffuse excess slow activity as suggested by previous EEG recordings.

3.1.2 *Interictal activity*

Frequent bursts of 3-4 Hz generalised spike and polyspike wave activity were also seen without associated obvious clinical semiology. During sleep, bursts of generalised irregular polyspike wave activity involving scalp and thalamic electrodes were seen without associated clinical changes. The thalamic electrodes were bilaterally involved.

3.1.3 *Seizures*

Very frequent typical absence seizures (5-15 seizures/hour) were seen associated with bursts of 3-4 Hz generalised polyspike wave activity, occasionally lasting up to 5 seconds. During these episodes, he stopped his on-going behavioural activity for 2-3 seconds, blinked repetitively and then resumed his activities.

3.1.3.1 *Visual inspection*

The seizures usually started with a bilateral high amplitude first discharge at the frontal scalp electrodes. This was followed by later discharges involving the thalamus. The onset of thalamic discharges was associated with an increase in rhythmicity of discharges, both in thalamus and cortex (figure 1a). The progressive decrement in amplitude of successive discharges was not as marked in the thalamus as on scalp. Some seizures showed thalamic slow activity preceding any other change but it was difficult to determine if this was part of spontaneous fluctuations of the background activity. The frontal spikes led the thalamus by 30ms in all generalised ictal discharges. The findings suggest that seizures started in the cortex but were maintained by rhythmic thalamo-cortical loops.

3.1.3.2 *Quantitative analysis* (figure 1b): Mean time shift values for segments $t_1$ and $t_2$ (which covered from one second before seizure onset to two seconds after seizure onset) revealed no statistically significant differences between cortical and thalamic electrodes. However during $t_3$ and $t_4$ segments (covering from 1 to 4 seconds after seizure onset) thalamic activity preceded cortical activity bilaterally (mean= -10.7 ms, p=0.005 for $t_3$, and mean= -11.4 ms, p=0.001 for $t_4$). In summary, quantitative analysis suggested that the thalamus started to lead after seizure onset.

**3.2 *Patient 2***

Patient 2 is a 24 years old woman with the diagnosis of idiopathic epilepsy with absences and generalised tonic-clonic seizures. She has no history of meningitis, encephalitis or febrile convulsions. Delivery was abnormal and she was described as a floppy baby and had oxygenation problems. There is no family history of epilepsy. She went through normal schooling and suffered fracture of the skull base at age 9 when she was attacked by a boy. Six months after the head injury, she had her first seizure which was a tonic-clonic seizure. Thereafter convulsive seizures occurred at a frequency of 2-3 seizures per month. She also had up to 30-100 absence seizures per day, with occasional seizure free days. Her absence seizures lasted from 2 seconds to 1 minute. During them, she moves her fingers, blinks or keep the eyes open and stares. At the time of referral, she suffered convulsive seizures often preceded by 80-100 absence seizures. Tonic-clonic seizures can happen at any time, starting with her ring fingers going up and non-forced head turning. There is no warning or prodromal signs, but occasionally there is an increase in heart rate and sometimes lip twitching occurring up to 2 hours before seizures. Seizures can be triggered by flashing lights and stress. At the time of assessment, she was taking sodium valproate and lamotrigine. She had been previously treated with levetiracetam. A 1.5T brain MRI was normal.

A scalp EEG telemetry showed normal background activity during wakefulness and sleep and multiple bursts of generalised spike-polyspike and wave discharges at 2-4 Hz, of abrupt onset and offset, lasting for 1-10 seconds. When the generalised spike and wave discharges lasted longer than three seconds, they were associated with cognitive impairment. Two generalised tonic-clonic seizures were recorded preceded by 5-10

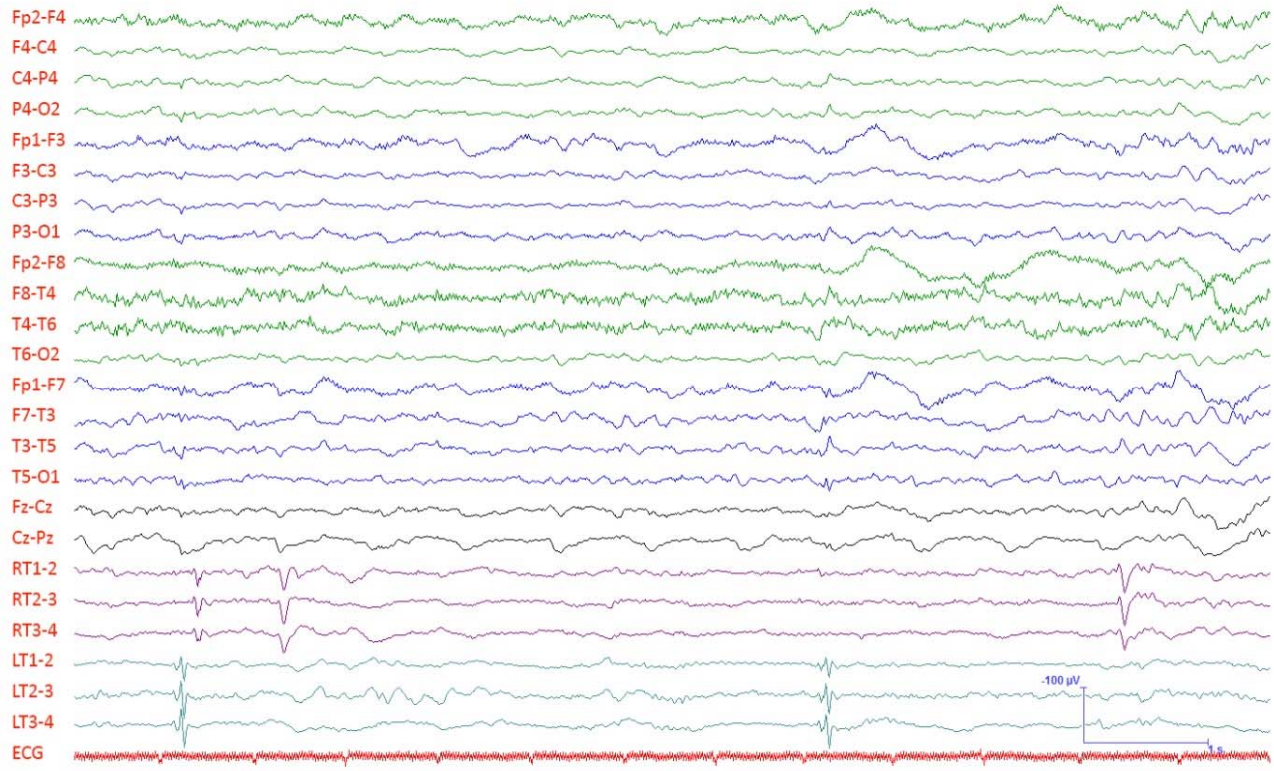


**Figure 2.** Scalp and thalamic EEG recordings showing bilateral independent thalamic interictal epileptiform discharges. Recordings are displayed in bipolar longitudinal montage. RT, right thalamic centromedian nucleus; LT, left thalamic centromedian nucleus.

seconds by generalised spike-and-wave discharges in the EEG.

3.2.1 *DBS telemetry*

One thalamic electrode bundle was implanted at the centromedian nucleus of the thalamus on each hemisphere for DBS. This was followed by a 4-day video-telemetry with standard scalp electrodes and thalamic DBS electrodes starting 48 hours after implantation.

3.2.2 *Interictal activity*

The interictal period showed runs of theta activity over frontal regions and occasional bilateral independent epileptiform discharges over the thalamic electrodes (figure 2). Very infrequent runs of activity at around 14 Hz were seen over the right thalamic electrodes without scalp involvement. In addition, there were frequent high amplitude generalised epileptiform discharges with frontal emphasis involving thalamus (figure 3). Occasional brief runs of generalised discharges at around 3Hz were also recorded without clinical manifestations.

3.2.3 *Seizures*

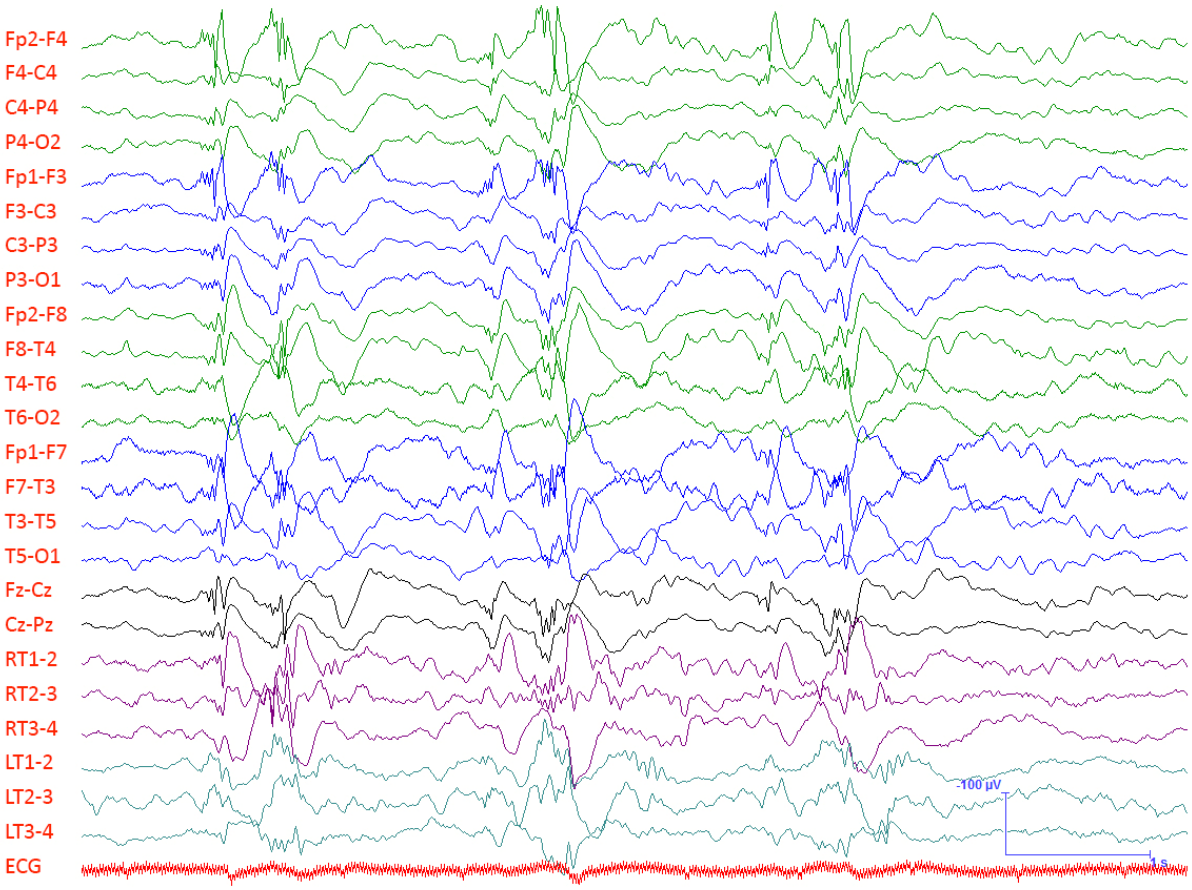


**Figure 3.** Scalp and thalamic EEG recordings showing generalised interictal epileptiform discharges. Recordings are displayed in bipolar longitudinal montage. RT, right thalamic centromedian nucleus; LT, left thalamic centromedian nucleus.

Recordings showed frequent periods of stereotyped absence seizures (1-3/hour) with generalised spike and wave discharges at around 3 Hz lasting for 5-10 seconds associated with staring, unresponsiveness and cognitive impairment (figure 4a). One episode evolved into a generalised tonic clonic seizure lasting about 1.5 minutes.

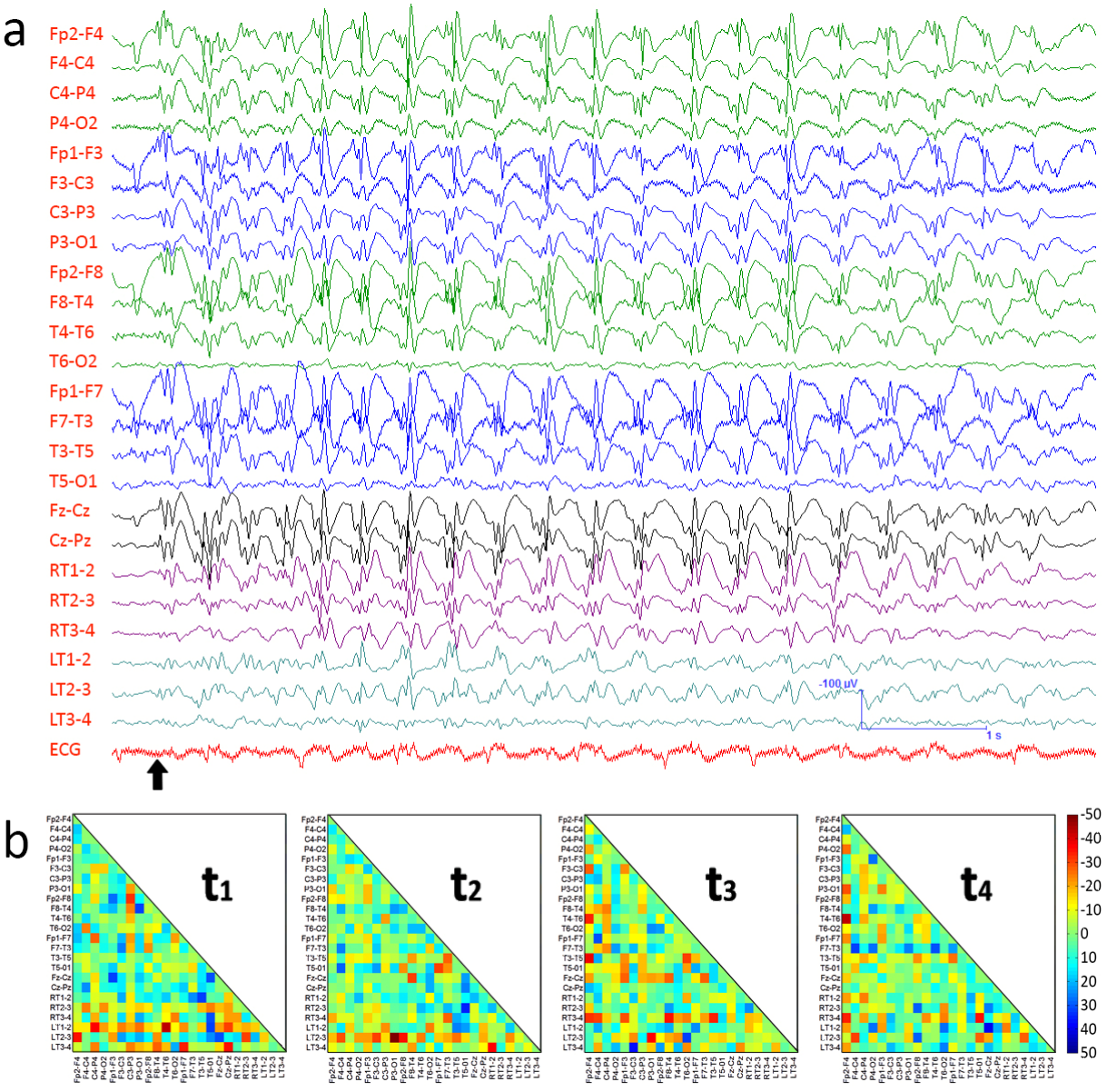


**Figure 4. A)** Scalp and thalamic EEG recordings during a typical absence seizure. Bursts of 3 Hz generalised polyspike wave activity are simultaneously recorded on the scalp and in the centromedian nucleus. Recordings are displayed in bipolar longitudinal montage. RT, right thalamic centromedian nucleus; LT, left thalamic centromedian nucleus. **B).** Colour matrix indicating the time differences (in milliseconds) between all possible channel pairs. Channels in the horizontal axis are compared to those in the vertical axis. Negative values (red) mean that to achieve the highest degree of association between both signals, the channel in the horizontal axis precedes (needs to be shifted to the right). Positive values (blue) indicate that to achieve the highest degree of association between both signals, the channel in the horizontal axis lags behind (needs to be shifted to the left). Note the preponderance of red-yellow squares over the five bottom rows in $t_1$ and $t_2$ (only $t_1$ is statistically significant) indicating that the thalamus started to lead the cortex around seizure onset.

3.3.3.1 *Visual inspection*

The first discharges on each burst were simultaneously recorded in frontal cortical and thalamic structures. One generalised tonic-clonic seizure was recorded showing an onset consisting of generalised spike and wave discharges simultaneously recorded on scalp and right thalamic electrodes (the left thalamic recordings were largely obscured by artefacts). The findings are consistent with a generalised seizure onset simultaneously involving cortex and thalamus.

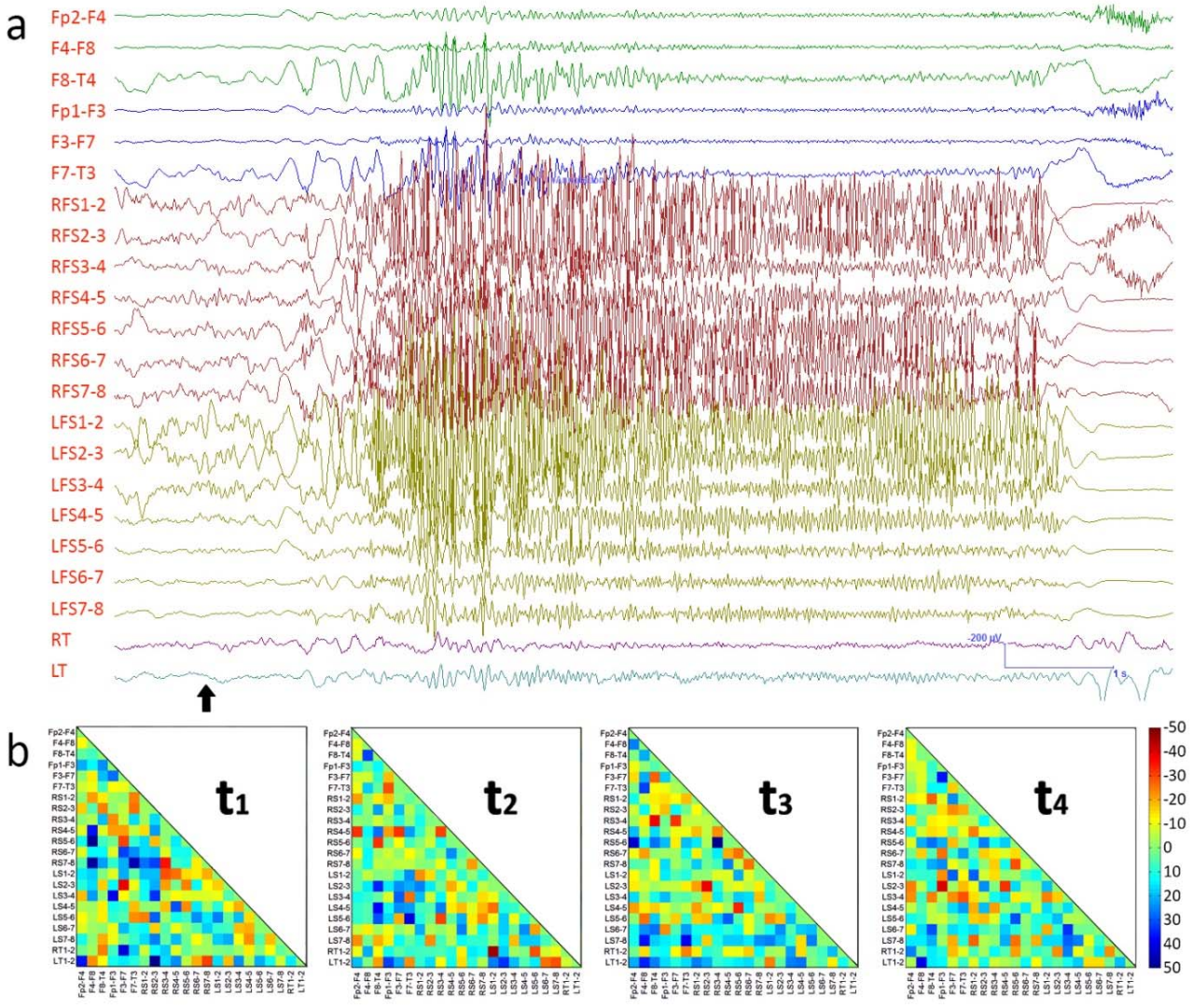


***Figure 5.*** *A) Scalp and bilateral intracranial subdural frontal strips in addition to thalamic depth electrode recordings during a frontal seizure. Seizure onset is located over the left frontal structures preceding thalamic activation. Recordings are displayed in bipolar longitudinal montage. RFS, right frontal strip; LFS left frontal strip; RT, right thalamic centromedian nucleus; LT, left thalamic centromedian nucleus.* ***B)*** *Colour matrix indicating the time differences (in milliseconds) between all possible channel pairs. Channels in the horizontal axis are compared to those in the vertical axis. Negative values (red) mean that to achieve the highest degree of association between both signals, the channel in the horizontal axis precedes (needs to be shifted to the right). Positive values (blue) indicate that to achieve the highest degree of association between both signals, the channel in the horizontal axis lags behind (needs to be shifted to the left). Note that no clear pattern is seen in $t_1$. However there is a preponderance of blue-green squares over the two bottom rows in $t_2$ and $t_3$ (only $t_3$ is statistically significant) indicating that the thalamus is lagging behind the cortex after seizure onset.*

3.3.3.2 *Quantitative analysis* (figure 4b)

Mean time shift values for $t_1$ segment (covering from one second before to one second after seizure onset) revealed statistically significant differences showing an earlier activation of thalamic electrodes compared to those at the cortex (mean= -6.1 ms, p=0.007). In the rest of the analysed segments no statistically significant differences between cortical and thalamic electrodes were observed. In this case, the findings suggest a leading role of the thalamus from early stages of the seizure.

**3.3 Patient 3**

Patient 3 is a 36 year old man with diagnosis of symptomatic focal epilepsy with seizures arising from the left hemisphere, probably frontal in origin. He has no history of meningitis, encephalitis or febrile convulsions. He had a normal birth and has no family history of epilepsy. His first seizure was a generalised tonic-clonic seizure occurring at age of 9, following a minor head injury. Since then, he has been having three types of attacks: infrequent blank spells (lasting for a few minutes), complex partial seizures and tonic-clonic seizures. He has around 35 complex partial seizures per month, with as many as 4 in a day and seizure-free periods of up to 1-4 days. Up to 3 times a month he suffers prolonged bursts of seizures lasting for over 15 minutes. Over the years he has been on phenytoin, vigabatrin, carbamazepine and valproate. He was seizure free for two years after introduction of clobazam. He had a vagus nerve stimulator implanted without benefit. He is currently on lamotrigine and primidone. A 1.5T brain MRI showed mild cerebral atrophy but no obvious focal intracranial abnormality. An EEG in childhood showed left frontal spiking.

3.3.1 *DBS telemetry*

Two 8-contact subdural strips were inserted over the frontal convexity bilaterally for DBS assessment, in addition to one thalamic electrode bundle implanted at each centromedian nucleus of the thalamus for DBS. Telemetry recording started 24 hours after implantation and lasted for 3 days.

3.3.2 *Interictal activity*

The interictal record showed a moderately and diffusely slowed background, possibly due to concomitant medication. Spike and spike-and-wave discharges were also seen predominantly over the right frontal region during waking. Bilaterally independent fronto-temporal discharges were recorded during sleep. There was no thalamic involvement in any interictal discharge.

3.3.3 *Seizures*

Eight stereotyped clinical seizures were recorded during sleep (figure 5a). They all showed a widespread left sided onset consisting of spikes and then polyspikes, or spike-polyspike activity with no thalamic activity. The thalamus is recruited 0.5-1s after seizure onset. During the seizures, he suffers a non-forced head version to the right and the right arm is raised. There is subsequent jerking on the right side and ipsilateral postictal Todd's paralysis.

3.3.3.1 *Visual inspection*

At the beginning of the seizure, the EEG shows the onset of bilateral, but predominantly left theta activity. The changes were suggestive of a left frontal focus.

3.3.3.2 *Quantitative analysis* (figure 5b)

Only $t_3$ (covering from 1 to 3 seconds after seizure onset) revealed statistically significant differences showing that the thalamus lagged behind the cortex (mean= 5.9 ms, p=0.019). No differences between cortical and thalamic electrodes were observed in the rest of the segments. The findings suggest that the thalamic activity lagged behind cortical activity.

**4. Discussion**

The three cases reported here illustrate the variety shown by the relative cortical and thalamic involvement in the different epilepsy types and to a degree supports the classical distinction between generalised and focal epilepsies. In the two patients with idiopathic generalised epilepsy, seizure onset is complex, with a variety of changes seen simultaneously or nearly simultaneously (<12ms latency difference) in cortical and subcortical structures, with time relations among structures shifting with seizure evolution. In patient 1, seizure onset was bilateral cortical and the belated onset of thalamic discharges was associated with an increase in rhythmicity of discharges, both in thalamus and cortex suggesting that seizures started in the cortex but were maintained by rhythmic thalamo-cortical loops. This is supported by quantitative analysis demonstrated that the thalamus led the cortex belatedly in the seizure. In patient 2, we observed bilateral independent interictal discharges restricted to the thalamus. However, ictal onset was diffuse involving cortex and thalamus though discharges were significantly larger in the cortex, but were led (6.1ms) by thalamic activity as shown by quantitative analysis. In contrast, seizure onset in patient 3 was largely restricted to frontal structures, with minimal thalamic involvement, confirming the focal nature of his seizures. However, even in such frontal seizures the thalamus comes involved belatedly and lagged behind the cortex. Overall the findings are consistent with a primarily cortical seizure onset with secondary involvement of the thalamus which may be involved in maintaining ictal duration and rhythmicity. In any case the thalamus appears to have some epileptogenic capacity as suggested by the finding of frequent bilateral independent discharges restricted to the thalamus in patient 2. This is a rather novel finding that suggests that the thalamus possesses epileptogenic potential of its own, a characteristic usually considered to be restricted to the cerebral cortex.

Several onset patterns have been described in generalised seizures. Some clinical reports illustrated with scalp EEGs revealed an early focal involvement of cortical regions prior to the onset of typical absence seizures [55–58]. The structures involved include mainly frontal cortices but also temporal and parieto-temporal areas. In addition, in humans focal frontal lesions can manifest with generalised discharges[59].

Simultaneous scalp and depth electrodes recordings have provided further insight into seizure onset patterns. In addition to the present study, we have found only four other such studies which report findings from small patient series [23–26]. In agreement with the findings of Velasco[26] and Tyvaert[35], we found that the thalamus appears to be involved in maintaining the rhythmicity of ictal discharges. However, our findings are consistent but not entirely in agreement of those of those of Spiegel and Wycis who described three patterns for the generation of generalised seizures in patients with generalised epilepsy[23]: a) Simultaneous appearance of the spike and wave discharges in thalamus (dorsomedial nucleus) and cortex in a patient suffering petit mal seizures operated under local anaesthesia; b) Discharges restricted to the thalamic electrodes in a patient under general anaesthesia, suggesting that generalisation of discharges could be prevented by anaesthetic drugs; and 3) Previous appearance of spike-and-wave discharges in the thalamus[24]: In a patient suffering grand and petit mal attacks, spike-wave discharges in the thalamus (dorsomedial nucleus region) appeared several seconds before those in frontal region. In this patient the burst of thalamic discharges outlasted cortical discharges. There were no cases of onset of spike-and-wave discharges in the cortex with secondary thalamic involvement. In five patients suffering generalised seizures studied with scalp and depth electrodes covering several thalamic nuclei, three modes of initiation of spike and wave discharges were observed[25]: Thalamic onset, simultaneous initiation in thalamic and extra-thalamic structures, and extra-thalamic onset (spike and wave discharges recorded from scalp electrodes and temporal structures preceding by at least half a second those in the thalamus). In patients with a cortical onset, thalamic epileptiform activities often showed a progressive increase in amplitude before stabilising. In contrast, those recordings with synchronous thalamic and extrathalamic onset showed high constant amplitude from the beginning. In two patients with thalamic onset, spike and wave discharges began bilaterally as small amplitude discharges in centromedian and anterior thalamic nuclei followed after half a second by a progressive increase in amplitude and frequency. The onset was usually bilateral, but in one instance it appeared first on one side. One second after the first discharge, spike and wave complexes appeared in extra-thalamic sites, sometimes showing atypical morphology and irregular frequency. When spike and wave discharges were simultaneously recorded from extra-thalamic and thalamic sites, regardless of whether this occurs from the beginning, the pattern became more rhythmic and

synchronous, as a typical 3 Hz pattern. In contrast, discharges showed more complex and asymmetrical morphology when the thalamus was not involved, and patterns became disorganized when the thalamus was no longer firing. It appears that generalised seizures may show different mechanisms of initiation, with various relative cortical and thalamic involvements, which may explain the apparent contradictory findings between different studies.

The specific timing and topography of the electrical changes during generalised absence seizures has been studied in a recent MEG study[36]. Standardized low resolution brain electromagnetic topography (SLORETA) identified a source of activity at the thalamus starting 50 ms before the beginning of the seizure, which was immediately followed by involvement of the lateral inferior frontal cortex. At the time of the first cortical spike, there was little activation at the thalamus but a prominent lateral inferior frontal source was present, with gradual cortical cranio-caudal recruitment leading to the generalised pattern. Interestingly they observed a source localised to the thalamus during the slow wave component of the spike and wave complex, suggesting a major involvement of the thalamus during the cortical "quiescent" period.

Patients 1 and 3 were recorded with a relatively low sampling rate of 256 Hz. According to Nyquist theorem, this will limit time resolution to signals below 125 Hz (8 ms time resolution). In the higher limit of this range (two samples per second at 125 Hz), this sampling rate may be insufficient for visual inspection, which typically requires at least 5-6 samples per cycle to identify waveforms. However, quantified signal analysis, such as the methods used here, will preserve frequency up to 125 Hz since two points per sample uniquely define a sine wave. The rat thalamo-cortical loop has a propagation delay in the range 8-60 ms which suggests that even the fastest loops occur within the limit of our resolution[60]. High frequency oscillations (ripples and fast ripples), which can go up to 500 Hz, were filtered out by the antialiasing filter and were not recordable at this sample rate. In any case, even at higher sampling rates, high frequency oscillations are commonly missed by macro electrodes[61], such as the scalp and intracranial electrodes used in the present study. This raises the issue whether some leading smaller high frequency seizure-like events in the thalamus could have been missed.

In summary, it appears that generalised seizures may show complex patterns of initiation, with various relative cortical and thalamic involvements. In the generalised seizures recorded in our patients, the thalamus may become involved early or late in the seizure but, once it becomes involved, it leads the cortex. Traditionally, it is considered that both thalamus and cortex become involved from start in generalized seizures. Therefore, these are novel findings suggesting that the thalamus may not always be involved in the initiation of generalized seizures but, when it is recruited, it becomes the leading structure, possibly maintaining and leading seizure activity in the cortex. This may be due to the various dynamical changes between cortical and subcortical structures as a result of multi-structure interplay, broadly consistent with the cortico-reticular model of generalised epilepsies. Such complex interactions have been predicted by computational models[62,63]. In contrast, the frontal seizures recorded in patient 3 suggest that the thalamus gets involved late in the seizure and, once it becomes involved, it lags behind the cortex. Other particularly novel findings are that the thalamus is capable of generating focal unilateral epileptiform discharges restricted to thalamic structures, and, though not always involved in seizure initiation, the thalamus may be responsible for maintaining the rhythmicity of ictal discharges.

**References**


1. 1F. Gibbs, H. Davis and W. Lennox, The electro-encephalogram in epilepsy and in conditions of impaired consciousness, *Arch. Neurolgy Psychiatry* **34** (1935) 1133–1148.
2. W. Penfield and H. Jasper, Epilepsy and the Functional Anatomy of the Human Brain (1954).
3. G. Buzsaki, The thalamic clock: emergent network properties, *Neuroscience* **41** (1991) 351–364.
4. P. Gloor, Generalized Cortico-Reticular Epilepsies Some Considerations on the Pathophysiology of Generalized Bilaterally Synchronous Spike and Wave Discharge, *Epilepsia* **9** (1968) 249–263.
5. H. K. M. Meeren, J. P. M. Pijn, E. L. J. M. Van Luijtelaar, A. M. L. Coenen and F. H. Lopes da Silva, Cortical focus drives widespread corticothalamic networks during spontaneous absence seizures in rats., *J. Neurosci.* **22** (2002) 1480–1495.
6. H. Jasper and J. Kershman, Electroencephalographic classification of the epilepsies, *Arch. Neurol. Psychiatry* **45** (1941) 903–943.
7. J. B. Hursh, Origin of spike and wave pattern of petit mal epilepsy, *Arch NeurPsych* **53** (1945) 274–282.

8. 8. Y. Futatsugi and J. J. Riviello Jr, Mechanisms of generalized absence epilepsy, *Brain Dev.* **20** (1998) 75–79.
9. F. Lewy and G. Gammon, Influence of sensory systems on spontaneous activity of cerebral cortex, *J. Neurophysiol* **3** (1940) 388–395.
10. E. W. Dempsey and R. S. Morison, The electrical activity of a thalamocortical relay system, *Am J Physiol* **138** (1943) 283–296.
11. R. S. Morison and E. W. Dempsey, Mechanisms of thalamocortical augmentation and repetition, *Am J Physiol* **138** (1943) 297–308.
12. H. Jasper and J. Droogleever-Fortuyn, Experimental studies on the functional anatomy of petit mal epilepsy, *Res. Publ. Ass. Nerv. Ment. Dis* **26** (1947) 272–298.
13. R. Hayne, L. Belinson and F. Gibbs, Electrical activity of subcortical areas in epilepsy, *Electroencephalogr. Clin. Neurophysiol.* **1** (1949) 437–445.
14. E. Niedermeyer, Depth EEG findings in epileptics with generalized spike-wave complexes, *Arch. Neurol.* **21** (1969) 51–58.
15. T. Starzl and W. Niemer, Cortical and subcortical electrical activity in experimental seizures induced by Metrazol, *J. Neuropathol. Exp. Neurol.* **12** (1953) 262–276.
16. E. Marcus and C. Watson, Synchronous Spike Wave Electrographic Patterns in the Cat, *Arch Neurol* **14** (1966) 601–610.
17. F. E. Bennett, Intracarotid and intravertebral metrazol in petit mal epilepsy., *Neurology* **3** (1953) 668–673.
18. J. Bancaud, J. Talairach, P. Morel, M. Bresson, A. Bonis, S. Geier, E. Hemon and P. Buser, "Generalized" epileptic seizures elicited by electrical stimulation of the frontal lobe in man, *Electroencephalogr. Clin. Neurophysiol.* **37** (1974) 275–282.
19. A. Valentin, M. Lazaro, N. Mullatti, S. Cervantes, I. Malik, R. P. Selway and G. Alarc??n, Cingulate epileptogenesis in hypothalamic hamartoma, *Epilepsia* **52** (2011) e35–39.
20. P. Gloor and R. G. Fariello, Generalized epilepsy: some of its cellular mechanisms differ from those of focal epilepsy, *Trends Neurosci.* **11** (1988) 63–68.
21. H. Wycis, A. Lee and E. Spiegel, Simultaneous records of thalamic and cortical (scalp) potentials in schizophrenics and epileptics, *Confin. Neurol.* **9** (1948) 264–272.
22. D. Williams, A study of thalamic and cortical rhythms in petit mal, *Brain* **73(1)** (1953) 50–69.
23. E. Spiegel, H. Wycis and V. Reyes, Diencephalic mechanisms in petit mal epilepsy, *Electroencephalogr. Clin.* … **3** (1951) 473–475.
24. E. Spiegel and H. Wycis, Thalamic recordings in man with special reference to seizure discharges, *Electroencephalogr. Clin. Neurophysiol.* **2** (1950) 23–27.
25. G. Rossi, R. Walter and P. Crandall, Generalized Spike and Wave Discharges and Nonspecific Thalamic Nuclei, *Arch Neurol* **19** (1968) 174–183.
26. M. Velasco, F. Velasco, a L. Velasco, M. Luján and J. Vázquez del Mercado, Epileptiform EEG activities of the centromedian thalamic nuclei in patients with intractable partial motor, complex partial, and generalized seizures., *Epilepsia* **30** (1989) 295–306.
27. M. Velasco, F. Velasco, H. Alcalá, G. Dávila and a E. Díaz-de-León, Epileptiform EEG activity of the centromedian thalamic nuclei in children with intractable generalized seizures of the Lennox-Gastaut syndrome., *Epilepsia* **32** (1991) 310–321.
28. M. Inoue, J. Duysens, J. M. H. Vossen and A. M. L. Coenen, Thalamic multiple-unit activity underlying spike-wave discharges in anesthetized rats, *Brain Res.* **612** (1993) 35–40.
29. T. Seidenbecher, R. Staak and H. C. Pape, Relations between cortical and thalamic cellular activities during absence seizures in rats., *Eur. J. Neurosci.* **10** (1998) 1103–12.
30. H. Meeren, Evolving concepts on the pathophysiology of absence seizures: the cortical focus theory, *Arch. Neurol.* **62** (2005) 371–376.
31. H. J. Luhmann, T. Mittmann, G. van Luijtelaar and U. Heinemann, Impairment of intracortical GABAergic inhibition in a rat model of absence epilepsy, *Epilepsy Res.* **22** (1995) 43–51.
32. A. Salek-Haddadi, L. Lemieux, M. Merschhemke, K. J. Friston, J. S. Duncan and D. R. Fish, Functional magnetic resonance imaging of human absence seizures., *Ann. Neurol.* **53** (2003) 663–7.
33. A. Labate and R. Briellmann, Typical childhood absence seizures are associated with thalamic activation., *Epileptic Disord.* **7** (2005) 373–377.
34. D. Fojtiková, M. Brázdil, J. Horký, M. Mikl, R. Kuba, P. Krupa and I. Rektor, Magnetic resonance spectroscopy of the thalamus in patients with typical absence epilepsy., *Seizure* **15** (2006) 533–40.
35. L. Tyvaert, S. Chassagnon, A. Sadikot, P. LeVan, F. Dubeau and J. Gotman, Thalamic nuclei activity in idiopathic generalized epilepsy: an EEG-fMRI study., *Neurology* **73** (2009) 2018–22.
36. J. R. Tenney, H. Fujiwara, P. S. Horn, S. E. Jacobson, T. a Glauser and D. F. Rose, Focal corticothalamic sources during generalized absence seizures: a MEG study., *Epilepsy Res.* **106** (2013) 113–22.
37. E. Millan, B. Abou-Khalil, D. Delbeke and P. Konrad, Frontal Localization of Absence Seizures Demonstrated by Ictal Positron Emission Tomography, *Epilepsy Behav.* **2** (2001) 54–60.
38. L. Bilo, R. Meo, M. F. De Leva, C. Vicidomini, M. Salvatore and S. Pappatà, Thalamic activation and cortical deactivation during typical absence status monitored using [18F]FDG-PET: A case report, *Seizure* **19** (2010) 198–201.

39. J. Gotman, C. Grova, a Bagshaw, E. Kobayashi, Y. Aghakhani and F. Dubeau, Generalized epileptic discharges show thalamocortical activation and suspension of the default state of the brain., *Proc. Natl. Acad. Sci. U. S. A.* **102** (2005) 15236–15240.
40. M. C. Prevett, J. S. Duncan, T. Jones, D. R. Fish and D. J. Brooks, Demonstration of thalarnic activation during typical absence seizures using H , I5O and PET, *Neurology* **2** (1995) 1369–402.
41. G. Alarcon, C. N. Guy, C. D. Binnie, S. R. Walker, R. D. Elwes, and C. E. Polkey, Intracerebral propagation of interictal activity in partial epilepsy: implications for source localisation. *J. Neurol. Neurosurg. Psychiatry* **57** (1994) 435–449.
42. G. Alarcon, J. J. Garcia Seoane, C. D. Binnie, M. C. Martin Miguel, J. Juler, C. E. Polkey, R. D. Elwes, J. M. and Ortiz Blasco, Origin and propagation of interictal discharges in the acute electrocorticogram. Implications for pathophysiology and surgical treatment of temporal lobe epilepsy. *Brain* **120** (1997) 2259–2282.
43. M. C. Martín Miguel, J. J. García Seoane, A. Valentín, E. Hughes, R. P. Selway, C. E. Polkey and G. Alarcón, EEG latency analysis for hemispheric lateralisation in Landau-Kleffner syndrome. *Clin. Neurophysiol.* **122** (2011) 244–252.
44. H. Adeli, S. Ghosh-Dastidar, and N. Dadmehr, A wavelet-chaos methodology for analysis of EEGs and EEG subbands to detect seizure and epilepsy. *IEEE Trans. Biomed. Eng.* **54** (2007) 205–211.
45. Y. Yang, T. Solis-Escalante, J. Yao, A. Daffertshofer, A. C. Schouten and F.C. Van der Helm, A General Approach for Quantifying Nonlinear Connectivity in the Nervous System Based on Phase Coupling. *Int. J. Neural Syst.* **25** (2015) 1550031.
46. S. Kalitzin, J. Parra, D. N. Velis, and F. H. Lopes Da Silva, Enhancement of phase clustering in the EEG/MEG gamma frequency band anticipates transitions to paroxysmal epileptiform activity in epileptic patients with known visual sensitivity. *IEEE Trans. Biomed. Eng.* **49** (2002) 1279–1286.
47. F. Wendling, P. Chauvel, A. Biraben, and F. Bartolomei, From intracerebral EEG signals to brain connectivity: identification of epileptogenic networks in partial epilepsy. *Front. Syst. Neurosci.* **4** (2010) 154.
48. A. Valentín, E. García Navarrete, R. Chelvarajah, C. Torres, M. Navas, L. Vico, N. Torres, J. Pastor, R. Selway, R. G. Sola and G. Alarcon, Deep brain stimulation of the centromedian thalamic nucleus for the treatment of generalized and frontal epilepsies., *Epilepsia* **54** (2013) 1823–33.
49. J. L. Fernández Torre, G. Alarcón, C. D. Binnie, J. J. Seoane, J. Juler, C. N. Guy and C. E. Polkey, Generation of scalp discharges in temporal lobe epilepsy as suggested by intraoperative electrocorticographic recordings., *J. Neurol. Neurosurg. Psychiatry* **67** (1999) 51–58.
50. N. Kissani, G. Alarcon, M. Dad, C. D. Binnie and C. E. Polkey, Sensitivity of recordings at sphenoidal electrode site for detecting seizure onset: Evidence from scalp, superficial and deep foramen ovale recordings, *Clin. Neurophysiol.* **112** (2001) 232–240.
51. G. Alarcón, J. Martinez, S. V Kerai, M. E. Lacruz, R. Q. Quiroga, R. P. Selway, M. P. Richardson, J. J. García Seoane and A. Valentín, In vivo neuronal firing patterns during human epileptiform discharges replicated by electrical stimulation., *Clin. Neurophysiol.* **123** (2012) 1736–44.
52. D. Flanagan, A. Valentín, J. J. García Seoane, G. Alarcón and S. G. Boyd, Single-pulse electrical stimulation helps to identify epileptogenic cortex in children, *Epilepsia* **50** (2009) 1793–1803.
53. M. E. Lacruz, J. J. García Seoane, A. Valentin, R. Selway and G. Alarcón, Frontal and temporal functional connections of the living human brain, *Eur. J. Neurosci.* **26** (2007) 1357–1370.
54. V. Kokkinos, G. Alarcón, R. P. Selway and A. Valentín, Role of single pulse electrical stimulation (SPES) to guide electrode implantation under general anaesthesia in presurgical assessment of epilepsy, *Seizure* **22** (2013) 198–204.
55. D. Craiu, S. Magureanu and W. van Emde Boas, Are absences truly generalized seizures or partial seizures originating from or predominantly involving the pre-motor areas?, *Epilepsy Res.* **70** (2006) 141–155.
56. Y. Kakisaka, A. V Alexopoulos, A. Gupta, Z. I. Wang, J. C. Mosher, M. Iwasaki and R. C. Burgess, Generalized 3 Hz spike-and-wave complexes emanating from focal epileptic activity in pediatric patients, **20** (2011) 103–106.
57. F. Kubota, N. Shibata, Y. Shiihara, S. Takahashi and T. Ohsuka, Frontal Lobe Epilepsy with Secondarily Generalized 3 Hz Spike-Waves: a Case Report, *Clin. Electroencephalogr.* **28** (1997) 166–171.
58. S. Sakakibara, F. Nakamura, M. Demise, J. Kobayashi, Y. Takeda, N. Tanaka, T. Koyama and M. Ito, Letter to the Editor Frontal lobe epilepsy with absence-like and secondary generalized seizures, *Psychiatry Clin. Neurosci.* **57** (2003) 455–456.
59. P. Pruvot, J. Bancaud, M. Delandsheer, M. Bordas-Ferrer and J. Talairach, Crises épileptiques généralisées et lésion corticale focale. (A propos d'une épilepsie frontale post-traumatique)., *Electroencephalogr Neurophysiol Clin* **2** (1972) 165–170.
60. D. R. Freestone, D. B. Grayden, A. Lai, T. S. Nelson, A. Halliday, A. N. Burkitt and M. J. Cook, The thalamocortical circuit and the generation of epileptic spikes in rat models of focal epilepsy, in *Proc. 31st Annu. Int. Conf. IEEE Eng. Med. Biol. Soc. Eng. Futur. Biomed. EMBC 2009* (2009), pp. 1533–1536.
61. M. Stead, M. Bower, B. H. Brinkmann, K. Lee, W. R. Marsh, F. B. Meyer, B. Litt, J. Van Gompel and G. A. Worrell, Microseizures and the spatiotemporal scales of human partial epilepsy, *Brain* **133** (2010) 2789–2797.
62. M. Breakspear, J. A. Roberts, F. R. Terry, S. Rodrigues, N. Mahant, P. A. Robinson,A unifying explanation of primary generalized seizures through nonlinear brain modeling and bifurcation analysis, *Cereb Cortex* **16** (2006) 1926–1313.
63. S. N. Kalitzin, J. Parra, D. N. Velis, F. H. Lopes da Silva, 2007, Quantification of unidirectional nonlinear associations between multidimensional signals, *IEEE Trans Biomed Eng* **54** (2007) 454–461.

# CHARACTERISING EEG CORTICAL DYNAMICS AND CONNECTIVITY WITH RESPONSES TO SINGLE PULSE ELECTRICAL STIMULATION (SPES)

**GONZALO ALARCÓN**

*Comprehensive Epilepsy Center Neuroscience Institute, Academic Health Systems, Hamad Medical Corporation, Doha, Qatar*

*Department of Clinical Neuroscience, King's College London, Institute Of Psychiatry, Psychology and Neuroscience, London, UK.*

*Department of Clinical Neurophysiology, King's College Hospital NHS FT, London, UK.*

*Departamento de Fisiología, Facultad de Medicina, Universidad Complutense, Madrid, Spain.*

**DIEGO JIMÉNEZ-JIMÉNEZ**

*Universidad San Francisco de Quito, School of Medicine, Quito, Ecuador.*

*Department of Clinical Neurophysiology, King's College Hospital NHS FT, London, UK.*

*Department of Clinical Neuroscience, King's College London, Institute Of Psychiatry, Psychology and Neuroscience, London, UK.*

**ANTONIO VALENTÍN**

*Department of Clinical Neuroscience, King's College London, Institute Of Psychiatry, Psychology and Neuroscience, London, UK.*

*Department of Clinical Neurophysiology, King's College Hospital NHS FT, London, UK.*

*Departamento de Fisiología, Facultad de Medicina, Universidad Complutense, Madrid, Spain.*

**DAVID MARTÍN-LÓPEZ**

*Department of Clinical Neurophysiology, Kingston Hospital NHS FT, London, UK.*

*Department of Clinical Neurophysiology, St George´s University Hospitals NHS FT, London, UK.*

*Department of Clinical Neuroscience, King's College London, Institute Of Psychiatry, Psychology and Neuroscience, London, UK.*

*Departamento de Fisiología, Facultad de Medicina, Universidad Complutense, Madrid, Spain.*

*E-mail: david.martin_lopez@kcl.ac.uk*

Objectives: To model cortical connections in order to characterize their oscillatory behavior and role in the generation of spontaneous electroencephalogram (EEG). Methods: We studied averaged responses to single pulse electrical stimulation (SPES) from the non-epileptogenic hemisphere of five patients assessed with intracranial EEG who became seizure free after contralateral temporal lobectomy. Second order control system equations were modified to characterize the systems generating a given response. SPES responses were modelled as responses to a unit step input. EEG power spectrum was calculated on the 20 seconds preceding SPES. Results: 121 channels showed responses to thirty-two stimulation sites. A single system could model the response in 41.3% and two systems were required in 58.7%. Peaks in the frequency response of the models tended to occur within the frequency range of most activity on the spontaneous EEG. Discrepancies were noted between activity predicted by models and activity recorded in the spontaneous EEG. These discrepancies could be explained by the existence of alpha rhythm or interictal epileptiform discharges. Conclusions: Cortical interactions shown by SPES can be described as control systems which can predict cortical oscillatory behaviour. The method is unique as it describes connectivity as well as dynamic interactions.

Keywords: Forced coupling, single pulse electrical stimulation, control systems, EEG.

## 1. Introduction

The dynamics of the oscillatory behaviour of neuronal systems are largely unknown. Traditional approaches to study electroencephalographic (EEG) brain connectivity and dynamics rely on identifying regions which are driving spontaneous cortical activity. When EEG activity propagates with preserved morphology, as in the case of epileptiform discharges, latency analysis identifying time differences between peaks can characterise propagation patterns and conduction times [1-3]. However, EEG waveforms can change with propagation because activity from different regions may add up and mutually interact. When waveforms are different between recording sites, the phase spectrum of Fourier analysis, spectral coherence and cross correlation have been used to identify leading regions and propagation patterns. Such methods suffer from relatively poor time resolution. Moreover, since Fourier analysis can only be defined for oscillatory (periodic) activity, when phase differences are recorded between two sites, it may be difficult or arbitrary to define which site is leading. A number of non-linear signal processing methods, have been developed over the last decades to overcome some limitations (for review, see [4]). These include non-linear regression analysis, amount of mutual information and chaos theory. Graph theory is emerging as a method for describing the global and local properties of brain networks (for review, see [5]). Each method is based on specific physiological and statistical assumptions. At present such assumptions tend to be largely theoretical, as it is unclear how multiple regions interact to generate electrical activity in the functioning human brain.

Because a region receives on-going functional contributions from many other brain areas simultaneously, it is difficult to tease out the relative contributions from all regions connected to a particular site. In addition, functional connections are typically reciprocal [6] and each region responds, modifying and feeding back activity from and to all other connected regions within milliseconds. In this process of mutual and multiple modulation of oscillatory activity by many regions, it is difficult to estimate the amount of coupling existing between any two regions.

The intracranial implantation of electrodes in patients being assessed for surgery to treat their epilepsy provides a unique opportunity to study human brain. In the present work we propose a new approach to estimate functional coupling between two regions and its contribution to spontaneous EEG activity, based on the response of neuronal networks to localised external stimulation. We have previously used responses to single pulse electrical stimulation (SPES) directly applied to the human cortex for interictal identification of hyperexcitable networks responsible to seizures [7-10]. Slight variations of this technique, sometimes denominated cortico-cortical evoked responses (CCEP), have been employed by other groups [11-20]. In addition, responses to SPES have increasingly been studied to map functional cortical connectivity [6, 11, 12, 14, 16-18, 21-24].

The pathophysiology of EEG responses to SPES is complex. Early and delayed EEG responses to SPES have been described. Early responses start immediately after stimulus, are seen when stimulating at most sites and can be largely considered as the normal response to stimulation [7]. Delayed responses tend to occur at the seizure onset site, and can be considered as a biomarker for epileptogenicity in children and adults [7-9, 25]. The morphology of early responses tends to be very consistent at each site but can vary largely among regions [7, 16]. Early responses often contain an early surface negative deflection (N1) at 22-36 ms and a second negative deflection (N2) usually at 113-164 ms [11, 12, 21, 26], sometimes showing a wider latency range from 7 to 127 ms [15]. However, the morphology of early responses can vary between regions, and N1 or N2 deflections may not be present. Early responses have also been described as an initial positive triphasic waveform (within 9.2-23.8 ms) or an initial negative biphasic waveform (within 25.4-39.4 ms) [17]. In later work, the authors classified response waveforms into 3 types [22]: a) Type N-P, the most common type, consisting of an initial negative peak (N1) followed by a positive peak (P1); b) Type N, consisting of N1 without P1; and c) Type P, consisting of P1 only.

Cortical responses to electrical stimulation show enormous morphological variability and frequently fail to fit into any of the above descriptions [7, 16]. Nevertheless, the overarching morphology of early responses appears to be that of several cycles of oscillations, sometimes resembling the damped sinusoids that describe the response of linear control systems to a step function input [27]. We suggest that single pulse stimuli can be interpreted as a transient function applied to the neuronal network, and waveforms of the EEG responses may reflect the transient steady-state response of the system (the cortex) until baseline level is reached. Excitatory and inhibitory postsynaptic potentials are related to the different response deflections in the anaesthetised cat [28]. The amplitude of early responses behaves broadly linearly over a range of amplitudes: the amplitude of early responses to SPES tend to increase with increasing stimulation intensity and with proximity to stimulating electrodes up to a ceiling [15, 29], suggesting that response amplitude is linearly related to stimulation intensity and that linear models could be appropriate to describe such responses. The amplitude of the response is broadly proportional to the strength of the connection and to the distance from stimulation.

One advantage of linear control theory is that it provides an estimate for the system's response to any frequency, regardless of the frequency composition of a particular input signal. In this sense, the application of control theory would provide an estimate of the ability (likelihood) of connections to generate each possible frequency, and therefore an estimate of the frequencies with which each connection is more likely to contribute to the spontaneous EEG. This is fundamental to the understanding of oscillatory systems such as those generating electrical cortical activity.

Our model assumes the following postulates with regard to cortical responses to SPES:

1) Presence of a cortical response to stimulation indicates the presence of a functional connection between the stimulated area and the area where a response is recorded.
2) A single electrical pulse applied to the cortex behaves as a transient input function.
3) The EEG response reflects the output of the cortical network activated by the connection between stimulated and recorded areas [27].

The aim of this work is to tests the following hypotheses:

a) Linear control models can be used to describe the morphology of early responses to SPES.
b) The frequency response of the connections activated by SPES can explain some of the oscillatory behaviour of the spontaneous EEG.

If these hypotheses are correct, SPES responses could be used to estimate functional coupling between two

Table 1. Patient information.

| Patient | Etiology | Age (years) | Age at seizure onset | Medication | Surgery performed |
|---|---|---|---|---|---|
| 1 | Mesial temporal sclerosis | 24 | 11 months | Carbamazepine, lamotrigine. | Right temporal lobectomy |
| 2 | Stroke | 34 | 24 years | Oxcarbazepine. | Right temporal lobectomy |
| 3 | Mesial temporal sclerosis | 39 | 7 years | Levetericetam, clobazam. | Right temporal lobectomy |
| 4 | Mesial temporal sclerosis | 40 | 13 years | Phenytoin, levetericetam, tegretol. | Left temporal lobectomy |
| 5 | Mesial temporal sclerosis | 32 | 15 years | Levetericetam, pregabalin, zopiclone. | Left temporal lobectomy |

regions (stimulated and recorded) and determine the relative contribution of the stimulated region to oscillatory mechanisms in the recorded region. This implies that SPES can be used to identify cortical connections in addition to describing their dynamics, a unique feature not present in any other method to date. In essence, the frequency response of the systems involved can be characterised as Bode plots which describe the system gain at each frequency. Thus, the peak of the Bode plot determines the frequency at which input gain is highest, and therefore the frequency at which the system is most likely to oscillate (the resonant frequency). In addition, the methodology described here can provide a uniform model to describe all response deflexions recorded with a small number of parameters sufficient to characterise oscillations, thus avoiding the use of multiple labels for latencies and amplitudes of peaks which are not always present.

## 2. Methods

### 2.1 Subjects

The study included five patients (table 1) assessed for surgery with chronic intracranial EEG recordings for the treatment of their epilepsy at King's College Hospital (London) between February 2007 and June 2009 who fulfilled the following inclusion criteria:

a) Patients had subdural or depth (intracerebral) electrodes bilaterally implanted in the temporal lobes.
b) Responses to SPES were recorded during assessment.
c) Patients underwent temporal lobectomy for the treatment of their epilepsy.
d) Patients became seizure free after surgery.

In order to estimate the behaviour of non-epileptic brain, only recordings from the non-epileptic temporal lobes were selected for analysis. Since all selected patients were seizure free after surgery, it is assumed that the remaining temporal lobe was not epileptogenic during the preoperative recordings used. Intracranial recordings cannot be compared with normal controls because it is impossible and unethical for normal subjects to undergo intracranial recordings. At present, the only clinical indication for chronic intracranial recordings is presurgical assessment of epilepsy which is the case of our patients. Therefore, the closest to normal control is the non-epileptogenic hemisphere in patients who become seizure free after resective surgery, which was the rationale for patient selection in our study. Furthermore, for the study of the mechanisms of the spontaneous EEG, each patient behaves as his/her own control since we compare the compound Bode plot and the spontaneous EEG generated in the same region.

The surgical procedure consisted on en-bloc temporal lobectomies which followed an anatomically standardised surgical technique[30]. En bloc temporal lobectomy was undertaken at King's College Hospital as originally described by Falconer [31], later modified to achieve a more complete removal of the hippocampus by use of the principles described by Spencer[32]. In effect, between 5·5 cm and 6·5 cm of the temporal lobe was removed. In the dominant hemisphere (the left) all superior temporal gyrus except the anterior 2 cm was spared. Such a resection would have included at least 50% of the amygdala and 2–3 cm of parahippocampal gyrus and hippocampus. The procedure removes most of the temporal lobe with its connections. Therefore, postsurgical seizure freedom after resection will be considered as the gold standard to demonstrate that the focus (including cortical pathology and associated epileptogenic connections) has been removed. Abolition of seizures after surgery suggests that the remaining cortex and connections are not epileptogenic. Some cortex previously connected to the removed focus will remain, which appear unable to generate seizures by itself. The choice of the hemisphere contralateral to the resection for analysis further minimizes the effect of the connections to and from the resected focus.

### 2.2 Electrodes

In accordance to the inclusion criteria above, all patients had bilateral subdural or depth electrodes implanted for intracranial EEG recordings during presurgical assessment. Subdural strip electrodes consisted of single rows of 4–8 platinum disk electrodes spaced at 10 mm between centres. The disks were embedded in a 0.7

mm thick polyurethane strip which overlapped the edges, leaving a diameter of 2.3 mm exposed, recessing approximately 0.1 mm from the surface plane. Multicontact flexible bundles of depth electrodes (AdTech Medical Instruments Corp., WI, USA) were implanted stereotactically under MRI guidance at temporal lobe locations. Each depth electrode bundle contained 6-10 cylindrical 2.3 mm platinum electrodes, with adjacent electrode centres separated by 5 mm. The location of electrodes was verified by post implantation skull X-ray, brain computed tomography (CT) or magnetic resonance imaging (MRI). The type, number and location of the electrodes were determined by the suspected location of the ictal onset region, according to non-invasive evaluation: clinical history, scalp EEG recordings obtained with the Maudsley system [33, 34], neuropsychology [35] and neuroimaging. The selection criteria and implantation procedure have been described elsewhere [36].

**2.3 Recording protocol**

The number of electrodes implanted is necessarily limited and was dictated by clinical practice. Recording of intracranial EEG started when the patient had recovered from the general anaesthesia applied for electrode implantation, at least 24 hours after the surgery for electrode implantation. Cable telemetry with up to 64 recording channels was used for data acquisition with simultaneous video monitoring. In all five patients, a Medelec-Profile system was used (Medelec, Oxford Instruments, United Kingdom). Data were digitized at 256 Hz and band pass filtered (0.05-70 Hz). The input range was 10 mV and data were digitized with a 22 bit analog-to-digital converter (an amplitude resolution of 0.153 nV). Interictal awake and sleep recordings in addition to ictal recordings and responses to SPES were permanently stored in hard drives. Data were recorded as common reference to a scalp electrode applied half way between Cz and Pz, and displayed for review in a variety of montages.

**2.4 Interictal spontaneous EEG activity**

*EEG selected for power spectrum:* Twenty seconds of spontaneous EEG recorded immediately prior to starting the SPES protocol were used as a sample of spontaneous EEG in order to estimate the frequency composition of spontaneous EEG activity between 0 and 50 Hz employing the periodogram method. EEG traces contained only periods of wakefulness with eyes open.

*Interictal epileptiform discharges*: The non-epileptogenic hemisphere often shows independent epileptiform discharges [1, 34]. Therefore, interictal telemetry recordings from all patients were inspected in order to identify the presence of interictal discharges in the non-epileptogenic hemisphere. If present, 25 of such interictal discharges were identified and averaged. When more than one type of epileptiform discharges (location or morphology) was observed, each type was averaged independently.

**2.5 SPES protocol**

SPES is used routinely in our centre to study cortical excitability and aid in the identification of epileptogenic cortex[7, 8, 25]. SPES was applied sequentially between pairs of adjacent electrodes with a constant current neurostimulator (Medelec ST10 Sensor, Oxford Instruments or Leadpoint, Medtronic) using monophasic single pulses (0.1 or 0.2 Hz, 1 ms, 5 mA). At least 10 identical stimuli were delivered at each stimulated site with each polarity. All pairs of consecutive electrodes were used to stimulate on successive trials. Monophasic pulses were chosen in order to increase spatial resolution because the cathode is more effective in exciting neurons. We applied 10 pulses with one polarity followed by another 10 pulses with reversed polarity, so that all electrodes were used as cathode at some point. These stimulation parameters are safe (for more details, see Valentin et al. 2002[7]) and charge delivered per second is 100 times lower than that applied for routine functional mapping. We have safely used this technique in over 200 patients assessed with intracranial electrodes for presurgical assessment of epilepsy. Essentially, 5 mA appears to provide the best compromise between safety and likelihood to record abnormal (delayed) responses while avoiding amplifier clipping as much as possible. EEG responses to each pulse were recorded by the non-stimulating electrodes. For each pair of stimulating electrodes and for each polarity, stimuli were stored and averaged for analysis.

A more detailed description of the experimental protocol for SPES is described elsewhere [7-9, 25].

### 2.6 Mathematical models

The mathematical development for open and closed second-order linear control models can be found in the Appendix section.

### 2.7 Measurement and modelling of responses

Software was designed and implemented in MatLab R2014a (The Math Works Inc., USA). Responses to identical SPES stimuli were averaged. Responses to stimuli of different polarities were averaged and analysed separately. Channels obscured by stimulus artefact or containing significant amount of noise were rejected from analysis. Channels that saturated (clipped) were excluded from analysis.

Intracranial responses to SPES were averaged by selecting 4 second epochs centred at the SPES artefact. The time point when the largest amplitude of the stimulation artefact was reached was set as the reference time point for analysis (time zero). Epochs comprising the first 1500ms after stimulus were used for modelling. Modelling was carried out in the recording montage (common reference to a scalp electrode located half way between Cz and Pz).

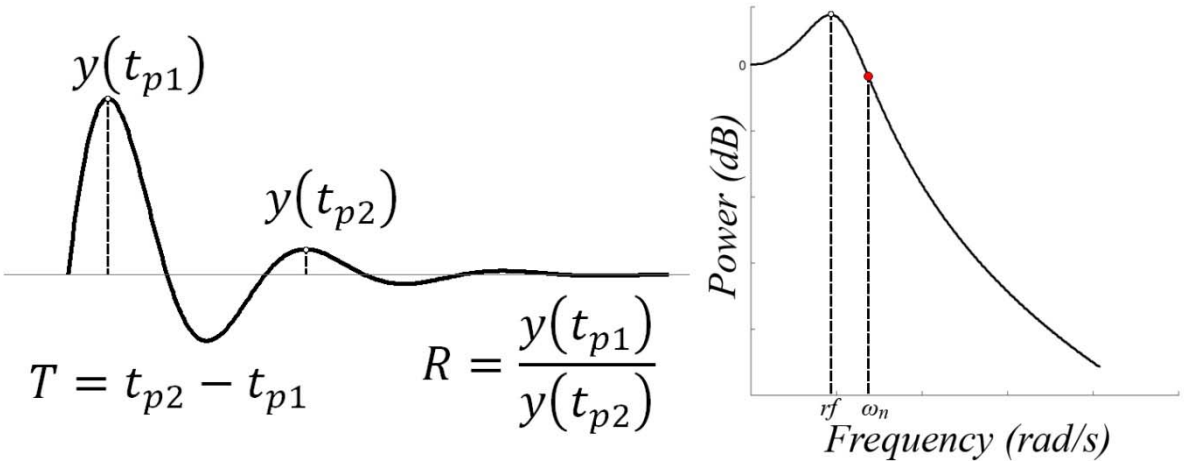


**Figure 1**. Representation of a damped oscillation showing the meaning of *T* (period) and *R* (subsidence ratio). The natural frequency of the oscillation (the inverse of *T*) corresponds to $2\pi/\omega_d$. $\omega_d$ is the angular frequency of the damped oscillation and equals $\omega_n\sqrt{(1-\zeta^2)}$. The envelope of the response is defined by two curves: $y(t) = 1 + e^{-\zeta\omega_n t}$ , and $y(t) = 1 - e^{-\zeta\omega_n t}$. The graph on the right represents the Bode diagram (frequency response) corresponding to a control system of the parameters shown on the left graph. The system gain decreases with frequency for frequencies above the cutoff frequency ($\omega_n$). The system gain is largest at a frequency (resonance frequency) to the left of the cutoff frequency (*rf*).The resonance frequency represents the frequency at which the system is most likely to oscillate.

Averaged responses to SPES were assumed to contain the unit step response of one or two control systems, each similar to those shown in figure 1 but differing in *R* and/or *T*. Response parameters (*R* and *T*) were measured by fixing manual cursors to the first two peaks of similar polarity in the first cycle of the response. *T* was defined as the time difference between both peaks. When only one deflection was present, the two peaks of opposite polarity were used and *T* was defined as twice the time difference between them. R was defined as the attenuation ratio between amplitudes of the first and second peaks (measured from peak to baseline, see *Figure 1*), that is, the amplitude attenuation between the first deflection and the second deflection. An example of response modelling is shown in figure 2.

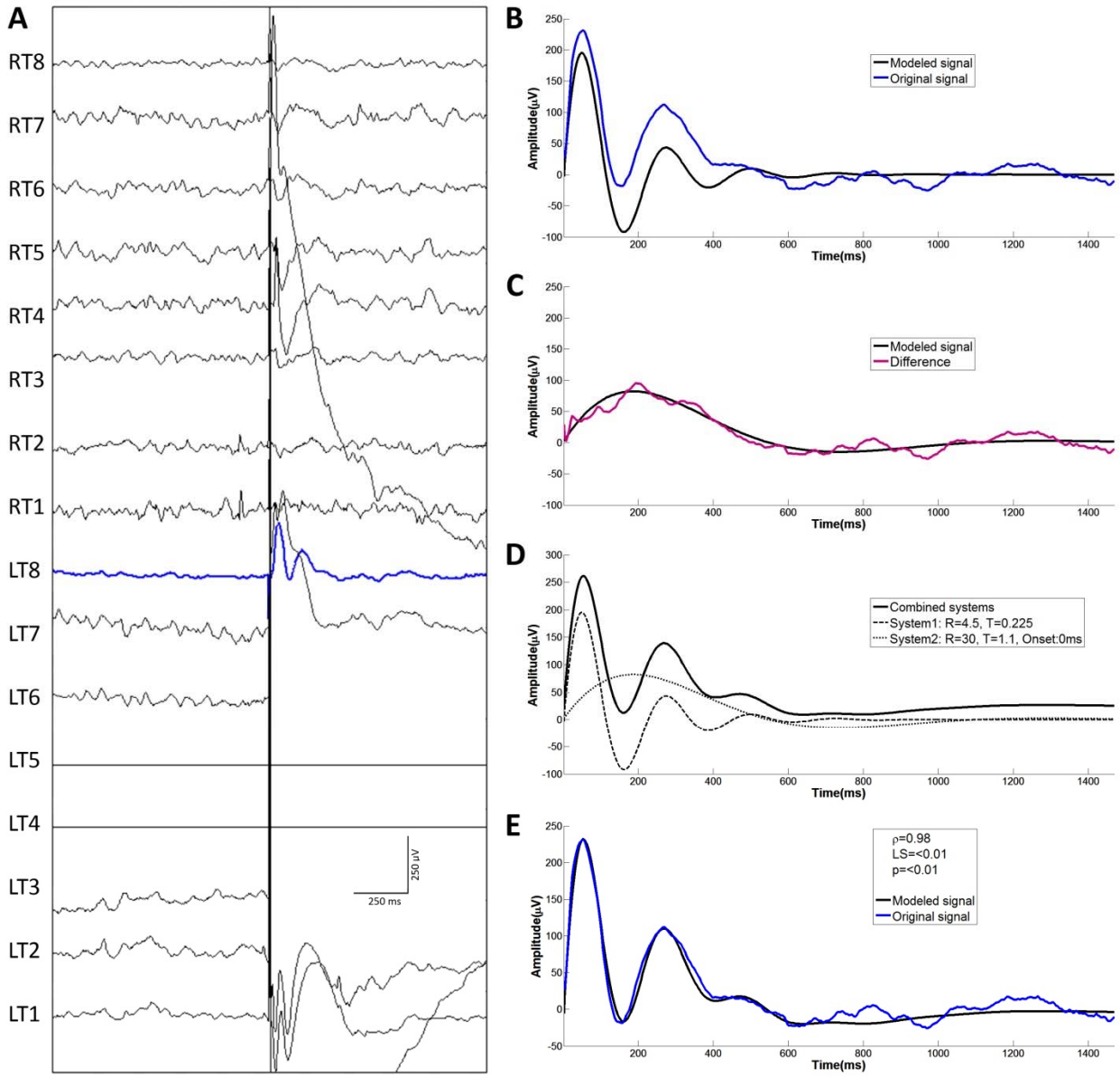


**Figure 2. Modelling process**. Patient implanted with subtemporal strips. A. Averaged responses to SPES delivered between electrodes LT4 and LT5 (flat traces). Note the high amplitude artefact recorded at channels close to the two stimulating electrodes. Response in channel LT8 (blue trace) has been selected for modelling. B. Recorded response (blue) and first control model (black). C. Difference (purple) between recorded response and first control model obtained in B, and the control system used to model the difference (second control model shown in black trace). D. Recorded response (solid line), first control system model (thick dotted line) and second control system model (thin dotted line). E. Comparison between recorded EEG response (blue line) and the final compound model (black line) obtained by adding first and second control models. RT: Right temporal, LT: Left temporal, R=Subsidence ratio, T=Period, ρ=Correlation coefficient, LS=Least square difference, p=significance.

As shown by the equations in the Appendix, *T* and *R* define $\omega_n$, $\omega_d$ and ζ, which are the parameters that determine the output response, *y(t)*. For the values of *T* and *R*, the model's response was calculated for the first 1500ms after stimulus. The first positive or negative deflections distinguishable from the stimulus artefact

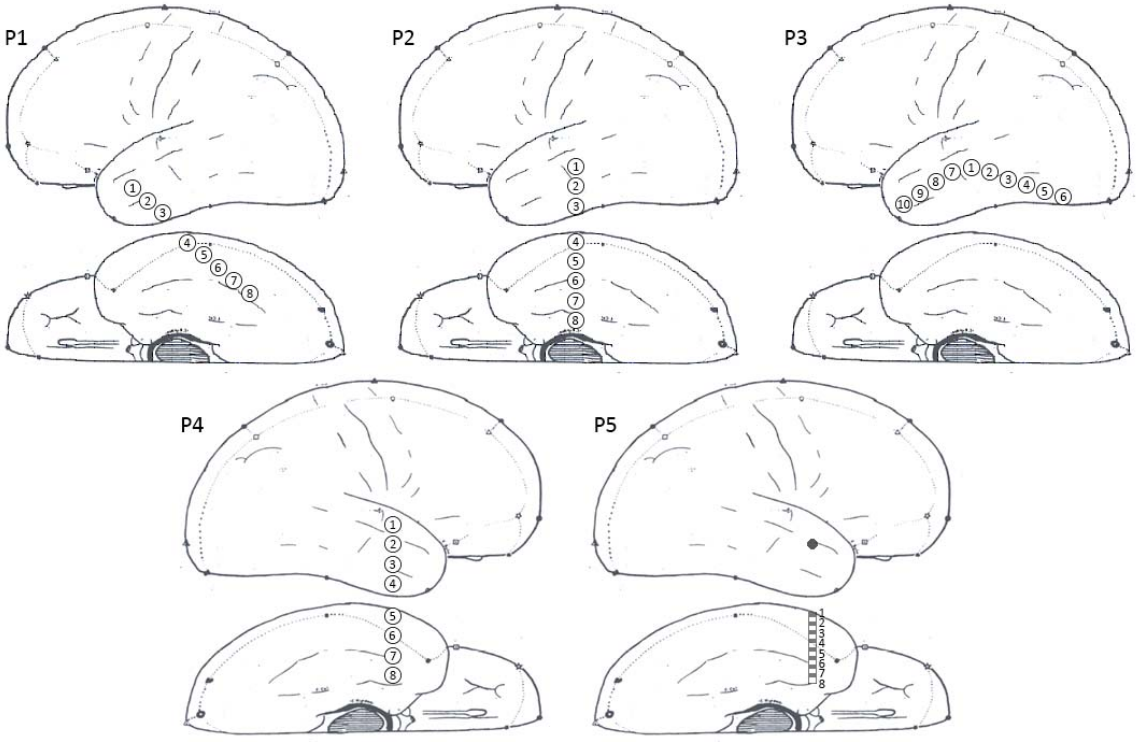


**Figure 3**. Electrode implantations in the "non-epileptogenic" temporal lobe. Patients 1 to 4 had subdural electrodes whereas patient 5 had depth electrodes.

were used to model the ***first control system***. Frequently the first deflection was followed by others of similar frequency of oscillation. In these cases, *T* and *R* values were identified as described above (figure 2) and the response predicted by the corresponding control system was calculated. Once the response predicted by the first control model was calculated, it was subtracted from the original recorded response (Figure 2B). If a remaining response distinguishable from the background noise was observed in the difference, the same modelling process was reiterated with the difference in order to obtain *T* and *R* for the ***second control system*** (Figure 2C). The interactions stopped if no oscillatory response distinguishable from the background noise was observed in the remaining signal. This was achieved with either one or two control systems in all cases. The amplitude of the models was automatically adjusted to obtain the lowest square difference between recorded response and model. In the last step, both models were added to obtain the ***final model*** (Figure 2D) which was compared with the original recorded response (Figure 2E). The degree of resemblance between final model and recorded response was quantified using Pearson correlation coefficients (ρ) and square difference. The significance level for the correlation coefficient was defined as $p<0.01$. Only those signals reaching a ρ value $>0.8$ and $p<0.01$ were considered similar. As explained in the Appendix, all systems involved in modelling are second order linear control systems. Thus, the terms "first" and "second" control systems refer to the fact that the first control system is the first system calculated to fit the response and also it is calculated from the first deflections on the recorded response. The second control system, if needed, is the second model calculated from the difference between the recorded response and the first control system.

**2.8 Modelling spontaneous EEG from responses to stimulation**

For each averaged response, bode diagrams reflecting the frequency-response for each control system were calculated and the peak resonance frequency identified (i.e., the frequency showing the highest gain). In addition, for each channel, the power spectrum of spontaneous EEG activity during the 20 second epoch previous to the first stimulation was calculated.

For each recording channel, Bode plots resulting from responses induced by stimulation applied to different sites were superimposed in order to compare them with frequency composition of the spontaneous EEG recorded in the same channel.

At a later stage, a grand average of Bode plots was carried out for each patient. All the obtained frequency-response Bode graphs from all channels were superimposed and the upper envelope of the graphs calculated. The hypothesis was tested that the power spectrum of the EEG can be estimated as the summation of all resonance frequencies from all active connections. However, the summation of all the recorded Bode plots renders a rather spiky graph since a relatively low number of connections are available for study due to the necessarily limited number of electrodes implanted. The envelope of the Bode plot peaks was used to integrate (summate) all the Bode plots, because the connections where no electrodes were implanted were not studied and were therefore missing. The envelope was used as a way to smooth the curve and allow for the Bode plots from missing connections, thus improving the estimation of the spontaneous EEG. A fifty-sample moving average (smoothing) was applied to the resulting envelope. The smoothed envelope was then superimposed to the average of the frequency composition of the spontaneous EEG from all channels from the same patient. Pearson correlation coefficients (ρ) were obtained in order to quantify the degree of resemblance between averaged power spectrum composition of the spontaneous EEG and the envelope of the Bode plots from all stimulations. Amplitudes of the Bode plot envelope were adjusted so that its maximal amplitude coincided with that of the power spectrum of the spontaneous EEG.

Sometimes resonance peaks in SPES Bode plots were observed which were not present in the power spectrum of the analysed sample of spontaneous activity. It was hypothesised that such peaks in the SPES Bode plots were due to oscillatory mechanisms which were either: a) Not active (or suppressed) during the sample of spontaneous EEG analysed (for instance, alpha activity not present with eyes open), or b) Their activity was too brief to be observed on the relatively long period of spontaneous EEG analysed with power spectrum (for instance, occasional interictal epileptiform discharges or sharp waves). When such discrepancies between Bode plots and spontaneous power spectrum were observed, the complete telemetry record was reviewed in search of epileptiform discharges, sharp waves or oscillatory activity not present in the 20 second EEG sample selected for power spectrum. If found, the frequencies of oscillatory activity and of epileptiform discharges (inverse of their average duration) were measured to establish if they coincided with the unexplained resonance frequencies in the SPES Bode plots at the same location. If frequencies coincided, it was assumed that SPES could identify the oscillatory mechanisms of the region even if their resulting oscillations were not observed in the 20 second EEG sample selected for power spectrum.

**2.8 Statistics**

Kolmogorov-Smirnov and Shapiro-Wilk tests were used to assess if variables are normally distributed within groups. Kruskal-Wallis H test was used to determine if there were statistically significant differences between different groups of variables. A Mann-Whitney U test with Bonferroni correction (p value was defined as $<0.01$) was performed to find specific differences between groups for the parameters that showed significant differences.

Table 2. Response types. Channels and responses are displayed in relation to the approximate distance to the stimulating electrodes.

| Distance (mm) | Type | | | | | | | Total |
|---|---|---|---|---|---|---|---|---|
| | A | B | C | D | No response | Stim artefact | Other artefacts | |
| **<10** | 10 | 2 | 1 | 6 | - | 53 | - | 72 |
| **10-20** | 6 | 7 | 4 | 18 | 3 | 10 | - | 48 |
| **20-30** | 5 | 4 | 2 | 19 | 8 | - | - | 38 |
| **30-40** | 1 | 1 | - | 14 | 3 | - | 1 | 20 |

## 3. Results

### 3.1 Patients

The study included artefact free intracranial SPES responses from five patients (2 males, 3 females, mean age = 30.6 years, range between 23 and 40 years) who underwent temporal lobectomy for the treatment of their epilepsy and became seizure free after surgery, with follow-up periods between 12 and 36 months. Four patients (P1-P4) had temporal subdural strips and one patient (P5) had depth electrodes implanted (Figure 3).

### 3.2 Distinction between response and stimulation artefact

In order to distinguish between stimulation artefact and cortical responses, an *in vitro* recording was carried out using gauze soaked with saline as a model for an inert conductor resembling the passive electrical properties the brain. Figure 4 compares recordings obtained *in vitro* and in a patient. Note the additional deflections (arrows) occurring after the artefact only in patient recordings, hence demonstrating that these are biological responses rather than artefacts.

Apart from overall morphology and amplitude, an additional criterion used to separate biological responses

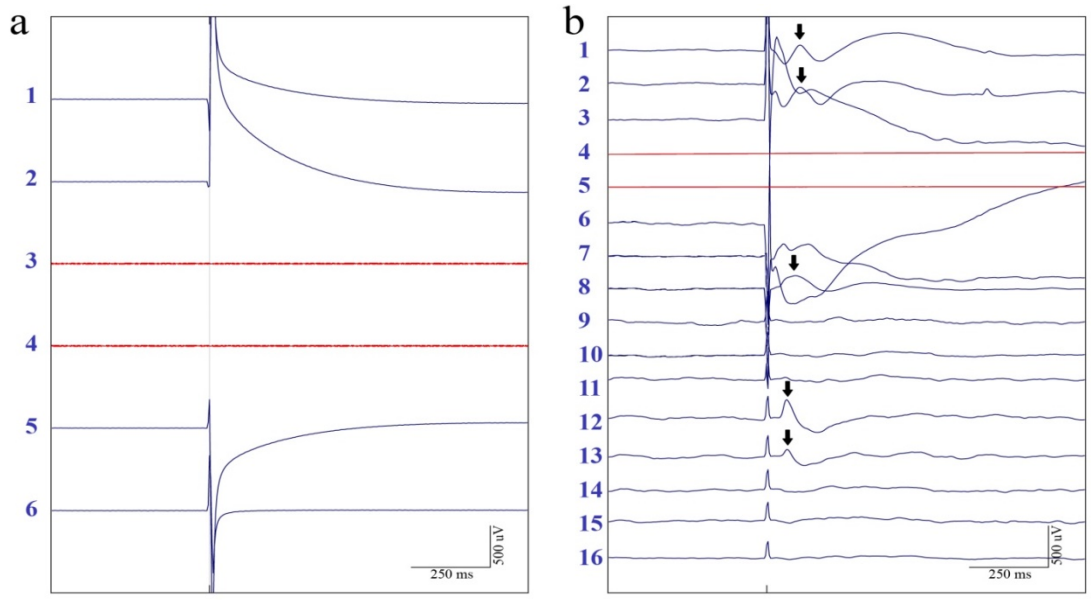


**Figure 4. *In vitro* vs *in vivo* recordings.** SPES in saline (a) and in a patient (b). Note the presence in vivo of additional deflections after the stimulus. Biological responses to SPES, no present in vitro, are marked with arrows.

from stimulation artefacts was that the polarity of biological responses does not change with changes in current polarity between the two stimulating electrodes, whereas the polarity of stimulation artefacts changes with changes in current direction between the stimulating electrodes.

### 3.3 Evaluation of model parameters

When an SPES response was present, signals were modelled following the procedures described in the methods section in order to define the existence of one or two control systems and their parameters.

We found that a response could be equally modelled as an open (K=0) or close loop (K≠0) system (figure 5). Therefore, in order to reduce the number of parameters involved, open loop systems were used for modelling in the remaining of the paper.

Responses to SPES showed variability in morphology. When more than one deflection was present, deflections tended to show higher duration with longer latency, e.g. late deflections were longer than earlier ones (see example in figure 5). This could not be modelled by a single linear control system but could be due to the presence of two control systems. This is the main reason why we embarked in modelling with more than one control system in the same response.

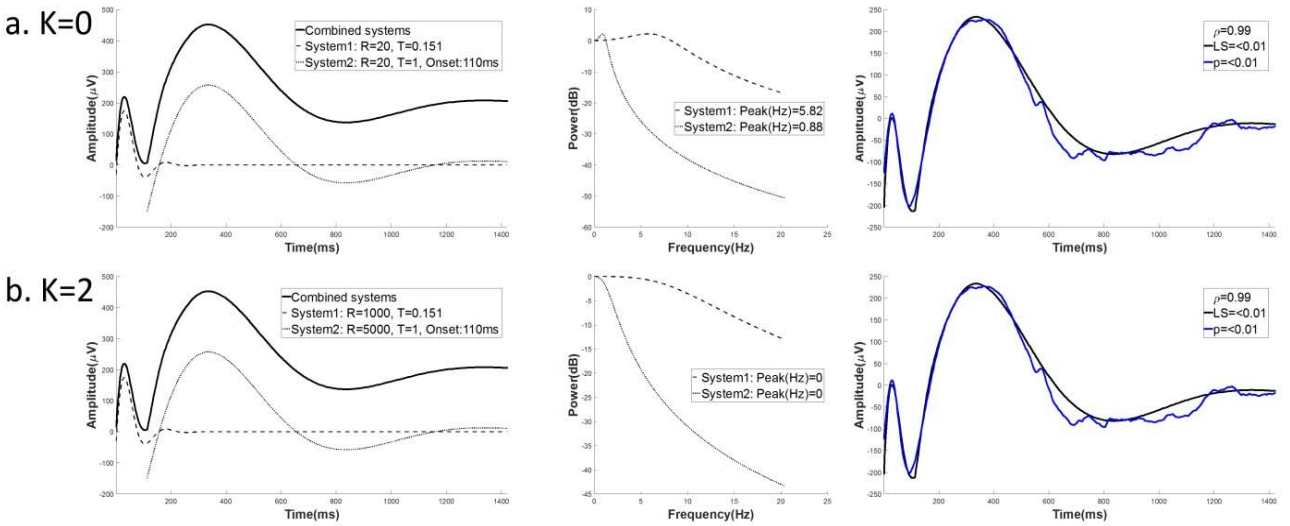


**Figure 5. Modelling the same recorded response (black trace) with open (a) and closed (b) loop control systems.** The figure shows the decomposition of the response in first and second systems in the time domain (left column), in the frequency domain (Bode plots, middle column) and the combination of both systems into the final model of the response (right column). Note that identical first (dash trace in left and middle columns) and second (grey trace in left and middle columns) control systems can be obtained with different combinations of *K* and *R* which render nearly final response models (right column). A higher *R* is translated into higher attenuation values on the frequency spectrum and a blunted resonance peak.

### 3.4 SPES responses

Out of 204 total recording channels, 121 channels showed responses to thirty-two stimulation sites. Thirty per cent of recording channels showed large stimulus artefact which obscured the EEG response (*Table 2*) and were always located in the vicinity of the pair of stimulating electrodes. 9.8% of channels failed to show a response.

Four response types have been identified and are illustrated in Figure 6. In summary the four types can be described as follows:

A) A single short surface-negative response of short duration lasting for less than 250 ms;

B) A longer surface-negative response lasting for longer than 250 ms;

C) A long surface-positive response, similar to type B but with opposite polarity.

D) Combination of morphologies described above.

These deflections were frequently followed by a number of increasingly smaller deflections (similar to those illustrated in figure 6). In as many as 71/204 (35%) of channels, two different superimposed responses of types A-C could be identified (D), which could be modelled as two different control systems. Their initial deflections showed shorter components resembling type A responses (D1) followed by later slower components similar to type B responses (D2). No surface-positive deflections (type C) were observed when two components were identified (type D).

Among artefact free responses (59.3%) recorded in a given channel, a single control system could model the response in 41.3% and two systems were required in 58.7%.

### 3.5 Modelling of SPES responses

Averaged SPES responses were modelled following the process described in methods section (*Figure 2 and 5*). As stated above, a single control system was identified in 50 responses and two control systems in 71 responses. Similarity between recorded responses and modelled responses was quantified. Traces reaching ρ values above 0.8 with statistical significance <0.01 were obtained in 79.04% of responses. ρ values of 0.9-1 were obtained in 55.65% of responses, ρ values between 0.8 and 0.9 in 23.39%, between 0.7 and 0.8 in 11.29%, between 0.6 and 0.7 in 3.23%, between 0.5 and 0.6 in 3.23%, and less than 0.5 was obtained in 3.23% of responses.

Five examples of modelled responses requiring two control systems are shown in figure 7. The left hand column shows the recorded response superimposed on the two control systems required to model it. The middle column shows the Bode diagrams for the two control systems, showing that each system has a frequency with largest amplitude, i.e. the resonance frequency. The right column shows recorded and modelled responses superimposed.

### 3.6 Properties of responses

Table 2 shows response type according to distance from recording to stimulating electrodes. Type A tends to occur closest to stimulating electrodes whereas types B and C are more common at 10-20 mm from the stimulating electrodes. Compound responses (type D) were the most common and widespread, showing maximal incidence around 20-30 mm from stimulating electrodes.

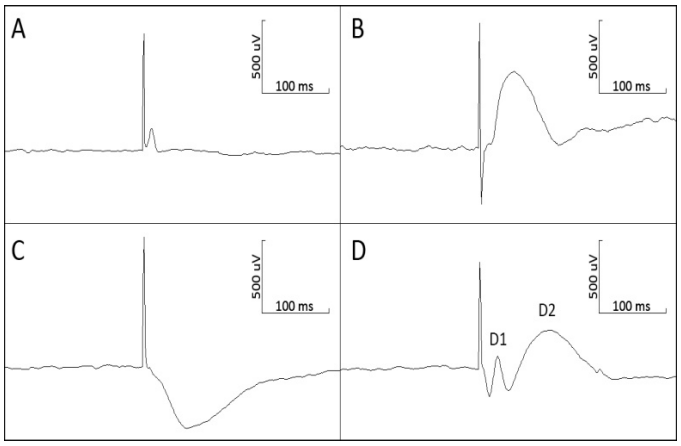


**Figure 6. Typical responses**. Examples A, B and C illustrate responses with a limited number of deflections (high R value) which are the simplest types of observed responses. Responses with more deflections illustrated in D can be considered as a combination of responses A and B (see text).

Table 2 shows response type according to distance from recording to stimulating electrodes. Type A tends to occur closest to stimulating electrodes whereas types B and C are more common at 10-20 mm from the stimulating electrodes. Compound responses (type D) were the most common and widespread, showing maximal incidence around 20-30 mm from stimulating electrodes.

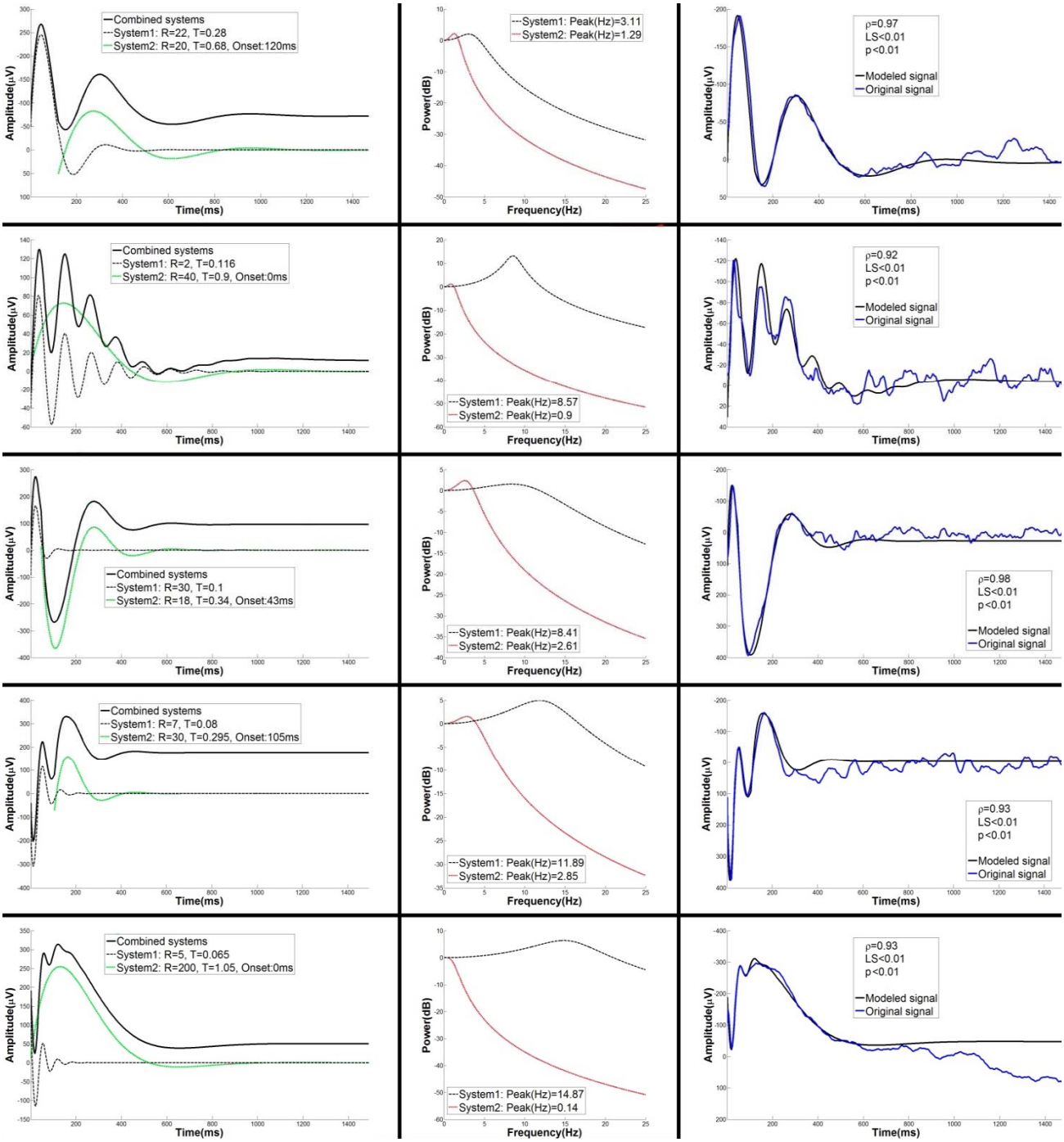


**Figure 7**: Modelled and original responses to SPES. Left column: Examples of responses (solid black line) modelled as the combination of two control systems (dashed black and green lines). Middle column: Bode plots for the control systems from each modelled response (dashed black and red lines). Right column: Overlapped original (blue line) and modelled (black line) signals.

R= Subsidence ratio, T=Period of the oscillation, ρ=Correlation coefficient, LS=Least squares difference.

Table 3. Median and interquartile range values (brackets) for latency, amplitude, period and distance to the stimulating electrode values within each group. T= Period, R= Subsidence ratio.

| Group | n | Onset Latency (ms) | Peak Latency (ms) | Amplitude (µV) | T (s) | Distance (mm) | R |
|---|---|---|---|---|---|---|---|
| **A** | 25 | 15.00 (15.00) | 59.06 (41.01) | 155.45 (142.38) | 0.12 (0.075) | 20.00 (20.00) | 40.00 (50.00) |
| **B** | 16 | 30.00 (88.00) | 199.65 (91.57) | 124,03 (179.94) | 0.49 (0.23) | 20.00 (10.00) | 10.00 (20.00) |

Table 3 shows parameters (peak latency, amplitude, period and distance between stimulating and recording electrodes) of the different response types (A, B, C, D1 and D2). Variables were not normally distributed within each group (Kolmogorov-Smirnov and Shapiro-Wilk tests)

Table 4. Statistical significance of Mann Whitney U with Bonferroni correction (p<0.01).

**Onset Latency**

| Group | **A** | **B** | **C** | **D1** | **D2** |
|---|---|---|---|---|---|
| A | - | *0.000** | 0.073 | 0.413 | *0.002** |
| B | *0.000** | - | 0.250 | *0.003** | 0.151 |
| C | 0.073 | 0.250 | - | 0.102 | *0.007** |
| D1 | 0.413 | *0.003** | 0.102 | - | *0.000** |
| D2 | *0.002** | 0.151 | *0.007** | *0.000** | - |

**Peak Latency**

| Group | **A** | **B** | **C** | **D1** | **D2** |
|---|---|---|---|---|---|
| A | - | *0.000** | *0.000** | 0.312 | *0.000** |
| B | *0.000** | - | 0.643 | *0.000** | 0.234 |
| C | *0.000** | 0.643 | - | *0.000** | 0.110 |
| D1 | 0.312 | *0.000** | *0.000** | - | *0.000** |
| D2 | *0.000** | 0.234 | 0.110 | *0.000** | - |

**T**

| Group | **A** | **B** | **C** | **D1** | **D2** |
|---|---|---|---|---|---|
| A | - | *0.000** | *0.000** | 0.255 | *0.000** |
| B | *0.000** | - | 0.926 | *0.000** | 0.491 |
| C | *0.000** | 0.926 | - | *0.000** | 0.945 |
| D1 | 0.255 | *0.000** | *0.000** | - | *0.000** |
| D2 | *0.000** | 0.491 | 0.945 | *0.000** | |

Significant differences were found in onset latency, peak latency, amplitude, *T* and distance values between response types (Kruskal-Wallis H test, onset latency $\chi2(2) = 72.117$, $p = 0.000$; peak latency $\chi2(2) = 137.150$, $p = 0.000$; amplitude $\chi2(2) = 10.283$, $p = 0.036$; T $\chi2(2) = 122.842$, $p = 0.000$; distance $\chi2(2) = 14.121$, $p = 0.007$). Mean values for these parameters within each group are displayed in *Table 3*.

No significant differences were found between the different types of responses in terms of *R* values (Kruskal-Wallis H test).

A Mann-Whitney U test with Bonferroni correction (p value was defined as <0.01) was performed to find specific differences between groups for the parameters that showed significant differences (amplitude, period and distance) *(Table 4)*.

The only significant difference in amplitude was found between C type and all other groups except type B (Mann-Whitney U test with Bonferroni correction). In terms of period and peak latency, there were no significant differences between A and D1, which were significantly different from B, C and D2 types. Similarly B, C and D2 types did not show significant differences among themselves but reached statistical significance when compared to A or D1. With regards to distance to stimulating electrode, only significant differences were found between D1-D2 and A.

In summary, there were no significant differences in terms of latency, amplitude and period neither between A and D1 types or between B and D2 types. C type was not significantly different to B and D2 types in terms of latency, period and distance to the stimulating electrode, but amplitude values were significantly different. This suggests that A responses and the first component of D responses can be considered equivalent and so can be B responses and the second component of D responses.

For the sake of completeness, table 5 shows the equivalence between previously described peak nomenclature and the control systems described in the present work.

### 3.7 Modelling spontaneous oscillations

For each patient, the power spectrum of the spontaneous EEG and Bode plots for each control model were obtained and calculated following the procedure described in the methods section. Figure 8 shows the Bode plots from all stimulations inducing a response in each channel (blue) and the power spectrum of the spontaneous EEG of each channel (red) for patient 2. The peaks of resonance in the Bode plots tend to occur within the frequency range of most activity on the spectrum of the spontaneous EEG (red), suggesting that the cortex tends to oscillate at the resonance peaks shown by the Bode plots of SPES responses.

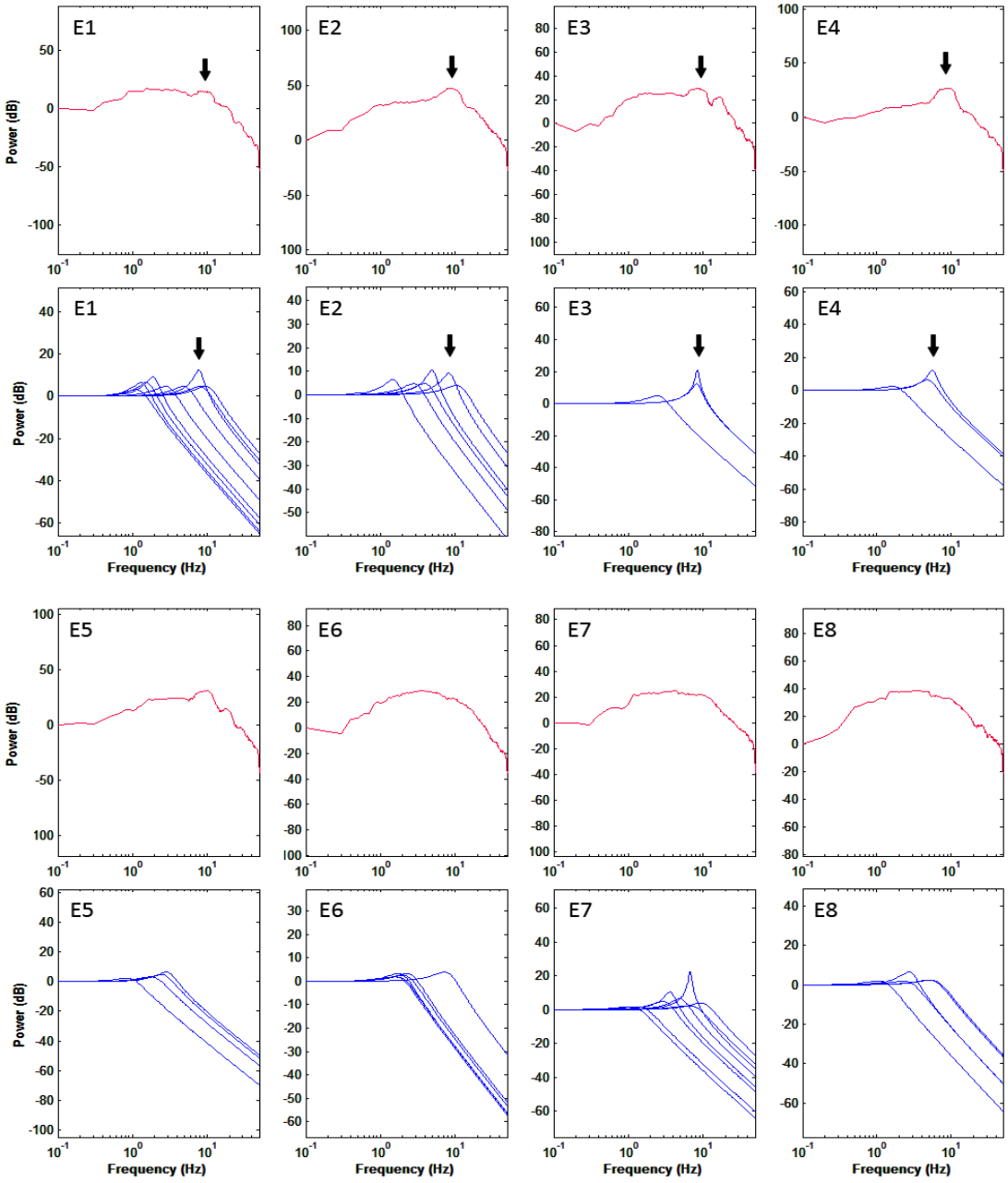


**Figure 8. Example of spontaneous oscillations modelling in patient 2.** Bode plot diagrams showing the power spectrum of spontaneous EEG activity contained within the 20 second epoch previous to the first electrical stimulation for each channel (red) and the frequency-responses for each control system (blue) identified for each electrode in patient 2. Note that some of the largest Bode plot peaks appear on the spontaneous EEG spectra as indicated by the inserted arrows.

Furthermore, in some channels (e.g. E3 and E4), the largest frequency on the Bode plot corresponded to specific peaks on the power spectrum (arrows in figure 8).

The clustering of resonance frequencies in the Bode plots of the responses around the frequencies showing larger power in the spontaneous EEG raised the question of whether the power spectrum of the spontaneous EEG can be estimated by the addition of the resonance frequencies from all regions projecting to the region where the EEG is recorded. In other words, resonance frequency from each Bode plot would show the frequency at which each connected site contributes to the spontaneous EEG of the region.

The number of electrodes implanted is necessarily limited. Consequently, it is not possible to know the Bode plot from all regions connected to any given one.

Table 5. Median values and interquartile ranges for latency, amplitude, period and distance to the stimulating electrode values within each group. *T*= Period, *R*= Subsidence ratio.

| Type | | Onset latency (ms) | Peak latency (ms) | Amplitude (μV) | *R* | *T* (s) | Distance (mm) |
|---|---|---|---|---|---|---|---|
| **N1 (A/D1)** | Median | 13.5 | 59.92 | 145.48 | 20.00 | 0.14 | 30.0 |
| | Interquartile range | 20.00 | 43.12 | 133.36 | 43.75 | 0.09 | 20.0 |
| **N2 (B/D2)** | Median | 70 | 249.49 | 121.70 | 20.00 | 0.55 | 30.0 |
| | Interquartile range | 155 | 124.49 | 132.07 | 42.00 | 0.34 | 20.0 |

The suggestion is that if we had more electrodes with more responses, we will end up with a higher degree of similarity between the compound Bode plot and the power of the spontaneous EEG spectrum from Bode plots by increasing the number of connections studied, we calculated a grand average of power spectra from all channels and superimposed the envelope of all Bode plots from all channels (the compound Bode plot) for each patient (figure 9). The averaged power spectrum and the compound frequency response curves in the Bode plots were similar in all 5 patients showing Pearson correlation coefficients above 0.9 ($p<0.01$).

Despite the overall similarity between power spectra and compound Bode plots seen in figure 9, some channels revealed isolated peaks in the frequencies of the compound Bode plot (arrows in figure 9) not corresponding to similar peaks in the compound power spectrum of the spontaneous EEG. Table 6 shows frequency and periods of the Bode plot peaks that do not appear in the power spectrum of the spontaneous EEG (unexplained peaks). The complete telemetry record was reviewed to find elements to explain such discrepancies. In all patients, there was either alpha activity or interictal activity at surprisingly similar frequencies to the unexplained Bode plot peaks, therefore providing an explanation for the Bode plot peaks

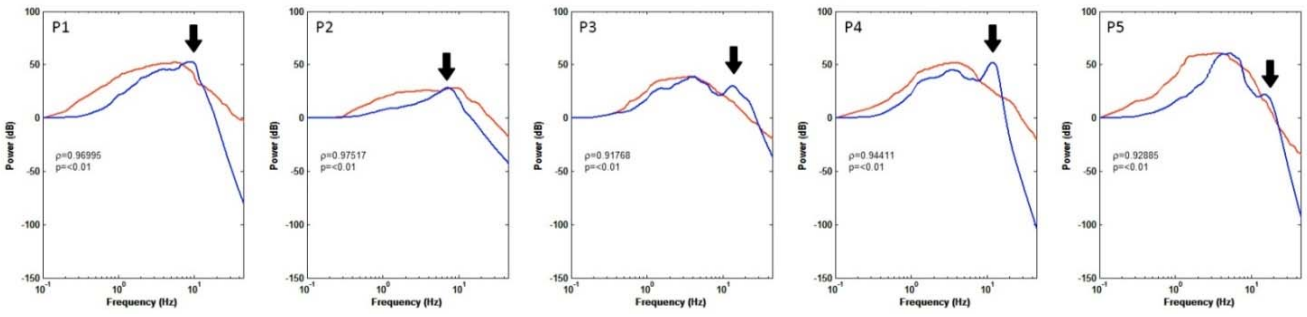


**Figure 9. Compound power spectrum versus compound frequency response curves (compound Bode plot).** For each patient, the red curve shows the averaged power spectrum from the spontaneous EEG for all channels (the compound power spectrum). The blue curve shows the addition of all Bode plots from all stimulation (i.e. the compound Bode plot) which represent the frequency response curves induced by all stimulations. The latter was computed by superimposing the Bode graphs from all channels and calculating the upper envelope of the graphs. A moving average was applied to the resulting envelope. Note that, despite their similarity, each patient showed peaks in the compound Bode plots (black arrows) which were not present in the compound power spectrum of the spontaneous EEG.

not present in the power spectrum.

In patient 1, the SPES responses responsible for the extra peak (at a frequency of 9.6 Hz) on the compound Bode plot were generated by the most posterior electrodes (electrodes 7 and 8 in figure 3). This is the region showing alpha activity at 9-10 Hz on eye closure, even though such activity was not present in the initial 20 sample of spontaneous EEG which was obtained with eyes open.

Table 6. Compound Bode plot peaks to be explained in each patient and EEG elements that justify them.

| Patient | Peak to be explained (frequency in Hz or period in ms) | Electrode number showing the peak to be explained | EEG element that explains the peak | Topography of EEG element that explains the peaks | Other elements in the spontaneous interictal EEG |
|---|---|---|---|---|---|
| 1 | 9.6 Hz or 104 ms | Post temp-occipital (7-8) | Alpha activity at 9-10 Hz | - | - |
| 2 | 7.1 Hz or 140 ms | Electrode 7 | Interictal spike wave discharge with period of 144ms | All channels but maximal at electrode 7. | - |
| 3 | 13.6 Hz or 74 ms | Electrodes 1, 2 | Interictal sharp waves with period of 86ms | Maximal at electrode 2 | Sharp waves of 300 ms maximal at electrode 10 |
| 4 | 11.8 Hz or 84.7 ms | Electrodes 3, 6 | Interictal sharp waves with period of 86ms | Electrodes 1-5<br>Maximal at electrode 4 | Spike-wave of 62 ms at electrodes 6-8 |
| 5 | 15.2 or 66 ms | Electrodes 1, 8 | Interictal spikes with period of 70ms | Electrode 8 | - |

Patients 2 to 5 showed unexplained peaks on their compound Bode plots with frequencies at 7.1 Hz, 13.6 Hz, 11.8 Hz and 15.2 Hz (i.e. periods corresponding to 140 ms, 74 ms, 84.7 ms and 66 ms, respectively). The four patients showed epileptiform discharges (spike wave discharges or sharp waves) of similar durations (periods at 144 ms, 86 ms, 86 ms and 70 ms respectively) which explained the corresponding peaks on the compound Bode plots (figure 10).

Patients 3 and 4 showed additional interictal discharges with durations of 300 ms and 62 ms, respectively, corresponding to frequencies (3.33 Hz and 16.13 Hz, respectively) outside the unexplained peaks for the same patients.

**4. Discussion**

We essentially describe a method to characterize connections and how they can contribute to spontaneous oscillations. We found it useful in explaining how connections contribute to the oscillatory nature of the spontaneous EEG generated in the regions were electrodes were implanted. Our results suggest that cortical interactions can be described as linear control systems. Responses to electrical stimulation can be explained as the superimposition of responses from one or two control systems which can be described with only 3-6 parameters (*R*, *T* and delay-phase for each control system). This method can characterise responses regardless of whether they show the standard deflexions and the method can be used to describe waveforms with few parameters. More importantly, the method can quantify the resonant frequency of functional coupling between two sites, and we suggest that the models can explain spontaneous EEG oscillations, teasing out the relative contributions to spontaneous oscillations from each pair of connected regions. Furthermore, the method appears to be able to identify oscillatory capabilities of the different regions of the cortex, potential oscillations which may not be present in an actual record of spontaneous EEG. This may be particularly relevant to predict, during the interictal period, impending seizures or the regions originating seizures as these

are characterised by transient oscillatory behaviour. Data were obtained from the non-epileptogenic hemisphere in patients becoming seizure free after surgery in order to maximise the chances of studying less abnormal brain tissue within the temporal lobe.

The principles of our proposed method are simple to understand. In essence, electrical stimulation activates functional coupling between connected regions, inducing cortical oscillations at the frequencies at which the regions involved are most likely to oscillate. The frequencies at which a connection is likely to oscillate after stimulation determine the largest peaks on the frequency response of the connected regions (the resonance frequencies) and the resonance frequencies of the local connections will determine the overall oscillatory behaviour of the region. In this context, it is easy to understand that interictal epileptiform discharges or seizures can arise when the resonance frequency of one connection dominates over others, and our method could, in principle, measure such dominance. This is a new way to interpret the EEG and cortical physiology in general, which opens a wide new area of research in neuroscience by providing objective measures of degree of functional coupling between connected regions in the amplitude and frequency domains.

*Control system models and cortical dynamics*

Brain dynamics display non-linear features (e.g. the behaviour on single neurons) in conjunction to linear characteristics (e.g. Weber's law, the sinusoidal behaviours of alpha and sigma activities). More specifically, the amplitude of early responses behaves broadly linearly over a range of amplitudes[15, 29], suggesting that linear models may be adequate for characterisation of the amplitude of response oscillations. In any case, in the end, the main purpose of our method is the characterization of brief oscillations with few parameters. The linear models used have been effective for this purpose. Overall the findings from this study are consistent with clinical practice. The EEG itself can be described as a low-pass filter in that the amplitude of oscillations decreases with increasing frequency as shown by the power spectrum of spontaneous EEG activity. Accordingly, the Bode plots obtained describe the response of the modelled system to any frequency. Above the cut-off frequency, Bode plots show higher signal attenuation the higher the frequency. Each Bode plot shows an amplitude peak at the so called resonance frequency, presumably the frequency which is easier to generate by the system.

We have treated the stimulus as a unit step function, when in fact it would be better described as a unit impulse function. Indeed, responses are transient oscillations returning to 0. It would be impossible to apply a true step function to the cortex as this would polarize the cortex for long enough to possibly induce tissue damage. Conceptually we could consider that each single pulse activates the neuronal network for a while, maintaining it on an activated state, which in itself could be considered as a pseudo-step function. The difference between considering the stimulus as a step or impulse function would probably be minimal, as we are essentially interested in characterizing the frequency of the resulting brief oscillations, and the method used appears effective for this purpose. The practical difference is that the mathematical development (appendix) is simpler for the step function.

Figure 9 suggests that the frequency composition of the spontaneous EEG can be predicted from the summation of the frequency responses from individual connections (compound Bode plots). In other words, the transfer functions of the corresponding control systems summate to generate cortical activity. This means that the control systems from different connections are largely arranged in parallel rather than in series since the transfer functions of controls systems arranged in parallel add up. The overall similarity found between traces shown in figure 9 (showing Pearson correlation coefficients above 0.9, $p<0.01$) despite the limited number of electrodes was very surprising and suggests that the study with more electrodes will increase such similarity.

Some peaks in the compound Bode diagram were not present in the power spectrum of the spontaneous EEG. Such peaks were found to be similar to the frequency of alpha activity or the instantaneous frequency of interictal epileptiform discharges recorded at the appropriate channel. Since the spontaneous EEG selected for

power spectrum was obtained with eyes open (alpha activity blocked) and epileptiform discharges are too brief to be observed in the power spectrum of a 20 second EEG, it is not surprising that their frequencies do not appear in the power spectrum of the spontaneous EEG, yet they are shown by the SPES Bode plots. Therefore, Bode plots obtained from responses to SPES could be a biomarker for the capacity of the cortex to generate activity which may or may not be present in the specific sample of EEG.

A puzzling finding is that despite their overall similarities the blue traces appear to be slightly shifted to the right (towards higher frequencies) than the red traces in figure 9. This may be due to the fact that pairs of neurons in driven neocortex have a shorter length scale than those found in spontaneous activity[37, 38]. Alternatively, this discrepancy could be explained by distortions in the stimulus step function induced by the resistance-capacitance properties of the brain tissue.

It could be claimed that the spectra of the spontaneous EEG shows very broad bandwidth, and this is why the sharp peaks in Bode plots are within the frequency range of the spontaneous EEG. As shown in figures 8 and 9, most EEG activity occurs below 12 Hz. The graph falls off thereafter and has therefore been omitted in the figures. The assertion that this band below 12 Hz is "broad" is subjective. One could equally take the opposite view, that it is extremely narrow. If the duration of action and postsynaptic potentials are 1-2 ms, electrical activity could in principle oscillate at up to 500-1000 Hz. The fact that most power is below 12 Hz can be taken as evidence that the band is surprisingly narrow. The main point is that most Bode plot peaks scatter within this band and are not present outside it. Therefore, we suggest that the EEG could be considered as the addition of all individual resonance peaks from all connections, in addition to the superimposed local activity not explored by SPES. Even some of the largest resonance peaks in the individual Bode plots can be seen on the spontaneous EEG in figure 8.

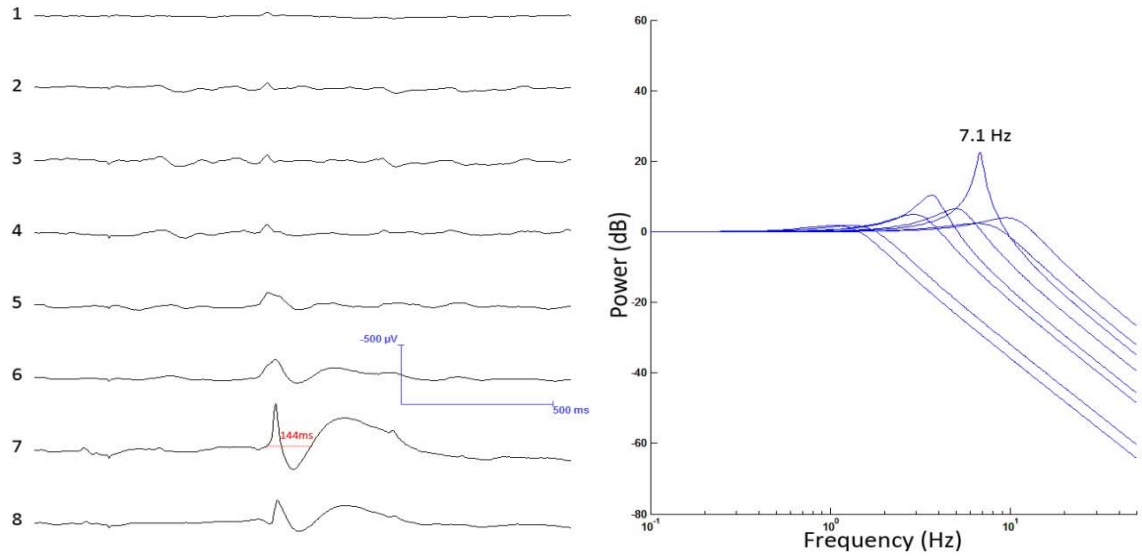


**Figure 10.** Patient 2. Left, averaged interictal discharge largest at electrode 7 showing duration of 144 ms (determining a frequency of 1/0.144 or 6.94 Hz). The frequency of this discharge is close to the largest peak (at 7.1 Hz) present in the Bode plots of SPES responses (right) which were recorded at the same electrode 7. Such interictal discharges were not present in the initial 20 second sample of spontaneous EEG. However, their frequency was prominent in SPES responses recorded by the same electrode, suggesting that the capacity of the corresponding connections to generate such discharges could be inferred from responses to stimulation, since the observed frequency peak is consistent with location and frequency with the interictal discharges.

*Physiological implications*

A very interesting observation was that late deflections tend to show longer duration than earlier deflections in nearly 60% of recorded responses (figures 5, 6D and 7). This cannot easily be modelled with a single control system, requiring the superimposition of two control systems to accurately model the response. Although both systems add up to form the standard N1, P1 and N2 deflections, the earlier deflections are dominated by fast oscillatory system, whereas later deflections are dominated by the slower system. Not all deflections are present in all responses, suggesting a different generation mechanism for different deflections [11, 12, 15, 21]. Indeed, simultaneous EEG and single cell recordings in animal and humans suggest that responses to SPES are composed of an earlier wave of excitation (lasting for less than 100 ms) followed by a longer period of inhibition (lasting for up to 700 ms) [28, 39-41]. Based on such duration for excitatory and inhibitory waves after stimulation, it would be tempting to speculate that the fast systems (such as responses type A and D1) tend to model excitation whereas the slower systems (such as responses B, C and D2) tend to model inhibition. Since interictal epileptiform discharges and responses to SPES show similar morphology and cellular mechanisms [41, 42], our method can also be used to model interictal epileptiform discharges.

Functional connectivity studies with SPES have tended to concentrate on the study of presence or absence of responses [6, 11, 12, 14, 16-18, 21-23]. The implication has been that the presence of response at site A when stimulating at site B implied the presence of functional connections from B to A. For equal distance between stimulating and recording electrodes, it is assumed that the strength of the connections is proportional to response amplitude. Thus, SPES responses provide information on the presence, strength and direction of functional connections. However, it is unclear if the morphology of responses is related to the nature of the connections. Our method goes one step ahead in estimating the coupling frequency between connected regions and the relative contribution of such coupling to the overall oscillatory activity. Consequently, we suggest that for a given recording site, our method could be used to tease out the relative contribution towards activity from each site connected to it, in addition to revealing the frequencies at which specific connections are capable of oscillating or most likely to oscillate. The damped oscillatory responses described here appear to be rather ubiquitous, possibly a manifestation of some generic cortical mechanism, suggesting that the method proposed could be used to model other electrical responses such as somatosensory evoked responses or high frequency oscillations. Furthermore, it appears that our method can detect the capability of a region to generate frequencies which may not be present in a sampled EEG record as suggested by table 6. For instance, the ability to generate alpha activity by temporo-occipital cortex was identified on the SPES Bode plots even when the sampled EEG and SPES responses were recorded with eyes open and did not show alpha activity (patient 1). The compound Bode plot for SPES responses showed a peak at the frequency of the alpha activity of that patient at the most posterior electrode which is precisely the electrode that recorded alpha activity when eyes were closed. An interpretation may be that SPES responses at the posterior electrode contain the alpha frequency because the underlying cortex is capable of generating alpha activity even if the brain was not actually generating alpha during the recording. Similarly, the capability to generate frequencies present in epileptiform discharges may have been identified by the method even when discharges were not present in the spontaneous EEG sampled (patients 2 to 5). The power spectrum of the EEG is unlikely to show a peak at the frequency of epileptiform discharges because discharges are either absent or very brief (one or few discharge lasting for 400 ms will be diluted in the power spectrum of a 20 second EEG). However, the frequencies of the discharges appear in the compound Bode plot at the appropriate channels. In fact, this finding is not all that surprising because we have described that SPES responses resemble the epileptiform discharges seen in the same channel[42]. A puzzling finding is that there were two patterns of epileptiform discharges which did not appear on specific peaks in the compound Bode plots (durations of 300ms in patient 3, and of 62ms in patient 4). This may reflect a limitation of stimulation with intracranial electrodes, since areas without implanted electrodes were not stimulated and consequently the frequency response of their connections not explored.

The question of whether this method could eventually be of use to draw conclusions about the normal brain is fascinating. Overall, the brain and EEG of people with and without epilepsy have many features in common.

Consequently, findings obtained from the use of this method may unmask some of the mechanisms of normal phenomena (such as the generation of the alpha rhythm and sleep phenomena, see for instance Voysey et al. 2015[43]) which may contribute to our understanding of the oscillatory behaviour of the non-epileptic brain in addition to that involved in generating seizures.

To conclude, we provide a method that describes the oscillatory behaviour of the EEG in terms of control theory while estimating oscillatory coupling between connected cortical regions. It may have the potential to identify frequencies at which cortical regions are able to oscillate, and possibly to separate excitatory and inhibitory activities between regions. The method is unique in that it has the potential to bring together dynamic and network models as it provides information on connectivity as well as network interactions and behaviour.

## References


1. Alarcon G., Guy C. N., Binnie C. D., Walker S. R., Elwes R. D. and Polkey C. E. 1994, "Intracerebral propagation of interictal activity in partial epilepsy: implications for source localisation," *J Neurol Neurosurg Psychiatry* **57**, 435-49.
2. Alarcon G., Garcia Seoane J. J., Binnie C. D., Martin Miguel M. C., Juler J., Polkey C. E., Elwes R. D. and Ortiz Blasco J. M. 1997, "Origin and propagation of interictal discharges in the acute electrocorticogram. Implications for pathophysiology and surgical treatment of temporal lobe epilepsy," *Brain* **120 ( Pt 12)**, 2259-82.
3. Martin Miguel Mdel C., Garcia Seoane J. J., Valentin A., Hughes E., Selway R. P., Polkey C. E. and Alarcon G. 2011, "EEG latency analysis for hemispheric lateralisation in Landau-Kleffner syndrome," *Clin Neurophysiol* **122**, 244-52.
4. Wendling F., Chauvel P., Biraben A. and Bartolomei F. 2010, "From intracerebral EEG signals to brain connectivity: identification of epileptogenic networks in partial epilepsy," *Front Syst Neurosci* **4**, 154.
5. Petkov G., Goodfellow M., Richardson M. P. and Terry J. R. 2014, "A critical role for network structure in seizure onset: a computational modeling approach," *Front Neurol* **5**, 261.
6. Lacruz M. E., Garcia Seoane J. J., Valentin A., Selway R. and Alarcon G. 2007, "Frontal and temporal functional connections of the living human brain," *Eur J Neurosci* **26**, 1357-70.
7. Valentin A., Anderson M., Alarcon G., Seoane J. J. G., Selway R., Binnie C. D. and Polkey C. E. 2002, "Responses to single pulse electrical stimulation identify epileptogenesis in the human brain in vivo," *Brain* **125**, 1709-1718.
8. Valentin A., Alarcon G., Garcia-Seoane J. J., Lacruz M. E., Nayak S. D., Honavar M., Selway R. P., Binnie C. D. and Polkey C. E. 2005, "Single-pulse electrical stimulation identifies epileptogenic frontal cortex in the human brain," *Neurology* **65**, 426-35.
9. Flanagan D., Valentin A., Garcia Seoane J. J., Alarcon G. and Boyd S. G. 2009, "Single-pulse electrical stimulation helps to identify epileptogenic cortex in children," *Epilepsia* **50**, 1793-803.
10. Kokkinos V., Alarcon G., Selway R. P. and Valentin A. 2013, "Role of single pulse electrical stimulation (SPES) to guide electrode implantation under general anaesthesia in presurgical assessment of epilepsy," *Seizure* **22**, 198-204.
11. Matsumoto R., Nair D. R., LaPresto E., Najm I., Bingaman W., Shibasaki H. and Luders H. O. 2004, "Functional connectivity in the human language system: a cortico-cortical evoked potential study," *Brain* **127**, 2316-30.
12. Matsumoto R., Nair D. R., Ikeda A., Fumuro T., Lapresto E., Mikuni N., Bingaman W., Miyamoto S., Fukuyama H., Takahashi R., Najm I., Shibasaki H. and Luders H. O. 2012, "Parieto-frontal network in humans studied by cortico-cortical evoked potential," *Hum Brain Mapp* **33**, 2856-72.
13. Iwasaki M., Enatsu R., Matsumoto R., Novak E., Thankappen B., Piao Z., O'Connor T., Horning K., Bingaman W. and Nair D. 2010, "Accentuated cortico-cortical evoked potentials in neocortical epilepsy in areas of ictal onset," *Epileptic Disord* **12**, 292-302.
14. Enatsu R., Matsumoto R., Piao Z., O'Connor T., Horning K., Burgess R. C., Bulacio J., Bingaman W. and Nair D. R. 2013, "Cortical negative motor network in comparison with sensorimotor network: a cortico-cortical evoked potential study," *Cortex* **49**, 2080-96.
15. Enatsu R., Piao Z., O'Connor T., Horning K., Mosher J., Burgess R., Bingaman W. and Nair D. 2012, "Cortical excitability varies upon ictal onset patterns in neocortical epilepsy: a cortico-cortical evoked potential study," *Clin Neurophysiol* **123**, 252-60.
16. Keller C. J., Honey C. J., Megevand P., Entz L., Ulbert I. and Mehta A. D. 2014, "Mapping human brain networks with cortico-cortical evoked potentials," *Philos Trans R Soc Lond B Biol Sci* **369**.
17. Terada K., Usui N., Umeoka S., Baba K., Mihara T., Matsuda K., Tottori T., Agari T., Nakamura F. and Inoue Y. 2008, "Interhemispheric connection of motor areas in humans," *J Clin Neurophysiol* **25**, 351-6.
18. Wilson C. L., Isokawa M., Babb T. L. and Crandall P. H. 1990, "Functional connections in the human temporal lobe. I. Analysis of limbic system pathways using neuronal responses evoked by electrical stimulation," *Exp Brain Res* **82**, 279-92.

19. Cherlow D. G., Dymond A. M., Crandall P. H., Walter R. D. and Serafetinides E. A. 1977, "Evoked response and after-discharge thresholds to electrical stimulation in temporal lobe epileptics," *Arch Neurol* **34**, 527-31.
20. Rosenblueth A. 1942, "Cortical responses to electric stimulation," *Amer J Physiol* **135**, 690-774.
21. Matsumoto R., Nair D. R., LaPresto E., Bingaman W., Shibasaki H. and Luders H. O. 2007, "Functional connectivity in human cortical motor system: a cortico-cortical evoked potential study," *Brain* **130**, 181-97.
22. Umeoka S., Terada K., Baba K., Usui K., Matsuda K., Tottori T., Usui N., Nakamura F., Inoue Y., Fujiwara T. and Mihara T. 2009, "Neural connection between bilateral basal temporal regions: cortico-cortical evoked potential analysis in patients with temporal lobe epilepsy," *Neurosurgery* **64**, 847-55; discussion 855.
23. Jimenez-Jimenez D., Abete-Rivas M., Martin-Lopez D., Lacruz M. E., Selway R. P., Valentin A. and Alarcon G. 2015, "Incidence of functional bi-temporal connections in the human brain in vivo and their relevance to epilepsy surgery," *Cortex* **65**, 208-18.
24. Donos C., Maliia M. D., Mindruta I., Popa I., Ene M., Balanescu B., Ciurea A. and Barborica A. 2016, "A connectomics approach combining structural and effective connectivity assessed by intracranial electrical stimulation," *Neuroimage* **132**, 344-58.
25. Valentin A., Alarcon G., Honavar M., Garcia Seoane J. J., Selway R. P., Polkey C. E. and Binnie C. D. 2005, "Single pulse electrical stimulation for identification of structural abnormalities and prediction of seizure outcome after epilepsy surgery: a prospective study," *Lancet Neurol* **4**, 718-26.
26. Enatsu R., Jin K., Elwan S., Kubota Y., Piao Z., O'Connor T., Horning K., Burgess R. C., Bingaman W. and Nair D. R. 2012, "Correlations between ictal propagation and response to electrical cortical stimulation: A cortico-cortical evoked potential study," *Epilepsy Research* **101**, 76-87.
27. Thompson S. 1989, Control systems. Engineering and design. (Longman group UK, United Kingdom).
28. Creutzfeldt O. D., Watanabe S. and Lux H. D. 1966, "Relations between EEG phenomena and potentials of single cortical cells. II. Spontaneous and convulsoid activity," *Electroencephalogr Clin Neurophysiol* **20**, 19-37.
29. Donos C., Mindruta I., Ciurea J., Maliia M. D. and Barborica A. 2016, "A comparative study of the effects of pulse parameters for intracranial direct electrical stimulation in epilepsy," *Clin Neurophysiol* **127**, 91-101.
30. Binnie C. D. and Polkey C. E. 1992, "Surgery for epilepsy," in Recent advances in clinical neurology, ed.^eds. Editior (Churchill Livingstone, London), pp. Churchill Livingstone.
31. Falconer M. A. 1971, "Genetic and related aetiological factors in temporal lobe epilepsy. A review," *Epilepsia* **12**, 13-31.
32. Spencer D. D., Spencer S. S., Mattson R. H., Williamson P. D. and Novelly R. A. 1984, "Access to the posterior medial temporal lobe structures in the surgical treatment of temporal lobe epilepsy," *Neurosurgery* **15**, 667-71.
33. Kissani N., Alarcon G., Dad M., Binnie C. D. and Polkey C. E. 2001, "Sensitivity of recordings at sphenoidal electrode site for detecting seizure onset: evidence from scalp, superficial and deep foramen ovale recordings," *Clin Neurophysiol* **112**, 232-40.
34. Fernandez Torre J. L., Alarcon G., Binnie C. D., Seoane J. J., Juler J., Guy C. N. and Polkey C. E. 1999, "Generation of scalp discharges in temporal lobe epilepsy as suggested by intraoperative electrocorticographic recordings," *J Neurol Neurosurg Psychiatry* **67**, 51-8.
35. Akanuma N., Alarcon G., Lum F., Kissani N., Koutroumanidis M., Adachi N., Binnie C. D., Polkey C. E. and Morris R. G. 2003, "Lateralising value of neuropsychological protocols for presurgical assessment of temporal lobe epilepsy," *Epilepsia* **44**, 408-18.
36. Kumar A., Valentin A., Humayon D., Longbottom A. L., Jimenez-Jimenez D., Mullatti N., Elwes R. C. D., Bodi I., Honavar M., Jarosz J., Selway R. P., Polkey C. E., Malik I. and Alarcon G. 2013, "Preoperative estimation of seizure control after resective surgery for the treatment of epilepsy," *Seizure-European Journal of Epilepsy* **22**, 818-826.
37. Nauhaus I., Busse L., Carandini M. and Ringach D. L. 2009, "Stimulus contrast modulates functional connectivity in visual cortex," *Nat Neurosci* **12**, 70-6.
38. Cowan J. D., Neuman J. and van Drongelen W. 2016, "Wilson-Cowan Equations for Neocortical Dynamics," *J Math Neurosci* **6**, 1.
39. Creutzfeldt O. D., Watanabe S. and Lux H. D. 1966, "Relations between EEG phenomena and potentials of single cortical cells. I. Evoked responses after thalamic and erpicortical stimulation," *Electroencephalogr Clin Neurophysiol* **20**, 1-18.
40. Barth D. S. and Sutherling W. 1988, "Current source-density and neuromagnetic analysis of the direct cortical response in rat cortex," *Brain Res* **450**, 280-94.
41. Alarcon G., Martinez J., Kerai S. V., Lacruz M. E., Quiroga R. Q., Selway R. P., Richardson M. P., Garcia Seoane J. J. and Valentin A. 2012, "In vivo neuronal firing patterns during human epileptiform discharges replicated by electrical stimulation," *Clin Neurophysiol* **123**, 1736-44.
42. Nayak D., Valentin A., Selway R. P. and Alarcon G. 2014, "Can single pulse electrical stimulation provoke responses similar to spontaneous interictal epileptiform discharges?," *Clinical Neurophysiology* **125**, 1306-1311.
43. Voysey Z., Martin-Lopez D., Jimenez-Jimenez D., Selway R. P., Alarcon G. and Valentin A. 2015, "Electrical Stimulation of the Anterior Cingulate Gyrus Induces Responses Similar to K-complexes in Awake Humans," *Brain Stimul* **8**, 881-90.

**Appendix**

**Mathematical models**

Second-order linear control models were developed and evaluated. Hereafter, *y(t)* will describe the recorded response to stimulation whereas *y'(t)* designates the modelled response of a control system.

This model assumes that human cortex can be described as a second order control system [27]. Each SPES pulse behaves as a unit step input (*U*) to the system. A generic response of such systems to a unit step function is shown in figure 1. The cortical response to SPES is regarded as the system output [*Y(t)*]. The response of the system to any frequency is determined by the response to a unit step function and will be displayed as standard Bode plots.

The transfer function [*G(s)*] of a second order open-llop (without feedback) control system is:

$$G(s) = \frac{O(s)}{I(s)} = \frac{\omega_n^2}{s^2+2\zeta\omega_n s+\omega_n^2} \quad (1)$$

Where: *O(s)* is the output (response); *I(s)* is the unit step input; $s = j\omega$; j=square root of -1; $\zeta$ is the dimensionless damping ratio and $\omega_n$ is the cut-off frequency:

$$\omega_n = \frac{\omega_d}{\sqrt{1-\zeta^2}} \quad (2)$$

Where $\omega_d$ is the system's natural undamped oscillatory angular frequency (i.e. angular frequency of the oscillation of the unit step response) of the response, which is:

$$\omega_d = \frac{2\pi}{T} \quad (3)$$

Where *T* is the period of the response oscillation (figure 1): $T=t_{p2}-t_{p1}$

The first peak would occur at latency $t_{p1}$:

$$t_{p1} = \frac{\pi}{\omega_d} \quad (4)$$

The second peak would occur at latency $t_{p2}$:

$$t_{p2} = \frac{3\pi}{\omega_d} \quad (5)$$

The relation between the amplitude of the response at the first and second peaks is characterised by the subsidence ratio (*R*):

$$y(t_{p1}) = Ry(t_{p2}) \tag{6}$$

$$R = \frac{y(t_{p1})}{y(t_{p2})} \tag{7}$$

Therefore *R* is the amplitude attenuation factor from one cycle to the next in the response (figure 1).

Most mathematical development of control theory deals with the design of systems to obtain responses of desired characteristics. Here we have the opposite problem: we are interested in characterising the system which is responsible for a given response. This can be obtained after a few algebraic manipulations as shown below. *R* and *T* characterise the system's response and can be estimated from the response itself according to the formulae shown above and in figure 1. To obtain the value of ζ in terms of *R*, we substitute for *y (t)* at the first two peaks, after shifting the y axis zero to 1, and taking natural logarithms:

$$e^{-\zeta\omega_n\frac{\pi}{\omega_d}} = Re^{-\zeta\omega_n\frac{3\pi}{\omega_d}} \tag{8}$$

$$log_e e^{-\zeta\omega_n\frac{\pi}{\omega_d}} = log_e R + log_e e^{-\zeta\omega_n\frac{3\pi}{\omega_d}} \tag{9}$$

$$-\zeta\omega_n\frac{\pi}{\omega_d} = log_e R - \zeta\omega_n\frac{3\pi}{\omega_d} \tag{10}$$

$$(-1+3)\zeta\omega_n\frac{\pi}{\omega_d} = log_e R \tag{11}$$

$$2\pi\zeta\frac{\omega_n}{\omega_d} = log_e R \tag{12}$$

$$2\pi\zeta\frac{\omega_d}{\omega_d\sqrt{1-\zeta^2}} = log_e R \tag{13}$$

$$\frac{2\pi\zeta}{\sqrt{1-\zeta^2}} = log_e R \tag{14}$$

$$\frac{4\pi^2\zeta^2}{1-\zeta^2} = (log_e R)^2 \quad (15)$$

$$4\pi^2\zeta^2 = (log_e R)^2 - \zeta^2(log_e R)^2 \quad (16)$$

$$\zeta^2(4\pi^2 + (log_e R)^2) = (log_e R)^2 \quad (17)$$

$$\zeta = \sqrt{\frac{(log_e R)^2}{4\pi^2 + (log_e R)^2}} \quad (18)$$

Equation (18) provides the value for ζ from *R*, which can be measured on the recorded systems response (in our case, on the EEG response to SPES). The expected (modelled) system time response, or *y'(t)*, can be calculated from the characteristic equation of the transfer function (1) and a standard partial-fraction expansion with its three poles (Thompson, Control systems…… pages 77-79) as:

$$y'(t) = 1 - \frac{e^{-\zeta\omega_n t}}{\sqrt{(1-\zeta^2)}}\left[\zeta \sin(\omega_d t) + \sqrt{(1-\zeta^2)}\cos(\omega_d \right. \quad (19)$$

By substituting ζ obtained from equation (18) into *y'(t)* in equation (19) we can calculate the expected (modelled) system's time response ignoring the DC of 1 introduced by the first term on the right of the equation.

A more stable model can in principle be achieved by adding a negative feedback loop (a closed loop system). If *G(s)* is the transfer function of the open loop system:

$$G(s) = \frac{N(s)}{D(s)} = \frac{\omega_n^2}{s^2 + 2\zeta\omega_n s + \omega_n^2} \quad (20)$$

Then the transfer function of the closed loop system for a simple proportional controller of *K* gain is [27]:

$$\frac{O(s)}{I(s)} = \frac{N(s)}{D(s) + KN(s)} \quad (21)$$

For the second order closed-loop control system, the transfer function then becomes:

$$\frac{O(s)}{I(s)} = \frac{\omega_n^2}{s^2 + 2\zeta\omega_n s + (K+1)\omega_n^2} \tag{22}$$

Note that the open loop system is the particular case of the closed loop system where K=0. The closed loop system characteristic equation is:

$$s(s^2 + 2\zeta\omega_n s + (K+1)\omega_n^2) = 0 \tag{23}$$

This system has three poles at *s*=0 and at:

$$s = -\zeta\omega_n \pm j\omega_n\sqrt{1 + K - \zeta^2} \tag{24}$$

Following complex number interpretation of the poles, the modulus of *s*, for *s* other than 0 is:

$$\sqrt{\zeta^2\omega_n^2 + \omega_n^2(1 + K - \zeta^2)} = \omega_n\sqrt{1+K} \tag{25}$$

and

$$\omega_d = \omega_n\sqrt{(1 + K - \zeta^2)} \tag{26}$$

Therefore,

$$\cos\theta_1 = \frac{\omega_d}{Modulus\ of\ s} = \frac{\omega_n\sqrt{(1+K-\zeta^2)}}{\omega_n\sqrt{1+K}} = \sqrt{1 - \frac{\zeta^2}{1+K}} \tag{27}$$

$$\sin\theta_1 = \frac{\zeta\omega_n}{\omega_n\sqrt{1+K}} = \frac{\zeta}{\sqrt{1+K}} \tag{28}$$

Following the same arithmetical operations as shown in pages 78-79 [27] but for the newly defined modulus and $\omega_d$, the time response to a step function of the closed loop second order system, *y'(t)*, is:

$$y'(t) = 1 - \frac{e^{-\zeta\omega_n t}}{\sqrt{(1-\zeta^2)}}\left[\frac{\zeta}{\sqrt{1+K}}\sin(\omega_d t) + \sqrt{\frac{1+K-\zeta^2}{1+K}}\cos(\omega_d t)\right] \quad (29)$$

$$y'(t) = 1 - \frac{e^{-\zeta\omega_n t}}{\sqrt{(1-\zeta^2)}\sqrt{1+K}}\left[\zeta\sin(\omega_d t) + \sqrt{1+K-\zeta^2}\cos(\omega_d t)\right] \quad (30)$$

The Bode diagram for the closed loop system can be derived as follows:

$$\frac{O(s)}{I(s)} = \frac{\omega_n^2}{s^2 + 2\zeta\omega_n s + (K+1)\omega_n^2} \quad (31)$$

$$\frac{O(s)}{I(s)} = \frac{1}{\frac{s^2}{\omega_n^2} + \frac{2\zeta\omega_n s}{\omega_n^2} + \frac{(K+1)\omega_n^2}{\omega_n^2}} = \frac{1}{K+1-\left(\frac{\omega}{\omega_n}\right)^2 + j2\zeta\left(\frac{\omega}{\omega_n}\right)} \quad (32)$$

The amplitude at each frequency is represented by the following function which corresponds to the Bode plot representation of amplitude versus frequency:

$$20\log_{10}[\text{Modulus of } O(s)/I(s)] = \quad (33)$$

$$= -20\log_{10}\sqrt{\left[K+1-\left(\frac{\omega}{\omega_n}\right)^2\right]^2 + 4\zeta^2\left(\frac{\omega}{\omega_n}\right)^2}$$

# 4. DISCUSSION

The work described above, shows that EEG activity recorded at the scalp level reflects a complex system originated by the interactions of superficial and deep cortical and subcortical structures. Such interactions simultaneously involve volume conduction and physiological activation and propagation along deep and superficial structures.

- ***Intracranial signatures: The realm beneath the waves***

The information obtained from depth electrodes can be helpful in the context of epilepsy. However, invasive recordings are not always available and we often only relay on scalp EEG recordings for the diagnosis of epilepsy. The qualitative analysis of scalp EEG is a routine practice in any Neurophysiology department, but many relevant information escapes the eye, hidden beneath the waves of higher amplitude background activity (Alarcon et al., 1994). Deep activity cannot be easily recorded on the scalp but can be estimated by their interplay with superficial sources and more directly by the methods outlined in our work about intracranial signatures(193). Overall, the classification performance of our algorithm reached a 65% accuracy. This might seem low compared with other studies just based in scalp data(149, 194) but it is an excellent result considering that we are detecting virtually invisible epileptiform discharges on the scalp while other methods count on prominent discharges on the scalp EEG. Increasing the length of the recordings to provide a higher number of examples, and increment the number of electrodes to improve spatial coverage would yield higher accuracy as suggested(195). Being able to detect what is hidden under the background noise from superficial activity would add a great value to the routine EEG analysis avoiding the need for repeated tests and possibly intracranial recordings. Hopefully,

with the perfection of this and other similar algorithms exploring the value of intracranial signatures, we will be able to reduce the need for invasive assessments and target well defined focal areas of increased epileptogenicity with a simple scalp EEG. A significant improvement in this field will not only improve diagnostic accuracy but would positively impact parallel fields such as automated seizure detection(196). Nowadays these devices are still precarious as they are dependent on the seizure type, which has great intra and inter-individual variability(196).

Our method has been further developed including deep convolutional networks to improve accuracy(157, 197). We have used deep learning to train the algorithm to use convolutional networks to learn meaningful features in a hierarchical process. As a result, the algorithm distinguishes not only between segments where there are or there are not definite epileptiform discharges, but also is able to classify how abnormal are the elements detected. This approach has demonstrated to be more accurate reaching an outstanding 89% accuracy possibly due to its ability of assimilate more complex information(157).

We cannot close this subject without a final methodological remark. A great variety of algorithms are trained to detect what is abnormal based in a pre-established definition but the performance of such automated systems for detection of epileptiform discharges is still poor compared with human detection. Even in the best case scenarios, some of the most popular methods combining wavelet transform, neural networks and artificial intelligence fail to identify a high proportion of spikes when compared with human expert detection(149) and what is worse, show a dangerous tendency to identify abnormalities which are not present, potentially hanging the long-life label of “epileptic” to a healthy individual. Developing an algorithm able to discriminate some particular activities among a

myriad of similar waveforms is not a simple task as it consists of providing a machine with the same ability to discriminate as a trained human subject: clinical judgement. This part of our job falls onto the trendy area of artificial intelligence systems. Our method is more "natural" in the way that we do not offer the algorithm a definition, but a precise timing to look at considering temporal, spectral and spatial parameters and we ask the algorithm to find similar circumstances in other recordings. Deep learning avoids the need for central representations(198) and falls in the field of what has been called "intelligence without representation"(199). This is a way to understand learning as an interactive process based on activity decomposition and self-experience rather than on a centrally predefined plan. The algorithm learns based on the interaction with the set of data decomposing it in a set of parameters. This concept might initially seem trivial, but it parallels what happens in human cognition as the meaning of a given concept ("interictal discharge" in this case) largely relies on the subject's previous experience(200). Exploiting our approach to the problem would hopefully yield better results in the mid-term in the field of automated spike detection.

- ***SPES and generation of physiological sleep features***

In our study about K-complexes, we have found that electrical stimulation of a particular area of the anterior cingulate gyrus generate responses similar to spontaneous sleep K-complexes consistent with a model in which the dorso-caudal anterior cingulate would act as a relevant trigger in the initiation of the cortical process leading to the generation of K-complexes. The fact that these responses are obtained in the awake subject is a rather striking finding apparently incompatible with our knowledge of sleep physiology.

What is the potential explanation for this paradox? As stimulation did not induced sleep or other sleep phenomena, we can assume that only part of the circuits involved in sleep were activated, probably sparing the subcortical loops. This would mean that K-complex generation is largely based on cortico-cortical connections as has been suggested elsewhere(183). The K-complex-like responses observed after electrical stimulation were not usually associated with spindle activity in contrast to spontaneous K-complexes which are often associated with sleep spindles(201). Sleep spindles generation requires activation of the reticular nucleus of the thalamus(184) and our findings suggest that during wakefulness, cingulate stimulation is unable to activate such circuits, either because the activated networks are possibly restricted to cortical loops or because a general sleep physiological environment is required for sleep spindles to be activated. Based on the first, it can be argued that we are only activating part of the network giving rise to the K-complex. This seems unlikely, as if that was the case, we would only expect to see the K-complex-like signals in a variable subset of the channels in contrast to our results showing a widespread distribution equivalent to that observed in physiological K-complexes.

The K-complex-like responses induced by SPES resemble spontaneous K-complexes in the same patient. In contrast to responses to stimulation physiological K-complexes would be the result of spontaneous interaction between neural sets resulting in cingular activation. The stimulation triggering spontaneous K-complexes would then be a physiological activation, possibly arriving from sensory networks (mainly somatosensory or auditory modalities) as classically proposed(202-204). Activation of the cingulate gyrus may arise from excitatory input from parietal association cortex or thalamic projections in the somatosensory or auditory pathways (ventral posterolateral, ventral posteromedial or the

medial geniculate nucleus of the thalamus)(205). Therefore, a direct thalamo-cortical excitatory input to the cingulate cortex cannot be excluded as the initiator of the sequence of cortical activations resulting in the bilaterally synchronous EEG element known as K-complex.

- ***Generalised seizures and the role of thalamo-cortical interactions***

The thalamus has a privileged relation with the cortex. Its nucleus diffusely project to most areas of the cortex, some nucleus transmitting sensory information to sensory cortex and multimodal association areas while others project to motor areas responsible for the post-processing of movement sequences and assess correct execution(205). As discussed in the introduction, this profuse anatomical interconnection and its midline situation has classically pointed to the thalamic structures as the origin of the synchronous epileptic phenomena known as generalised seizures but evidence from animal models and humans has often provided contradictory evidence for the relative contribution of cortical and thalamic structures in generalised seizures.

In our study we analysed qualitative and quantitatively three patients studied with simultaneous scalp and thalamic centromedian electrodes. We had the rare opportunity of assessing the centromedian nucleus via implanted electrodes for deep brain stimulation and studied the thalamic behaviour during focal and generalised seizures. Each case shows a different scenario demonstrating the complex relation between thalamus and cortex in the context of generalised and focal epilepsy.

Patients with generalised epilepsy showed simultaneous or nearly simultaneous onset of epileptiform activities at scalp and thalamic EEG recordings. In one case the onset was cortical while in the other was simultaneous in cortex and thalamus. However, what was common for both was that once the thalamus was involved it became the leading structure and induced a higher degree of rhythmicity and homogeneity to the epileptiform abnormalities observed. In the patient with focal epilepsy, as it can be expected the thalamus only became involved after the seizure was already established.

A surprising but significant finding was the presence of frequent spontaneous independent epileptiform abnormalities in the thalamus bilaterally in one patient. This finding suggests that the thalamus has some intrinsic epileptiform capability of its own. Despite of this, the findings do not consistently demonstrate a leading role of the thalamus in the initiation of seizures but do support a role for the thalamus in maintaining seizures.

In the last decade a new concept has emerged to describe the pathophysiology of generalised epilepsy as a "system epilepsy" (206). The focal "trigger" has lost some importance as the new concept of a diffuse increase in excitability (altered functional connectivity) has emerged. This model assumes that the root of the problem lies in a large-scale increase in circuit excitability. Evidence for this concept has been provided from basic quantitative EEG studies(207), graph theory analysis(208, 209), combined EEG-fMRI studies(210-212) and magnetoencephalography studies(213). The scenario allows for a great variety of mechanisms being able to initiate the spark that leads to the development of the seizure. Theoretically any excitatory stimulus able to overcome the excitability threshold would act as the trigger in a fashion that is less anatomically specific. This would explain the discrepancies observed in the literature and would provide a broader conceptual

frame replacing previous theories suggesting a rather complex relation between thalamo-cortical circuits at seizure onset.

What our findings suggest is that irrespective of the structure where the seizure actually originates, the characteristic rhythmicity and seizure maintenance observed in the ictal EEG is determined in part by thalamic involvement. Perhaps therapeutic approaches aiming to stop this rhythmic behaviour would help in the reduction of the incidence and duration of generalised seizures but it is difficult to predict how the hyperexcitable network would behave without the regulatory influence of the thalamus. This would vary depending on whether the basic spreading mechanism would just initially involve locally connected areas(214) or distant spreading(215). Based on SPES data we can first hypothesise that the latter is more likely, but this is unlikely as simultaneous activation occurs within milliseconds in the practical totality of the cortex(216). In contrast, although theoretically more complex, spreading through layer V has demonstrated to be faster(214). We cannot predict the effects of such hyperexcitable state at a cellular level but there is some evidence supporting intracortical spreading(119) and therefore this hypothesis cannot be excluded. Perhaps the use of SPES and quantification of forced coupling in subjects with generalised epilepsy would add further evidence in one direction or the other (see section “Forced coupling and epilepsy”).

- ***Forced coupling a new window to study functional connectivity***

In our last and perhaps more relevant study, we have demonstrated that cortico-cortical interplay can be characterised by a set of control systems acting together in response to a given stimulus. Despite of the complexity of the mathematical development, the principles of our model are simple. Essentially, induced coupling assumes that electrical stimulation forces functional coupling between brain regions (neural masses) synaptically connected, inducing oscillations at the frequencies at which the cortical regions involved are most likely to oscillate. The frequencies at which a connection is likely to oscillate after stimulation determine the largest peaks on the frequency response of the connection (the resonance frequencies) and the resonance frequencies of the local connections will determine the overall oscillatory behaviour of the region. In this context, it is easy to understand that interictal epileptiform discharges or seizures can arise when the resonance frequency of one connection dominates over others, and our method can measure such dominance. This is a new way to interpret the electroencephalogram and cortical physiology in general, which opens a wide new area of research in neuroscience by providing objective measures of degree of functional coupling between connected regions in the frequency domain.

The brain is composed by a large number of neurons profusely interconnected by tracts of white matter. It is relatively simple to estimate the behaviour of a single neuron or small group of neurons with a limited number of equations, but the behaviour of larger populations is rather complex and frequently cannot be predicted by the summation or interconnection of a large number of the individual elements(69, 70). Failure of such models can be attributed to the practical impossibility of describing all the connections of each neuron in the brain and their relative strength. At a larger populational level it is perhaps more practical to describe the brain as a group of larger sets of neurons (the neural masses)

and then analyse the populational dynamics between them(72). Neural mass theory assumes that when a large number of non-linear elements (the neurons) influence each other reciprocally over an extended time and space, a hypothetical higher order structure (the mass) emerges with totally different properties, including linear properties. Due to its configuration, minor changes at cellular level can trigger sudden changes in the overall state of the neural mass. The opposite is also true, as minor variations in the sequence or number of small elements (neurons) activated within a neural mass may not change the response (42, 44). The overall behaviour of the mass is the result of large-scale spatio-temporal interaction of neurons exceeding the microscopic level ultimately leading to large scale synchronisation giving rise to what has been called “macrostates” of activity(72). These changes translate into the macroscopic and often sudden changes observed in the EEG.

Our method develops an approach to describe functional connectivity between large groups of cortical neurons. The concept of functional connectivity implies either a direct synaptic connection between two groups of neurons or a more complex interaction with several networks intercalated in the chain and mutually interacting. Whichever is the case, the final result is a variation in the local field potential expressed as a deflection or group of deflections. These intracranial EEG deflexions allow us to employ a phenomenological approach to infer some oscillatory properties of the group of neurons in the proximity of the electrode. Our work aimed at characterising the generation of these EEG elements: the early responses to single pulse electrical stimulation. These responses have proven to be ubiquitous to all cortical regions, including healthy tissue, and therefore are most likely physiological responses(159). Their morphological variations are still nowadays unexplained and although many descriptive approaches have been attempted, no theories have arisen to

justify their morphology until now. In an initial approximation we observed that the outcome of the neuronal activation after SPES can often be described as dampened sinusoids, resembling the response of second order linear control systems to a transient input(191). A control system is composed of multiple components connected or related in such manner that they act as an entire unit(191). This is in our case, the neural mass or masses contained within the cortical region surrounding the recording electrodes. We suggest that during SPES, electrical stimulation acts as a forced input that destabilises the balanced state of the system embodied by the cortex. The induced early responses would be a product of the transient responses of the system (the cortex) until a baseline equilibrium level is reached again (the steady-state).

Brain activities can be described as a conjunction of non-linear and linear features. Responses to SPES show a quasi-linear increase in amplitude with increase in stimulation intensity(165, 217). In addition, control theory has previously been employed to model cortical activity by different authors (72, 218-222). Model based predictor-controller systems as the Kalman filter (222), can calculate a particular system state (as a neuronal population) and the control vectors that modulate it. An important part of the defining process of these models is the definition of a number of initial conditions whose variation significantly affects the outcome of the system. These control models have been successfully employed to replicate a variety of dynamic patterns spontaneously produced by the mammalian brain (220) and modulate them in terms of oscillation frequency and spatiotemporal parameters (221).

Studies in SPES have demonstrated that linear variations in stimulus intensities lead to significant changes in response amplitude (158, 163, 165, 170, 217) and morphology (168,

170) of the induced responses up to a limit of intensity of stimulation. In our study, cortical responses obtained from electrodes close to the stimulating pair showed highest amplitudes. Other authors(168, 170) have observed higher amplitudes and response damping (fewer oscillations) with increasing stimulation intensities. By contrast, lower intensities and longer recording distance from stimulation are associated with lower amplitude responses and higher number of oscillations. This would suggest that the parameters of the control systems involved change with stronger stimuli. We could hypothesise that as a response to a strong stimulation, the cortex reacts with a strong inhibitory response with strong oscillation damping. By contrast, weaker stimulation induces a milder inhibitory response, allowing the cortical connections to oscillate for longer. The fact that R and T values change in response to different intensities means that cortex possesses high versatility, reacting with stronger or milder inhibitory patterns as required depending on the input.

- ***Evaluation of cortical excitability: insights from transcranial magnetic stimulation (TMS)***

In order to explain the subjacent mechanisms supporting the control systems, we need to understand the interplay between excitatory and inhibitory cortical processes. In our model we have assumed that feedback loops are mainly mediated by surround tonic inhibition. Indeed, inhibitory postsynaptic potentials observed in single cell recordings coincide in time with the macroscopic slow EEG response deflections in anaesthetised cats (223) and with the responses to SPES observed in human recordings(94). We can gain some insight into what can be happening in the cortical circuits during SPES by examining the neuronal

behaviour resulting after TMS. The complexity of cortical excitability has been profusely studied with TMS in the motor cortex has disclosed several mechanisms of facilitation and inhibition. TMS and electrical stimulation share common principles of action. Both can activate a descending volley through the corticospinal tract, but there are some slightly different mechanisms involved in each modality of stimulation. Epidural electrical cortical stimulation excites the neuron perpendicularly at the axon hillock whereas during magnetic stimulation, activation is mediated by interneurons due to the orientation of the induced electric field, parallel with the scalp(224). When examining corticospinal tract responses at motor threshold intensities, a single prominent wave (the D-wave) is characteristically elicited by electrical stimulation followed by variable smaller waves with slightly longer latencies (the I-waves) while magnetic stimulation predominantly or exclusively generates I-waves(225). These I-waves are mediated by interneurons or by connections proceeding from other pyramidal cells from layer V with complex dendritic trees(226). However, when employing supra-threshold magnetic intensities evoking latero-medial induced currents, the obtained pyramidal tract responses are similar to those induced by electrical stimulation producing both types of responses, D and I-waves.

For our purpose, the study of intracortical inhibition and facilitation after subthreshold TMS pulses is highly relevant(227). There is a variety of mechanisms from the pharmacological point of view that can help us to illustrate such complex balance between inhibition and excitation after electrical stimuli. When a conditioning stimulus is delivered to the cortex, there is an initial period of inhibition (short intracortical inhibition - SICI), mediated by GABA-A and dopamine, lasting for 1-4ms(228) and a later period, between 50 and 200ms (long intracortical inhibition – LICI)(229) mediated by GABA-B(230). In addition, the silent

period (a pause in ongoing voluntary muscle contraction) consistently occurs after delivering a TMS pulse and is also mediated by GABA-B receptors(231). This is a slightly more complex phenomenon as it is not purely cortical. The entire silent period lasts between 200-300ms, but the initial 50-75ms of this inhibition are attributed to spinal mechanisms while intracortical inhibition accounts for the remaining time(232). Interestingly after peripheral somatosensory stimulation, other periods of cortical inhibition are described at 20 and 200ms (short afferent and long afferent inhibition – SAI and LAI) which are mediated by cholinergic effects(233). In terms of longer cortical projection phenomena, stimulation of the primary motor cortex has demonstrated to produce inhibition on the contralateral primary cortex at 10 and 40ms after the motor cortex stimulus (transcallosal or interhemispheric inhibition)(234) and similarly premotor cortex stimulation produces ipsi and contralateral inhibition(235, 236). Interestingly interhemispheric inhibition is affected by LICI, SICI and LAI meaning a hierarchical predominance of these GABA-mediated mechanisms(237, 238) but there is also some conflicting evidence questioning this preponderance (239). On the other side, after the TMS pulse there is a period of facilitation between 6-20ms (intra-cortical facilitation - ICF)(227) mediated by glutamatergic mechanisms(240, 241). We can infer some parallelism between these periods of change in cortical excitability and the early responses after SPES. Previous studies with simultaneous single cell and EEG recordings during SPES have demonstrated and early period of neuronal activation lasting less than 100ms followed by a period of inhibition up to 700ms(94, 223, 242, 243). This then suggests that the earlier responses can correspond with a period of increased neuronal firing in keeping with excitation while that later wave would reflect inhibition. Combined pharmacological and SPES studies would help to shed light into the

specific role of each cortical neurotransmitter after electrical stimulation. Our study revealed that the initial and generally shorter deflections (responses A and D1) occurred with latencies of around 13.1 ms. This would fall in the interval where intracortical facilitation applies and interestingly would have its maximal expression in areas in the vicinity of the electrode. We can hypothesise that glutamatergic activation underlies the generation of such responses. Similarly, the second group of responses showing longer duration and more prolonged latencies with onset around 70ms (B and D2 responses), fall in the interval of late intracortical inhibition and cortical silent period, suggesting a predominantly GABA-B-mediated generation but also coincide with the long afferent inhibition suggesting a cholinergic mechanism.

- ***The role of control systems in cortical dynamics***

The original idea behind our approach to control system theory was to find the mathematical explanation for the variety of waveforms observed after electrical stimulation. However, the model soon demonstrated its utility beyond this goal. As an emergent property it can predict the overall populational behaviour in terms of the power spectrum.

The morphology of the responses modelled (dampened sinusoids) resembles other biological responses obtained from the brain. For example, we can for instance consider the somatosensory evoked potentials or the slow waves that frequently follow epileptiform discharges. These activities possibly obey to similar mechanisms producing such waveforms based in control systems acting in response to a stimulus (physiological in the case of

evoked potentials and pathological in the case of epileptiform discharges). This may be a clue for understanding the majority of sinusoidal activities observed in the EEG.

Our method assumes that SPES activates functional coupling between connected regions. We suggest that the induced responses oscillate at the frequencies at which the neural masses involved are most likely to oscillate. From our model and based in the morphology of the responses, we can determine the resonance frequencies of the local connections based on the frequency of the response and the attenuation between contiguous deflections. With these parameters, a function of the expected amplitude of frequencies for each control system can be expressed as a diagram (Bode plot). Such diagrams showed resonance peaks, reflecting the frequencies at which each system is most likely to resonate. Thus, the relative contribution to spontaneous oscillations for each pair of connected regions can be established with this method. But what would be the processes generating such oscillations at a cellular level? Based in the nature of our responses and in the deductions inferred from TMS investigations we can theorise that the initial deflection (most likely glutamatergic) is therefore generated as an effect of pyramidal cell activation and resonance, while the later deflections (most likely GABA-ergic) would arise from inhibitory interneurons to counteract the excitatory effect of the initial pyramidal cell response.

At a given region, after stimulating at multiple sites we can summate the obtained Bode plots obtained by stimulating at each connected site in order to determine the overall oscillatory behaviour of the region studied. In other words, we suggest that the transfer functions of the control systems for a particular area with their peaks, summate to generate the EEG. This essentially means that these control systems are arranged in parallel rather

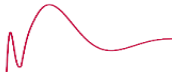

than in series, since the transfer functions add up. For each region we only obtained a low number of stimulations due to the limited number of electrodes inserted, but even considering this limitation, the degree of similarity between recorded and simulated EEG power spectra is surprisingly high. The differences may arise from connections from other regions not implanted and therefore not examined by SPES. We hypothesise that a study with a higher number of electrodes implanted will increase such similarity ultimately achieving a perfect modelling in a theoretical setting with a high number of electrodes.

The resulting overall prediction for the response power spectrum shows a high degree of similarity with the spectrum of spontaneous EEG. This interesting result provides a new explanation for the low-pass property of the EEG. It is well known that the amplitude of brain oscillations decreases with increasing frequency as shown by the power spectrum of spontaneous EEG activity. In general lines the magnitude of power tends to be inversely related to temporal frequency(244, 245). Our model also predicts a similar behaviour, showing a predominance of “slower” frequencies grossly below 12 Hz, and a steep attenuation of frequencies above the cut-off frequency. This attenuation is particularly dramatic in high frequencies corresponding with the high frequency oscillation spectrum, therefore explaining the extremely low amplitude observed for the highest frequencies. It can be argued that the compound Bode plots obtained by our model have a more marked attenuation than those observed in the EEG at the highest frequencies of the spectrum. This can be explained by the use of a second order model that shows more specificity when it comes to describing frequencies while showing steeper high frequency falloff rates. There are many potential explanations for this behaviour at the cellular level. Firs, this property is mainly attributed to the dendrites(246, 247), particularly to those in pyramidal due to their

length and activation. Some authors have also linked this phenomena to the capacitive properties of the extracellular medium(248), but the capacity of the extracellular medium is negligible in practice(104). In addition, the neurons as a group also have some features that can explain this low-pass filter behaviour from a network point of view. The number of neurons that can be recruited in response to a given stimulus is limited by time. Therefore, it is easy to understand that if we increase the time window, we can recruit a higher number of neurons, adding their potentials to the overall field. Faster frequencies would not allow a sufficient number of neurons to be activated synchronously and therefore the resulting amplitude of the local field potential would then be smaller(18, 24). Also, this process depends on the time constant of a particular neurotransmitter and this would determine the type of activity generated. For instance, NMDA and GABA-B receptors have slow time constants while AMPA or GABA-A have faster time constants(18, 106). In addition, due to the phase-amplitude coupling phenomenon, the phase of slow oscillations modulates the power of faster oscillations limiting their duration(24, 48, 249).

In our work, the majority of the recorded responses required the algebraic addition of two control systems to be modelled. Usually early deflections were shorter and yielded faster frequency peaks while late deflections showed longer duration and therefore slower frequency peaks. But not always two control systems were required as sometimes only one type of oscillation was present(161, 162, 165, 174) and the response could be modelled with only one control system (one resonant frequency).

With our paradigm, in contrast to physiological stimuli, we introduce an external electrical input able to produce supramaximal recruitment of connections. It is precisely due to the nature of our method, that connections that were indeed inactive in certain physiological

conditions can be activated by SPES and produce corresponding peaks of activity in the Bode plot. For instance, our method was able to successfully identify resonance peaks in the alpha frequency when activating connections to the occipital region even with eyes open(192), even when such peaks corresponding with the alpha frequency were not present in the power spectrum of the spontaneous EEG because eyes were open during recording. Analysis of the alpha rhythms in the same subject revealed that resonant frequencies predicted by our method were similar to the patient's mean alpha frequencies. In a recent work with SPES, the amplitudes of early responses tend to vary depending on the baseline power of alpha and beta frequencies(250). In essence, the authors interpreted that alpha and beta oscillations can modulate local excitability demonstrated by enhanced amplitude in SPES responses. Integrating this information in our model adds a further explanation to this interesting phenomenon. We can consider that a given cortical area has the latent capacity of producing a certain rhythm and as we have demonstrated, this can be detected even when the rhythm is not actually happening.

Lastly, we can hypothesise that our analysis would prove useful to assess situations where the cortex properties are altered either due to drug-induced effects like anaesthesia or secondary to pathological conditions such as encephalopathies or disorders of consciousness. Some evidence has been obtained in TMS studies revealing abnormal cortical excitability with reduced inter-neuronal transmission (reduced intracortical inhibition and facilitation) in vegetative state(251). SPES can be employed to assess cortical excitability and dynamics in this and similar contexts.

- ***Forced coupling and epilepsy***

Neural mass models have been created to simulate the behaviour of large cortical populations according with a few parameters. This has been employed not only to understand the generation of physiological background rhythms(72), but also pathological phenomena. Seizures have successfully been simulated employing neural masses-based models(252). In this model, changes in the inhibitory or excitatory gain lead to the generation or seizure-like rhythmic patterns. For this purpose, changes in pyramidal cells excitatory time are necessary in order to generate instability. Either a reduction of GABAergic tone(253) or an increase in the speed of secretion of excitatory neurotransmitters by the pyramidal cells(252) would then lead to the unstable-hyperexcitable state of the cortex that characterises seizures.

Translating into our approach, when prominent peaks (resonant peaks) are predicted by our model, a high likelihood of oscillating at a particular frequency arises (instability). This increases the tendency to oscillate, with the property of progressively recruiting an increasing number of circuits, which is in essence what characterises epileptic seizures. Our method can detect and quantify when a particular resonance frequency of one connection dominates over the rest due to the model's ability to estimate the functional coupling between connected regions at each frequency (even when not oscillating at the resonant frequencies). The sharper and larger the peak is, the more likely that the connection will resonate at the peak frequency, supposedly transforming into a seizure.

We have already discussed the ability of control system theory to detect background frequencies characteristic for certain cortical regions, even when the typically required

conditions are not met (alpha rhythm detection with eyes opened), but this is not only true for background rhythmic activities, but also for transient phenomena. Our analysis showed that disagreements in resonance peaks between the recorded EEG spectrum and our predicted peaks could often be explained by the presence of transient EEG phenomena later in the record. As epileptiform discharges occur occasionally, they may be too infrequent to be detected in the selected period of EEG for analysis. Similarly, in contrast to the interpretation of a standard EEG usually lasting for 20-90 minutes, our method may allow us to establish the capability of the cortex to generate epileptiform discharges even if such discharges were not present during the necessarily limited duration of the standard EEG. The implications of this for the study of propagation of interictal and seizure activity are enormous and can lead to the future development of specific therapeutic tools and protocols for mapping of brain areas involved in the initiation and spreading of epileptiform activity. This could lead to improved resections in epilepsy surgery, avoiding unnecessary removal of functionally independent areas and focusing on relevantly connected cortices.

This is not the first time that SPES has proved its ability to demonstrate the presence of connections activating epileptogenic circuits. Its role in detecting the seizure onset zone relies on the induction of delayed responses(159, 163, 165, 169, 171, 172, 177, 178). Furthermore, there is also some evidence suggesting that electrodes showing more early responses are associated with the epileptogenic cortex (seizure onset area)(254). Although this can just possibly correlate with adequate location of the stimulating electrodes in well-connected areas, it can also be attributed to increased effective connectivity of the ictal-onset zone. The reasons for this are unknown but could be potentially attributed to reinforcement of the connections or to some intrinsic properties of the dysplastic

tissue(255). Our group has demonstrated the usefulness of SPES to reproduce responses with similar morphology to the patient's habitual interictal epileptiform discharges after electrical stimulation of epileptogenic areas(93), and they not only share similar morphology but also common cellular mechanisms (94, 256). Therefore, as suggested earlier, our method could prove useful to model epileptiform discharges and ensuing slow waves, and get further insight of the mechanisms that generate these abnormalities interictally as opposed to ictal events.

Seizure spreading to contiguous regions is most likely the consequence of impaired GABA-A inhibition in horizontal axonal transmission in layer V(214). Spreading to neighbouring areas occurs faster but propagation time to more distant areas is longer and may obey to other mechanisms. It has been proposed that indirect spread to non-connected areas and secondary generalization could be linked with reduced inhibition over the large cortical areas rather than direct axonal spreading(215). In this direction, SPES ability to map functional connectivity(77, 161, 162, 164, 166-168, 174-176, 255) and the added value of forced coupling analysis could increase our understanding of the behaviour of focal circuits in the areas involved, allowing us to estimate if spreading correlates with altered inhibition or to facilitation. Comparison of bode plot data obtained from cortical areas with different role in seizure generation and spreading would theoretically help to distinguish between regions of healthy or abnormal hyperexcitable tissue based on the bode plot profiles with strong resonance peaks due to uncontrolled oscillations after SPES.

- ***High frequency oscillations (HFOs) and SPES***

HFOs are low amplitude highly fast oscillations between 80 and 800 Hz(257), divided into ripples band defined (between 80-250 Hz) and the fast ripples (between 250-500 Hz)(258). These phenomena have recently gained importance in the field of epilepsy as there is strong evidence suggesting their potential role as a biomarker for epileptogenic tissue in human micro and macro-electrode recordings(259-262), suggested by the better postsurgical results obtained after removal of HFO-generating tissue(263). SPES ability to induce HFOs has been demonstrated by other groups(254, 264). Interestingly, SPES stimulation in the seizure onset zone provokes a significant increase in HFO compared with other non-seizure onset locations. Although the diagnostic role of HFO is increasingly being accepted and incorporated to the clinical practice, some studies suggest that its reliability as a seizure onset marker is not superior to that of spikes(265). A potential explanation for this lies in the fact that while epileptiform activity is only rarely found in healthy cortex, HFOs can be encountered in a variety of tissues and physiological conditions such as in the occipital areas while visual processing(266), in sensorimotor cortex in the context of motor activity(267) or in the hippocampus during slow wave-sleep(268).

Can we use our model to study HFOs? We have already mentioned a tendency for the shorter duration (higher frequency) oscillations to generate closer in time to the SPES stimulus. We can hypothesise that circuits generating faster oscillations show an early activation. Therefore, networks responsible for the generation of HFOs would then fire closer to the electrical stimulus. HFOs have been the object of study of recent works with SPES. A recent study employing higher sampling frequency than ours looked for the presence of HFOs during the first N1 deflection (corresponding to types A and D1 in our study) and the second N2 deflection (corresponding with B and D2). Their analysis revealed

an increase in HFOs power during the early period after stimulation but decreased power afterwards(264). This is consistent with the presence of bursts of action potentials shortly after SPES, followed by longer periods of inhibition (94).This is strongly in line with the assumptions of our model where the faster deflexions take place first. In summary, SPES-HFOs studies have done its first steps but more detailed analysis is required to assess which are the complex neuronal events underlying these high frequency activities and what is their exact relation with epileptiform phenomena.

# 5. CONCLUSION

- ***Specific conclusions obtained from the papers***

From the first paper we have deduced the following conclusion:

- It is possible to detect scalp-visible and nonscalp-visible intracranial IED signatures on the scalp EEG employing a mathematical algorithm.
- The probabilistic classifier provided successful detections with a low number of false positives both, when trained with within-subject data and when trained on a pool of patients with epilepsy.

From the second paper we obtained the following conclusions:

- Electrical stimulation of the anterior cingulate gyrus initiates widespread synchronous activity that resembles K-complexes.
- Cingulate stimulation can induce responses similar to K-complexes during wakefulness.

The third paper concludes with the following points:

- Generalised seizures may show complex patterns of initiation, with various relative cortical and thalamic involvements.
- In the generalised seizures recorded in our patients, the thalamus may become involved early or late in the seizure but, once it becomes involved, it leads the cortex.
- In frontal seizures the thalamus gets involved late in the seizure and, once it becomes involved, it lags behind the cortex.

- The thalamus is capable of generating focal unilateral epileptiform discharges restricted to thalamic structures

And the fourth paper provides the following conclusions:

- It is possible to describe the oscillatory behaviour of the EEG in terms of control theory while estimating oscillatory coupling between connected cortical regions.
- The method may have the potential to identify frequencies at which cortical regions are able to oscillate.

## • *General conclusions*

It is well known that EEG activity is made by the interplay (interactions) of superficial and deep cortical and subcortical structures within a conductive medium. Our hypothesis is tha such interplay can be characterised by a set of control systems susceptible to be described according with the morphology of responses induced after SPES. The resulting properties of the summated systems can help to identify intrinsic properties of the cortex such as the ability to produce the explicit or latent background rhythms, epileptiform activity or seizures. The study of functional connectivity and the frequency-behaviour of distant cortical areas is at our grasp thanks to our newly developed approach (forced coupling).

In addition, the ability to produce physiological cortically-generated phasic events can also be examined by SPES as demonstrated by the generation of K-complex-like responses after stimulation of the cingulate gyrus. This suggest that the initiation of K-complex largely relies on cortical structures.

We have also found that it is possible to detect epileptiform activities (as those generated in deep areas of the mesial temporal lobe) at the scalp level. This shows that there is a significant amount of unused information available on the scalp EEG arising from deep sources (the intracranial signatures). Due to its low amplitude, this information is not identifiable by human experts' eye but detectable by more sophisticated analytical methods.

The role of deep mesial structures in generalised seizures has been assessed with thalamic centromedian electrodes. We conclude that generalised seizures can show complex initiation patterns with earlier or later involvement of the thalamus. Despite the presence of interictal thalamic epileptiform discharges, there is no consistent evidence of an exclusive initiation role at the thalamus, but once it becomes involved imposes a leading role over the cortex acting as a pacemaker for the generalised seizures.

As a final remark this work also exemplifies how quantitative methods can help us to improve our understanding of the relative contribution of deep structures to the EEG and the interplay between different areas leading to physiological and pathological scenarios.

# 6. BIBLIOGRAPHY


1. Fisher RS, van Emde Boas W, Blume W, Elger C, Genton P, Lee P, et al. Epileptic seizures and epilepsy: definitions proposed by the International League Against Epilepsy (ILAE) and the International Bureau for Epilepsy (IBE). Epilepsia. 2005;46(4):470-2.
2. Fisher RS, Acevedo C, Arzimanoglou A, Bogacz A, Cross JH, Elger CE, et al. ILAE official report: a practical clinical definition of epilepsy. Epilepsia. 2014;55(4):475-82.
3. Fiest KM, Sauro KM, Wiebe S, Patten SB, Kwon CS, Dykeman J, et al. Prevalence and incidence of epilepsy: A systematic review and meta-analysis of international studies. Neurology. 2017;88(3):296-303.
4. Kim LG, Johnson TL, Marson AG, Chadwick DW, group MMS. Prediction of risk of seizure recurrence after a single seizure and early epilepsy: further results from the MESS trial. Lancet Neurol. 2006;5(4):317-22.
5. Shinnar S, Berg AT, Moshe SL, O'Dell C, Alemany M, Newstein D, et al. The risk of seizure recurrence after a first unprovoked afebrile seizure in childhood: an extended follow-up. Pediatrics. 1996;98(2 Pt 1):216-25.
6. Hauser WA, Rich SS, Annegers JF, Anderson VE. Seizure recurrence after a 1st unprovoked seizure: an extended follow-up. Neurology. 1990;40(8):1163-70.
7. Krumholz A, Wiebe S, Gronseth G, Shinnar S, Levisohn P, Ting T, et al. Practice Parameter: evaluating an apparent unprovoked first seizure in adults (an evidence-based review): report of the Quality Standards Subcommittee of the American Academy of Neurology and the American Epilepsy Society. Neurology. 2007;69(21):1996-2007.
8. Brodtkorb E. Common imitators of epilepsy. Acta Neurol Scand Suppl. 2013(196):5-10.
9. Morrell MJ. Differential diagnosis of seizures. Neurol Clin. 1993;11(4):737-54.
10. Baldin E, Hauser WA, Buchhalter JR, Hesdorffer DC, Ottman R. Yield of epileptiform electroencephalogram abnormalities in incident unprovoked seizures: a population-based study. Epilepsia. 2014;55(9):1389-98.
11. Binnie CD, Prior PF. Electroencephalography. Journal of neurology, neurosurgery, and psychiatry. 1994;57(11):1308-19.
12. King MA, Newton MR, Jackson GD, Fitt GJ, Mitchell LA, Silvapulle MJ, et al. Epileptology of the first-seizure presentation: a clinical, electroencephalographic, and magnetic resonance imaging study of 300 consecutive patients. Lancet. 1998;352(9133):1007-11.
13. Schreiner A, Pohlmann-Eden B. Value of the early electroencephalogram after a first unprovoked seizure. Clinical EEG. 2003;34(3):140-4.
14. Smith SJ. EEG in the diagnosis, classification, and management of patients with epilepsy. Journal of neurology, neurosurgery, and psychiatry. 2005;76 Suppl 2:ii2-7.
15. Caton R. The electric currents of the brain. BMJ. 1873;2:278-.
16. Berger H. Ueber das Elektroenkephalogramm des Menschen. Archiv für Psychiatrie und Nervenkrankheiten. 1929;87(1):527-70.
17. Adrian ED, Matthews BH. The interpretation of potential waves in the cortex. The Journal of physiology. 1934;81(4):440-71.
18. Buzsaki G, Anastassiou CA, Koch C. The origin of extracellular fields and currents--EEG, ECoG, LFP and spikes. Nat Rev Neurosci. 2012;13(6):407-20.
19. Nunez PL, Srinivasan R. Electric fields of the brain : the neurophysics of EEG. 2nd ed. Oxford ; New York: Oxford University Press; 2006. xvi, 611 p. p.
20. Tipler PA, Mosca G. Physics for scientists and engineers : with modern physics. 6th, extended . ed. New York: W.H. Freeman; 2008. xxxii, 1412, 7, 30, 51, 26 p. p.

21. Azevedo FA, Carvalho LR, Grinberg LT, Farfel JM, Ferretti RE, Leite RE, et al. Equal numbers of neuronal and nonneuronal cells make the human brain an isometrically scaled-up primate brain. J Comp Neurol. 2009;513(5):532-41.
22. Drachman DA. Do we have brain to spare? Neurology. 2005;64(12):2004-5.
23. R LdN. A study of nerve physiology. Stud Rockefeller Inst Med Res Repr. 1947;132:1-548.
24. Buzsáki G. Rhythms of the brain. Oxford ; New York: Oxford University Press; 2006. xiv, 448 p. p.
25. Linden H, Tetzlaff T, Potjans TC, Pettersen KH, Grun S, Diesmann M, et al. Modeling the spatial reach of the LFP. Neuron. 2011;72(5):859-72.
26. Spruston N. Pyramidal neurons: dendritic structure and synaptic integration. Nat Rev Neurosci. 2008;9(3):206-21.
27. Attal Y, Bhattacharjee M, Yelnik J, Cottereau B, Lefevre J, Okada Y, et al. Modeling and detecting deep brain activity with MEG & EEG. Conf Proc IEEE Eng Med Biol Soc. 2007;2007:4937-40.
28. Nunez PL. Electric fields of the brain : the neurophysics of EEG. New York: Oxford University Press; 1981. xix, 484 p. p.
29. Wong RK, Prince DA, Basbaum AI. Intradendritic recordings from hippocampal neurons. Proceedings of the National Academy of Sciences of the United States of America. 1979;76(2):986-90.
30. Riedner BA, Hulse BK, Murphy MJ, Ferrarelli F, Tononi G. Temporal dynamics of cortical sources underlying spontaneous and peripherally evoked slow waves. Progress in brain research. 2011;193:201-18.
31. Llinas RR. The intrinsic electrophysiological properties of mammalian neurons: insights into central nervous system function. Science. 1988;242(4886):1654-64.
32. Silva LR, Amitai Y, Connors BW. Intrinsic oscillations of neocortex generated by layer 5 pyramidal neurons. Science. 1991;251(4992):432-5.
33. Pike FG, Goddard RS, Suckling JM, Ganter P, Kasthuri N, Paulsen O. Distinct frequency preferences of different types of rat hippocampal neurones in response to oscillatory input currents. The Journal of physiology. 2000;529 Pt 1:205-13.
34. Buzsaki G, Bickford RG, Ponomareff G, Thal LJ, Mandel R, Gage FH. Nucleus basalis and thalamic control of neocortical activity in the freely moving rat. The Journal of neuroscience : the official journal of the Society for Neuroscience. 1988;8(11):4007-26.
35. Bennett MV, Zukin RS. Electrical coupling and neuronal synchronization in the Mammalian brain. Neuron. 2004;41(4):495-511.
36. Jefferys JG. Nonsynaptic modulation of neuronal activity in the brain: electric currents and extracellular ions. Physiol Rev. 1995;75(4):689-723.
37. McCormick DA, Contreras D. On the cellular and network bases of epileptic seizures. Annu Rev Physiol. 2001;63:815-46.
38. He BJ, Snyder AZ, Zempel JM, Smyth MD, Raichle ME. Electrophysiological correlates of the brain's intrinsic large-scale functional architecture. Proceedings of the National Academy of Sciences of the United States of America. 2008;105(41):16039-44.
39. Kang J, Jiang L, Goldman SA, Nedergaard M. Astrocyte-mediated potentiation of inhibitory synaptic transmission. Nat Neurosci. 1998;1(8):683-92.
40. Alarcon G, Guy CN, Binnie CD, Walker SR, Elwes RD, Polkey CE. Intracerebral propagation of interictal activity in partial epilepsy: implications for source localisation. Journal of neurology, neurosurgery, and psychiatry. 1994;57(4):435-49.
41. Cohen MX. Where Does EEG Come From and What Does It Mean? Trends in neurosciences. 2017;40(4):208-18.
42. Luczak A, Bartho P, Harris KD. Spontaneous events outline the realm of possible sensory responses in neocortical populations. Neuron. 2009;62(3):413-25.
43. Womelsdorf T, Valiante TA, Sahin NT, Miller KJ, Tiesinga P. Dynamic circuit motifs underlying rhythmic gain control, gating and integration. Nat Neurosci. 2014;17(8):1031-9.

44. Abeles M, Prut Y. Spatio-temporal firing patterns in the frontal cortex of behaving monkeys. J Physiol Paris. 1996;90(3-4):249-50.
45. Abeles M. Corticonics : neural circuits of the cerebral cortex. Cambridge ; New York: Cambridge University Press; 1991. xiv, 280 p. p.
46. Gerstein GL, Williams ER, Diesmann M, Grun S, Trengove C. Detecting synfire chains in parallel spike data. J Neurosci Methods. 2012;206(1):54-64.
47. Harris KD, Bartho P, Chadderton P, Curto C, de la Rocha J, Hollender L, et al. How do neurons work together? Lessons from auditory cortex. Hear Res. 2011;271(1-2):37-53.
48. Canolty RT, Knight RT. The functional role of cross-frequency coupling. Trends Cogn Sci. 2010;14(11):506-15.
49. Jiang H, Bahramisharif A, van Gerven MA, Jensen O. Measuring directionality between neuronal oscillations of different frequencies. NeuroImage. 2015;118:359-67.
50. Cosandier-Rimele D, Merlet I, Badier JM, Chauvel P, Wendling F. The neuronal sources of EEG: modeling of simultaneous scalp and intracerebral recordings in epilepsy. NeuroImage. 2008;42(1):135-46.
51. Khadem A, Hossein-Zadeh GA. Quantification of the effects of volume conduction on the EEG/MEG connectivity estimates: an index of sensitivity to brain interactions. Physiol Meas. 2014;35(10):2149-64.
52. van den Broek SP, Reinders F, Donderwinkel M, Peters MJ. Volume conduction effects in EEG and MEG. Electroencephalography and clinical neurophysiology. 1998;106(6):522-34.
53. Cuffin BN, Schomer DL, Ives JR, Blume H. Experimental tests of EEG source localization accuracy in spherical head models. Clinical neurophysiology : official journal of the International Federation of Clinical Neurophysiology. 2001;112(1):46-51.
54. Roth BJ, Ko D, von Albertini-Carletti IR, Scaffidi D, Sato S. Dipole localization in patients with epilepsy using the realistically shaped head model. Electroencephalography and clinical neurophysiology. 1997;102(3):159-66.
55. Cuffin BN. Effects of fissures in the brain on electroencephalograms and magnetoencephalograms. J Appl Phys. 1984;57:146-53.
56. Nicholson PW. Specific impedance of cerebral white matter. Experimental neurology. 1965;13(4):386-401.
57. Baumann SB, Wozny DR, Kelly SK, Meno FM. The electrical conductivity of human cerebrospinal fluid at body temperature. IEEE Trans Biomed Eng. 1997;44(3):220-3.
58. Geddes LA, Baker LE. The specific resistance of biological material--a compendium of data for the biomedical engineer and physiologist. Med Biol Eng. 1967;5(3):271-93.
59. Yan Y, Nunez PL, Hart RT. Finite-element model of the human head: scalp potentials due to dipole sources. Med Biol Eng Comput. 1991;29(5):475-81.
60. Heasman BC, Valentin A, Alarcon G, Garcia Seoane JJ, Binnie CD, Guy CN. A hole in the skull distorts substantially the distribution of extracranial electrical fields in an in vitro model. J Clin Neurophysiol. 2002;19(2):163-71.
61. Nolte G, Bai O, Wheaton L, Mari Z, Vorbach S, Hallett M. Identifying true brain interaction from EEG data using the imaginary part of coherency. Clinical neurophysiology : official journal of the International Federation of Clinical Neurophysiology. 2004;115(10):2292-307.
62. Stam CJ, Nolte G, Daffertshofer A. Phase lag index: assessment of functional connectivity from multi channel EEG and MEG with diminished bias from common sources. Hum Brain Mapp. 2007;28(11):1178-93.
63. Vinck M, Oostenveld R, van Wingerden M, Battaglia F, Pennartz CM. An improved index of phase-synchronization for electrophysiological data in the presence of volume-conduction, noise and sample-size bias. NeuroImage. 2011;55(4):1548-65.
64. Pascual-Marqui RD, Michel CM, Lehmann D. Low resolution electromagnetic tomography: a new method for localizing electrical activity in the brain. Int J Psychophysiol. 1994;18(1):49-65.

65. Gorodnitsky IF, George JS, Rao BD. Neuromagnetic source imaging with FOCUSS: a recursive weighted minimum norm algorithm. Electroencephalography and clinical neurophysiology. 1995;95(4):231-51.
66. Baillet S, Garnero L. A Bayesian approach to introducing anatomo-functional priors in the EEG/MEG inverse problem. IEEE Trans Biomed Eng. 1997;44(5):374-85.
67. Amblard C, Lapalme E, Lina JM. Biomagnetic source detection by maximum entropy and graphical models. IEEE Trans Biomed Eng. 2004;51(3):427-42.
68. Daunizeau J, Mattout J, Clonda D, Goulard B, Benali H, Lina JM. Bayesian spatio-temporal approach for EEG source reconstruction: conciliating ECD and distributed models. IEEE Trans Biomed Eng. 2006;53(3):503-16.
69. Taylor PN, Wang Y, Kaiser M. Within brain area tractography suggests local modularity using high resolution connectomics. Sci Rep. 2017;7:39859.
70. Traub RD. Neocortical pyramidal cells: a model with dendritic calcium conductance reproduces repetitive firing and epileptic behavior. Brain research. 1979;173(2):243-57.
71. David O, Friston KJ. A neural mass model for MEG/EEG: coupling and neuronal dynamics. NeuroImage. 2003;20(3):1743-55.
72. Freeman WJ. Mass action in the nervous system : examination of the neurophysiological basis of adaptive behavior through the EEG. New York: Academic Press; 1975. xx, 489 p. p.
73. Wendling F, Hernandez A, Bellanger JJ, Chauvel P, Bartolomei F. Interictal to ictal transition in human temporal lobe epilepsy: insights from a computational model of intracerebral EEG. J Clin Neurophysiol. 2005;22(5):343-56.
74. Suffczynski P, Kalitzin S, Lopes Da Silva FH. Dynamics of non-convulsive epileptic phenomena modeled by a bistable neuronal network. Neuroscience. 2004;126(2):467-84.
75. Alarcon G, Garcia Seoane JJ, Binnie CD, Martin Miguel MC, Juler J, Polkey CE, et al. Origin and propagation of interictal discharges in the acute electrocorticogram. Implications for pathophysiology and surgical treatment of temporal lobe epilepsy. Brain : a journal of neurology. 1997;120 ( Pt 12):2259-82.
76. Martin Miguel Mdel C, Garcia Seoane JJ, Valentin A, Hughes E, Selway RP, Polkey CE, et al. EEG latency analysis for hemispheric lateralisation in Landau-Kleffner syndrome. Clinical neurophysiology : official journal of the International Federation of Clinical Neurophysiology. 2011;122(2):244-52.
77. Lacruz ME, Garcia Seoane JJ, Valentin A, Selway R, Alarcon G. Frontal and temporal functional connections of the living human brain. The European journal of neuroscience. 2007;26(5):1357-70.
78. Sirven JI, Sperling MR, French JA, O'Connor MJ. Significance of simple partial seizures in temporal lobe epilepsy. Epilepsia. 1996;37(5):450-4.
79. Palmini A, Gloor P. The localizing value of auras in partial seizures: a prospective and retrospective study. Neurology. 1992;42(4):801-8.
80. Penfield W, Jasper H. Epilepsy and the Functional Anatomy of the Human Brain: Boston, Little, Brown 1954.
81. Cooper R, Winter AL, Crow HJ, Walter WG. Comparison of Subcortical, Cortical and Scalp Activity Using Chronically Indwelling Electrodes in Man. Electroencephalography and clinical neurophysiology. 1965;18:217-28.
82. Ray A, Tao JX, Hawes-Ebersole SM, Ebersole JS. Localizing value of scalp EEG spikes: a simultaneous scalp and intracranial study. Clinical neurophysiology : official journal of the International Federation of Clinical Neurophysiology. 2007;118(1):69-79.
83. Tao JX, Baldwin M, Ray A, Hawes-Ebersole S, Ebersole JS. The impact of cerebral source area and synchrony on recording scalp electroencephalography ictal patterns. Epilepsia. 2007;48(11):2167-76.
84. Tao JX, Ray A, Hawes-Ebersole S, Ebersole JS. Intracranial EEG substrates of scalp EEG interictal spikes. Epilepsia. 2005;46(5):669-76.

85. Kobayashi K, Yoshinaga H, Ohtsuka Y, Gotman J. Dipole modeling of epileptic spikes can be accurate or misleading. Epilepsia. 2005;46(3):397-408.
86. Hill NJ, Gupta D, Brunner P, Gunduz A, Adamo MA, Ritaccio A, et al. Recording human electrocorticographic (ECoG) signals for neuroscientific research and real-time functional cortical mapping. J Vis Exp. 2012(64).
87. Ebersole JS. Non-invasive pre-surgical evaluation with EEG/MEG source analysis. Electroencephalogr Clin Neurophysiol Suppl. 1999;50:167-74.
88. Foldvary N, Klem G, Hammel J, Bingaman W, Najm I, Luders H. The localizing value of ictal EEG in focal epilepsy. Neurology. 2001;57(11):2022-8.
89. Alarcon G, Kissani N, Dad M, Elwes RD, Ekanayake J, Hennessy MJ, et al. Lateralizing and localizing values of ictal onset recorded on the scalp: evidence from simultaneous recordings with intracranial foramen ovale electrodes. Epilepsia. 2001;42(11):1426-37.
90. Spencer SS, Williamson PD, Bridgers SL, Mattson RH, Cicchetti DV, Spencer DD. Reliability and accuracy of localization by scalp ictal EEG. Neurology. 1985;35(11):1567-75.
91. Bautista RE, Spencer DD, Spencer SS. EEG findings in frontal lobe epilepsies. Neurology. 1998;50(6):1765-71.
92. Quesney LF, Constain M, Rasmussen T, Stefan H, Olivier A. How large are frontal lobe epileptogenic zones? EEG, ECoG, and SEEG evidence. Adv Neurol. 1992;57:311-23.
93. Nayak D, Valentin A, Selway RP, Alarcon G. Can single pulse electrical stimulation provoke responses similar to spontaneous interictal epileptiform discharges? Clinical neurophysiology : official journal of the International Federation of Clinical Neurophysiology. 2014;125(7):1306-11.
94. Alarcon G, Martinez J, Kerai SV, Lacruz ME, Quiroga RQ, Selway RP, et al. In vivo neuronal firing patterns during human epileptiform discharges replicated by electrical stimulation. Clinical neurophysiology : official journal of the International Federation of Clinical Neurophysiology. 2012;123(9):1736-44.
95. Rosenow F, Luders H. Presurgical evaluation of epilepsy. Brain : a journal of neurology. 2001;124(Pt 9):1683-700.
96. Jayakar P, Gotman J, Harvey AS, Palmini A, Tassi L, Schomer D, et al. Diagnostic utility of invasive EEG for epilepsy surgery: Indications, modalities, and techniques. Epilepsia. 2016;57(11):1735-47.
97. Kahane P, Landre E, Minotti L, Francione S, Ryvlin P. The Bancaud and Talairach view on the epileptogenic zone: a working hypothesis. Epileptic disorders : international epilepsy journal with videotape. 2006;8 Suppl 2:S16-26.
98. Bancaud J, Talairach J, Bonis A, Schaub C, Szikla G, Morel P. La stéréoencéphalographie dans l'épilepsie. Paris: Masson; 1965.
99. Zijlmans M, Jacobs J, Kahn YU, Zelmann R, Dubeau F, Gotman J. Ictal and interictal high frequency oscillations in patients with focal epilepsy. Clinical neurophysiology : official journal of the International Federation of Clinical Neurophysiology. 2011;122(4):664-71.
100. Bartolomei F, Nica A, Valenti-Hirsch MP, Adam C, Denuelle M. Interpretation of SEEG recordings. Neurophysiol Clin. 2018;48(1):53-7.
101. Ramantani G, Dumpelmann M, Koessler L, Brandt A, Cosandier-Rimele D, Zentner J, et al. Simultaneous subdural and scalp EEG correlates of frontal lobe epileptic sources. Epilepsia. 2014;55(2):278-88.
102. Koessler L, Cecchin T, Colnat-Coulbois S, Vignal JP, Jonas J, Vespignani H, et al. Catching the invisible: mesial temporal source contribution to simultaneous EEG and SEEG recordings. Brain topography. 2015;28(1):5-20.
103. Wieser HG, Elger CE, Stodieck SR. The 'foramen ovale electrode': a new recording method for the preoperative evaluation of patients suffering from mesio-basal temporal lobe epilepsy. Electroencephalography and clinical neurophysiology. 1985;61(4):314-22.

104. Alarcon G, Binnie CD, Garcia Seoane JJ, Martin Miguel MC, Fernandez Torre JL, Polkey CE, et al. Mechanisms involved in the propagation of interictal epileptiform discharges in partial epilepsy. Electroencephalogr Clin Neurophysiol Suppl. 1999;50:259-78.
105. Fernandez Torre JL, Alarcon G, Binnie CD, Seoane JJ, Juler J, Guy CN, et al. Generation of scalp discharges in temporal lobe epilepsy as suggested by intraoperative electrocorticographic recordings. Journal of neurology, neurosurgery, and psychiatry. 1999;67(1):51-8.
106. Niedermeyer E, Lopes da Silva FH. Electroencephalography : basic principles, clinical applications, and related fields. 5th ed. Philadelphia: Lippincott Williams & Wilkins; 2005. xiii, 1309 p. p.
107. Nayak D, Valentin A, Alarcon G, Garcia Seoane JJ, Brunnhuber F, Juler J, et al. Characteristics of scalp electrical fields associated with deep medial temporal epileptiform discharges. Clinical neurophysiology : official journal of the International Federation of Clinical Neurophysiology. 2004;115(6):1423-35.
108. Tatum WO, Rubboli G, Kaplan PW, Mirsatari SM, Radhakrishnan K, Gloss D, et al. Clinical utility of EEG in diagnosing and monitoring epilepsy in adults. Clinical neurophysiology : official journal of the International Federation of Clinical Neurophysiology. 2018;129(5):1056-82.
109. Bartolomei F, Wendling F, Vignal JP, Kochen S, Bellanger JJ, Badier JM, et al. Seizures of temporal lobe epilepsy: identification of subtypes by coherence analysis using stereo-electro-encephalography. Clinical neurophysiology : official journal of the International Federation of Clinical Neurophysiology. 1999;110(10):1741-54.
110. Bartolomei F, Wendling F, Bellanger JJ, Regis J, Chauvel P. Neural networks involving the medial temporal structures in temporal lobe epilepsy. Clinical neurophysiology : official journal of the International Federation of Clinical Neurophysiology. 2001;112(9):1746-60.
111. Salanova V, Morris HH, 3rd, Van Ness PC, Luders H, Dinner D, Wyllie E. Comparison of scalp electroencephalogram with subdural electrocorticogram recordings and functional mapping in frontal lobe epilepsy. Archives of neurology. 1993;50(3):294-9.
112. Elsharkawy AE, Alabbasi AH, Pannek H, Schulz R, Hoppe M, Pahs G, et al. Outcome of frontal lobe epilepsy surgery in adults. Epilepsy research. 2008;81(2-3):97-106.
113. Chibane IS, Boucher O, Dubeau F, Tran TPY, Mohamed I, McLachlan R, et al. Orbitofrontal epilepsy: Case series and review of literature. Epilepsy & behavior : E&B. 2017;76:32-8.
114. Ramantani G, Maillard L, Koessler L. Correlation of invasive EEG and scalp EEG. Seizure. 2016;41:196-200.
115. Bonini F, McGonigal A, Trebuchon A, Gavaret M, Bartolomei F, Giusiano B, et al. Frontal lobe seizures: from clinical semiology to localization. Epilepsia. 2014;55(2):264-77.
116. Gibbs F, Davis H, Lennox W. The electro-encephalogram in epilepsy and in conditions of impaired consciousness. Arch Neurolgy Psychiatry 1935;34:1133-48.
117. Buzsaki G. The thalamic clock: emergent network properties. Neuroscience. 1991;41(2-3):351-64.
118. Gloor P. Generalized cortico-reticular epilepsies. Some considerations on the pathophysiology of generalized bilaterally synchronous spike and wave discharge. Epilepsia. 1968;9(3):249-63.
119. Meeren HK, Pijn JP, Van Luijtelaar EL, Coenen AM, Lopes da Silva FH. Cortical focus drives widespread corticothalamic networks during spontaneous absence seizures in rats. The Journal of neuroscience : the official journal of the Society for Neuroscience. 2002;22(4):1480-95.
120. Meeren H, van Luijtelaar G, Lopes da Silva F, Coenen A. Evolving concepts on the pathophysiology of absence seizures: the cortical focus theory. Archives of neurology. 2005;62(3):371-6.
121. von Krosigk M, Bal T, McCormick DA. Cellular mechanisms of a synchronized oscillation in the thalamus. Science. 1993;261(5119):361-4.
122. Spiegel EA, Wycis HT. Thalamic recordings in man with special reference to seizure discharges. Electroencephalography and clinical neurophysiology. 1950;2:23-7.

123. Spiegel EA, Wycis HT, Reyes V. Diencephalic mechanisms in petit mal epilepsy. Electroencephalography and clinical neurophysiology. 1951;3(4):473-5.
124. Hayne RA, Belinson L, Gibbs FA. Electrical activity of subcortical areas in epilepsy. Electroencephalography and clinical neurophysiology. 1949;1(4):437-45.
125. Niedermeyer E, Laws ER, Jr., Walker EA. Depth EEG findings in epileptics with generalized spike-wave complexes. Archives of neurology. 1969;21(1):51-8.
126. Craiu D, Magureanu S, van Emde Boas W. Are absences truly generalized seizures or partial seizures originating from or predominantly involving the pre-motor areas? Some clinical and theoretical observations and their implications for seizure classification. Epilepsy research. 2006;70 Suppl 1:S141-55.
127. Kakisaka Y, Alexopoulos AV, Gupta A, Wang ZI, Mosher JC, Iwasaki M, et al. Generalized 3-Hz spike-and-wave complexes emanating from focal epileptic activity in pediatric patients. Epilepsy & behavior : E&B. 2011;20(1):103-6.
128. Sakakibara S, Nakamura F, Demise M, Kobayashi J, Takeda Y, Tanaka N, et al. Frontal lobe epilepsy with absence-like and secondarily generalized seizures. Psychiatry and clinical neurosciences. 2003;57(4):455-6.
129. Kubota F, Shibata N, Shiihara Y, Takahashi S, Ohsuka T. Frontal lobe epilepsy with secondarily generalized 3 Hz spike-waves: a case report. Clinical EEG. 1997;28(3):166-71.
130. Bancaud J, Talairach J, Morel P, Bresson M, Bonis A, Geier S, et al. "Generalized" epileptic seizures elicited by electrical stimulation of the frontal lobe in man. Electroencephalography and clinical neurophysiology. 1974;37(3):275-82.
131. Valentin A, Lazaro M, Mullatti N, Cervantes S, Malik I, Selway RP, et al. Cingulate epileptogenesis in hypothalamic hamartoma. Epilepsia. 2011;52(5):e35-9.
132. Martin-Lopez D, Jimenez-Jimenez D, Cabanes-Martinez L, Selway RP, Valentin A, Alarcon G. The Role of Thalamus Versus Cortex in Epilepsy: Evidence from Human Ictal Centromedian Recordings in Patients Assessed for Deep Brain Stimulation. International journal of neural systems. 2017;27(7):1750010.
133. Lodder SS, van Putten MJ. A self-adapting system for the automated detection of inter-ictal epileptiform discharges. PloS one. 2014;9(1):e85180.
134. Grouiller F, Thornton RC, Groening K, Spinelli L, Duncan JS, Schaller K, et al. With or without spikes: localization of focal epileptic activity by simultaneous electroencephalography and functional magnetic resonance imaging. Brain : a journal of neurology. 2011;134(Pt 10):2867-86.
135. Zhou J, Schalkoff RJ, Dean BC, Halford JJ. Morphology-based wavelet features and multiple mother wavelet strategy for spike classification in EEG signals. Conf Proc IEEE Eng Med Biol Soc. 2012;2012:3959-62.
136. Liu YC, Lin CC, Tsai JJ, Sun YN. Model-based spike detection of epileptic EEG data. Sensors (Basel). 2013;13(9):12536-47.
137. Ghosh-Dastidar S, Adeli H, Dadmehr N. Mixed-band wavelet-chaos-neural network methodology for epilepsy and epileptic seizure detection. IEEE Trans Biomed Eng. 2007;54(9):1545-51.
138. De Lucia M, Fritschy J, Dayan P, Holder DS. A novel method for automated classification of epileptiform activity in the human electroencephalogram-based on independent component analysis. Med Biol Eng Comput. 2008;46(3):263-72.
139. Janca R, Jezdik P, Cmejla R, Tomasek M, Worrell GA, Stead M, et al. Detection of interictal epileptiform discharges using signal envelope distribution modelling: application to epileptic and non-epileptic intracranial recordings. Brain topography. 2015;28(1):172-83.
140. Wilson SB, Emerson R. Spike detection: a review and comparison of algorithms. Clinical neurophysiology : official journal of the International Federation of Clinical Neurophysiology. 2002;113(12):1873-81.

141. Wilson SB, Turner CA, Emerson RG, Scheuer ML. Spike detection II: automatic, perception-based detection and clustering. Clinical neurophysiology : official journal of the International Federation of Clinical Neurophysiology. 1999;110(3):404-11.
142. Acharya UR, Sree SV, Alvin AP, Yanti R, Suri JS. Application of non-linear and wavelet based features for the automated identification of epileptic EEG signals. International journal of neural systems. 2012;22(2):1250002.
143. Gotman J, Gloor P. Automatic recognition and quantification of interictal epileptic activity in the human scalp EEG. Electroencephalography and clinical neurophysiology. 1976;41(5):513-29.
144. Acir N, Oztura I, Kuntalp M, Baklan B, Guzelis C. Automatic detection of epileptiform events in EEG by a three-stage procedure based on artificial neural networks. IEEE Trans Biomed Eng. 2005;52(1):30-40.
145. Gotman J, Ives JR, Gloor P. Automatic recognition of inter-ictal epileptic activity in prolonged EEG recordings. Electroencephalography and clinical neurophysiology. 1979;46(5):510-20.
146. Harner R. Automatic EEG spike detection. Clin EEG Neurosci. 2009;40(4):262-70.
147. Gabor AJ, Seyal M. Automated interictal EEG spike detection using artificial neural networks. Electroencephalography and clinical neurophysiology. 1992;83(5):271-80.
148. Cui J, Wong W. The adaptive chirplet transform and visual evoked potentials. IEEE Trans Biomed Eng. 2006;53(7):1378-84.
149. Argoud FI, De Azevedo FM, Neto JM, Grillo E. SADE3: an effective system for automated detection of epileptiform events in long-term EEG based on context information. Med Biol Eng Comput. 2006;44(6):459-70.
150. Adeli H, Ghosh-Dastidar S, Dadmehr N. A wavelet-chaos methodology for analysis of EEGs and EEG subbands to detect seizure and epilepsy. IEEE Trans Biomed Eng. 2007;54(2):205-11.
151. Vahabi Z, Amirfattahi R, Shayegh F, Ghassemi F. Online Epileptic Seizure Prediction Using Wavelet-Based Bi-Phase Correlation of Electrical Signals Tomography. International journal of neural systems. 2015;25(6):1550028.
152. Bao FS, Gao JM, Hu J, Lie DY, Zhang Y, Oommen KJ. Automated epilepsy diagnosis using interictal scalp EEG. Conf Proc IEEE Eng Med Biol Soc. 2009;2009:6603-7.
153. Wang C, Zou J, Zhang J, Wang M, Wang R. Feature extraction and recognition of epileptiform activity in EEG by combining PCA with ApEn. Cogn Neurodyn. 2010;4(3):233-40.
154. Martis RJ, Acharya UR, Tan JH, Petznick A, Tong L, Chua CK, et al. Application of intrinsic time-scale decomposition (ITD) to EEG signals for automated seizure prediction. International journal of neural systems. 2013;23(5):1350023.
155. Yuan Q, Zhou W, Yuan S, Li X, Wang J, Jia G. Epileptic EEG classification based on kernel sparse representation. International journal of neural systems. 2014;24(4):1450015.
156. Gaspard N, Alkawadri R, Farooque P, Goncharova, II, Zaveri HP. Automatic detection of prominent interictal spikes in intracranial EEG: validation of an algorithm and relationsip to the seizure onset zone. Clinical neurophysiology : official journal of the International Federation of Clinical Neurophysiology. 2014;125(6):1095-103.
157. Antoniades A, Spyrou L, Martin-Lopez D, Valentin A, Alarcon G, Sanei S, et al. Detection of Interictal Discharges With Convolutional Neural Networks Using Discrete Ordered Multichannel Intracranial EEG. IEEE Trans Neural Syst Rehabil Eng. 2017;25(12):2285-94.
158. Adrian ED. The spread of activity in the cerebral cortex. The Journal of physiology. 1936;88(2):127-61.
159. Valentin A, Anderson M, Alarcon G, Seoane JJG, Selway R, Binnie CD, et al. Responses to single pulse electrical stimulation identify epileptogenesis in the human brain in vivo. Brain : a journal of neurology. 2002;125:1709-18.
160. Purpura DP, Pool JL, Ransohoff J, Frumin MJ, Housepian EM. Observations on evoked dendritic potentials of human cortex. Electroencephalography and clinical neurophysiology. 1957;9(3):453-9.

161. Matsumoto R, Nair DR, LaPresto E, Najm I, Bingaman W, Shibasaki H, et al. Functional connectivity in the human language system: a cortico-cortical evoked potential study. Brain : a journal of neurology. 2004;127(Pt 10):2316-30.
162. Matsumoto R, Nair DR, Ikeda A, Fumuro T, Lapresto E, Mikuni N, et al. Parieto-frontal network in humans studied by cortico-cortical evoked potential. Hum Brain Mapp. 2012;33(12):2856-72.
163. Iwasaki M, Enatsu R, Matsumoto R, Novak E, Thankappen B, Piao Z, et al. Accentuated cortico-cortical evoked potentials in neocortical epilepsy in areas of ictal onset. Epileptic disorders : international epilepsy journal with videotape. 2010;12(4):292-302.
164. Enatsu R, Matsumoto R, Piao Z, O'Connor T, Horning K, Burgess RC, et al. Cortical negative motor network in comparison with sensorimotor network: a cortico-cortical evoked potential study. Cortex; a journal devoted to the study of the nervous system and behavior. 2013;49(8):2080-96.
165. Enatsu R, Piao Z, O'Connor T, Horning K, Mosher J, Burgess R, et al. Cortical excitability varies upon ictal onset patterns in neocortical epilepsy: a cortico-cortical evoked potential study. Clinical neurophysiology : official journal of the International Federation of Clinical Neurophysiology. 2012;123(2):252-60.
166. Keller CJ, Honey CJ, Megevand P, Entz L, Ulbert I, Mehta AD. Mapping human brain networks with cortico-cortical evoked potentials. Philos Trans R Soc Lond B Biol Sci. 2014;369(1653).
167. Terada K, Usui N, Umeoka S, Baba K, Mihara T, Matsuda K, et al. Interhemispheric connection of motor areas in humans. Journal of clinical neurophysiology : official publication of the American Electroencephalographic Society. 2008;25(6):351-6.
168. Wilson CL, Isokawa M, Babb TL, Crandall PH. Functional connections in the human temporal lobe. I. Analysis of limbic system pathways using neuronal responses evoked by electrical stimulation. Experimental brain research. 1990;82(2):279-92.
169. Cherlow DG, Dymond AM, Crandall PH, Walter RD, Serafetinides EA. Evoked response and after-discharge thresholds to electrical stimulation in temporal lobe epileptics. Arch Neurol. 1977;34(9):527-31.
170. Rosenblueth A. Cortical responses to electric stimulation. Amer J Physiol. 1942;135:690-774.
171. Valentin A, Alarcon G, Garcia-Seoane JJ, Lacruz ME, Nayak SD, Honavar M, et al. Single-pulse electrical stimulation identifies epileptogenic frontal cortex in the human brain. Neurology. 2005;65(3):426-35.
172. Valentin A, Alarcon G, Honavar M, Garcia Seoane JJ, Selway RP, Polkey CE, et al. Single pulse electrical stimulation for identification of structural abnormalities and prediction of seizure outcome after epilepsy surgery: a prospective study. Lancet neurology. 2005;4(11):718-26.
173. Flanagan D, Valentin A, Garcia Seoane JJ, Alarcon G, Boyd SG. Single-pulse electrical stimulation helps to identify epileptogenic cortex in children. Epilepsia. 2009;50(7):1793-803.
174. Matsumoto R, Nair DR, LaPresto E, Bingaman W, Shibasaki H, Luders HO. Functional connectivity in human cortical motor system: a cortico-cortical evoked potential study. Brain : a journal of neurology. 2007;130(Pt 1):181-97.
175. Umeoka S, Terada K, Baba K, Usui K, Matsuda K, Tottori T, et al. Neural connection between bilateral basal temporal regions: cortico-cortical evoked potential analysis in patients with temporal lobe epilepsy. Neurosurgery. 2009;64(5):847-55; discussion 55.
176. Jimenez-Jimenez D, Abete-Rivas M, Martin-Lopez D, Lacruz ME, Selway RP, Valentin A, et al. Incidence of functional bi-temporal connections in the human brain in vivo and their relevance to epilepsy surgery. Cortex; a journal devoted to the study of the nervous system and behavior. 2015;65:208-18.
177. Valentin A, Alarcon G, Barrington SF, Garcia Seoane JJ, Martin-Miguel MC, Selway RP, et al. Interictal estimation of intracranial seizure onset in temporal lobe epilepsy. Clinical neurophysiology : official journal of the International Federation of Clinical Neurophysiology. 2014;125(2):231-8.

178. Kokkinos V, Alarcon G, Selway RP, Valentin A. Role of single pulse electrical stimulation (SPES) to guide electrode implantation under general anaesthesia in presurgical assessment of epilepsy. Seizure : the journal of the British Epilepsy Association. 2013;22(3):198-204.
179. de Andres I, Garzon M, Reinoso-Suarez F. Functional Anatomy of Non-REM Sleep. Front Neurol. 2011;2:70.
180. Amzica F, Steriade M. Short- and long-range neuronal synchronization of the slow (< 1 Hz) cortical oscillation. Journal of neurophysiology. 1995;73(1):20-38.
181. Cash SS, Halgren E, Dehghani N, Rossetti AO, Thesen T, Wang C, et al. The human K-complex represents an isolated cortical down-state. Science. 2009;324(5930):1084-7.
182. Contreras D, Steriade M. Cellular basis of EEG slow rhythms: a study of dynamic corticothalamic relationships. The Journal of neuroscience : the official journal of the Society for Neuroscience. 1995;15(1 Pt 2):604-22.
183. Steriade M, Nunez A, Amzica F. A novel slow (< 1 Hz) oscillation of neocortical neurons in vivo: depolarizing and hyperpolarizing components. The Journal of neuroscience : the official journal of the Society for Neuroscience. 1993;13(8):3252-65.
184. Steriade M, Contreras D, Curro Dossi R, Nunez A. The slow (< 1 Hz) oscillation in reticular thalamic and thalamocortical neurons: scenario of sleep rhythm generation in interacting thalamic and neocortical networks. The Journal of neuroscience : the official journal of the Society for Neuroscience. 1993;13(8):3284-99.
185. Roth M, Shaw J, Green J. The form voltage distribution and physiological significance of the K-complex. Electroencephalography and clinical neurophysiology. 1956;8(3):385-402.
186. Wennberg R, Cheyne D. On noninvasive source imaging of the human K-complex. Clinical neurophysiology : official journal of the International Federation of Clinical Neurophysiology. 2013;124(5):941-55.
187. Murphy M, Riedner BA, Huber R, Massimini M, Ferrarelli F, Tononi G. Source modeling sleep slow waves. Proceedings of the National Academy of Sciences of the United States of America. 2009;106(5):1608-13.
188. Dang-Vu TT, Desseilles M, Laureys S, Degueldre C, Perrin F, Phillips C, et al. Cerebral correlates of delta waves during non-REM sleep revisited. NeuroImage. 2005;28(1):14-21.
189. Czisch M, Wehrle R, Stiegler A, Peters H, Andrade K, Holsboer F, et al. Acoustic oddball during NREM sleep: a combined EEG/fMRI study. PloS one. 2009;4(8):e6749.
190. Voysey Z, Martin-Lopez D, Jimenez-Jimenez D, Selway RP, Alarcon G, Valentin A. Electrical Stimulation of the Anterior Cingulate Gyrus Induces Responses Similar to K-complexes in Awake Humans. Brain Stimul. 2015;8(5):881-90.
191. Thompson S. Control systems engineering and design. Harlow, Essex, England: Longman Scientific & Technical;Wiley; 1989.
192. Alarcon G, Jimenez-Jimenez D, Valentin A, Martin-Lopez D. Characterizing EEG Cortical Dynamics and Connectivity with Responses to Single Pulse Electrical Stimulation (SPES). International journal of neural systems. 2018;28(6):1750057.
193. Spyrou L, Martin-Lopez D, Valentin A, Alarcon G, Sanei S. Detection of Intracranial Signatures of Interictal Epileptiform Discharges from Concurrent Scalp EEG. International journal of neural systems. 2016;26(4):1650016.
194. Halford JJ, Schalkoff RJ, Zhou J, Benbadis SR, Tatum WO, Turner RP, et al. Standardized database development for EEG epileptiform transient detection: EEGnet scoring system and machine learning analysis. J Neurosci Methods. 2013;212(2):308-16.
195. Yamazaki M, Tucker DM, Fujimoto A, Yamazoe T, Okanishi T, Yokota T, et al. Comparison of dense array EEG with simultaneous intracranial EEG for interictal spike detection and localization. Epilepsy research. 2012;98(2-3):166-73.
196. Ulate-Campos A, Coughlin F, Gainza-Lein M, Fernandez IS, Pearl PL, Loddenkemper T. Automated seizure detection systems and their effectiveness for each type of seizure. Seizure. 2016;40:88-101.

197. Antoniades A, Spyrou L, Martin-Lopez D, Valentin A, Alarcon G, Sanei S, et al. Deep Neural Architectures for Mapping Scalp to Intracranial EEG. International journal of neural systems. 2018;28(8):1850009.
198. Schmidhuber J. Deep learning in neural networks: an overview. Neural Netw. 2015;61:85-117.
199. Brooks A. Intelligence without representation. Artificial Intelligence. 1991;47(1-3):139-59.
200. Buccino G, Colage I, Gobbi N, Bonaccorso G. Grounding meaning in experience: A broad perspective on embodied language. Neurosci Biobehav Rev. 2016;69:69-78.
201. Manual for the Scoring of Sleep and Associted Events, (2007).
202. Amzica F, Steriade M. The functional significance of K-complexes. Sleep Med Rev. 2002;6(2):139-49.
203. Johnson LC, Karpan WE. Autonomic correlates of the spontaneous K-complex. Psychophysiology. 1968;4(4):444-52.
204. Niiyama Y, Satoh N, Kutsuzawa O, Hishikawa Y. Electrophysiological evidence suggesting that sensory stimuli of unknown origin induce spontaneous K-complexes. Electroencephalography and clinical neurophysiology. 1996;98(5):394-400.
205. Haines DE, Mihailoff GA. Fundamental neuroscience for basic and clinical applications. Fifth edition. ed. Philadelphia, PA: Elsevier; 2018. xi, 516 pages p.
206. Avanzini G, Manganotti P, Meletti S, Moshe SL, Panzica F, Wolf P, et al. The system epilepsies: a pathophysiological hypothesis. Epilepsia. 2012;53(5):771-8.
207. Clemens B, Szigeti G, Barta Z. EEG frequency profiles of idiopathic generalised epilepsy syndromes. Epilepsy research. 2000;42(2-3):105-15.
208. Chen PC, Castillo EM, Baumgartner J, Seo JH, Korostenskaja M, Lee KH. Identification of Focal Epileptogenic Networks in Generalized Epilepsy Using Brain Functional Connectivity Analysis of Bilateral Intracranial EEG Signals. Brain topography. 2016;29(5):728-37.
209. Clemens B, Puskas S, Besenyei M, Spisak T, Opposits G, Hollody K, et al. Neurophysiology of juvenile myoclonic epilepsy: EEG-based network and graph analysis of the interictal and immediate preictal states. Epilepsy research. 2013;106(3):357-69.
210. Zhang Z, Liao W, Chen H, Mantini D, Ding JR, Xu Q, et al. Altered functional-structural coupling of large-scale brain networks in idiopathic generalized epilepsy. Brain : a journal of neurology. 2011;134(Pt 10):2912-28.
211. Xue K, Luo C, Zhang D, Yang T, Li J, Gong D, et al. Diffusion tensor tractography reveals disrupted structural connectivity in childhood absence epilepsy. Epilepsy research. 2014;108(1):125-38.
212. Caeyenberghs K, Powell HW, Thomas RH, Brindley L, Church C, Evans J, et al. Hyperconnectivity in juvenile myoclonic epilepsy: a network analysis. NeuroImage Clinical. 2015;7:98-104.
213. Elshahabi A, Klamer S, Sahib AK, Lerche H, Braun C, Focke NK. Magnetoencephalography Reveals a Widespread Increase in Network Connectivity in Idiopathic/Genetic Generalized Epilepsy. PloS one. 2015;10(9):e0138119.
214. Telfeian AE, Connors BW. Layer-specific pathways for the horizontal propagation of epileptiform discharges in neocortex. Epilepsia. 1998;39(7):700-8.
215. Enatsu R, Jin K, Elwan S, Kubota Y, Piao Z, O'Connor T, et al. Correlations between ictal propagation and response to electrical cortical stimulation: a cortico-cortical evoked potential study. Epilepsy research. 2012;101(1-2):76-87.
216. D'Arcangelo G, D'Antuono M, Biagini G, Warren R, Tancredi V, Avoli M. Thalamocortical oscillations in a genetic model of absence seizures. The European journal of neuroscience. 2002;16(12):2383-93.
217. Donos C, Mindruta I, Ciurea J, Maliia MD, Barborica A. A comparative study of the effects of pulse parameters for intracranial direct electrical stimulation in epilepsy. Clinical neurophysiology : official journal of the International Federation of Clinical Neurophysiology. 2016;127(1):91-101.

218. Freeman WJ. Measurement of oscillatory responses to electrical stimulation in olfactory bulb of cat. J Neurophysiol. 1972;35(6):762-79.
219. Freeman WJ. Analysis of function of cerebral cortex by use of control systems theory. Mesoscopic brain dynamics. London: Springer; 2000. p. 95-123.
220. Huang XY, Troy WC, Yang Q, Ma HT, Laing CR, Schiff SJ, et al. Spiral waves in disinhibited mammalian neocortex. Journal of Neuroscience. 2004;24(44):9897-902.
221. Schiff SJ, Sauer T. Kalman filter control of a model of spatiotemporal cortical dynamics. J Neural Eng. 2008;5(1):1-8.
222. Schiff SJ. Kalman Meets Neuron: The Emerging Intersection of Control Theory with Neuroscience. Ieee Eng Med Bio. 2009:3318-21.
223. Creutzfeldt OD, Watanabe S, Lux HD. Relations between EEG phenomena and potentials of single cortical cells. II. Spontaneous and convulsoid activity. Electroencephalogr Clin Neurophysiol. 1966;20(1):19-37.
224. Ueno S, Sekino M. Biomagnetics : principles and applications of biomagnetic stimulation and imaging. Boca Raton: CRC Press, Taylor & Francis Group; 2016. xix, 343 pages p.
225. Di Lazzaro V, Oliviero A, Profice P, Saturno E, Pilato F, Insola A, et al. Comparison of descending volleys evoked by transcranial magnetic and electric stimulation in conscious humans. Electroencephalography and clinical neurophysiology. 1998;109(5):397-401.
226. Rusu CV, Murakami M, Ziemann U, Triesch J. A model of TMS-induced I-waves in motor cortex. Brain Stimul. 2014;7(3):401-14.
227. Ziemann U, Rothwell JC, Ridding MC. Interaction between intracortical inhibition and facilitation in human motor cortex. The Journal of physiology. 1996;496 ( Pt 3):873-81.
228. Di Lazzaro V, Oliviero A, Meglio M, Cioni B, Tamburrini G, Tonali P, et al. Direct demonstration of the effect of lorazepam on the excitability of the human motor cortex. Clinical neurophysiology : official journal of the International Federation of Clinical Neurophysiology. 2000;111(5):794-9.
229. Sanger TD, Garg RR, Chen R. Interactions between two different inhibitory systems in the human motor cortex. The Journal of physiology. 2001;530(Pt 2):307-17.
230. McDonnell MN, Orekhov Y, Ziemann U. The role of GABA(B) receptors in intracortical inhibition in the human motor cortex. Experimental brain research. 2006;173(1):86-93.
231. Werhahn KJ, Kunesch E, Noachtar S, Benecke R, Classen J. Differential effects on motorcortical inhibition induced by blockade of GABA uptake in humans. The Journal of physiology. 1999;517 ( Pt 2):591-7.
232. Wasserman E, Epstein CM, Ziemann U. The Oxford handbook of transcranial stimulation. Oxford ; New York: Oxford University Press; 2008. xiv, 747 p. p.
233. Di Lazzaro V, Oliviero A, Profice P, Pennisi MA, Di Giovanni S, Zito G, et al. Muscarinic receptor blockade has differential effects on the excitability of intracortical circuits in the human motor cortex. Experimental brain research. 2000;135(4):455-61.
234. Ferbert A, Priori A, Rothwell JC, Day BL, Colebatch JG, Marsden CD. Interhemispheric inhibition of the human motor cortex. The Journal of physiology. 1992;453:525-46.
235. Civardi C, Cantello R, Asselman P, Rothwell JC. Transcranial magnetic stimulation can be used to test connections to primary motor areas from frontal and medial cortex in humans. NeuroImage. 2001;14(6):1444-53.
236. Mochizuki H, Huang YZ, Rothwell JC. Interhemispheric interaction between human dorsal premotor and contralateral primary motor cortex. The Journal of physiology. 2004;561(Pt 1):331-8.
237. Lee H, Gunraj C, Chen R. The effects of inhibitory and facilitatory intracortical circuits on interhemispheric inhibition in the human motor cortex. The Journal of physiology. 2007;580(Pt.3):1021-32.
238. Kukaswadia S, Wagle-Shukla A, Morgante F, Gunraj C, Chen R. Interactions between long latency afferent inhibition and interhemispheric inhibitions in the human motor cortex. The Journal of physiology. 2005;563(Pt 3):915-24.

239. Chen R. Interactions between inhibitory and excitatory circuits in the human motor cortex. Experimental brain research. 2004;154(1):1-10.
240. Schwenkreis P, Witscher K, Janssen F, Addo A, Dertwinkel R, Zenz M, et al. Influence of the N-methyl-D-aspartate antagonist memantine on human motor cortex excitability. Neuroscience letters. 1999;270(3):137-40.
241. Ziemann U, Chen R, Cohen LG, Hallett M. Dextromethorphan decreases the excitability of the human motor cortex. Neurology. 1998;51(5):1320-4.
242. Creutzfeldt OD, Watanabe S, Lux HD. Relations between EEG phenomena and potentials of single cortical cells. I. Evoked responses after thalamic and erpicortical stimulation. Electroencephalography and clinical neurophysiology. 1966;20(1):1-18.
243. Barth DS, Sutherling W. Current source-density and neuromagnetic analysis of the direct cortical response in rat cortex. Brain research. 1988;450(1-2):280-94.
244. Milstein J, Mormann F, Fried I, Koch C. Neuronal shot noise and Brownian 1/f2 behavior in the local field potential. PloS one. 2009;4(2):e4338.
245. Miller KJ, Sorensen LB, Ojemann JG, den Nijs M. Power-law scaling in the brain surface electric potential. PLoS Comput Biol. 2009;5(12):e1000609.
246. Gold C, Henze DA, Koch C, Buzsaki G. On the origin of the extracellular action potential waveform: A modeling study. Journal of neurophysiology. 2006;95(5):3113-28.
247. Pettersen KH, Hagen E, Einevoll GT. Estimation of population firing rates and current source densities from laminar electrode recordings. J Comput Neurosci. 2008;24(3):291-313.
248. Bazhenov M, Lonjers P, Skorheim S, Bedard C, Dstexhe A. Non-homogeneous extracellular resistivity affects the current-source density profiles of up-down state oscillations. Philos Trans A Math Phys Eng Sci. 2011;369(1952):3802-19.
249. Belluscio MA, Mizuseki K, Schmidt R, Kempter R, Buzsaki G. Cross-frequency phase-phase coupling between theta and gamma oscillations in the hippocampus. The Journal of neuroscience : the official journal of the Society for Neuroscience. 2012;32(2):423-35.
250. Usami K, Milsap GW, Korzeniewska A, Collard MJ, Wang Y, Lesser RP, et al. Cortical Responses to Input From Distant Areas are Modulated by Local Spontaneous Alpha/Beta Oscillations. Cerebral cortex. 2018.
251. Bagnato S, Boccagni C, Sant'Angelo A, Prestandrea C, Rizzo S, Galardi G. Patients in a vegetative state following traumatic brain injury display a reduced intracortical modulation. Clinical neurophysiology : official journal of the International Federation of Clinical Neurophysiology. 2012;123(10):1937-41.
252. Shayegh F, Bellanger JJ, Sadri S, Amirfattahi R, Ansari-Asl K, Senhadji L. Analysis of the behavior of a seizure neural mass model using describing functions. J Med Signals Sens. 2013;3(1):2-14.
253. Liley DT, Bojak I. Understanding the transition to seizure by modeling the epileptiform activity of general anesthetic agents. J Clin Neurophysiol. 2005;22(5):300-13.
254. Mouthaan BE, van 't Klooster MA, Keizer D, Hebbink GJ, Leijten FSS, Ferrier CH, et al. Single Pulse Electrical Stimulation to identify epileptogenic cortex: Clinical information obtained from early evoked responses. Clinical neurophysiology : official journal of the International Federation of Clinical Neurophysiology. 2016;127(2):1088-98.
255. Parker CS, Clayden JD, Cardoso MJ, Rodionov R, Duncan JS, Scott C, et al. Structural and effective connectivity in focal epilepsy. NeuroImage Clinical. 2018;17:943-52.
256. Nayak D, Valentin A, Selway RP, Alarcon G. Can single pulse electrical stimulation provoke responses similar to spontaneous interictal epileptiform discharges? Clinical Neurophysiology. 2014;125(7):1306-11.
257. Menendez de la Prida L, Staba RJ, Dian JA. Conundrums of high-frequency oscillations (80-800 Hz) in the epileptic brain. J Clin Neurophysiol. 2015;32(3):207-19.

258. Jefferys JG, Menendez de la Prida L, Wendling F, Bragin A, Avoli M, Timofeev I, et al. Mechanisms of physiological and epileptic HFO generation. Progress in neurobiology. 2012;98(3):250-64.
259. Bragin A, Engel J, Jr., Wilson CL, Vizentin E, Mathern GW. Electrophysiologic analysis of a chronic seizure model after unilateral hippocampal KA injection. Epilepsia. 1999;40(9):1210-21.
260. Bragin A, Engel J, Jr., Wilson CL, Fried I, Mathern GW. Hippocampal and entorhinal cortex high-frequency oscillations (100--500 Hz) in human epileptic brain and in kainic acid--treated rats with chronic seizures. Epilepsia. 1999;40(2):127-37.
261. Jirsch JD, Urrestarazu E, LeVan P, Olivier A, Dubeau F, Gotman J. High-frequency oscillations during human focal seizures. Brain : a journal of neurology. 2006;129(Pt 6):1593-608.
262. Urrestarazu E, Chander R, Dubeau F, Gotman J. Interictal high-frequency oscillations (100-500 Hz) in the intracerebral EEG of epileptic patients. Brain : a journal of neurology. 2007;130(Pt 9):2354-66.
263. Jacobs J, Zijlmans M, Zelmann R, Chatillon CE, Hall J, Olivier A, et al. High-frequency electroencephalographic oscillations correlate with outcome of epilepsy surgery. Annals of neurology. 2010;67(2):209-20.
264. Kobayashi K, Matsumoto R, Matsuhashi M, Usami K, Shimotake A, Kunieda T, et al. High frequency activity overriding cortico-cortical evoked potentials reflects altered excitability in the human epileptic focus. Clinical neurophysiology : official journal of the International Federation of Clinical Neurophysiology. 2017;128(9):1673-81.
265. Roehri N, Pizzo F, Lagarde S, Lambert I, Nica A, McGonigal A, et al. High-frequency oscillations are not better biomarkers of epileptogenic tissues than spikes. Annals of neurology. 2018;83(1):84-97.
266. Singer W, Gray CM. Visual feature integration and the temporal correlation hypothesis. Annu Rev Neurosci. 1995;18:555-86.
267. Murthy VN, Fetz EE. Synchronization of neurons during local field potential oscillations in sensorimotor cortex of awake monkeys. Journal of neurophysiology. 1996;76(6):3968-82.
268. Buzsaki G, Horvath Z, Urioste R, Hetke J, Wise K. High-frequency network oscillation in the hippocampus. Science. 1992;256(5059):1025-7.